UNIVERSITÀ
DI PAVIA

Dipartimento di Biologia e Biotecnologie "L. Spallanzani"

Development of non-invasive approaches for seed quality assessment

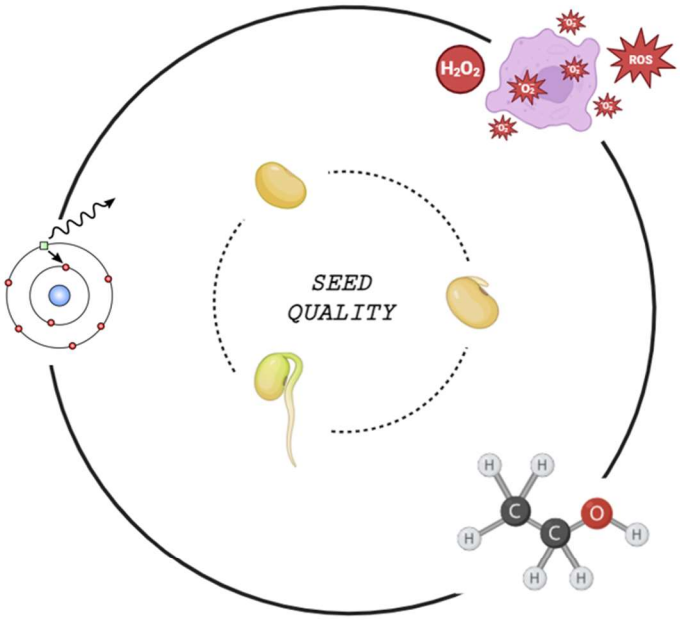

Adriano Griffo

Dottorato di Ricerca in
Genetica, Biologia Molecolare e Cellulare
Ciclo XXXVII – A.A. 2023-2024

Table of Contents

Abstract

Agriculture plays a crucial role in influencing the world's population health and economy. Since the current global food production is not adequate to meet the steady population growth and the impact of climate change, multiple joined approaches are required to improve agricultural production in a more sustainable fashion. In this context, a more extensive utilization of high-quality seeds for agricultural production can markedly improve crop production. Seed quality is defined as the set of physical (morphology, weight, color), physiological (viability, vigor), and genetic features (genetic purity).

High-quality seeds present optimal germination performances, in terms of germination rate, positively correlated with optimal plant growth, and consequently, improved crop production and yield. Given the importance of seed quality for crop production, the use of cost-effective, rapid, and accurate methods for seed quality assessment represents one of the major objectives of seed companies and consumers for maximizing the economic return. Although most of the conventional methods currently applied for seed quality estimation, such as germination and tetrazolium tests, are standardized for being applied in a multitude of different species, the time required for the analysis, as well as limited number of information collected are limiting factors that confine their application to specific contexts. Moreover, the invasiveness, relating to the consumption of seed material required, that characterizes these tests is in contrast with the need for sustainable approaches employed in agriculture to save natural resources. For these reasons, in recent years optical technologies (machine vision, NIR, Raman spectroscopy, thermal, x-ray, and hyperspectral imaging) have been adapted and optimized for the non-invasive seed quality estimation. Although these technologies present an elevated efficiency and accuracy in detecting seed quality, the cost and the complexity associated with their use, can limit their large-scale employment.

In the present work, different approaches for the non-invasive seed quality estimation were developed. Approaches based on the detection of different markers of seed quality, such as reactive oxygen species (ROS), volatile organic compounds (VOCs), ultra-weak photon emission (UPE), and delayed luminescence (DL), were tested on different species. Seeds with contrasting characteristics (high- *versus* low-quality) were obtained either through priming treatments or heat shock, natural and artificial aging protocols. Although the developed approaches are based on different mechanisms, the obtained results highlighted their feasibility in estimating seeds quality. While ROS detection can be considered as the most rapid, easy-to-use and cost-effective approach, the detection of UPE/DL and VOCs, provide a much higher quantity and accuracy of data, but require advanced equipment and skills to be performed and analyzed.

Abbreviations

AA (artificial aging)

ABA (abscisic acid)

ABI 1/2/3/4/5 (abscisic acid intensive 1/2/3/4/5)

AOSA (Association of Official Seed Analysts)

APX (ascorbate peroxidase)

AUC (area under the curve)

BRs (brassinosteroids)

CAT (catalase)

CTRL (control)

CVG (coefficient of velocity)

DB (dry-back)

DCFH-DA (2'7'-dichloro-dihydro-fluorescein diacetate)

DL (delayed luminescence)

DOG1 (delay of germination 1)

FOX-1 (ferrous oxidation-xylenol orange)

GAs (gibberellins)

FAO (Food and Agriculture Organization)

H_2O_2 (hydrogen peroxide)

HP (hydropriming)

HS (heat stress)

ISTA (International Seed Testing Association)

KNN (k-nearest neighbor)

LEA (late embryogenesis abundant)

MC (moisture content)

MGR (mean germination rate)

MGT (mean germination time)

NIR (near-infrared)

PCA (principal component analysis)

PMT (photomultiplier)

PV (peak value)

QTLs (quantitative trait loci)

QRT-PCR (quantitative Real-Time Polymerase Chain Reaction)

RBOH (plant respiratory burst oxidase homolog)

RH (relative humidity)

ROS (reactive oxygen species)

SOD (superoxide dismutase)

SVM (support vector machine)

TFs (transcription factors)

TTC (2,3,5-triphenyl tetrazolium chloride)

U (uncertainty index)

UPE (ultra-weak photon emission)

VOCs (volatile organic compounds)

Z (synchronicity index)

1. General Introduction

1.1 Seed quality in the context of agricultural production

Agriculture has a crucial role in global food production. Agricultural production is not only fundamental to improving nutrition but is also the main source of income for many nations. The increase in crop production is determinant to end hunger, as well as for economic and social development. Over the past two decades, the global agricultural production volumes of primary crops showed a steady upward trend (**Fig. 1.1**). The production of maize (**Fig 1.1a**) and soybean (**Fig 1.1b**), two of the most consumed crops in the world, presented a continuous increase over the past twenty years. This growth can be mostly due to the improved technologies related to agriculture and the intensification of farming activities (FAO 2022).

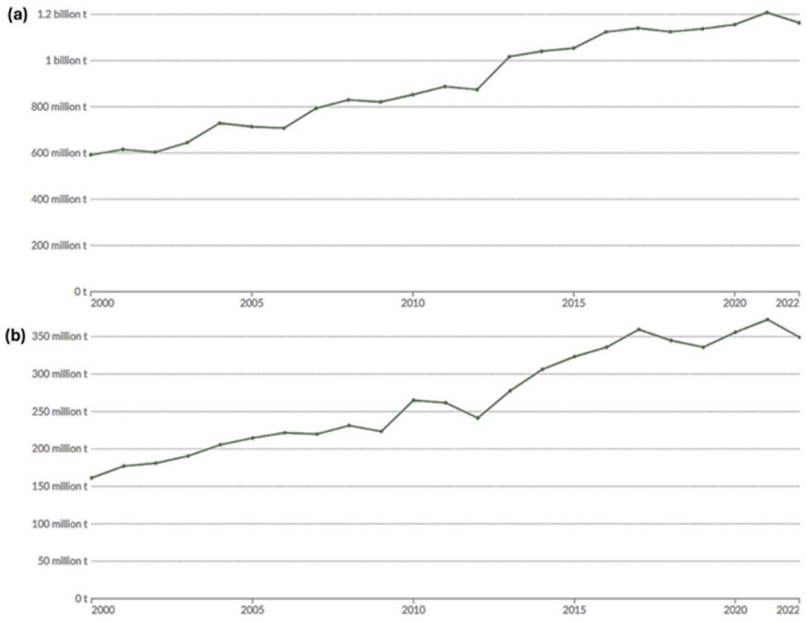

Figure 1.1. Global production of **(a)** maize and **(b)** soybean from 2000 to 2022, expressed as billion or million tons (t). UN Food and Agriculture Organization (FAO), FAOSTAT 2023 https://www.fao.org/faostat/en/#data/QCL/visualize.

Despite this trend, the current crop production is not sufficient to meet the future global demand. A meta-analysis on projected global food demand estimated the need to increase food production by 45% - 56%, against the more pessimistic prevision of FAO, ranging between 60% - 110 % (Van Dijk et al., 2021). Regardless of the perspective, food production must be increased to ensure food security for a steadily growing world population. The global population reached 7.8 billion by mid-2020, an increase from 7 billion in 2010, 6 billion in 1998, and 5 billion in 1986. The average annual growth rate was approximately 1.1% between 2015 and 2020, which gradually declined after reaching a peak of 2.3% in the late 1960s (Gu et al., 2021).

Based on popular projections, the future global population will reach 10 billion by 2100 (Lee, 2011). In this context, the geographical distribution of population growth is an important index to be considered. As shown in **Fig. 1.2**, most of the countries with the highest growth rate are characterized by poor economic development and are unable to provide enough food and good quality services to the current population (Ezeh et al., 2012).

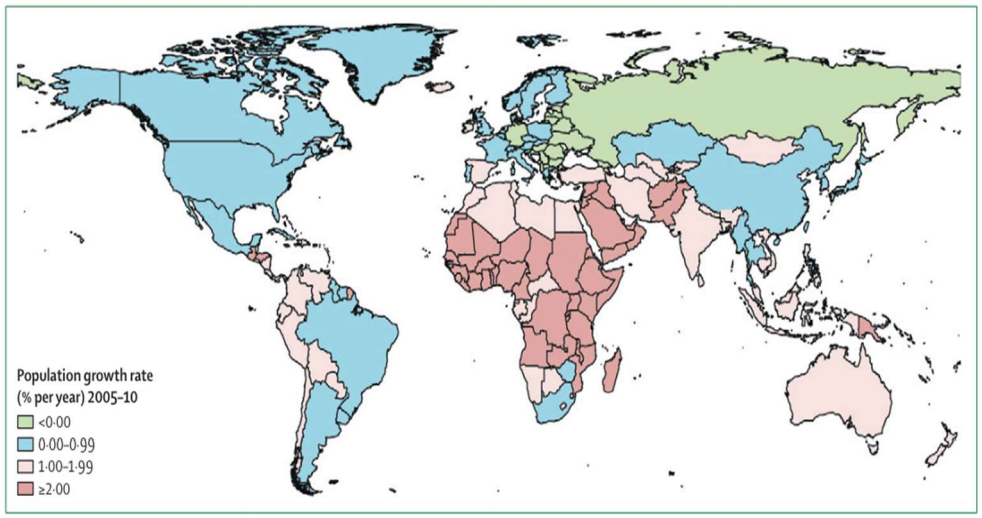

Figure 1.2. Population growth rate per year by country in the period 2005-2010. The countries with rapid growth (growth rate greater or equal to 2%) are indicated in red, with a moderate growth (rate between 1-1,99%) in light pink, low or no growth countries (0-0,99%) in blue, and population decline countries in green (Ezeh et al., 2012).

In a complex scenario where global and local food production needs to be boosted to be in line with the current population demands and future projections, other factors play a negative role in reducing crop yields. Climate changes are generally associated with the loss of agricultural productivity. It was reported that the global mean surface temperature had increased by 0.85ºC during 1880-2012. Furthermore, the global annual mean precipitation had shown substantial changes over the period 1901-2008. The most significant aspect of this climatic variation is the discrepancy in the spatial-temporal characteristics of these two variables across different regions of the world. In fact, the rate of temperature change in the Arctic was almost twice as much as the global mean value in the past century, while the rate of precipitation increased particularly in eastern North and South America, northern Europe, and northern and central Asia, in comparison to the Mediterranean, southern Africa, and parts of southern Asia, where a drying trend is observed (Shi and Chen, 2018). The frequency of extreme events, defined as climatic events that occur rarely within the climatic context of recent decades, represents an important feature of climatic changes. Intense precipitations, floods, storms, tornadoes, and prolonged periods of drought became more frequent and characterized the climatic conditions of several regions (Zwiers et al., 2013). This marked change in the global climatic condition is the result of enhanced human activities that altered the composition of the atmosphere through

the massive release of greenhouse gases, including methane (CH_4), carbon dioxide (CO_2), and nitrous oxide (N_2O) (Malhi et al., 2021). Through an estimation of the impact of climate change, agriculture is revealed to be the most vulnerable sector. Several studies highlight the negative effect of climatic events, like high temperatures and rainfall, on the yield of crops. Moreover, the occurrence of adverse climate-related events not only has a profound impact on the production of food but also on its distribution, quality, and accessibility. Considering that food security is inextricably linked with public health, all these events will result in the spreading of hunger, poverty, and disease (Arora, 2019).

In recent years, multiple approaches have been employed to overcome this complex challenge. The reduction of greenhouse gas emissions represents the initial step in limiting the influence of climatic changes on food production. In this context, technologies based on decarbonization and reduced CO_2 emissions, including renewable energy, fuel switching, efficiency gains, nuclear power, carbon capture, storage, and utilization, are being proposed. In particular, the production of sustainable energy represents one of the priorities that drives current scientific research. Innovative technologies, such as photovoltaic solar power, concentrated solar power, solar thermal power for heating and cooling applications, wind power, hydropower, marine power, geothermal power, biomass power, and biofuels, have become common tools for producing new forms of renewable energy (VijayaVenkataRaman et al., 2012). Despite these premises, the intermittent nature/variability in power production is a limiting factor affecting the large-scale production of sustainable energy forms. Moreover, non-technical factors, like renewable energy investments, government stability, and administrative procedures may delay the expansion of these technologies (Fawzy et al., 2020). Along with the reduction of greenhouse gas emissions, the enhancement of crop production is an important step to counterbalance the damage caused by climate change to agriculture. The current agricultural practice has been influenced by the utilization of chemical fertilizers to boost crop production (Delgado et al., 2016). Conventional fertilizers present low utilization efficiency by plants due to fixation, leaching, microbial degradation, photolysis, and volatilization. However, the repeated application of these products, which is required to achieve maximum yield, negatively impacts on the environment, polluting the underground water sources (Elemike et al., 2019). A potential alternative is represented by the application of waste products of biomass anaerobic digestion as sustainable and efficient fertilizers (Vaneeckhaute et al., 2013). In addition, the knowledge of the different roles of amino acids in plant yield and growth allowed the development of a novel and safer form of chemical fertilizer with low environmental impact (Souri, 2016).

Traditional plant breeding, based on the selection of the most productive species and varieties under optimal conditions, represents a method responsible for the linear increase in food production observed in the last decades. However, this strategy does not ensure the best production levels in low-yield environments (Tester and Langridge, 2010). The advances in genetic knowledge regarding the factors affecting the resistance to stress conditions are driving modern plant breeding processes, which preserve crop productivity under non-optimal growing conditions (Lamichhane and

Thapa, 2022). New plant breeding technologies (NPBT) constitute the results of recent biotechnological innovations applied to plant breeding and crop production improvement. These technologies, which include different approaches of genome editing such as oligonucleotide-directed mutagenesis (ODM) and sequence-specific nuclease (SSN), variants of conventional transformation methods including cisgenesis and intragenesis, grafting, agro-infiltration, and manipulation of epigenetic landscape (RNA-dependent DNA methylation, RdDM), are emerging as a reliable solution to enhance plant stress tolerance and yield (Enfissi et al., 2021). Although the benefits of the NPBT approach are discussed in several studies (Raman, 2017; Singh et al., 2022), the utilization of genetically modified (GM) crops represents probably the most divisive symbol of modern agriculture and is at the center of political, environmental, and scientific debates. Generally, one of the main limitations of modern and artificial plant breeding methods is the adverse effect on biodiversity. The potential effect of GM crops in inducing the progressive loss of biodiversity (Schmeller and Henle, 2008) is in contrast with the purpose of improving crop production, as the loss of species affects food security and availability (Ceccarelli, 2009). In the view of prioritizing the utilization of species with high resistance to adverse climatic conditions and biodiversity preservation, the inclusion of lesser-known local crops can enhance the final production. Orphan legumes, defined as those leguminous crops that have been utterly ignored by policymakers and are considered underutilized, are receiving increased attention from the scientific community due to their tolerance to drought as well as high and low temperatures (Chongtham et al., 2022; Balestrazzi et al., 2024). These legumes have adapted to hostile environments through the development of a combination of morphological, physiological, biochemical, cellular, and molecular mechanisms to rapidly respond to stress (Cullis et al., 2018; Balestrazzi et al., 2024). Presently, different studies report good germinability of orphan seeds in regions where few conventional crops can grow (Cullis and Kunert, 2017; Popoola et al., 2022; Balestrazzi et al., 2024).

In agriculture, seeds represent the fundamental input factor influencing crop productivity. Seed germination is indeed a critical initial stage in plant's life, as it enables the survival of plant species in natural environments and influences crop yield in agriculture (Bailly and Roldan, 2023). Moreover, seeds are crucial elements for the preservation of biodiversity and agrobiodiversity, referring to the species that are critical for food production, influencing local and global food security (Pimbert, 2022). The importance of seeds for sustainable and adequate food production explains the growth of the global market in previous years. The global seed market is an important part of the agriculture sector, covering the production, manufacture, distribution, and sale of seeds for a variety of crops. From the year 2000, the size of the global seed market expanded from around 10 billion US dollars to a value of 52 billion in 2014 (OECD, 2018). Future projections confirm the same trend for the following years, as indicated in **Fig. 1.3**. The market size indicates a continuous increase, starting from 113.96 billion dollars in the current year to a value of around 189 billion in 2031, with a compound annual growth rate (CAGR) of 6.50%.

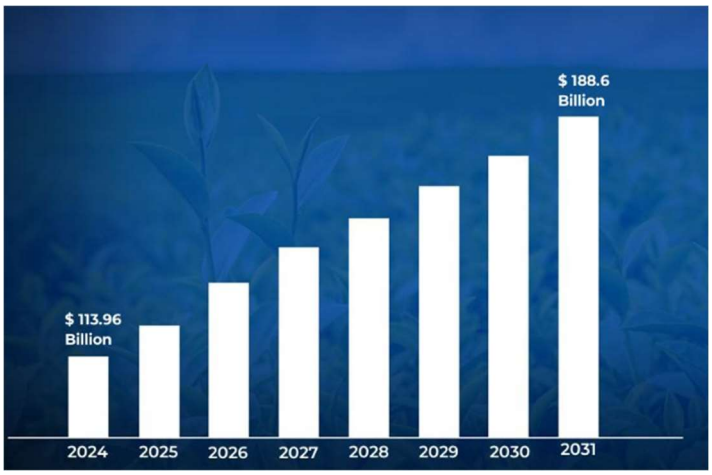

Figure 1.3. Current global seed market value (in US dollars, USD) trend. Verified Market Research. In-Depth Industry Outlook: Seed Market Size & Forecast https://www.verifiedmarketresearch.com/product/seed-market/.

In this scenario, several factors are likely to be the driving forces of the observed future growth. As discussed above, the growth of the world's population and the effects of climate change require increased crop production, which in turn requires an increase in the seeds used and produced. In addition, innovative seed treatments and recent advances in seed storage also contribute to market value expansion. In particular, strategies for the preservation and improvement of seed quality have a profound impact on the global market.

The concept of seed quality is broad and includes multiple features of seed biology. Seed quality (**Fig. 1.4**) is defined as the set of physical, physiological, and genetic characteristics of seeds (Raman and Cho, 2016; Domergue et al., 2019).

Figure 1.4. Physical, psychological, and genetic features defining seed quality (https://novogoldseeds.com/quality-policy/).

Seed quality has a crucial role in agricultural production and in preserving plant biodiversity since high-quality seeds present superior germination performances and are more resistant to deterioration during long-term storage (Matthews et al., 2012)

and to pathogen infestation (Kulik, 2020). Moreover, good seed quality assures high germination percentage levels under non-optimal growth conditions, such as high temperatures (Kumar, 2012).

The physical status of seeds is mainly influenced by environmental conditions during growth and harvest (Barnard and Calitz, 2011) and includes all the features regarding the overall external structure, like morphology, weight, and color. Seeds with optimal physical quality present uniform size, weight, and color, and are free from diseases and coat damage (Sundareswaran et al., 2023). All these features can individually influence the germination capacity (Zabala et al., 2011). For instance, seed weight influences water uptake during the early stage of germination, thus affecting seedling growth (Hay et al., 2022). Considering its relevant effect on seed germination, the observation of differences, in terms of seed weight, among species distributed in different climatic conditions provides pieces of evidence on how this physical feature responds to environmental factors as an adaptive trait, preserving plant fitness. Li et al. (2015) documented a within-species variation in seed weight and germination attributes, observing a correlation between physical parameters, time and percentage of germination. Another study conducted on six populations of false Rhodes grass (*Chloris crinita*) species from different humid and arid regions subjected to osmotic stress indicates a strong correlation between stress tolerance and seed weight. Although seed weight is a genetically stable feature, defined by a specific evolutionary history, studies support the hypothesis of seed weight as an adaptive trait to promote plant growth under stress conditions (Marinoni et al., 2022). Similarly, seed morphology and color are important physical features reflecting germination potential. These traits show a correlation with seed maturation level (Puga-Guzmán et al., 2023), as well as with some chemical compounds involved in biological processes during germination (Shimada et al., 2021). In a recent study conducted on native *Tulipa* species, seed morphology, and color were both correlated with the ratio of embryotic length to seed length, an indicator of good germination potential. Interestingly, the two physical characteristics were not reciprocally correlated, suggesting they represent independent features both influencing germination capacity (Zhang et al., 2023). The presence of damage has a variable effect on seed germination, and it is often associated with animal/insect predation. Although seed predation by animals or damage induced by pests affects seed integrity, germination potential can be maintained if the embryo is not involved in the damage (Pérez et al., 2008). Generally, partial seed predation has a variable effect, depending on the species and the external structure of the seeds. Interestingly, the response to seed damage can be an accelerated germination dynamic, probably induced by the breaking of physical dormancy due to the scarification of the seed coat (Vallejo-Marín et al., 2006). However, in most cases seed damage induced by pests promotes seed aging, resulting in a loss of germination capacity (Pérez et al., 2008). In this context, pest infestation is one of the physical characteristics that mostly affects seed germination. Numerous studies report a marked loss of germination performances due to post-harvest infection. A recent work on different varieties of chickpeas (*Cicer arietinum*) reports a significant decrease in germination rate in all the growing districts in Ethiopia caused by insect infestation. The analyses on seeds led to the

identification of twelve different species of insects involved in the infestation, but *Callosobruchus chinensi*s was the most prevalent species, accounting for roughly 92.21% of the entire population (Berhe et al., 2023). Therefore, all physical characteristics are directly related to seed quality, influencing the germination ability. In some circumstances, these features allow plant adaptation and fitness preservation in non-optimal growth conditions, acting as adaptive traits.

Aside the physical characteristics, physiological features are strongly related to seed quality and include all the aspects that reflect germination behavior. Seed viability and seed vigor are the main attributes related to the physiological state of seeds. Seed viability corresponds to the portion of living seeds in a sample and represents an essential prerequisite for germination and plant growth (Pradhan et al., 2022). Although is often related to the concept of viability, seed vigor has a more elaborate meaning. The term is used to refer to the concepts of "driving force" and "shooting strength" of germinating seedlings, with the purpose of highlighting seeds that produced seedlings with longer roots in comparison to those from "weaker" seeds from the same lot (Marcos Filho, 2015). Physiological seed quality is mainly estimated through the calculation of germination indices, reflecting the portion of seeds germinated, the speed and the uniformity of germination, the length of shoots and roots (Ranal and Santana, 2006). These aspects will be explored in-depth in the next chapter.

Genetic purity constitutes an important part of the overall seed quality. The germination performances of species and varieties in a specific environment are strictly dependent on the genetic background of the seeds used by farmers. Hence, it is important to evaluate the genetic purity to ensure optimal agricultural production (Sedah et al., 2023). The biological basis is the presence of genes that are functionally related to different aspects of seed quality. Currently, omics technologies, involved in genome, epigenome, and transcriptome analyses, have facilitated the identification of different genes and quantitative trait loci (QTLs) that are involved in seed quality (Zhang et al., 2022). The current knowledge of DNA sequences linked to seed quality includes different species of high relevance for food production. For instance, the *POWR1* (*Protein, Oil, Weight, Regulator 1*) gene was found to be involved in seed protein and oil content in *Glycine max*, influencing both weight and chemical composition. *POWR1* is a domestication gene mainly expressed in developing coat that regulates nutrient transport and lipid metabolism, controlling the equilibrium between oil and protein synthesis (Goettel et al., 2022). The *SWEET* gene, first identified in *Arabidopsis thaliana* and *G. max*, is another important regulator of seed weight through the control of oil content. SWEET proteins are sugar transporters that induce the uptake of sugars into embryos from maternal tissues, promoting embryo cell division and expansion and lipid synthesis to the detriment of protein production (Wang et al., 2020). Additional regulators of seed size are genes involved in plant hormone synthesis, such as brassinosteroids (BRs), which were identified in *Oryza sativa* (*OsBRD1, OsBRD2, OsD2, OsDWARF4, OsDWARF11*), and *Zea mays* (*ZmDWF1*, *ZmDWF4*, *ZmDET2*, *ZmUPA1*) (Sun et al., 2021). Seed viability is another feature influenced by the information present in plant genome. The study of Li et al. (2023) reported a negative correlation between seed viability and the

presence of mutant alleles of the *HXK* genes in several species. These genes encode for hexokinases, key enzymes involved in glucose metabolism and signal transduction that affect several physiological processes, influencing seed size, viability, and germination. Similarly, raffinose family oligosaccharides (RFO) biosynthetic genes, such as genes encoding for galactinol synthase, raffinose synthase, and stachyose synthase, affect seed vigor. RFOs are essential sugars that protect against desiccation damage during seed maturity and provide energy for the effective establishment of new seedlings during seed germination (Salvi et al., 2022). Many QTLs involved in seed vigor have also been identified. A QTLs mapping work on artificially aged *Triticum aestivum* seeds identified eight DNA sequences correlated with eight traits related to seed vigor. Gene identification within the target DNA sequences revealed seven genes involved in metabolic and cellular processes, catalytic activity, and biological regulation (Shi et al., 2020). The identification of QTLs related to seed quality represents an important step in improving food production. By employing QTL analyses, it is possible to select molecular markers for stress tolerance, germination potential, and physical/chemical structure, to optimize crop yield and production (Csanádi, 2001). A more detailed description of other approaches used for seed quality estimation will be provided in one of the next chapters.

1.2 Metabolic aspects of seed germination

Seed germination represents a crucial phase in the life cycle of a plant, directly influencing its growth and the yield of the crop. This complex event is the consequence of a multitude of morphological, molecular, and biochemical processes activated at specific time points to initiate seed germination under specific circumstances. In recent decades, consistent research has been dedicated to the study of seed germination, resulting in a significant accumulation of knowledge regarding the biological processes that regulate and define this event. However, an analysis of seed germination as a separate event within the plant development cycle provides an incomplete understanding of the true complexity and significance of this process. Numerous aspects of seed germination behavior are strictly linked to other stages of plant development, such as seed maturation and dormancy establishment, as well as biotic and abiotic factors (Penfield, 2017).

Seed maturation follows embryogenesis and can be divided into two stages: morphogenesis and maturation. During seed maturation, seeds undergo a period of embryo growth and accumulate storage molecules (Sajeev et al., 2019). Seed maturation ends with a desiccation phase, after which the embryo enters a dormant state (Gutierrez et al., 2007). Seed dormancy is an important physiological process linked to seed maturation and germination. It is defined as the inhibition of seed germination in viable seeds under unfavorable conditions. This event, which arrests the activation of germination processes, is crucial in many species to facilitate seed dispersal and to postpone germination until optimal conditions occur, thereby optimizing the possibility of successful plant growth (Rehmani et al., 2022). Seed

dormancy occurs in two different stages of the plant development cycle. The first dormancy occurs at the end of seed maturation (primary dormancy). Once primary dormancy is lost in response to specific post-harvest environmental conditions, seeds enter in a secondary dormancy stage if the conditions required to induce germination are absent. This secondary dormancy allows seed dispersal and activation of the germination process at optimal conditions (Finch-Savage and Leubner-Metzger, 2006). Although the molecular mechanisms that induce seed dormancy remain largely unknown, different studies pinpoint at different biological events. During dormancy, the embryo undergoes a quiescent state in which germination-promoted genes are not actively expressed. In this scenario, chromatin structure determines gene expression, regulating the maintenance of the dormancy state or the activation of the germination process. Hence, many epigenetic regulatory-related genes associated with chromatin remodeling are involved in seed dormancy and germination phases (Shu et al., 2016). In this context, the principal components of the chromatin remodeling process are abscisic acid (ABA) and gibberellins (GAs), which have been reported by several studies as the key regulators of dormancy and germination phases (Sano and Marion-Poll, 2021). ABA and GA are phytohormones actively involved in the modification of chromatin structure, influencing the expressions of histone methyltransferase and histone acetyltransferase genes (Zheng et al., 2012; Shu et al., 2016). However, the pivotal role of ABA and GA in seed dormancy maintenance and the transition to germination is not limited to the regulation of chromatin structure. Specifically, the dynamic balance between ABA and GA represents the central point which determines the induction of seed dormancy and germination events (Liu and Hou, 2018).

ABA is the main inducer and protector of seed dormancy. This evidence is supported by studies that observed faster germination in ABA-deficient mutants and transgenic plants constitutively expressing the ABA biosynthesis genes maintaining deep seed dormancy (Shu et al., 2016). ABA starts accumulating after the embryogenesis step of seed maturation phase, where it inhibits embryo growth and positively regulates reserve accumulation and at later stages induces primary dormancy and desiccation tolerance. Its biosynthesis is a multi-step process which starts with the cleavage of cis-isomers of the oxygenated carotenoids, violaxanthin and neoxanthin, by a 9-cis epoxycarotenoid dioxygenase (NCED). The 15-carbon product, xanthoxin, is then transported from plastids to cytosol and converted into abscisic aldehyde by a short-chain alcohol dehydrogenase, encoded by the *ABA2* gene. The final biosynthesis step is catalyzed by an abscisic aldehyde oxidase, which produces the ABA active hormone (Wu et al., 2023). Although ABA accumulation shows a peak in the middle of the maturation phase, genetic studies indicates that an initial source of this hormone translocate from maternal tissues to seeds. According to studies conducted on *Arabidopsis thaliana*, NCED3 is the main contributor to ABA production in vegetative maternal tissues, while other dioxygenase forms are mainly involved in the hormone synthesis inside seed tissues, such as NCED6, NCED5, and NCED9 proteins (Chauffour et al., 2019). Once synthetized, ABA operates in a complex signaling network and triggers the activation of downstream signaling genes involved in seed maturation and dormancy. In this complex network ABA interacts with

specific receptors which are reported by different studies to have an essential role in seed, the PYL/RCAR family proteins. As illustrated in **Fig. 1.5**, in the absence of ABA, PYLs proteins promote the release of protein phosphatase type 2C (PP2C) and activate its phosphatase function. PP2C proteins, including ABA-insensitive 1/2 (ABI1/2) and ABA-hypersensitive germination 3 (AHG3), serve as negative regulators within the ABA signaling system, suppressing the activities of downstream ABA signaling protein like sucrose nonfermenting 1-related protein kinase 2s (SnRK2s) through protein phosphorylation. This results in the inhibition of the downstream ABA signaling network. In the presence of ABA, the PYR/PYL/RCAR protein-ABA complex binds to the PP2C proteins, thereby inhibiting their phosphatase activity and resulting in the release and activation of SnRK2s function (Zhang et al., 2015; Ali et al., 2021). SnRK2s are a plant-specific protein kinase family that function as positive regulators of the ABA signaling network. Despite the family's composition of 10 distinct members (SnRK2.1–2.10), the ABA-related activation is observed to occur through the involvement of SnRK2.2, 2.3, and 2.6 proteins. SnRK2 substrates, including the basic region/leucine zipper motif (bZIP) transcription factors AREBs (ABA-responsive element binding factors), regulate the expression of genes involved in seed maturation and dormancy (Jakoby et al., 2002; Wang et al., 2013).

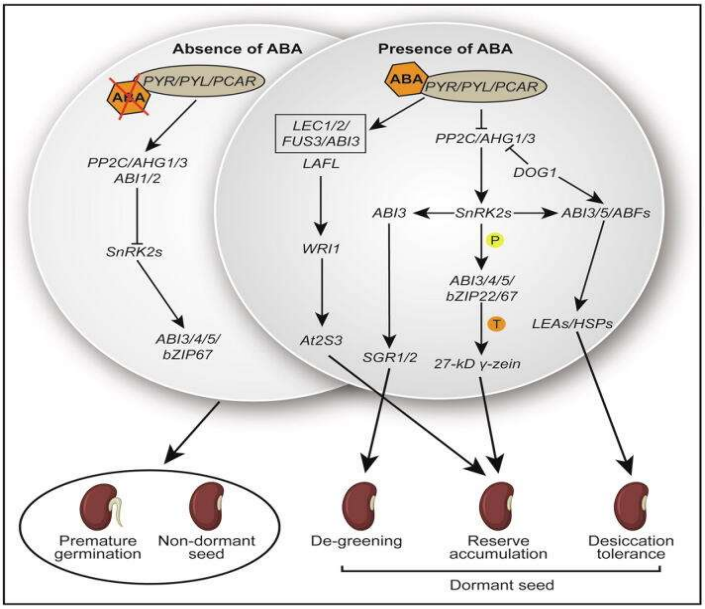

Figure 1.5. The ABA signaling pathway involved in seed development (Ali et al., 2021).

During seed maturation, important molecules activated during ABA signaling are master regulator genes, such as abscisic acid intensive 3 and 5 (*ABI3* and *ABI5*) (**Fig. 1.5**), FUSCA3 (*FUS3*), leafy cotyledon 1 and 2 (*LEC1* and *LEC2*), which are involved in the regulation of maturation-related genes. Specifically, ABI3 and ABI5 are the main master-regulators operating in maturing seeds, directly involved into the control of late embryogenesis abundant (LEA) and dehydrin expression (Gutierrez et

al., 2007; Zinsmeister et al., 2016). *LEA* genes are highly expressed during seed maturation and are responsible for the production of proteins actively involved in the establishment of desiccation tolerance, acting as osmoprotectants or chaperones (Delseny et al., 2001). At the end of seed maturation, primary dormancy is established. In this context, one of the most investigated proteins associated to ABA activity is DOG1. DELAY OF GERMINATION1 (DOG1) is a heme-binding protein identified for the first time in seeds of *A. thaliana* and subsequently found in many other species, such as *Hordeum vulgare*, *T. aestivum*, *O. sativa*, *Z. mays*. Although DOG1 is involved in numerous phases of plant life, from seed maturation to germination, its essential role in inducing temperature-dependent primary dormancy is well documented. The expression of *DOG1* starts in the early stages of seed maturation, and its strongly regulated by external temperature to be markedly reduced in mature dry seeds. The activation of *DOG1* gene is related to the activity of bZIP-transcription factor 67 (bZIP67), which binds its promoter regions. Protein synthesis is accompanied by their self-dimerization to form a fully activated complex, which is able to bind PP2C ABA Hypersensitive Germination 1 (AHG1), enhancing ABA signaling and the establishment of primary dormancy. The essential role of bZIP67 in DOG1 synthesis suggests that this protein is not crucial for ABA activity, however, the improvement of ABA activity induced by DOG1 is essential for primary dormancy establishment (Carrillo-Barral et al., 2020; Matilla, 2020). When unfavorable germination conditions persist, a novel phase of dormancy (secondary dormancy) is induced, probably triggered by *de novo* ABA synthesis. Although primary and secondary dormancy are similar physiological events induced by the activation of the ABA-dependent pathways, the response to the environmental conditions is markedly different. These studies support the hypothesis of other regulatory pathways that are involved in enhancing ABA activity during secondary dormancy. For instance, DOG1 is actively involved in an environment-sensing pathway during primary dormancy establishment but its activity is not documented in secondary dormancy (Murphey et al., 2015). Although the nature of the sensory mechanisms remains undetermined, specific environmental factors can directly modify the metabolic status and favor secondary dormancy establishment. In the work of Hourston et al. (2022), low temperatures promote ABA biosynthesis and inhibit ABA degradation, leading to ABA accumulation. This event follows the accumulation of numerous oleosin and LEA proteins and the modification of chromatin structure through histone methylation and acetylation. An additional component in the mechanism of secondary dormancy establishment may be played by ABA-Insensitive 5 (ABI5), potentially involved in integrating stress signaling and phytohormone levels (Buijs, 2020). During seed germination, ABA levels decrease and ABA signaling is repressed. However, this trend does not imply that ABA signaling is not involved in germination. Although all the ABA-associated genes exhibit a reduced transcription, many of them operate in seed germination process. The transcription factor ABI5, for instance, plays a critical role in ABA signaling as a positive regulator, affecting the expression of *PYL11* and *PYL12* genes by binding to their promoters, which generates a PYL–ABI5–PYL feedback loop to maintain ABA signaling under a basal level during seed germination. At this stage, the binding of exogenous ABA with PYL receptors induces a further activation of the SnRK2s-

ABI5 pathway and the expression of ABA-associated genes and promotes the expression of *PYL* genes (Yang et al., 2023). Hence, ABI5 acts in different aspects and triggers both seed dormancy and germination. The key that explains the controversial role of ABI5 is represented by the different expression and function of *PYL* genes. Among the 12 *PYL* genes detected in seeds, the expression of *PYR1*, *PYL1*, *PYL2* or *PYL4* is associated with germination inhibition and stomatal closure, while the expression levels of *PYL7*, *PYL9*, *PYL11*, and *PYL12* decrease significantly during seed germination. The complexity and diversity of the expression patterns and biochemical properties of *PYL*s may probably explain the different roles of ABA signaling and its components (Zhao et al., 2020).

Together with ABA, GAs represent a central component in the plant life cycle. These hormones are essential for numerous developmental processes, including seed germination, stem elongation, leaf expansion, trichome development, pollen maturation, and the induction of flowering. Despite the number of GAs identified in plants, fungi, and bacteria exceeding 130, only a few have been demonstrated to possess biological activity. A considerable number of non-bioactive GAs are present in plants, serving as precursors for bioactive forms or as deactivated metabolites. The primary bioactive GAs include GA1, GA3, GA4, and GA7, with GA1 and GA4 representing the most prevalent bioactive GAs in plants (Kozaki and Aoyanagi, 2022). GAs are biosynthesized from geranylgeranyl diphosphate (GGDP), a common C20 precursor for diterpenoids. Two terpene synthases (TPSs) located in the plastids, *ent*-copalyl diphosphate synthase (CPS) and *ent*-Kaurene synthase (KS), are involved in the conversion of GGDP to the tetracyclic hydrocarbon intermediate *ent*-Kaurene. *Ent*-Kaurene is then converted to GA12 by two cytochrome P450 monooxygenases (P450s) and to GA9 through three oxidations catalyzed by soluble 2-oxoglutarate–dependent dioxygenases (2ODDs) GA 20-oxidase (GA20ox). A first bioactive gibberellin, GA4, is formed from GA9 by a second 2ODD, the GA 3-oxidase (GA3ox). Other bioactive forms of GAs are produced from GA12 and involve different enzymatic reactions (Yamaguchi, 2008). The network of interaction in which GAs are involved includes a large number of different components. Studies conducted in *A. thaliana* and *O. sativa* indicated as key molecules of the GAs pathway the GA receptor gibberellin insensitive dwarf (GID1 and 2), the DELLA transcription regulators (DELLAs), and the F-box proteins sleepy1 (SLY1) (Davière and Achard, 2013). In the GA signaling scheme, GAs are perceived by a plasma membrane receptor GID1, inducing the formation of a GA-GID1-DELLA complex. DELLAs are key intracellular proteins involved in repressing GA responses. The putative identification of distinct DELLAs proteins in numerous plant species reflects their importance in the GA pathway. Distinct DELLAs proteins are involved in different events, from seed germination to floral development (Locascio et al., 2013). When GAs are not linked to their receptors, DELLAs accumulate and repress seed germination, growth, and almost all known GA-dependent processes, interfering with the DNA-binding capacity of transcription factors or inhibiting the activity of transcriptional regulators. Moreover, DELLAs operate as transcription factors and directly activate the transcription of downstream genes (Hirsch and Oldroyd 2009). The formation of the GA-GID1-DELLA complex promotes DELLAs proteasome-

dependent degradation, inducing conformational changes in DELLAs proteins and favoring their binding with F-box proteins. F-box proteins are E3 ubiquitin-ligase complexes that catalyze the attachment of polyubiquitin chains to target proteins for their subsequent degradation by the 26S proteasome (Davière and Achard, 2013).

Although GAs are mainly involved in seed germination, where the dynamic balance between ABA and GAs is shifted toward GAs biosynthesis, some studies indicate their involvement also in maturation and dormancy stages. This evidence supports the results of many studies that observed how pea (*Pisum sativum*) GA-deficit mutants as well as overexpression of *GA2ox* caused seed abortion. A possible explanation is given by the potential activity of GAs on specific components involved in seed maturation, like leafy cotyledon 1 (LEC1), which can activate *ABI3* and *FUS3*, regulators of seed maturation and part of ABA signaling (Kozaki and Aoyanagi, 2022). GAs might cover a similar effect during seed dormancy, where an active biosynthesis of GA precursor GA9 and GA20 was found, as well as the production of active forms (GA1 and GA4). However, the ratio ABA:GA during seed dormancy is high. In fact, the biosynthesis of GAs is associated with a rapid degradation of these compounds, keeping the dynamic balance between ABA and GA shifted toward the first hormone. Furthermore, GAs are not reported to be actively involved in the seed dormancy molecular network, reflecting a marginal activity, compared to ABA, in seed dormancy establishment (Finch-Savage and Leubner-Metzger, 2006).

Favorable germination conditions, such as increased temperature and presence of light, induces *DOG1* gene repression and lead to a more efficient catabolism of ABA. The absence of downstream components of ABA-dependent signaling (ABI3, ABI4, and ABI5) promotes the biosynthesis of GAs, which in turn leads to the degradation of DELLAs protein. This series of molecular events markedly shifts the dynamic equilibrium between ABA and GA, favoring the second hormone (Zuo and Xu, 2020). While ABA is a key component in seed maturation and dormancy, GAs constitute the central component of the germination molecular network, which induces the synthesis of transcription factors that promote seed germination. Ogawa et al. (2003) investigated the identities of the GA-regulated genes and found a large number of genes upregulated and downregulated with a different time response to GAs. Most of the genes upregulated are positive regulators of ABA involved in different functions. Genes encoding for expansins, heat-shock proteins, hydrolases, and proteinases are included in the early-upregulated genes group. The presence of expansin genes suggests an activity of wall hydrolyses. Among the mid and late-upregulated genes group (6h and 12h after GA induction), cytochrome P450 monooxygenase genes are reported, reflecting an intense metabolism of GA intermediates to form bioactive GAs. Moreover, GA4 directly induces the production of the transcription factor AtMyb34/ATR1, which operates as a positive regulator of the *ASA1* gene. *ASA1* gene encodes for the α-subunit of anthranilate synthase, involved in the first committed step in tryptophan biosynthesis. Overall, this study indicates that the main effect of GA involves the downregulation of ABA-upregulated genes and endosperm weakening (Ogawa et al., 2003). The more recent study of Tuan et al. (2019) supports these results, suggesting that GAs have two main roles in

controlling germination. The first one is to enhance the weakening of the endosperm by inducing the expression of genes involved in cell wall hydrolyses, such as β-mannanase, expansin, β-1,3-glucanase, and chitinase, while the second role is to stimulate the growth potential of the embryo.

Although the dynamic equilibrium between ABA and GAs is the main factor in seed maturation, dormancy establishment, and germination, other hormones operate as well either influencing the ABA:GAs ratio or directly regulating the expression of specific genes. **Fig. 1.6** illustrates the main hormones that support ABA and GAs activity and regulate seed dormancy and germination. Auxin is involved in both seed dormancy and germination through cooperative work with ABA. Many biochemical and genetic analyses showed that auxin is required to activate ABI3, inducing the release of auxin response factors 10 and 16 (ARF10 and ARF16) from AXR2/3 (Liu et al., 2013). ARF10 and ARF16 also promote germination activating the transcriptional function of ABI5 and interacting with jasmonate zim-domain (JAZ), repressors of jasmonic acid (JA) signaling (Mei et al., 2023).

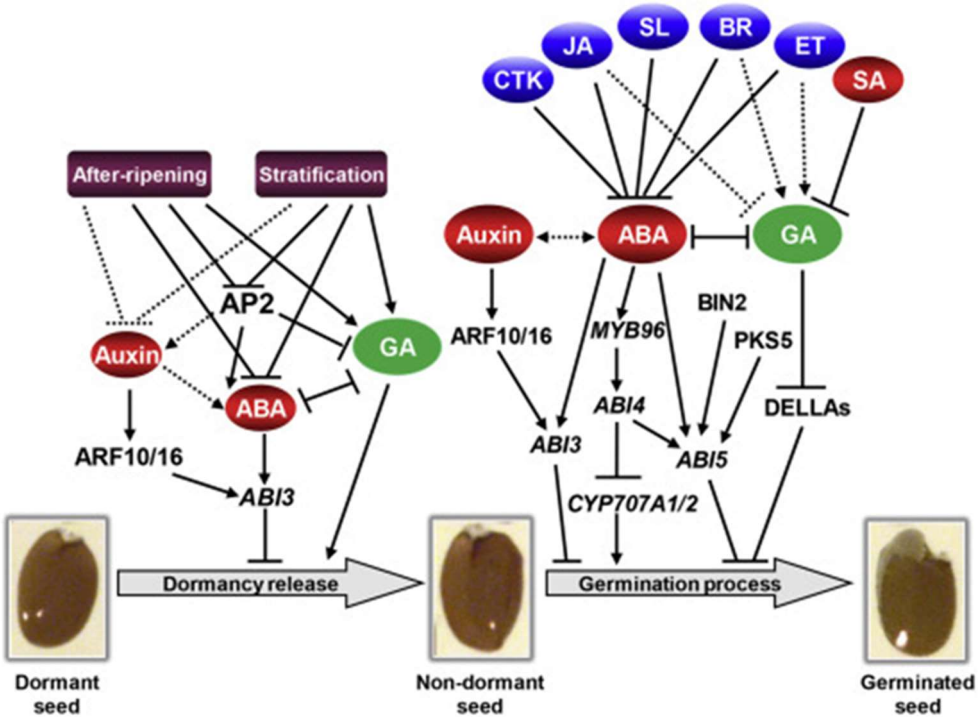

Figure 1.6. Network of main phytohormones (ABA, GA, auxinx) interaction involved in the control of seed dormancy and germination (Shu et al., 2016).

Jasmonates are a class of lipid-derived hormones able to interact both with GA and ABA to modulate seed germination. These molecules are recognized by the receptor coronatine-insensitive protein (COI1) and the jasmonate domain (JAZ) transcriptional repressor, which results in the degradation of JAZ proteins and the release of transcription factors, including MYC2/3/4, which are included in ABA and

GA signaling pathways. MYC2 can interact with the regulatory component of ABA receptor (PYL6), support the release of ABI5, and ABI3, enhancing ABA signaling to inhibit or delay germination. The preservation of ABA signaling mediated by JA is also active during seed germination. The degradation of DELLA protein RGL2 induced by GA stimulates JAs production, which releases ABI5 and supports ABA biosynthesis (Stamm et al., 2012; Pan et al; 2023). BRs are a class of plant steroids widely distributed in the plant kingdom and active at small concentrations. Although the crosstalk between BRs and ABA is unknown, some studies suggest a role of BRs in promoting seed germination by interacting with the activity of ABA (Xue et al., 2009). Similarly, cytokinins (CTKs) promote seed germination by antagonizing ABA and inducing ABI5 degradation. Moreover, CTKs induce the expression of Arabidopsis Response Regulators (*ARRs*) genes that are involved in attenuating the ABA-mediated inhibition of germination (Smolikova et al., 2021). Ethylene also counteracts the effect of ABA, promoting seed dormancy breaking. A role of ethylene in reducing ABA biogenesis through the binding with the ETR1 and ETR2 (ethylene response 1 and 2) receptors has been reported, while the potential crosstalk with GAs is so far unknown (Shu et al., 2016).

Overall, the process of seed germination can be divided into three phases (**Fig. 1.7**). Phase I is characterized by a rapid uptake of water, essential for activating the metabolic processing promoting germination. Phase II follows the initial step of imbibition and constitutes the point at which most of the metabolic reactions triggered by water uptake occur. While phases I and II are indicative for the so-called pre-germinative metabolism, phase III is representative for the post-germination stage (Macovei et al., 2017; Smolikova et al., 2021).

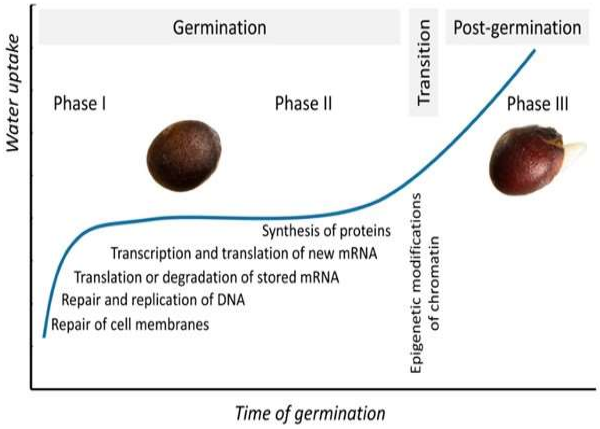

Figure 1.7. Main phases of seed germination (Smolikova et al., 2021).

1.2.1 Pre-germinative metabolism and seed priming

As largely stated, seed germination is a complex process intrinsically related to seed maturation and dormancy. The transition to different stages is determined by a complex molecular network of several factors, which respond to changes in environmental conditions. When optimal growth conditions occur, seed dormancy is broken, and the germination process starts. One of the key events that determine the transition between dormancy and germination is water uptake. This is required for the reactivation of metabolic reactions, which ensures an appropriate germination. The fact that water imbibition represents the initial stage of metabolic reawakening is supported by analyses of seed respiration (estimated through the CO_2 efflux), which indicate an increased release of carbon dioxide (Marler, 2019). The set of metabolic events occurring during germination, known as pre-germinative metabolism, represents an influential aspect of seed viability. The activation of pre-germinative metabolism is strictly related to seed imbibition and appropriate water uptake and occurs during the second stage of germination. Overall, the main events related to pre-germinative metabolism include the production of energy, the reparation of DNA and cell membranes, and changes in the transcriptome, proteome, and metabolome profiles (Macovei et al. 2017).

Energy production is achieved through cell respiration, which requires the direct consumption of oxygen and the presence of intact and functional mitochondria. The generation of active mitochondria, known as mitochondrial biogenesis, represents one of the earliest events of seed germination. Mitochondrial biogenesis is a complex process currently described by two distinct models: the growth and division model and the maturation model. Following the growth and division model, novel mitochondria are generated through the binary fission of pre-existing mitochondria and generally occur during cell mitosis, while the mitochondrial mass increases during interphase. The second model is strictly associated with the concept of promitochondria, structurally and biochemically simple organelles that respond to specific signals, maturing into fully developed and metabolically active mitochondria. Many studies support that mitochondrial biogenesis occurring during seed germination follows the maturation model and it is induced by sequential and dynamic events of gene expression, protein turnover, and post-translational modifications (Logan et al., 2001). Specifically, the synthesis of proteins is an essential step for mitochondrial maturation. Among mitochondrial proteins, several enzymes involved in metabolism (aldehyde dehydrogenase, monodehydroascorbate reductase, glyceraldehyde-3-phosphate dehydrogenase), respiration (Rieske protein, cytochrome *c*, the alpha and beta subunits of ATP synthase), TCA and carbon metabolism (the alpha and beta subunits of pyruvate dehydrogenase E1, citrate synthase, malate dehydrogenase, phosphoenolpyruvate carboxykinase), import/transport (Tom40, voltage-dependent anion channel (VDAC), adenine nucleotide translocator), stress response (manganese superoxide dismutase) and development (late embryogenesis abundant protein), as well as chaperones and proteins of the proteolytic system (Hsp60, Hsp70, mitochondrial processing peptidase), exhibit high abundance in seed mitochondria. Another key event involved in mitochondrial maturation is represented by the post-translational modifications

(PTMs) of proteins, which affect protein localization, stability, and activity. Carbonylation, phosphorylation, and *S*-nitrosylation have been identified in numerous mitochondrial proteins during seed germination (Czarna et al., 2016). Cytochrome *c* (CYTc) is an important component involved in mitochondrial biogenesis and energy production. The work of Racca et al. (2022) indicates that *CYTC* genes are actively expressed during the early stages of germination and the overproduction of the CYTc protein is positively associated with the increased production of ATPs occurring during seed imbibition. These results indicate that *CYTC* gene expression is a part of pre-germinative metabolism that influences mitochondrial biogenesis and cell respiration activation during seed germination.

The dynamic balance between protein synthesis and hydrolysis is an important event in the pre-germinative metabolism. Many genes involved in redox and metabolic processes are actively transcribed in messenger RNAs (mRNAs) during early seed imbibition and translocate into polysomes for the synthesis of novel proteins. The active recruitment of polysomes is probably one of the main strategies for optimizing the synthesis of proteins and is proved by an over-accumulation of ribosomal subunits that support mRNA translation during seed germination (Pagano et al., 2023). The intense turnover of proteins during seed germination is also supported by a recent study on protein accumulation in carrot seeds during imbibition. In this context, ribosomal and proteasome-related proteins exhibited the highest abundance levels, as well as proteins involved in photosynthesis (photosystem II and photosystem I proteins, ATP synthase subunit, cytochrome and ferredoxin-NADP reductase proteins) and in carbohydrate metabolism (isocitrate lyase, malate synthase, succinate dehydrogenase, malic enzyme, sucrose synthase, 6-phosphofructokinase, fructose-bisphosphate aldolase, glucose 6-phosphate dehydrogenase) (Zhao et al., 2022).

DNA repair is an essential process occurring during pre-germinative metabolism. The germination process coincides with an increase in cell cycle activity, including cell division and DNA replication. The potential accumulation of DNA lesions during this stage has dramatic consequences in seed quality, since the elevated rate of mutagenesis negatively affect radicle protrusion, seedling growth and development (Waterworth et al., 2022). Genome integrity is preserved through the coordinated action of different DNA repair pathways, such as nucleotide and base excision repair (NER, BER), homologous recombination (HR), and non-homologous end joining (NHEJ) which play a critical role in preserving genome stability (**Fig. 1.8**) (Balestrazzi et al., 2011; Ventura et al., 2012; Waterworth et al., 2019). Among these, BER is highly active during seed germination (Pagano et al., 2019) and is involved in the removal of oxidative base damage, alkylation, deamination, and abasic sites (apurinic and/or apyrimidinic, AP). BER includes DNA glycosylases, enzymes able to catalyze the hydrolysis of the N-glycosidic bond of the damaged deoxynucleoside, causing the excision of the damaged bases. Single nucleotide (Short-Patch repair, SP, carried out by the DNA polymerase *b*) or several nucleotides (Long-Patch repair, LP, performed by replicative DNA polymerases *d* or *ε*) are afterward inserted to fill the gap, while the ends are rejoined by DNA Ligase III (SP-BER) and DNA Ligase I (LP-BER) (Ventura et al., 2012; Waterworth et al., 2019). Many genes involved in BER, such as the 8-oxoguanine DNA glycosylase/ lyase (*OGG1*) and the

formamidopyrimidine-DNA glycosylase (*FPG*) are up-regulated during seed imbibition (Balestrazzi et al., 2011), alongside tyrosyl-DNA phosphodiesterase (*TDP1*), which encodes for an enzyme responsible for the repair of topo I-mediated damage (Macovei et al., 2010; Forti et al., 2020).

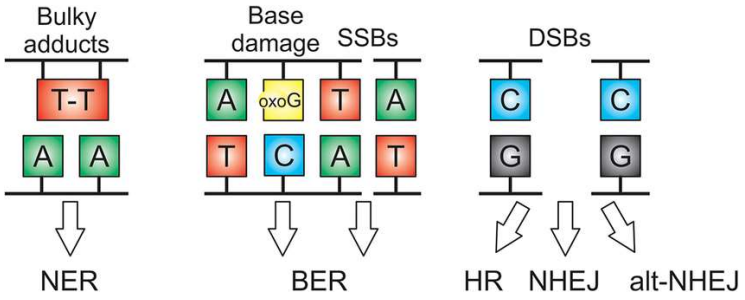

Figure 1.8. Overview of DNA repair pathways in seeds. NER, nucleotide excision repair; BER, base excision repair; HB, homologous recombination; NHEJ, non-homologous end joining; alt-NHEJ, alternative NHEJ; Oxo G, 8-oxo guanine (Waterworth et al., 2019).

The NER pathway operates by removing the cyclobutane pyrimidine dimers (CPDs), phosphor-products and other bulky lesions that cause helix distortions. Recognition of lesion, incision of the damaged DNA strand on each side of the lesion, and release of the oligonucleotide that harbors the lesion, are the processing step of NER. This system is composed of two sub-pathways: the transcription coupled-nucleotide excision repair (TC-NER), which removes damage from the transcribed strands of active genes, and the global genome-nucleotide excision repair (GG-NER), responsible for repairing lesions throughout the whole genome. While TC-NER remove different lesions at a similar rate, GG-NER efficiency is related to the type of lesion. Although both TC-NER and GG-NER require the activity of the transcription elongation factor-IIH (TFIIH) to unwind the DNA helix around the damaged site, the recognition mechanism of the lesion among the sub-pathways is different. TC-NER is activated by the stalling of RNA polymerase II (RNAPII) during transcription, while in GG-NER the lesion is detected by a molecular complex that includes the UV-Damaged DNA-Binding protein complex (UV-DDB), the Xeroderma Pigmentosum group C and the centrin proteins (Balestrazzi et al., 2011). HR and NHEJ are involved in repairing the double-strand breaks, highly cytotoxic DNA lesions which occur spontaneously in the cell, especially during DNA replication and under oxidative stress. A central player in HR is the strand-exchange protein Rad51, which promotes the formation of a physical connection between the invading DNA substrate and homologous duplex DNA, leading to the formation of heteroduplex DNA. The activation of Rad 51 is related to the interaction with Replication Protein A complex (RPA). Although HR system is also characterized by alternative pathways (single-strand annealing, SSA), the recruitment and the activation of Rad51 is always required (Waterworth et al., 2019). In comparison to HR, which involves a homologous sequence to guide repair, NHEJ directly ligates two ends without the need for a homologous sequence. NHEJ can be subdivided into two classes depending on the pathway used to repair the damage. The first one is Ku-dependent classical/canonical NHEJ (c-NHEJ) repair, which involves the activity of Ku, a

heterodimeric complex of 70 and 80 kDa subunits, that binds to broken DNA ends to prevent degradation and facilitate alignment for the subsequent ligation step mediated by DNA Ligase IV. An alternative NHEJ pathway (Alt-NHEJ) operates through the DNA polymerase θ (PolQ) when the recruitment of Ku proteins is not required (Raina et al., 2021).

The pre-sowing treatment triggering pre-germinative metabolism is the main principle behind seed priming, a technique that allows controlled seed rehydration to elicit the metabolic processes normally activated during the early phase of germination but preventing the seed transition towards full germination. Priming is a well-known approach for enhancing seed quality, improving the germination performances in terms of percentage, speed, and synchrony, along the resistance to pathogens and abiotic stresses (Paparella et al., 2015; Pagano et al., 2023). Although a large number of studies documented the positive effect of seed priming in different species, such as *Allium cepa* (Selvarani and Umarani, 2011), *G. max* (Lewandowska et al., 2020; Griffo et al., 2023) along many other legume species (Rastin et al., 2013; Maurya et al., 2020), *O. sativa* (Farooq et al., 2007), and *T. aestivum* (Harris et al., 2008), the efficacy of the treatment is strongly influenced by plant species/genotype and physiology, seed lot and vigor, as well as to the priming method applied (Pagano et al., 2023). As shown in **Fig. 1.9**, seed priming includes various techniques dedicated to improving germination performance, seedling growth, and crop yield.

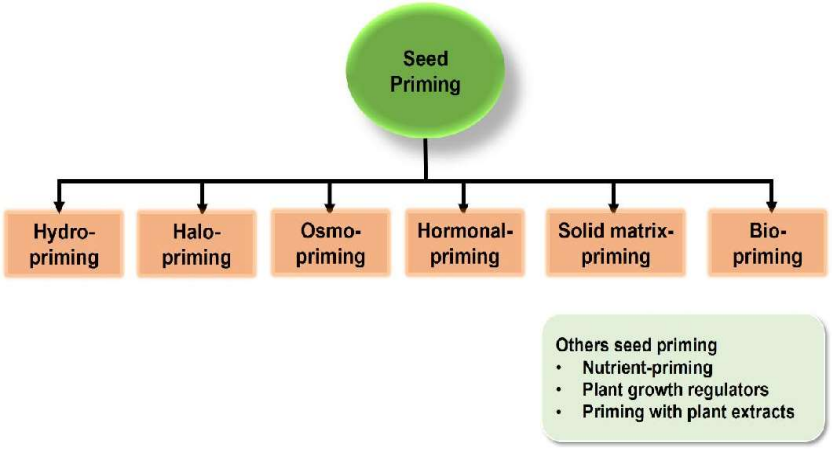

Figure 1.9. Schematic representation of seed priming techniques (Rhaman et al., 2020).

Hydropriming consists of soaking the seeds in water before sowing and may or may not be followed by air-drying of the seeds. Controlled water imbibition is a crucial passage to ensure optimal activation of seed metabolism, thus seed soaking must be monitored to avoid disproportionate water uptake and seed damage (Nawaz et al., 2013). One of the primary benefits associated with the hydropriming technique is the utilization of only water, which makes this approach simple and inexpensive (Jisha et al., 2013). Hydropriming was successfully utilized to improve the germination performances of many crop species (Damalas et al., 2019; Kaburu et al., 2024). Instead, solid-matrix priming (SMP) is a technique in which seeds are mixed with a

solid material and water in known proportions. This mixture allows the seeds to imbibe and attain a threshold moisture content preventing radicle emergence (Wu et al., 2019). SMP has been successfully used to improve the quality of different species (Ermiş et al., 2016; Sen and Mandal, 2016). Differently, halopriming relies on soaking the seeds in inorganic salt solutions, i.e., NaCl, $CaCl_2$, KNO_3, etc. Similarly to drought stress, the inorganic salt solution lowers the seed water potential, promoting the activation of mechanisms that act on plant stress memory to make plants respond quickly to imminent abiotic stress. As a consequence, this treatment can promote tolerance to other upcoming stresses and exhibits positive effects in enhancing plant tolerance to adverse environmental conditions (Kumar et al., 2016; El-Sanatawy et al., 2021). In the case of osmopriming, seeds are soaked in osmotic solutions, still with decreased water potential, to control the water absorption rate and ensure the activation of membrane repairing systems and metabolic processes (Bray, 2017). Although different osmopriming agents can be utilized, such as $CaCl_2$, KNO_3, KCl, K_3PO_4, NaCl, and mannitol, polyethylene glycol (PEG) is one of the most suitable and utilized agents for osmopriming, as it is chemically inert and does not induce damage to seed embryos. Moreover, PEG is non-damaging to proteins and does not penetrate seed tissues due to its large molecular size (Lei et al., 2021). Alternatively, the treatment using hormone solutions is referred to as hormo-priming and is based on the utilization of plant growth regulators during seed imbibition. Regulators such as ABA, GAs salicylic acid, ascorbic acid, cytokinins, auxins, kinetin, ethylene, and polyamines are commonly used since they are well-known molecules involved in controlling seed germination (Rhaman et al., 2020). On the other hand, biopriming integrates biological (inoculation of seed with beneficial organisms to protect seed) and physiological aspects (seed hydration) for enhancing seed quality. It represents an ecological approach that uses selected microorganisms that limit the toxic effect of soil- and seed-borne pathogens (Reddy and Reddy, 2013). One of the main advantages related to microbes inoculation in biopriming is that their utilization promotes nutrient acquisition via nitrogen fixation and solubilization of insoluble minerals, organic acids, antimicrobial metabolites, lytic enzymes, growth regulators, and stress-responsive/induced phytohormones, alleviating abiotic stress such as drought, high soil salinity, and extreme temperatures (Chakraborti et al., 2022). Apart from the priming techniques mentioned so far, novel priming approaches (e.g., nano-priming, green-priming, use of physical agents like temperature, electric fields, microwaves, atmospheric plasma) have been developed and optimized to enhance the germination performances of seeds. There are many pieces of evidence suggesting that exposing seeds to a modest high-temperature stress (HTS) stimulus can improve the resistance to the same or different stress factors. This is the principle behind the thermo-priming approach, which has been applied to different species to improve seed quality and stress tolerance (Wang et al., 2014).

At a molecular level, the response to priming-induced stress rapidly triggers the appropriate physiological, biochemical, and molecular adjustments, through the activity of second messengers like calcium ions (Ca^{2+}) and reactive oxygen species (ROS). This leads to a rapid adaptation in the genetic machinery, achieved through a network of transcription factors (TFs) and microRNAs (miRNAs) (Khan et al., 2022).

ROS constitutes a group of molecules at the center of seed physiology. A crucial event of pre-germinative metabolism is indeed the production of ROS triggered with the start of water uptake. ROS are key components of different signal transduction pathways in seeds and many studies suggest that seed germination can be achieved only when the ROS content is maintained under a critical threshold, called "oxidative window for germination", in which the ROS-mediated signaling mechanisms can be induced (Bailly et al., 2008; Ventura et al., 2012). However, the impact of ROS in seed physiology is not limited to their activity on seed germination but they also operate in different stages of the plant life cycle.

1.2.2 Reactive oxygen species (ROS): an overview and roles in germination

ROS are intracellular chemical species that contain oxygen (O_2) and exhibit reactivity towards lipids, proteins, and DNA. The category of ROS includes the superoxide anion ($O_2^{\bullet-}$), hydrogen peroxide (H_2O_2), and hydroxyl radicals (OH•). ROS are more chemically reactive than O_2 and can trigger a variety of biological events. As shown in **Fig. 1.10**, different biochemical processes are responsible for ROS production in plant cells. One of the main sources of ROS is linked to cell respiration in mitochondria. The three sites mainly involved in ROS production are complex I, II, and III within the mitochondrial respiratory chain, which is located in the inner mitochondrial membrane. These complexes generate $O_2^{\bullet-}$ by the one-electron reduction of molecular O_2 and release it into the mitochondrial matrix. Complex III can also release $O_2^{\bullet-}$ into the intermembrane space (Glasauer and Chandel, 2013).

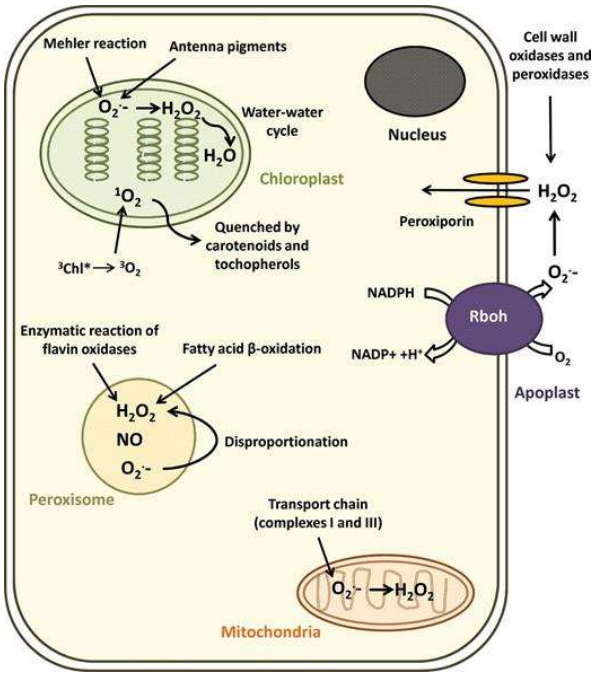

Figure 1.10. Major sites of ROS production in plant cells (Bose et al., 2014).

1. General Introduction

Peroxisomes are subcellular organelles with a single membrane involved in the production of H_2O_2 and $O_2^{\cdot-}$ in plant cells. According to different studies, peroxisomes represent the main source of intracellular H_2O_2, which results from different biochemical processes, such as the photorespiratory glycolate oxidase (GOX) reaction, the main enzyme of fatty acid β-oxidation, acyl-CoA oxidase, the enzymatic reaction of flavin oxidases and the spontaneous or enzymatic dismutation of $O_2^{\cdot-}$ radicals. Together with mitochondria and chloroplasts, peroxisomes produce $O_2^{\cdot-}$ occurring in two different sites. The first site of $O_2^{\cdot-}$ production is the organelle matrix, in which the generating system is xanthine oxidase (XOD), an enzyme that catalyzes the oxidation of xanthine and hypoxanthine to uric acid. The other side of $O_2^{\cdot-}$ production is the peroxisomal membrane, where a small electron transport chain appears to be involved. This is composed of the flavoprotein NADH: ferricyanide reductase of about 32 kDa and a cytochrome b protein and utilizes NADH and NADPH as the electron donor for $O_2^{\cdot-}$ production (Bose et al., 2014; Del Río and López-Huertas, 2016). Chloroplasts produce ROS through both photosystems. In photosystem II (PSII), the excess energy produced leads to the formation of the triplet state of light-excited chlorophyll (3Chl), which transfers the absorbed energy to ground-state oxygen (O_2), facilitating the production of highly reactive singlet oxygen ($^1O_2$). PSII is also involved in the production of $O_2^{\cdot-}$, H_2O_2, and OH•. Electron leakage on the PSII electron acceptor side produces $O_2^{\cdot-}$, which leads to the dismutation and to the generation of H_2O_2, which is further converted to OH• by non-heme iron. H_2O_2 can also be produced by an alternative pathway that starts with incomplete water oxidation. In PSI, the stepwise production of $O_2^{\cdot-}$ and H_2O_2 is dependent on ineffective photochemical and non-photochemical quenching (NPQ), in which PSII-derived electrons are transferred to O_2 through PSI-associated electron transport components (Li and Kim, 2022). ROS are also produced by NOX proteins, which are primarily localized to the plasma membrane, in the endoplasmic reticulum and mitochondria membranes. The catalytic subunit of FOX proteins utilizes electrons donated by NADPH to generate $O_2^{\cdot-}$ through the one-electron reduction of O_2 (Glasauer and Chandel, 2013).

ROS intrinsic chemical properties direct their reactivity toward specific biological targets. One of the main targets of ROS is represented by proteins, which can be damaged and/or inhibited by ROS-induced direct oxidation of amino acids. Different interactions between amino acids and ROS have been elucidated. ROS can oxidate arginine (Arg), lysine (Lys), proline (Pro), and threonine (Thr) residues, which generate carbonyl groups in the side chains, inhibiting or altering their activities. Sulfur-containing amino acids, and thiol groups specifically, are very susceptible sites to ROS oxidation. Activated oxygen can abstract an H atom from cysteine residues to form a thiyl radical (RS·) that reacts with a second thiyl radical to form disulfide bridges. Membrane phospholipids are continually subjected to oxidation induced by ROS, a phenomenon known as lipid peroxidation. The process of lipid peroxidation in a membrane includes a set of chain reactions that are triggered by the abstraction of a hydrogen atom (from a C – H bond), in an unsaturated fatty acyl chain of a polyunsaturated fatty acid (PUFA) residue induced by ROS. The lipid radical (L•) can bind an oxygen molecule to form a lipid peroxyl radical (LOO•), which in turn can

further propagate the peroxidation chain reaction by abstracting a hydrogen atom from adjacent PUFA side chains. The resulting lipid hydroperoxide (LOOH) can easily decompose into several reactive species, including lipid alkoxyl radicals (LO•), aldehydes alkanes, lipid epoxides, and alcohols. The main consequence of lipid peroxidation is the loss of membrane fluidity, which can lead to damage to membrane proteins, and the inactivation of receptors, enzymes, and ion channels (Garg and Manchanda, 2009). Another important ROS target is the DNA, which reflects cell integrity. Although all four DNA bases can be oxidated by ROS, the pyrimidines (cytosine and, especially, thymine) appear to be most susceptible. Base oxidations can lead to ring saturation, ring opening, ring contraction, and hydroxylation reactions, which result in the formation of local distortions in the double helix. Moreover, the degradation of bases triggered by ROS induces the formation of several toxic products, such as 8-hydroxyguanine, 8-oxoguanine, hydroxymethyl urea, urea, thymine glycol, and thymine. The phosphodiester backbone can also be oxidated by ROS. The resulting damage to the sugar and phosphate sites leads to strand breaks and requires the activation of DNA repair mechanisms to restore DNA integrity and maintain cell vitality. A further consequence of ROS-induced oxidation of DNA is the cross-linking of DNA to proteins, which can block DNA transcription (Garg and Manchanda, 2009; Storr et al., 2013).

Despite their attitude toward biological targets, only high levels of ROS are associated with toxic effect. Aside the detrimental effects induced by over-production, ROS are key signaling molecules involved in many biological events in plant cells, such as control and regulation of cell growth, programmed cell death (PCD), hormone signaling, plant responses to biotic and abiotic stress, and the development of tissues. This duality depicts a scenario in which ROS play different and opposite roles: as signaling molecules regulating many processes in plants under normal and adverse conditions, and as toxic by-products involved in oxidative stress and cell damage (Dat et al., 2000; Mittler et al., 2011). As signaling molecules, ROS operate in a complex network of biochemical pathways to control several molecular processes of seed maturation, dormancy, and germination (Martin et al., 2022). Low levels of ROS have been associated with control of maturation and dormancy stages, while the increase of radicals accumulation is an important factor promoting the dormancy breaking and the start of germination. The main hypothesis suggests that ROS production, accumulation, and scavenging are included in the complex pathways of ABA and GAs networks (Wojtyla et al., 2016) (**Fig. 1.11**). GAs, as germination-promoting hormones, stimulate the production of OH•, involved in promoting radicle protrusion. GAs are also associated with H_2O_2 production, which is the most stable radicle form associated with different signaling events. ABA, which operates by maintaining seed dormancy and inhibiting germination, is involved in the inhibition of the Fenton reaction, a process in which H_2O_2 oxidizes iron (II) to form iron (III) and releases OH•. Additionally, ABA also suppresses H_2O_2 production (Jhanji et al., 2024). According to previous evidence, H_2O_2 promotes ABA degradation in several manners. The main mechanism of H_2O_2-dependent ABA degradation includes the activation of ABA-8-hydroxylase, an ABA catalytic enzyme (Mizutani and Todoroki, 2006), but a direct oxidation of ABA by H_2O_2 can also occur.

ROS are involved in the biosynthesis of hormones as well. H_2O_2 promotes GAs synthesis through the activation of mitogen-activated protein kinase (MAPK) cascades, supporting the evidence that ROS have a positive impact on facilitating dormancy release and promoting seed germination, inducing both GA synthesis and ABA degradation (Jhanji et al., 2024). ROS also act as secondary messengers in other plant hormonal signaling. Auxin and ROS signaling are closely related to each other and are merged into a hormonal network that regulates seed germination and various growth and developmental processes. An increase in H_2O_2 synthesis after exogenous auxin application indicates that ROS can have effects on auxin biosynthesis. H_2O_2 and other ROS can also affect auxin transport, metabolism, and signaling (Krishnamurthy and Rathinasabapathi, 2013). ROS influence the activity of ethylene, acting as secondary messengers for HCN (hydrogen cyanide) to activate several transcription factors involved in ethylene signaling pathway to release seed dormancy and promote germination. Moreover, H_2O_2 can stimulate ethylene biosynthesis (Ishibashi et al., 2013).

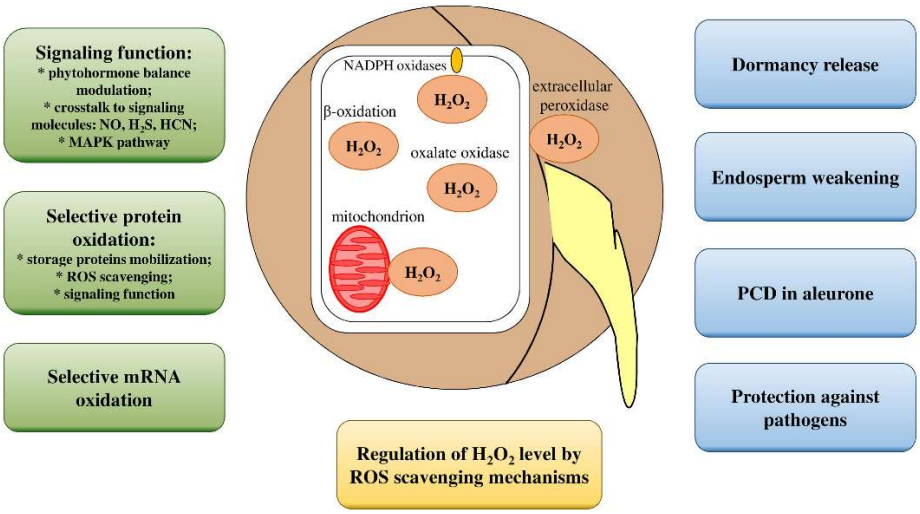

Figure 1.11. Representation of H_2O_2 functions in relation to seed germination. H_2O_2 levels are controlled by antioxidant mechanisms. Signaling functions and crosstalk with other molecules and phytohormones, along with the selective oxidation of proteins and mRNA, play key roles in regulating germination. H_2O_2 directly interrupts dormancy, weakens the endosperm, induces programmed cell death (PCD) in aleurone cells, and can have antimicrobial properties (Wojtyla et al., 2016).

Given the fact that the activity of ROS is strictly associated with their intracellular levels, a complex system of ROS scavenging operates to balance the processes involved in radical production and maintain specific concentrations. ROS-decomposing enzymes represent an essential part of the ROS scavenging system since they promote plant survival under stress conditions, when ROS overproduction occurs. The first group of enzymes involved in the antioxidant defense is constituted by the superoxide dismutases (SODs), which decompose $O_2^{\cdot -}$ to H_2O_2. In plant cells, the principal SODs are FeSOD and MnSOD, characterized by different cofactors

present at their active site. Individual SOD isozymes are compartmentalized into mitochondria, peroxisomes, cytosol, chloroplast stroma, thylakoids, and nucleus (Alscher et al., 2002). Catalases (CATs) are responsible for the detoxification of the overproduced H_2O_2, catalyzing the decomposition of H_2O_2 to H_2O and O_2. Several CAT isozymes have been found in numerous plant species and are mainly localized in photosynthetic, vascular, and reproductive tissues (Sharma and Ahmad, 2014). The presence of multiple CAT isozymes indicates that these exhibit functional versatility. Indeed, CAT isoforms are indispensable for the plant response to stress, including drought and salt, where CAT1 and CAT3 are involved, or heat and heavy metals, where CAT2 is required (Dvořák et al., 2021). Ascorbate peroxidases (APXs) are an important group of heme-containing peroxidases involved in detoxifying H_2O_2 through the electron transfer from ascorbate to form monodehydroascorbate (MDHA) and H_2O. Different APX isozymes have been found in plants and are encoded by a multi-gene family. These isozymes have also different localization and exhibit different kinetic properties like catalytic rate, optimal pH, stability, and molecular weight (Wu and Wang, 2019). Glutathione peroxidases (GPXs) are a family of isozymes that catalyze the conversion of H_2O_2,, hydroperoxides, and lipid hydroperoxides, in water by using glutathione. Four different groups of GPXs have been characterized, encoded by a small family of genes having different localization in plant cells, from cytosol to chloroplast stroma (Ozyigit et al., 2016).

These enzymatic antioxidant defenses respond directly to ROS accumulation in plant cells, triggering a series of signaling reactions to influence the expression of the enzyme-encoding genes. For many radicals, the sensing process involves specific radical receptors capable of transducing signals from extracellularly produced ROS into intracellular signaling cascades. For instance, a group of receptor kinases specific to H_2O_2, the hydrogen-peroxide-induced Ca^{2+} increases 1 (HPCA1) are involved in sensing hydrogen peroxide (Dvořák et al., 2021). However, one of the most effective manners to trigger the expression of genes encoding for the ROS scavenging enzymes involves the activation of the mitogen-activated protein kinase (MAPK) signaling pathway. This system consists of MAPKKKs (MAP3Ks), MAPKKs (MAP2Ks), and MAPKs, which are consecutively phosphorylated, leading to the activation/inactivation of a wide range of target proteins, including TFs. ROS directly react and activate MAPKKKs and phragmoplast localized kinases (ANPs), through oxidation of cysteines or sulfenylation reactions, starting the phosphorylation cascade of the MAPK system (Son et al., 2011). ROS can also influence the expression of genes involved in the enzymatic antioxidant systems by modifying Ca^{2+} cytosolic concentrations. Ca^{2+} is an important secondary messenger functioning in intra- and extracellular signaling networks able to activate Ca^{2+} channels, ion pumps, plasma membrane- and organelle-membrane-embedded Ca^{2+} transporters, Ca^{2+}-binding proteins (calmodulin), and various Ca^{2+}-dependent protein kinases, in response to ROS production (Görlach et al., 2015).

In addition to the enzymatic system, the non-enzymatic antioxidant defense is mediated by low molecular weight metabolites such as α-tocopherol, carotenoids, and flavonoids. α-Tocopherol is one of the eight forms of “vitamin E″ and is universally distributed in the plant kingdom, being the major form accumulating in

photosynthetic tissues and, hence, in chloroplasts. It is part of a well-coordinated network necessary to protect the chloroplasts from damage induced by radicals. In particular, α-tocopherol cooperates with β-carotene in modulating the levels of $^1O_2$ and has a unique role in stopping the propagation of lipid peroxidation (Mesa and Munné-Bosch, 2023). Carotenoids are also involved in the antioxidant defense in plant cells through the inactivation of $^1O_2$ radicals. Moreover, they participate in the protection of the photosynthetic machinery from excessive light, since they can dissipate excess energy via xanthophyll-mediated non-photochemical quenching (NPQ) (Cazzonelli, 2011). Although the mechanisms underlying flavonoid-mediated ROS reduction in plants are still unclear, their presence in the chloroplast suggests a role as scavengers of singlet oxygen and stabilizers of the chloroplast's outer envelope membrane (Agati et al., 2012).

1.3 Seed storage and seed deterioration

One of the most intriguing aspects of seed physiology is the capacity to enter a quiescent state and maintain viability under different stress conditions for extended periods. This quiescent state is established during the desiccation process that occurs in the late seed maturation phase. This specific feature results in an optimization of seed longevity, defined as the total time span during which seeds remain viable (Sano et al., 2016). Seed longevity is an important factor that affects the reproductive success of higher plants. Elevated seed longevity allows optimal seed dispersal, avoiding competition for nutrients with other plant species and permits the start of germination under favoring conditions. This complex parameter is strongly dependent on the species and it is influenced by intrinsic and external factors. **Fig. 1.12** illustrates the most relevant factors that influence seed longevity (Zinsmeister et al., 2020), which are discussed below.

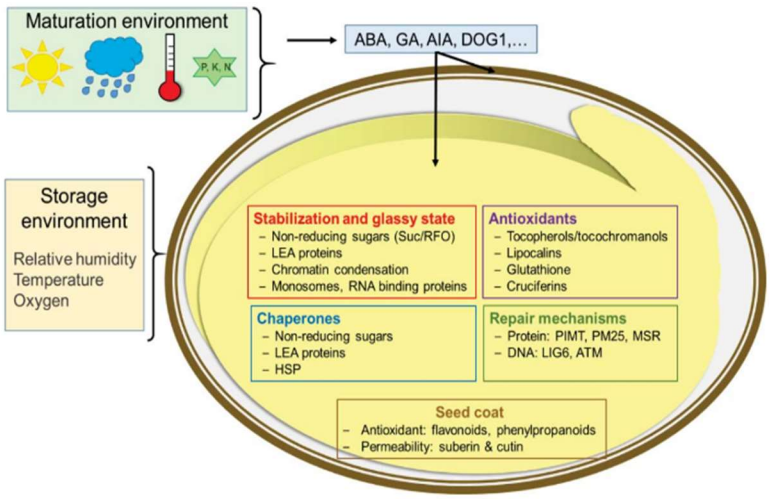

Figure 1.12. Graphical representation of features affecting seed longevity (Zinsmeister et al., 2020).

Intrinsic features are determined during the maturation phase, under the influence of maternal plant tissues. These include a range of molecules, such as lipophilic and water-soluble antioxidant compounds, stress proteins (HSP and LEA proteins), RNA binding proteins that conserve mRNA in the dry seeds, and non-reducing sugars (sucrose and oligosaccharides) that prevent protein denaturation, protect membranes, and participate to the formation of a glassy state. Among the intrinsic factors, there are the mechanisms that repair genome lesions and preserve genome integrity (Zinsmeister et al., 2020; Waterworth et al., 2024). The levels of these molecules are strictly regulated by several hormones involved in seed dormancy and maturation.

The LAFL transcriptional regulators (i.e., LEC1, ABI3, FUS3, and LEC2), belonging to ABA-dependent downstream signaling, are mainly involved in seed longevity acquisition. Downstream of ABI3, there are several genes involved in seed longevity, such as *HSFA9* (heat shock factor A9), belonging to transcription factors that regulate the expression of genes encoding for HSPs (heat shock proteins). In addition, ABI4 and ABI5 are regulators of seed longevity. ABI4 is hypothesized to coordinate the dismantling of chloroplasts during seed maturation and the subsequent attainment of seed longevity, acting in synergy with ABI5. ABI5 is strictly regulated by DOG1, operating during the first stages of the plant life cycle (maturation and dormancy). Since DOG1 participates in an environment-sensing pathway, it links the maturation environment to the intrinsic features involved in seed longevity acquisition (Pirredda et al., 2023).

External factors involved in seed longevity represent a key point for seed storage practices since they constitute the storage environment. These factors are related to the loss of seed quality during long-term storage, a process defined as seed aging. Maintaining seed quality during storage is essential for the propagation of food crops, as seeds are the first link in the food chain and the ultimate symbol of food security. In addition, preserving seed quality helps conserve biodiversity, which is essential to ensure food security under changing climatic conditions. Therefore, the purpose of seed storage is to maintain seeds in a viable state for a long time and to delay the aging processes in order to preserve genetic diversity and avoid wasting seed material (Bakhtavar and Afzal, 2020). The main external factors affecting seed viability during storage are the moisture content (MC), temperature, and the proportion of oxygen. Moisture content influences dry seed longevity during storage, by affecting the rate of viability loss. Elevated levels of MC have been associated with rapid seed deterioration in different species, like soybean (Ali et al., 2014), wheat (Malaker et al., 2008), rice (Genkawa et al., 2008), and onion (Tripathi and Lawande, 2014). One explanation for the effect of high MC on seed deterioration is that an increase in seed water content promotes the reactivation of metabolism. Specifically, the oxidative reactions, mainly due to mitochondrial activity, are largely responsible for aging in dry seeds, since they promote the production of ROS (Kibinza et al., 2006). As largely stated in the previous subchapter, high levels of ROS are associated with loss of membrane integrity, reduced energy metabolism, impairment of RNA and protein synthesis, and DNA degradation. Moreover, lipid peroxidation occurring during seed aging is directly related to ROS accumulation and has been demonstrated to be one of the processes mostly affecting seed aging in long-term stored seeds. Additionally,

an oxidative environment promotes Maillard reactions, responsible for the inactivation of proteins (Zhang et al., 2021). Similarly to elevated MC, a high storage temperature is associated with increased viability loss rates, since it increases the respiration rate and enzyme activity. Indeed, numerous studies documented that seeds stored at low-temperatures exhibit better germination performances than those stored at high-temperatures, regardless of the storage period (van Treuren et al., 2018; Gebeyehu, 2020). The detrimental effect of oxygen during storage has been documented to induce chromosome aberrations during cell division, promoting the accumulation of DNA lesions in seeds. Long-term storage under elevated concentrations of oxygen is indeed linked to loss of seed quality (Groot et al., 2012). Other factors can decrease seed longevity during storage, such as infestations caused by insects and pests. Biotic factors are indeed responsible for weight loss, loss of flavor, mold growth, and the production of toxins, which in turn determines the loss of seed quality (Santos et al., 2016; Berhe et al., 2023). A prolonged life span after drying is not an inner characteristic of all seeds. Optimal storage practices allow the preservation of the viability of orthodox seeds (or desiccation-tolerant seeds), which endure drying process and can be stored at freezing temperatures for long periods. Recalcitrant (or desiccation-sensitive) seeds, which are sensitive to drying, cannot be stored under conventional practices, thus limiting the long-term storage (Barbedo et al., 2013). In summary, depending on the internal characteristics that affect seed longevity, the storage environment can be adapted to optimize seed quality maintenance. Nevertheless, even the implementation of the most optimal storage conditions is unable to entirely prevent the deterioration of seeds.

As shown in **Fig. 1.13**, the typical trend of seed deterioration assumes the shape of a sigmoid curve. The internal and external features involved in seed longevity can alter the rates of seed quality loss and modify the typical pattern of seed deterioration, emphasizing or reducing the sigmoid shape. The curve of seed deterioration is characterized by an initial phase, called “asymptomatic phase”. During this stage, no apparent loss of seed viability can be observed; however, the following reduction in seed quality suggests that specific aging processes are occurring (Walters et al., 2010). One of the main events involved in seed deterioration is the accumulation of ROS during seed storage, which can be prompted by high temperatures and MC as well as elevated oxygen concentrations during storage.

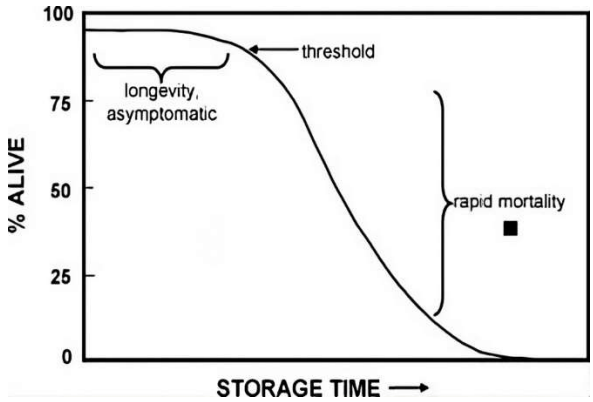

Figure 1.13. Schematic diagram of the typical trend of seed viability responses to storage time (Walters et al., 2010).

Membrane damage, a consequence of ROS-induced lipid peroxidation, is one of the main events associated with seed aging during long-term storage. This event can occur from the early stages of deterioration and alters the seed structural integrity, inducing oxidative damage. Another event is the depletion of the stored reserves, occurring during storage at relatively high humidity conditions. These are essential to provide the metabolic needs of the embryo until the seedling reaches autotrophy. Since aged seeds are metabolically active during storage, reserve molecules are directly consumed to produce energy, impairing the maintenance of cells, and tissues (Ebone et al., 2019). As largely stated, DNA and RNA are susceptible to ROS reactivity. Seed aging is indeed associated with chromosome aberration, changes in telomere length, DNA methylation, and abnormal gene expression (Waterworth et al., 2019). Specifically, the oxidation of guanidine represents a type of DNA lesion commonly found in aged seeds. Considering its single-stranded structure and the absence of repair systems, RNA is particularly vulnerable to oxidation and inevitably leads to a decrease in protein synthesis (López-Fernández et al., 2018; Ebone et al., 2019).

Despite the current knowledge of the processes ongoing during seed storage and the factors involved in seed deterioration, the explanation or the prediction of seed quality loss during storage is limited. One of the main reasons is that the structural modifications of seeds during storage affect the rates of oxidative and metabolic processes, thus they need to be considered to estimate seed viability loss rate. In recent years, different models have been developed for predicting the rates of seed quality loss. One of the first and most popular models for seed viability loss prediction during storage is the Robert-Ellis equation, which was developed on the assumption that there is no interaction between the storage temperature and seed moisture content that influences seed viability. Although this model had an important and positive impact on the research of seed longevity under storage, it is only applicable within a limited temperature range, and it is not suitable for predicting the longevity of seeds stored at -20°C. Moreover, the interaction between storage temperature and seed moisture is not regarded, but it affects seed viability (Tang et al., 2000; Zhou et al.,

2016). Despite these limitations, the Robert-Ellis equation represents the basis of novel models for seed longevity prediction during long-term storage. The Avrami equation, which describes the cooperative reactions based on visco-elastic properties, has been used to predict the pattern of seed aging through the formula $\ln(N_0/N) = (t/\Phi)^n$, where t is storage time and N_0/N is the reciprocal of percentage germination. The coefficients and n describe the shape of the sigmoidal curve, with the abruptness at which viability declines increasing as n increases above 1, and Φ is the time coefficient, which is dependent on the temperature of storage (Walters et al., 2005).

An additional factor that constrains the investigation of the seed deterioration process is the duration of the process itself. Seed deterioration is a gradual and prolonged process, during which a series of biochemical reactions are initiated at specific intervals. The approach that most contributed to the increase of knowledge regarding the molecular aspects of seed deterioration is the artificial aging test, which is based on the assumption that an adverse storage environment (in terms of moisture content and temperature) promotes the increase in the speed of seed quality loss without modifying the molecular pathway that acts during natural aging. Thus, this approach allows the production of the so-called artificially aged seeds, theoretically presenting the same characteristics as the naturally aged seeds (TeKrony, 2005).

1.3.1 Artificial seed aging

Artificial aging (AA) is a widely used approach to estimate the physiological quality of seed lots with similar emergence behavior. This method simulates stress conditions, promoting the triggering of the biochemical processes that cause seed deterioration. The principle of this test is to promote a fast seed deterioration by exposing them to high temperatures and relative air humidity, conditions that intensify the aging process. Seeds with high vigor will maintain viability or be little affected by stress conditions, while seeds with low vigor undergo a marked reduction of viability, making it possible to establish differences in the physiological potential of the lots (Fantazzini et al., 2018). One of the principal benefits of the AA test is the capacity to collect data regarding seed quality and storage potential in a relatively short period of time. This approach is one of the methods approved and standardized for seed quality estimation by the International Seed Testing Association (ISTA) to ensure its reproducibility across different species and varieties (TeKrony, 2005). As previously stated, the fundamental assertion of AA is the increase in seed deterioration rate through the induction of similar molecular and biochemical mechanism that occurs during natural aging. In addition to the estimation of seed quality, this approach has also been employed to elucidate the events that lead to deterioration. Although this test is commonly utilized to rapidly obtain aged seeds for a variety of analytical purposes, several studies have indicated that accelerated aging may result in the activation of physiological processes that do not occur during normal aging. Nevertheless, most studies on artificial aging conclude that the biochemical alterations occurring during accelerated aging are similar to those

observed in natural aging, with the primary distinction being the rate at which these changes occur (Freitas et al., 2006).

The protocol of accelerated aging differs based on tested species. ISTA has defined very specific protocols of AA tests for many species, including *Brassica* spp. and *Glycine max*. Following ISTA rules for AA tests, seeds are stored for a defined period in sealed containers at a high temperature and humidity up to 100% relative humidity (RH). In contrast to ISTA indications, other studies performed AA tests at lower RH and a range of cool to high temperatures (typically between 5 and 65°C), depending on how quickly viability is lost. Since the effect of AA parameters is dependent on the species tested, the Ellis-Roberts equation can be utilized to quantify the viability loss based on moisture content, temperature, the initial viability of the seed sample, and the 'inherent' longevity of the seeds of that species (Hay et al., 2019). However, the conventional AA procedure has several limitations when applied to species that produce relatively small seeds. One limiting factor is the non-uniform water absorption among seed samples, which can result in different levels of deterioration and, consequently, compromise the standardization of germination results after aging (Rodo and Marcos Filho, 2003). A well-known alternative consists of controlling RH to specific ranges by using saturated salt solutions, that is a mixture of distilled water and a chemically pure salt. This approach, defined as saturated salt accelerated aging (SSAA), allows to control the high RH and temperature to which seeds remain exposed during the AA test, thus resulting in a controlled deterioration that can be adapted to the species tested (Rodo and Marcos Filho, 2003; Bennett et al., 2004).

1.3.2 Volatile organic compounds (VOCs)

The pattern of seed deterioration is characterized by a first stage of stable viability (asymptomatic phase), which is rapidly accompanied by a second phase in which a rapid loss of quality occurs. This non-gradual transition between the two phases suggests the existence of a threshold that leads to permanent loss of seed quality. As a result, metabolic and oxidative processes involved in seed deterioration must be active during the asymptomatic phase, even if no reduction in seed quality is observed at this stage. Several chemical reactions occur under dry conditions and are responsible for seed deterioration, including fermentation, glycation (Maillard reaction), oxidation, and peroxidation, the latter triggered or promoted by ROS. A consistent group of products of these reactions is represented by small molecular weight carbonyl compounds that escape into the air as volatile molecules. Since these volatile organic compounds (VOCs) constitute the major byproduct of catabolic reactions and can be rapidly detected, their assessment can be used to estimate the chemical reactions occurring during the long-term storage of dry seeds (Mira et al., 2016). Several studies investigated the VOCs released from seeds of different species during natural or artificial seed ageing by using gas chromatography analyses. Overall, all these works revealed that ethanol, methanol, and acetaldehyde are the most abundantly released VOCs from seeds. Moreover, the levels of VOCs released

are dependent on the status of seed deterioration; more deteriorated seeds or seeds stored for longer time exhibit higher levels of released VOCs (Umarani et al., 2020; Zhang et al., 2022). However, the set of volatiles emitted is extensive and includes different aldehydes, alcohols, ketones, alkanes, alkenes, terpenes, and furans (Lee et al., 2000; Mira et al., 2010). From these works it emerges that several features can affect the final volatilome profile, including storage conditions (in terms of temperature and RH) and seed chemical composition. These factors can promote different chemical reactions or biochemical processes involved in seed deterioration, which in turn leads to the emission of specific VOCs. In this context, the work of Colville et al. (2012) provides insights into the principal processes occurring in dry seeds and the highly emitted VOCs for each process (**Fig. 1.14**). Lipid peroxidation, a process representative for seed deterioration, is initiated by ROS-induced oxidation of fatty acids or from lipoxygenases activity. The products of lipid peroxidation include aldehydes, alcohols (obtained from the conversion of aldehydes by alcohol dehydrogenases), and methyl ketones. Alcoholic fermentation can also occur during seed aging, favored by stress conditions, when pyruvate formed by glycolysis is converted to acetaldehyde by pyruvate decarboxylase. This may be converted to ethanol by alcohol dehydrogenase or it can be oxidized to acetic acid by aldehyde dehydrogenase. Acetone is produced during the decarboxylation of pyruvate, while methanol arises from the demethoxylation of pectin by methyl pectin esterases and can subsequently participate in the formation of methyl acetate through esterification with acetic acid. Degradation of carotenoids is an additive reaction occurring during seed aging responsible for the release of xylene. The aldehydes produced by lipid peroxidation can participate in Maillard reactions (M) with reducing sugars, to give rise to dicarbonyl compounds and promote the release of 2,3-butanedione (Colville et al., 2012).

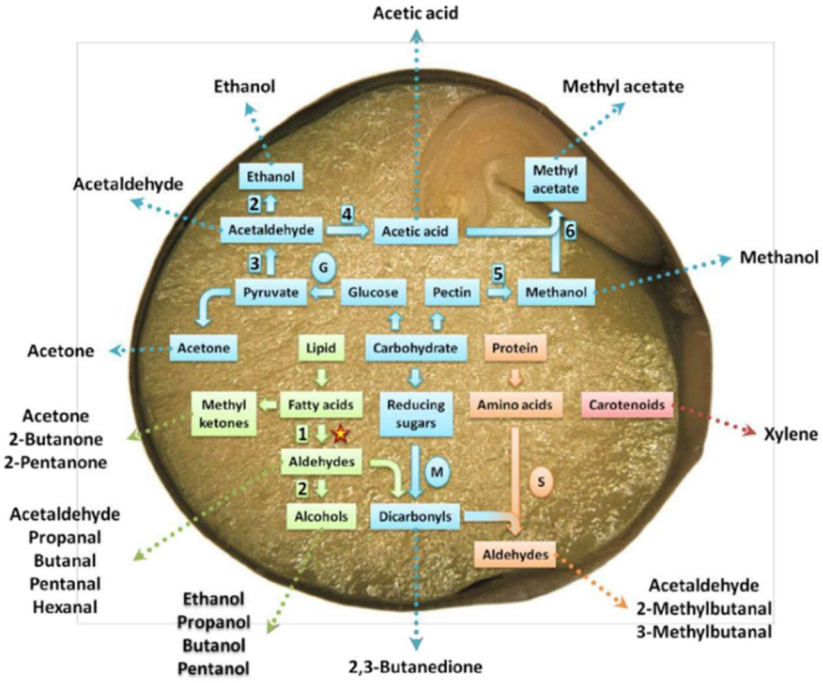

Figure 1.14. Schematic representation of biochemical reactions occurring in dry seeds during long-term storage illustrated through their respective VOCs emitted (Colville et al., 2012).

In genebanks, the use of sealed containers during long-term storage represents a factor that contributes to the preservation of seed quality. However, in this case VOCs released from aged seeds can operate from the storage environment to accelerate the rate of viability loss. Several studies have documented the deleterious effects of specific volatile compounds on seed quality. While the detrimental activity of commonly released VOCs, such as acetone, ethanol, methanol, and acetic acid has been observed in some species and ranges of RH and temperature, acetaldehyde has been proven to cause significant viability losses in multiple species and under a wide range of storage conditions (Zhang et al., 1994; Taylor et al., 1999; Chinnasay et al., 2022). Since VOCs constitute the byproduct of several metabolic reactions, their emission can be indicative of the activation of germination mechanisms, in which several processes are triggered. The analysis of VOCs in germinating seeds of *Cyclopia genistoides* and *Cyclopia subternata* revealed both similarities and differences in emitted volatiles, suggesting that common and different signaling pathways responsible for inducing volatiles during germination may exist. Although the germination process presents common mechanisms among seeds of different species, the variations in emitted VOCs indicate that the metabolic status in germinating seeds is influenced by other features, such as genetic variability and chemical composition (Motsa et al., 2017). In summary, VOCs are significant byproducts of catabolic reactions that occur in both dry and imbibed seeds. Since

their release from seeds is strongly related to the deterioration process, they can be utilized as biomarkers for rapid and reproducible assessment of seed quality. Considering that the asymptomatic phase of seed deterioration is immediately followed by a rapid loss of seed quality (Walters et al., 2010), the detection of VOCs during this stage may contribute to assessing the processing activated at this level and responsible for the subsequent reduction of seed viability.

1.4 Methods to measure seed quality

Overall, national and international seed systems ensure the production and distribution of high-quality seeds, following specific rules for seed sampling and testing. In this context, the existence of national and international organizations for seed testing favors the trade of high-quality seeds, promoting the preservation of seed security (McGuire and Sperling, 2016). The International Seed Testing Association (ISTA) is an international organization that provides international seed analysis certificates, produce rules for seed sampling and testing, promotes research toward the development of innovative methods for seed quality assessment and the spread of knowledge in seed science in technology (https://www.seedtest.org/en/home.html). North American countries follow the Association of Official Seed Analysts (AOSA) rules, which differ only in minor aspects from that of the ISTA (https://analyzeseeds.com/). A variety of methods are currently available and approved by ISTA for the assessment of seed quality, employed by seed industries and germplasm genebanks. These approaches allow the estimation of seed quality through the exploration of several features, such as physical structure and morphology, chemical composition, seed viability and vigor, and genetic purity. A common characteristic of all these methods is represented by the need to destruct or consume seed materials to collect information related to seed quality. Although these invasive approaches represent the most known and universally used approaches for seed quality estimation, part of the current research regarding seed science concerns the development of non-invasive methods, including the application of different technologies for the sensitive detection of the external and internal seed structure, seed viability, and chemical composition. Despite their effectiveness, the large-scale implementation is frequently constrained by several limitations, including high costs and specialized personnel. Consequently, no universal approach has yet been developed, with the selection of the method dependent on the context of the application. The present section explores the different approaches available for seed quality estimation, divided into invasive and non-invasive methods.

1.4.1 Invasive methods

The invasive approaches require the consumption of the analyzed seeds. These conventional approaches are currently approved and standardized by ISTA to ensure the reproducibility of the tests to a broad range of species. Below, a list of the main invasive approaches with their respective description is provided.

Germination test represents the universal quality standard test for seed quality assessment. The main scope of the test is to assess seed viability - defined as the maximum germination capacity, in terms of embryo protrusion and development to a seedling - under favorable germination conditions (Milošević et al., 2010). Different aspects are described by ISTA rules, such as the number of seeds and replicates, as well as the time of germination (Schmidt, 2007). A more complex analysis of the germination test results, achieved through the count of the germinating seeds during each day of the germination time, allows the estimation of seed vigor, a physical feature of seed quality that reflects the germination rate in function of the time required for the seedling emergence (Scott et al., 1984; Matthews et al., 2012). This analysis permits the calculation of indexes that reflect the percentage, speed, and synchronicity of germination. The work of Ranal and Santana describes many commonly used germination indexes:

- Percentage of germination $(G)\% = \left(\frac{number\ of\ germinated\ seeds)}{total\ number\ of\ seeds}\right) \times 100$
- Mean germination time $(MGT) = \frac{\sum_{i=1}^{k} ni\ x\ ti}{\sum_{i=1}^{k} ni}$
- Synchronicity index $(Z) = \frac{\sum Cni,2}{\sum ni\ x\ \sum(ni\ \ \frac{1}{2})}$

where *ni* is the number of seeds germinated in the time *i* (not the accumulated number, but the number correspondent to the *ith* observation), *ti* corresponds to the time from the start of the experiment to the *ith* observation (day), *k* is the last time of germination, and *Cni,2* = *ni* (*ni*-1)/2. The Z index can assume values comprises between 1, which indicates a complete synchrony among germinating seeds, and 0, reflecting the total absence of synchrony (Ranal and Santana, 2006).

The tetrazolium test is a method used for a rapid estimation of seed viability and vigor. The reduction of tetrazolium salt (2,3,5-triphenyl tetrazolium chloride - TTC) (**Fig. 1.15**) is catalyzed by specific dehydrogenase enzymes, which catalyze respiratory reactions in the mitochondria, during glycolysis (glyceraldehyde-3-phosphate) and citric acid cycle, or Krebs cycle. In the reduced form, the TTC-salt is a red-colored, stable, no-diffusible substance called triphenyl formazan or formazan. When a seed is immersed in the colorless TTC solution, the TTC penetrates into the seed tissues, interfering with the reduction processes of the living cells by accepting a hydrogen ion. The reduction of TTC in triphenyl formazan in the tissue indicates the presence of living cells, which assumes a red color. Thus, the resulting red color is a positive indication of viability, while in the case of non-viable seed tissues, no reduction occurs and the seeds remain colorless (França-Neto and Krzyzanowski, 2022). Different seed tissues can respond to tetrazolium staining, such as the embryo, cotyledons, radicles, and nutritive endosperm tissues (França-Neto and Krzyzanowski, 2019).

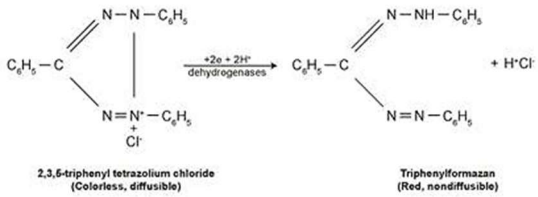

Figure 1.15. Illustration of the reduction reaction of 2,3,5-triphenyl tetrazolium chloride in triphenyl formazan occurring within living seed cells (França-Neto and Krzyzanowski, 2019).

Compared to germination tests, the utilization of TTC solution allows to estimate seed viability and vigor levels in less than 20 h for the majority of crops. Moreover, the TTC test is not influenced by environmental or intrinsic factors, such as seed dormancy (Sores et al., 2016; França-Neto and Krzyzanowski, 2019). Despite the amount of information provided, the interpretation of the results of the test requires marked decision-making capability of expert seed analysts, making this approach difficult to be utilized by non-specialists (França-Neto and Krzyzanowski, 2019).

Given the influence of water content on the physiological and metabolic status of seeds, its estimation within seeds represents a sensitive approach to assess seed quality. The conventional method approved by ISTA for seed moisture content estimation consists of measuring seeds weight before and after an oven-drying treatment (Obi et al., 2016; Hay et al., 2023). A crucial point in the application of the oven drying method is the selection of a temperature that allows the exclusive release of water. In this context, the chemical composition and structure of the seeds represent the main features that affect the selection of the temperature and the duration of the drying process. Although ISTA reference methods include a drying phase in the oven of 103°C for 17 h, different tests on multiple species indicated more rapid alternative treatments (130°C for 1 or 2 h) (Hay et al., 2023). The oven drying method belongs to the direct, or primary, approaches for seed moisture content estimation, which involve water removal.

Secondary approaches, involving some physical or chemical characteristics, are also used to measure seed moisture content. Among these, the most common is the electrical conductance method, a rapid and easy to use technique, although it requires prior calibrations (Chen, 2003). The electrical conductivity (EC) test represents an ISTA-approved method, which involves measuring the ability to conduct electric current directly on seed or seed-steep water. Seed samples are soaked in deionized water and the EC of the soak water is measured after 24 h (Matthews and Powell, 2006). The test is based on the link between conductivity and seed vigor/viability. Seeds imbibed with water exude ions, sugars, and other metabolites from the beginning of the imbibition period due to changes in the integrity of the cell membranes as a function of the amount of water and the degree of seed deterioration. In degraded seeds, the repair mechanism is absent or inefficient, or the membranes are completely damaged, resulting in leaching of larger amounts of electrolytes

(Fessel et al., 2006). Accelerated aging is an additional method for evaluating seed quality. As described in detail in the previous sections, the ability of seeds to maintain its quality under stress conditions is a characteristic of high-quality seeds (Fantazzini et al., 2018).

In addition to the specific seed quality detection methods described, biochemical and molecular techniques can be used to study the chemical composition and genetic purity of seeds. Several works have performed quality estimation by detecting chemical composition and metabolic profiling in seeds of different species using liquid chromatography approaches (Wang et al., 2012; Hou et al., 2018), as well as electrophoretic techniques for estimating genetic purity (Zheng et al., 2017; Anupama et al., 2020).

1.4.2 Non-invasive methods

In the last decades, several non-destructive technologies have been developed for the rapid, accurate, reliable, and simple evaluation of seed quality. Most of the methods mentioned in this section are optical technologies. One of the most promising technologies is machine vision (**Fig. 1.16**), an artificial intelligence technique that emulates the processes of human vision.

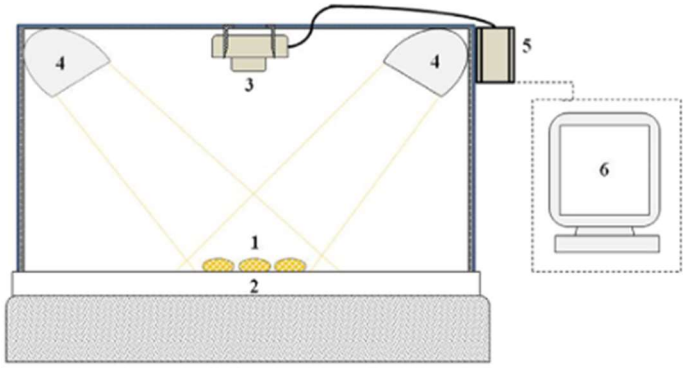

Figure 1.16. Illustration of the components of a typical machine vision system, which includes the seed sample (1), sample holding platform (2), camera (3), light sources (4), frame grabber (5), and the computer (6).

A conventional machine vision system comprises a sample holding platform (which also serves as the imaging background), a camera for capturing the image, a light source for optimal illumination, and a computer for data elaboration (**Fig. 1.16**). The digital information of the object is obtained from the acquired image, improving the use of specific processing algorithms. A computer executes the processing of the acquired digital image utilizing techniques such as image resizing, enhancement, noise removal, edge detection, and filtering. An additional image segmentation operation performed by the computer is necessary to separately identify individual seeds from the background. This is achieved through a variety of methods, including

threshold-based, region-based, gradient-based, or classification-based approaches. The final stages of machine vision operation are recognition and interpretation. Sample recognition is performed using a computer learning algorithm, which ranges between the intuitive decision trees to a more complex neural network algorithm (Rahman and Cho, 2016; Vithu and Moses, 2016). The main advantage related to the application of machine vision for seed quality estimation is the ability to collect high-quality physical information, such as seed size, color, and morphology (Rahman and Cho, 2016), as well as the presence of insects or microbial infestations (Vithu and Moses, 2016). Moreover, machine vision technology demonstrated marked affordability in seed identification, which requires the expert skills of seed analysts (Zhao et al., 2022). This approach has been successfully used to assess the quality of pepper (Tu et al., 2018), rice (Ansari et al., 2021), wheat (Fazel-Niari et al., 2022), and soybean (Mahajan et al., 2018) seeds. Despite its potential, this system is not able to detect seed chemical composition and internal insect infestation, important factors reflecting seed quality. Moreover, the results are highly affected by operating/environmental conditions and by the selection of the learning algorithm (Vithu and Moses, 2016).

Spectroscopy has been used to assess the chemical composition of seeds (Rahman and Cho, 2016). The most common spectroscopy techniques used for seed testing are near-infrared (NIR) and Raman. NIR spectroscopy deals with the near-infrared region of the electromagnetic spectrum (from 780 to 2500 nm) which presents a longer wavelength and lower frequency than visible light. As a vibrational technology, it is based on molecular overtone and combined vibrations that penetrate deeper into the seed sample and induce the vibration of molecules. Since the energy emitted by an oscillating molecule is influenced by intramolecular interactions, the vibrations around the equilibrium position are non-symmetric and specifically related to different chemical groups (Reich, 2005; Siesler, 2007). The absorptions measured by NIR spectroscopy correspond mostly to overtones and combinations of vibrational modes involving C-H, O-H, and N-H chemical bonds. Recording the electromagnetic radiation absorbed by these molecular bonds in the NIR wavelengths produces spectra that are unique to a sample and operate as a "fingerprint". The collected spectra contain data about the chemical and physical properties of the organic molecules in the sample, and therefore important information about the composition of the sample (Prieto et al., 2017). Although Raman spectroscopy also belongs to the vibrational spectroscopies group, the principle behind this technique is different from the NIR spectroscopy. This technology utilizes the Raman effect, which is the inelastic scattering of photons on a quantized molecular system. Thus, during Raman spectroscopy, the vibrational excitation generated by the excitation source of the device induces a photon scattering process, which is distinct for every molecule. Therefore, the obtained Raman spectra can be interpreted as a type of characteristic “molecular fingerprint” of an examined inorganic, organic or biological molecule or more complex systems, such as biological cells and tissue (Cialla-May et al., 2019; Moon et al., 2023). The main advantages related to the application of spectroscopy technologies are related to their elevated sensitivity, as they accurately detect the internal chemical composition, the presence of damage/pest infestations of the seed

material. However, many limitations related to the cost of the instruments and the complexity of the data generated restrains the large-scale use of these approaches (Rahman and Cho, 2016). NIR and Raman spectroscopies have been comparatively utilized to assess the quality of corn (Ambrose et al., 2016), pepper (Seo et al., 2016), and wheat seeds (Liu et al., 2019).

Imaging technologies have also been successfully applied as non-invasive seed quality assessment. X-ray imaging is a rapid and easy-to-use method applied to detect the seed's internal structure and morphology. Although X-rays are potentially harmful, seeds are exposed to relatively low doses during the test to not provoke adverse effects. The dose that determines the radiograph density, degree of contrast, and image quality, can be optimized for different species (Gagliardi and Marcos-Filho, 2011). This method has recently been used to estimate the quality of tomato (*Solanum lycopersicum* L.) (Pessoa et al., 2023) and sugar beet (*Beta vulgaris* L.) seeds (Hamdy et al., 2024). Similarly, thermal imaging technology has been adapted to assess the seed quality in soybean (França-Silva et al., 2023) and pea (Men et al., 2017). This technique records the infrared radiation emitted by seeds using infrared detectors without the need for an illumination source. Since the infrared radiation emitted from the object depends principally on its temperature, this thermal information is converted into two-dimensional thermal pictures to show the temperature gradient on the surface of the seeds. Given that the thermal properties reflect many features related to seed quality, this type of imaging allows a rapid and accurate evaluation. Compared to classical methods of temperature measurements, this approach provides the recording of the temperature for all spots in the whole examined material without direct contact with the seeds tested (ElMasry et al., 2020). The limiting aspect of thermal imaging technology is represented by the different features that can influence the performance of the imaging system, divided into environmental (ambient temperature, atmospheric temperature, relative humidity, and shadow effects of nearby objects), related to the software (color pallet used for image visualization), and the object (distance between the object and the camera, moisture and thermal properties of objects) (Rahman and Cho, 2016; ElMasry et al., 2020). A complex imaging system is represented by the hyperspectral imaging technique, which can be used for seed classification and grading, viability and vigor detection, damage and pests/insects' infestation detection, and internal seed composition (Feng et al., 2019). The main advantage related to hyperspectral imaging technology is the ability to acquire both spectral and spatial information simultaneously, combining the advantages of spectroscopic and imaging techniques (Reddy et al., 2022). Given the quality of the information provided, this approach has been used to detect seed quality in different species, such as tomato (Shrestha et al., 2016) and corn (Zhu et al., 2012; Ambrose et al., 2016).

A common point in all the mentioned optical technologies utilized for seed quality estimation is data elaboration and interpretation. Although different approaches collect distinct types of data, the high quantity of information gathered requires the application of sophisticated hardware and programs. In this context, the application of machine-learning algorithms for data classification markedly improved the data processing step, allowing a more affordable and accurate interpretation of

spectroscopic and imaging information. Classification algorithms, such as deep learning, support vector machine (SVM), k-nearest neighbor (KNN) algorithm, are combined with hyperspectral imaging (Nie et al., 2019; Wonggasem et al., 2024), NIR spectroscopy (Zhu et al., 2024), and X-ray (Hamdy et al., 2024) to enhance data processing and allow the prediction in different seed quality groups. This trend indicates the potential improvements related to seed quality assessment promoted by the integration of artificial intelligence (AI) models.

2. Aim of the research

Given the status of the state-of-the-art presented in the Introduction, the objective of the current PhD thesis was to develop non-invasive methods to sustainably assess seed quality. Considering the multidisciplinary of seed quality, encompassing different features, the work focused on the development of different approaches, based on the detection of distinct markers of seed quality.

The first method developed was based on ROS detection, using two biochemical assays (FOX-1 and DCFH-DA), which provide different information regarding ROS types and levels. FOX-1 was used to assess the concentration of hydrogen peroxide and peroxidic radicals' concentration [ROOH] released from seeds, while DCFH-DA provides a general measure of the oxidative stress level. The two methods were tested in a contrastive system constituted by high-quality (primed) and low-quality (heat shock) seeds of *Glycine max*, *Solanum lycopersicum*, and *Triticum aestivum*. ROS levels were also measured during seed imbibition, in order to evaluate the time course of ROS production.

The second approach was based on the detection of two phenomena related to photons emission, respectively the ultra-weak photon emission (UPE) and the delayed luminescence (DL). An experimental light analyzer (LIANA©, provided by the Super-Lab company) was used for testing different accessions belonging to five legume species (*Lathyrus sativus*, *Cicer arietinum*, *Vicia faba*, *Pisum sativum*, *Phaseolus vulgaris*). In this work, the contrastive system of high and low-quality seeds was constituted by seeds stored for more than ten years either at -18°C (standard approach of seed storage) or at room temperature (22-24°C, naturally-aged seeds). This work was performed in collaboration with the Leibnitz Institute for Plant Genetics and Crop Plant Research (IPK, Gatersleben, Germany), holding one of the biggest genebank germplasm collections in the world.

The last approach focused on the detection of volatile organic compounds (VOCs). The technology applied was based on the proton transfer reaction-quadruple ion guide-time of flight-mass spectrometry (PTR-Qi-TOF-MS), a method able to rapidly and accurately detect VOCs in real-time. High and low-quality seeds, obtained through hydropriming and artificial aging, were used. The species investigated included two commercial *G. max* accessions (OL996 and EM PURA), and three orphan legume species, with two accessions each (*P. sativum var. arvense*, accessions Forrimax and Guifredo; *L. sativus*, accessions Maleme-107 and Sofades; *T. foenum-graecum* accessions Rayhane and Tborsek). This work was performed in collaboration with the INFRA-VOL phenotyping platform, hosted at the Italian National Research Council – Institute for Sustainable Plant Protection (CNR-IPSP, Portici, Italy).

3. Noninvasive methods to detect reactive oxygen species as a proxy of seed quality

The work included in this chapter was published on March 3rd, 2023 in the journal *Antioxidants* (Impact Factor 6.0) with the title "Noninvasive Methods to Detect Reactive Oxygen Species as a Proxy of Seed Quality" (https://www.mdpi.com/2076-3921/12/3/626). My contribution to this article is hereby described. I was involved in the identification of the optimal hydropriming and heat shock treatments, hence development and characterization of the experimental system with high- and low-quality seeds. I also optimized the use of FOX-1 and DCFH-DA assays for seeds, as well as participated in the gene expressions analysis studies through qRT-PCR. Additionally, I performed data representation, statistical analysis, and results interpretation.

Abstract

ROS homeostasis is crucial to maintain radical levels in a dynamic equilibrium within physiological ranges. Therefore, ROS quantification in seeds with different germination performance may represent a useful tool to predict the efficiency of common methods to enhance seed vigor, such as priming treatments, which are still largely empirical. In the present study, ROS levels were investigated in an experimental system composed of hydroprimed and heat-shocked seeds, thus comparing materials with improved or damaged germination potential. A preliminary phenotypic analysis of germination parameters and seedling growth allowed the selection of the best-performing priming protocols for species like soybean, tomato, and wheat, having relevant agroeconomic value. ROS levels were quantified by using two noninvasive assays, namely dichloro-dihydro-fluorescein diacetate (DCFH-DA) and ferrous oxidation-xylenol orange (FOX-1). qRT-PCR was used to assess the expression of genes encoding enzymes involved in ROS production (respiratory burst oxidase homolog family, RBOH) and scavenging (catalase, superoxide dismutase, and peroxidases). The correlation analyses between ROS levels and gene expression data suggest a possible use of these indicators as noninvasive approaches to evaluate seed quality. These findings are relevant given the centrality of seed quality for crop production and the potential of seed priming in sustainable agricultural practices.

3.1 Introduction

Seed quality can be defined based on the set of physical, genetic, and physiological characteristics, as per the guidelines given by the International Seed Testing Association (ISTA) (Milivojević et al., 2018). Because seed quality affects germination, its evaluation has become increasingly important for consumers and seed companies, as it constitutes a valuable tool to optimize crop production, with practical and economic benefits (Huang et al., 2015). This can be achieved through the development of approaches aimed at determining seed quality in an efficient,

noninvasive manner (Rahman and Cho, 2016). The current standard approach to monitoring seed viability is mostly based on germination tests which are time-consuming and destructive (Hay et al., 2017). Research efforts dedicated to improving seed viability testing are constantly performed, but so far no universal approach has been developed.

Starting from the primordial state of development on the mother plant, seeds undergo endogenous and exogenous stresses that may undermine cellular structures and functions. As a consequence, reactive oxygen species (ROS) are produced during all phases of seed development, from seed dehydration to storing and germination, posing different outcomes on seed longevity and quality (Bailly, 2019; Pagano et al., 2019; Rehmani et al., 2022). In addition to ROS, more recently reactive nitrogen species (RNS) and especially nitric oxide (NO) have also been shown to carry essential functions in seed biology, from their intervention in the regulation of seed dormancy, germination, and aging, to their possible use as seed pretreatments to increase seed quality (Ciacka et al., 2022).

ROS production is a side effect of many metabolic pathways (e.g., mitochondrial and plastid electron transport chains, peroxisomal reactions, lipid autooxidation) occurring both under physiological and stress conditions (Richards et al., 2015; Ishibashi et al., 2018; Farooq et al., 2022; Klupczyńska et al., 2022). Uncontrolled ROS accumulation causes oxidative damage and compromises seed viability (Kurek et al., 2019; Juan et al., 2021). Aside from detrimental effects, positive physiological functions of ROS were highlighted during the pre-germinative metabolism, related to signaling, dormancy release, reservoir mobilization, and radicle elongation (Bailly et al., 2008; Macovei et al., 2017; Doria et al., 2019; El-Maarouf-Bouteau, 2022). Thus, ROS play a key role in the activation of pre-germinative metabolism (Macovei et al., 2017; Doria et al., 2019). Accumulation of ROS in seeds has been well documented in multiple species and at different developmental stages (Schopfer et al., 2001; Bailly et al., 2002; Jurdak et al., 2022). At the cellular level, several components (e.g., mitochondria, peroxisomes, cell membrane, and apoplast) act as preferred production sites. The reactivation of metabolism during seed imbibition causes an enhanced accumulation of ROS, generally resulting from electron leakage within the mitochondrial electron transport chain (Kranner et al., 2010). Due to their dual nature, ROS must be kept under stringent control by antioxidant defenses. If the balance between ROS production and scavenging is lost, the seeds undergo oxidative stress which can induce seed death. In this view, the presence and diffusion of ROS throughout the cell compartments are spatially and temporally regulated to avoid damage (Mittler et al., 2011; Wrzaczek et al., 2013). Given the double nature of ROS functions in seeds, the concept of an “oxidative window” of germination is used to evidence this critical range in which ROS can play a positive role in seed metabolism without being detrimental (Bailly, 2019).

Fast and uniform seed germination and successful seedling establishment are high priorities for enhancing crop yields. Technologies designed to improve germination performance (generally known as seed priming) can contribute to building up dynamic and sustainable agriculture practices (Devika et al., 2021; Reed et al., 2022;

Pagano et al., 2023). Seed priming is the process of regulating seed germination by managing a series of parameters during the initial stages of germination (Paparella et al., 2015; Mal et al., 2019; Marthandan et al., 2020). For instance, the so-called "on-farm" seed priming, a low-cost technique consisting of soaking seeds in water before sowing, has led to 22% faster seed emergence translated into a 21% yield increase, whereas under stress conditions the plants proved to be more tolerant, gaining up to 22–28% in yield improvements (Carrillo-Reche et al., 2018). The main effect of priming is the activation of the metabolic processes triggered during the early phase of germination, or the pre-germinative metabolism (Paparella et al., 2015; Macovei et al., 2017; Pagano et al., 2023). Although the success of seed priming is strongly correlated to plant species, genotype, seed lot, and vigor, it has also been proven to be effective in improving germination performances during environmental constraints (Paparella et al., 2015; Mal et al., 2019; Rhaman et al., 2020; Johnson and Puthur, 2021; Yang et al., 2022). Among the different priming treatments, hydropriming (water soaking with or without aeration) is especially useful in those agricultural areas where crop cultivation is impaired by adverse climate conditions, and it does not require the use of chemical substances (Carrillo-Reche et al., 2018; Forti et al., 2020; Forti et al., 2020; Adhikari et al., 2021; Forti et al., 2021). Despite its simplicity, hydropriming has been reported to improve germination performances (in terms of germination time, speed, and percentage) in many species (Dezfuli et al., 2008; Damalas et al., 2019; Forti et al., 2020; Forti et al., 2020; Adhikari et al., 2021; Forti et al., 2021; Colombo et al., 2023). In the case of some practices (e.g., osmopriming, chemopriming), several studies have indicated that these act by delaying water entrance into the seed and thus may limit ROS oxidative injury (Marta et al., 2016; Lechowska et al., 2019; Mirmazloum et al., 2020), whereas in most cases priming acts at the level of seed transition from dormancy toward full germination, touching processes like the activation of DNA repair and antioxidant mechanisms, essential to obtain seeds with improved quality (see comprehensive reviews Paparella et al., 2015; Macovei et al., 2017; Pagano et al., 2023). When considering the antioxidant response, enhanced enzymatic activity or increased expression of genes encoding antioxidant enzymes (e.g., SOD, APX, CAT, GR), were evidenced during seed germination and priming treatments (Wojtyla et al., 2006; Lee et al., 2010; Balestrazzi et al., 2011; Macovei et al., 2014).

As seed priming is still an empirical procedure, hallmarks useful to monitor the seed response to priming and to discriminate between high- and low-quality lots are necessary to enable the development of efficient protocols (Pagano et al., 2019; Forti et al., 2020; Forti et al., 2020; Forti et al., 2021). Because ROS play a vital role in seed dormancy and germination, measuring their levels can provide relevant information about seed viability under different conditions. ROS levels have been evaluated as a possible indicator of overpriming seed performance in *Medicago truncatula*, showing that their accumulation during dehydration positively correlates with the loss of desiccation tolerance (Pagano et al., 2022). ROS levels were also used as a tool to monitor seed quality in *Solanum melongena*, pinpointing that low-quality seed lots defined by low germination rates were characterized by enhanced accumulation of ROS (Forti et al., 2020). Additionally, in *Pisum sativum*, accessions

with low ROS levels were associated with long-lived seeds, which maintained good germination profiles, whereas short-lived seeds were characterized by higher ROS accumulation (Giannella et al., 2022).

Despite recent advances, the thresholds at which ROS induces toxicity are unknown and conditioned by many factors. Moreover, the necessity to avail of a palette of universal, cost-effective, and noninvasive tools or techniques to monitor seed quality, is highly requested by seed technologists working in industry and seed banks. To this purpose, the current study employed two different biochemical assays, namely dichloro-dihydro-fluorescein diacetate (DCFH-DA) and ferrous oxidation-xylenol orange (FOX-1), to quantify ROS levels in seeds subjected to contrastive treatments leading to enhanced (hydropriming) or impaired (heat-shock) seed quality, in different plant species. These data were also integrated with the expression profiles of genes encoding enzymes involved in ROS production and scavenging.

3.2 Materials and Methods

3.2.1 Seed materials and treatments

Seeds of *Glycine max* (commercial variety, provided by Sipcam Oxon SpA, Milan, Italy), *Solanum lycopersicum* (commercial variety, provided by ISI Sementi S.p.A., Fidenza, Italy), and *Triticum aestivum* (commercial variety, provided by ITQB NOVA, Oeiras, Portugal) were used. The seeds were collected from the respective providers and stored at 4 °C until use. Hydropriming (HP) treatments were conducted in a species-specific manner, especially regarding the time spent during the seed imbibition phase. For instance, in soybean seeds, HP treatments were carried out for 2, 4, and 8 h of imbibition (**Fig. 3.1**). Considering the *S. lycopersicum* and *T. aestivum* systems, the HP treatments based on seed imbibition in water were carried out at different intervals of time, namely 2 h, 8 h, 24 h for tomato, and 2 h, 4 h, 6 h for wheat seeds. Subsequently, the seeds were air-dried overnight at room temperature to perform the dry-back (DB) phase of the priming treatment. The heat-shock (HS) treatment was carried out in an oven at 90 °C for 30 min for *G. max* and *T. aestivum*, while *S. lycopersicum* seeds were kept in the oven for 3 h. Nontreated controls (CTRL) consisting of dry seeds were also used in the experimental system. A schematic representation of the experimental design representative for *G. max* treatments is given in **Fig. 3.1**.

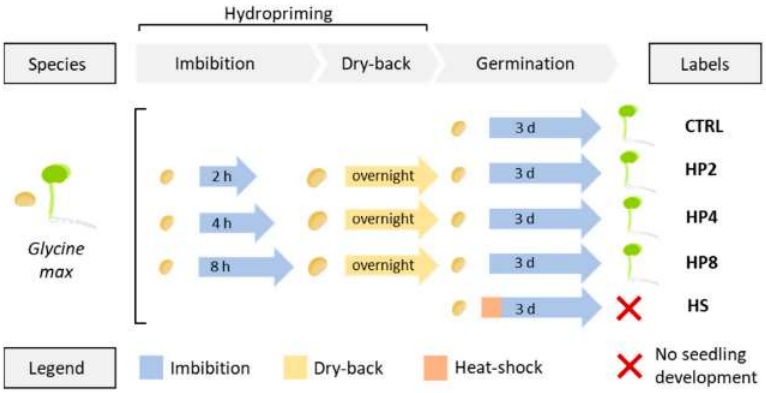

Figure 3.1. Example of the experimental system applied to *Glycine max* seeds. Imbibition steps are indicated in blue, dry-back is indicated in yellow, and heat-shock is indicated in orange. CTRL, non-treated control; HP2, hydropriming for 2 h; HP4, hydropriming for 4 h; HP8, hydro-priming for 8 h; HS, heat-shock.

3.2.2 Germination parameters

For germination tests, treated/untreated seeds were monitored in parallel compatibly with the guidelines provided by ISTA (Milivojević et al., 2018). For this purpose, all germination tests were performed in triplicate, where 20 seeds/replicate were placed in Petri dishes containing a filter of blotting paper moistened with 2.5 mL water. All containers were kept in a growth chamber at 25 °C under light conditions with a photon flux density of 150 µmol m^{-2} s^{-1}, a photoperiod of 16/8 h, and 70–80% relative humidity. Germination was assessed daily for a period of three days for soybean, five days for wheat, and six days for tomato seeds. At the end of the indicated periods, the following germination indices were calculated: germinability (G), peak value (PV), mean germination time (MGT), mean germination rate (MGR), coefficient of velocity (CVG), uncertainty index (U), and synchronicity index (Z) (Ranal and de Santana, 2006). G is defined as the percentage (%) of germinated seeds at the end of the germination test. PV is the highest ratio between the number of germinated seeds at a given time point and the corresponding time, providing an indication of germination rates both in terms of percentage and speed. MGT calculates the average germination time, in which lower MGT values indicate a faster germination. MGR is calculated as the reciprocal of MGT, and it provides an estimation of germination frequency, in which higher MGT values correspond to higher germination frequency. CVG is calculated as the MGR expressed in percentage (%); hence it provides an estimation of germination frequency, in which higher CVG values correspond to higher germination frequency. U is associated with the distribution of germination during the germination test timespan, and higher U values indicate lower synchronization and more dispersion. Z is relative to the synchrony of germination during the experimental monitoring, in which higher Z values indicate a high degree of synchronization and lower dispersion in time (Ranal and de Santana, 2006). The formulas used for the calculation of these parameters are shown in **Table. 3.1**.

Table 3.1. Germination parameters used in this study to assess seed germination as reported by Ranal and Garcia de Santana (2006). For each parameter, definition, formula, limits of measurement, and unit are shown. *, *ti* is the time from the start of the experiment to the *ith* observation (day); *ni*: number of seeds germinated in the time *i* (not the accumulated number, but the number correspondent to the *ith* observation), and *k* is the last time of germination. **, *fi* is the relative frequency of germination, *ni* the number of seeds germinated on the day *i*, and *k* the last day of observation. ***, *Cni,2* is the combination of the seeds germinated in the time *i*, two together, and *ni* is the number of seeds germinated in time *i.*

Parameter	Formula	Limits	Unit
G% (percentage of germination)	G = (100*n. of germinated seeds)/ total n. of seeds	$0 \leq G \leq 100$	%
PV (peak value)	PV = {Ni/Ti = Nmax}	$0 \leq PV \leq$ N	N/day
MGT (mean germination time)*	$(MGT) = \frac{\sum_{i=1}^{k} ni\ x\ ti}{\sum_{i=1}^{k} ni}$	$0 < t \leq k$	day
CVG (coefficient of velocity of germination)	$CVG = (\sum_{I=1}^{k} fi\ /\ \sum_{I=1}^{k} fi\ xi) * 100$	$0 < CVG \leq 100$	%
MGR (mean germination rate)	$v = CV/100$	$0 < v \leq 1$	day-1
U (uncertainty associated with the distribution of the relative frequency of germination)**	$\bar{E} = (\sum_{I=1}^{k} fi \log_2 fi)$ being $fi = ni/\sum_{I=1}^{k} ni$	$0 \leq U \leq \log 2\ n$	bit
Z (synchronization index) ***	$Z = \frac{\sum Cni,2}{\sum ni\ x\ \sum(ni - \frac{1}{2})}$	$0 \leq Z \leq 1$	Z score

Aside from the germination parameters, seedling growth was biometrically assessed. The seedling growth was monitored at the end of the experiment by using ImageJ (https://imagej.nih.gov/ij/) software. To this purpose, at least five seedlings/replicates were photographed and used to determine the seedling length (in terms of roots and/or aerial parts).

3.2.3. DCFH-DA assay

ROS levels were quantified in CTRL and HP, HS, and DB seeds. The assay was carried out by using the fluorogenic dye 2,7-dichlorofluorescein diacetate (DCFH-DA; Sigma-Aldrich, Milan, Italy). The dye is converted to a nonfluorescent molecule following deacetylation mediated by esterases, and it is subsequently oxidized by ROS into the fluorescent compound 2,7-dichlorofluorescein (DCF), which can be detected by fluorescence spectroscopy with maximum excitation and emission spectra of 495 nm and 529 nm, respectively. The assay was carried out as described by Pasqualini et al., with the following modifications (Pasqualini et al., 2011). Seed samples (1 seed/replicate for *G. max* and *T. aestivum* and 10 seeds/replicate for *S. lycopersicum*) were incubated for 30 min with 500 µL of 10 µM DCFH-DA (for *G. max* and *T. aestivum*) and 70 µL of 50 µM DCFH-DA (for *S. lycopersicum*) or for 15 min. Five replicates were used per sample. Subsequently, the fluorescence sensor (at 517 nm) of the Rotor-Gene 6000 PCR apparatus (Corbett Robotics, Brisbane, Australia) was used, setting the program for one cycle of 30 s at 25 °C. A sample containing only DCFH-DA was used as a negative technical control to subtract the baseline fluorescence. Data were expressed as relative fluorescence units (RFU).

3.2.4. FOX-1 assay

Peroxyl radicals and hydrogen peroxide (H_2O_2) concentrations were quantified in control and treated seeds at the indicated time points as presented in Section 3.2.1. The assay was carried out by using the reagent xylenol orange (Carlo Erba, Milan, Italy), which reacts with Fe^{3+} (derived from the oxidation of Fe^{2+} induced by peroxyl radicals and H_2O_2) to give a blue-violet complex with an absorption maximum at 560 nm. The working solution (FOX-1 solution) was prepared as described by Bridi et al., 2015. A solution containing ammonium ferrous (II) sulphate $(NH_4)2Fe(SO_4)2{\cdot}6H_2O$ 25 mM (Merk's Reagents, Darmstadt, Germany) in H_2SO_4 0.25 M (Honeywell, Charlotte, NC, USA) was added to a Milli-Q water solution containing Xylenol Orange 125 µM (Carlo Erba, Milan, Italy) and D-sorbitol 100 mM (Duchefa Biochemie, Haarlem, The Netherlands) in a ratio of 1:100. The solutions were mixed gently until the color became uniform. Seed samples (1 seed/replicate for *G. max* and *T. aestivum* and 10 seeds/replicate for *S. lycopersicum*) were incubated in a sufficient volume (1.5 mL for *S. lycopersicum* and 3 mL for *T. aestivum* and *G. max*) of FOX-1 working solution to allow seeds complete immersion for 45 min. Five replicates were used per sample. Subsequently, 1 mL of medium was recovered from each sample and the absorbance was determined at 560 nm by using a Biochrom WPA Biowave (Biochrom Ltd., Cambridge, United Kingdom) spectrophotometer. A calibration curve (**Fig. 3.2**) was performed by using FOX-1 solution with different concentrations (0, 1.25, 2.50, 5 µM) of H_2O_2, and data were represented as [ROOH] concentration values.

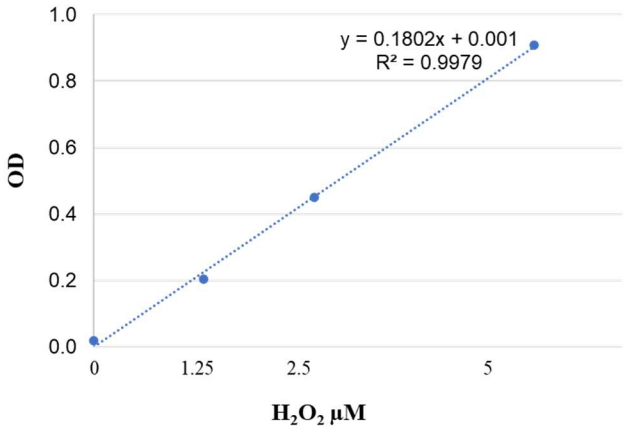

Figure 3.2. FOX-1 calibration curve performed with several concentrations (0, 1.25, 2.50, 5 µM) of hydrogen peroxide (H_2O_2).

3.2.5. Quantitative real-time-polymerase chain reaction (qRT-PCR)

Total RNA was isolated from *G. max* treated/untreated seeds by using TRIzol™ (Thermo Fisher Scientific, Monza, Italia), as indicated by the provider. Subsequently, a DNase (Thermo Fisher Scientific) treatment was performed. RNA was quantified by using NanoDrop (Biowave DNA, WPA, Thermo Fisher Scientific). Subsequently, cDNAs were obtained by using the RevertAid First Strand cDNA Synthesis Kit (Thermo Fisher Scientific) according to the manufacturer's suggestions. The qRT-PCR reactions were performed with the Maxima SYBR Green qPCR Master Mix (Thermo Fisher Scientific) according to the supplier's indications, by using a CFX Duet, Real-Time PCR System (BIO-RAD, Milano, Italy). Amplification conditions were as follows: denaturation at 95 °C for 10 min, and 45 cycles of 95 °C for 15 s and 60 °C for 60 s. Oligonucleotide sequences (**Table 3.2**) were designed by using Primer3Plus1 (https://primer3plus.com/) and verified with Oligo Analyzer.2 (https://eu.idtdna.com/pages/tools/oligoanalyzer).

Table 3.2. List of oligonucleotide sequences used for the qRT-PCR analysis

Gene	Phytozome Accession No.	Primer Forward (5'-3')	Primer Reverse(5'-3')
MnSOD	Glyma.04G221300	GGTGTGGCTTGGTCTGG	CATGCTCCCAAACATCAATACC
SOD1	Glyma.19G240400	GAGGGTGTCACTGGAACTATTTTC	GTAGTGTCCCCCAAGGCA
CAT5	Glyma.06G017900	GAACGTGTTGTCCATGCCA	GCTACCACGCTCATGAATGAC
CAT1	Glyma.17G261700	CTCATCGTCCGTTTCTCCA	GTGGGACTTGGGGTTGG
APX2	Glyma.12G073100	CCGTTGAGAAGGCGAAGAAG	CGGAGGGGTGCTTTATGG
RbohE2	Glyma.08G005900	GAGGGCAAGAGAGGGTGAG	AAGAGCAGAGCGAGCATCA
RbohC2	Glyma.06G162300	TTTCTATAACCTCCGCCCCT	GTCCACTCTTGCCGTTGTC
CYP	Glyma.12G024700	ACGACGAAGACGGAGTGG	CGACGACGACAGGCTTGG
RP40S	Glyma05G37470	TTCCACCTCGCAACCATGAT	CGAAGCAAACTCCCTCTTGG

Relative quantification was carried out by using the *CYP* (peptidyl-prolyl cis-trans isomerase) and RP40S (ribosomal protein 40S) as reference genes (Wan et al., 2017). Raw fluorescence data provided by Software 1.7 (BIO-RAD) were used to determine

the threshold cycle number (Ct) values for each transcript quantification. Relative quantification of transcript accumulation was performed as described by Thomsen et al. by using the X_0 method in which a conversion of the exponentially related Ct values is introduced to arrive to linearly related values, representing the amount of starting material in a qPCR reaction (Thomsen et al., 2010). All reactions were performed in triplicate. The choice of investigated genes was based on in silico gene expression data mining obtained from *Arabidopsis thaliana* and *Glycine. max* orthologues, recovered from BAR ePLANT (http://bar.utoronto.ca/eplant_soybean/) (Severin et al., 2010) and Arabidopsis eFP browser (http://bar.utoronto.ca/efp/cgi-bin/efpWeb.cgi) (Bassel et al., 2008), respectively. The selected genes encoding enzymes involved in ROS production and scavenging include superoxide dismutase (*SOD*1, Phytozome accession No. Glyma.19G240400) manganese superoxide dismutase (*MnSOD*, Phytozome accession No. Glyma.04G221300), catalase 1 (*CAT*1, Phytozome accession No. Glyma.06G017900), catalase 5 (*CAT*5, Phytozome accession No. Glyma.17G261700), ascorbate peroxidase 2 (*APX*2, Phytozome accession No. Glyma.12G073100), respiratory burst oxidase homolog E2 (*RbohE*2, Phytozome accession No. Glyma.08G005900), and respiratory burst oxidase homolog C2 (*RbohC*2, Phytozome accession No. Glyma.06G162300).

3.2.6. Statistical analyses

Germination data were analyzed with the Student *t*-test by using the Microsoft Excel package using as threshold the *p-value* < 0.05 ('*'). Estimation of oxidative stress and ROS data were analyzed by two-way ANOVA and Tuckey–Kramer test, where $p < 0.05$ is considered as significantly different, by using the software developed by Assaad et al., 2015. Letters were used to indicate significant differences among all samples. For correlation analyses, Pearson's correlation coefficient and the relative *p*-values were determined by using MetaboAnalyst 5.0 (https://www.metaboanalyst.ca/) (Pang et al., 2021). The same software was also used for principal component analysis (PCA) performed by using the germination parameters and ROS detection data. The obtained "biplot" and "score plot" graphics show how the different sample groups are clustered according to the results obtained in the performed analyses.

3.3 Results

3.3.1 Hydropriming improves germination performance in multiple species

Because hydropriming has been already proven to be effective in improving seed germination potential (Carrillo-Reche et al., 2018; Forti et al., 2020; Forti et al., 2020; Adhikari et al., 2021; Forti et al., 2021), this initial part of the work was dedicated to select the most appropriate time points of seed imbibition as this is generally dependent not only on plant variety/genotype but also on the respective seed lots (Paparella et al., 2015; Forti et al., 2020). To test the efficiency of hydropriming treatment in improving seed germination, we first focused on soybean, as it is one of the most cultivated species that dominate global agriculture (Karges et al., 2022). It has a sequenced and well-annotated genome (Schmutz et al., 2010), with data present in several bioinformatics platforms (e.g., Phytozome, BAR ePLANT). Due to the time-specific sensitivity of hydropriming treatments, several imbibition time points were tested. Additionally, to develop a competent experimental design, HS treatments were implemented to decrease seed quality and germination were included along with the control (CTRL). The experimental system described was validated and the results are shown in **Fig. 3.3**.

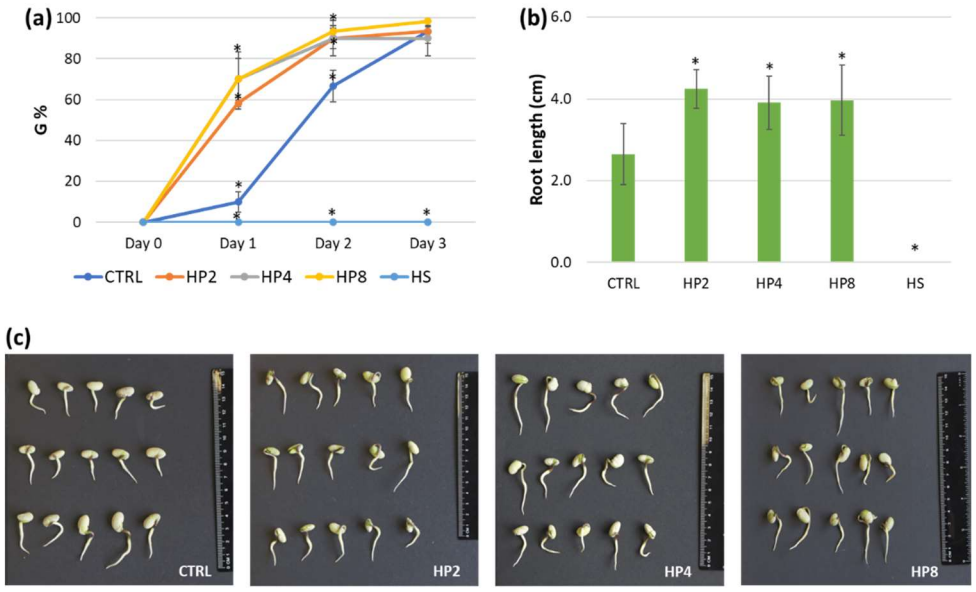

Figure 3.3. Evaluation of hydropriming efficiency in *Glycine max* seeds. (**a**) Germination percentage (%). (**b**) Root length (cm). (**c**) Representative images of germinated soybean seedlings after three days of treatments. Statistical differences among treatments and control are represented with asterisks (*). $P \leq 0.05$. CTRL, non-treated control; HP2, hydropriming for 2 h; HP4, hydropriming for 4 h; HP8, hydropriming for 8 h; HS, heat-shock.

3. ROS and seed quality

The analyses indicated that hydropriming resulted in a significantly enhanced germination percentage (G%) compared to CTRL (**Fig. 3.3a**) for all the tested treatments during the first two days of monitoring. This improved G% was also translated into significantly enhanced root growth when measured at the end of the experiment (after three days) (**Figs 3.3b** and **3.3c**). Data collected for other germination parameters shown in **Table 3.3** confirm that HP improves germination performance.

Table 3.3. Germination parameters calculated for *Glycine max*. Statistical differences among treatments and control are represented with asterisks (*), $P \leq 0.05$. Formulas and measure units for each parameter are provided in the supplementary materials. PV, peak value; MGT, mean germination time; MGR, mean germination rate; CVG coefficient of velocity; U, uncertainty index; Z, synchronicity index; CTRL, nontreated control; HP2, hydropriming for 2 h; HP4, hydropriming for 4 h; HP8, hydropriming for 8 h; HS, heat-shock.

	CTRL	HP2	HP4	HP8	HS
PV	6.67 ± 0.76	11.67 ± 0.58 *	14 ± 2.65 *	14 ± 2 *	0 ± 0 *
MGT	2.18 ± 0.09	1.41 ± 0.06 *	1.22 ± 0.12 *	1.33 ± 0.17 *	n.d.
MGR	0.46 ± 0.02	0.71 ± 0.03 *	0.82 ± 0.08 *	0.76 ± 0.10 *	n.d.
CVG	45.89 ± 1.87	70.98 ± 2.76 *	82.24 ± 7.84 *	75.7 ± 9.95 *	n.d.
U	1.28 ± 0.08	1.1 ± 0.13	0.72 ± 0.21 *	1 ± 0.34	0 ± 0 *
Z	0.43 ± 0.02	0.48 ± 0.03	0.65 ± 0.13 *	0.56 ± 0.15	0 ± 0 *

Specifically for soybean, all the imposed HP treatments showed significant differences compared to CTRL, in terms of PV, MGT, MGR, and CVG, whereas the U and Z parameters were improved only with the HP4 treatment. This indicates that the best time point at which to stop the priming treatment for this soybean commercial variety is after 4 h of imbibition in water, a treatment that brings positive outcomes in terms of germination percentage, speed, and uniformity. The HS treatment was highly damaging and no seed germinated, showing that this can be used as a system to decrease seed quality.

To confirm that these treatments can be universally implemented for different plant species and seed types, the experiments were also performed on *S. lycopersicum* (**Fig. 3.4a,b**) and *T. aestivum* seeds **(Fig. 3.4c,d**), which show the time course of G% and the average length of roots and shoots. Roots/ shoots average length was measured from the images collected and illustrated in Fig. 21. Moreover, additional germination parameters were calculated and illustrated in **Table 3.4**. The gathered results show

that HP2 and HP8 treatments were efficient in improving germination and seedling growth in tomatoes, whereas for wheat the only significant data regarded G% after one day of monitoring. The results indicate that hydropriming treatments are efficient in boosting germination, but the imbibition time points need to be tailored for each species/genotype/seed lots, as evidenced in other cases (Forti et al., 2020; Forti et al., 2020; Adhikari et al., 2021; Forti et al., 2021).

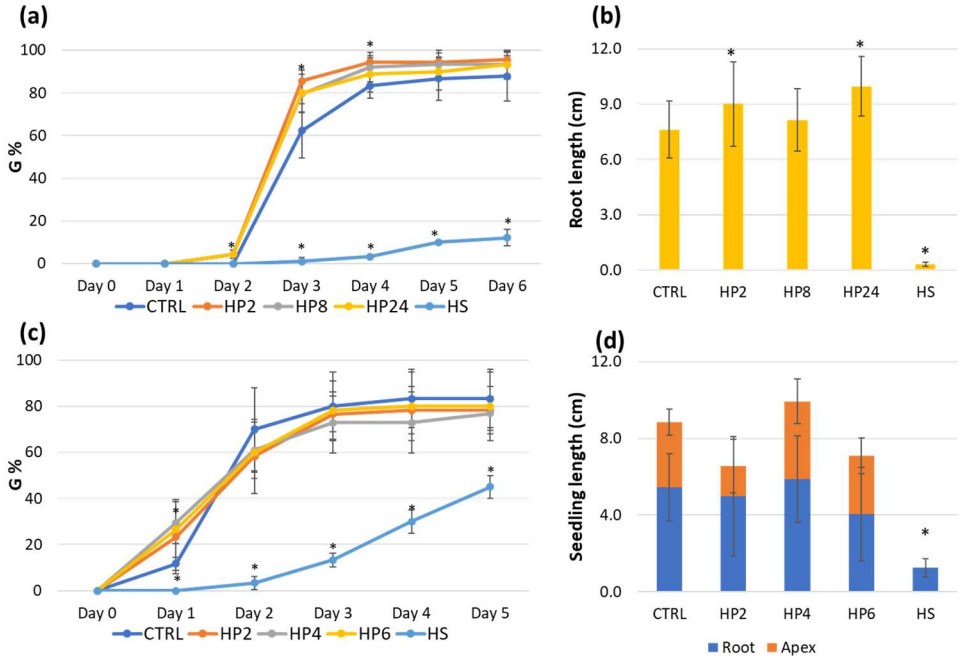

Figure 3.4. Evaluation of hydropriming efficiency in tomato (*Solanum lycopersicum*) and wheat (*Triticum aestivum*) seeds. **(a)** Germination percentage (%) measured daily in tomato for a time period of six days. **(b)** Root length (cm) measured in 6-days-old tomato seedlings. **(c)** Germination percentage (%) measured daily in wheat for a time period of five days. **(d)** Seedling length (cm) measured in terms of roots and aerial parts in 5-days-old wheat plantlets. Statistical differences among treatments and control are represented with asterisks (*), $P \leq 0.05$. CTRL, non-treated control; HP2, hydropriming for 2 h; HP4, hydropriming for 4 h; HP6, hydropriming for 6 h; HP8, hydropriming for 8 h; HP24, hydropriming for 24 h; HS, heat shock.

Table 3.4. Germination parameters calculated for *Solanum lycopersicum*, and *Triticum aestivum*. Statistical differences among treatments and control are represented with asterisks (*), *p-value* < 0.05. PV, peak value; MGT, mean germination time; MGR, mean germination rate; CVG coefficient of velocity; U, uncertainty index; Z, synchronicity index; CTRL, non-treated control; HP2, hydro-priming for 2 h; HP4, hydropriming for 4 h; HP8, hydropriming for 8 h; HS, heat shock.

S.lycopersicum	CTRL		HP2		HP8		HP24	
I	Media	St. dev.	Media	St. dev	Media	St. dev	Media	St. dev.
Peak Value	6,64 ± 0,97		8,56 ± 0,50*		7,89 ± 0,96		8,00 ± 0,88	
MGT	3,35 ± 0,05		3,08 ± 0,12*		3,11 ± 0,07*		3,18 ± 0,14	
MGR	0,30 ± 0,00		0,33 ± 0,01*		0,32 ± 0,01*		0,31 ± 0,01	
CVG	29,85 ± 0,43		32,50 ± 1,28*		32,17 ± 0,67*		31,46 ± 1,38	
U	0,98 ± 0,13		0,76 ± 0,21		0,90 ± 0,20		0,98 ± 0,14	
Z	0,56 ± 0,03		0,73 ± 0,08*		0,66 ± 0,08		0,66 ± 0,05*	

T.aestivum	CTRL		HP2		HP4		HP6	
I	Media	St. dev.	Media	St. dev	Media	St. dev	Media	St. dev.
Peak Value	7,00 ± 1,80		6,06 ± 1,23		6,00 ± 1,80		6,17 ± 0,76	
MGT	2,07 ± 0,11		1,99 ± 0,48		1,94 ± 0,30		1,91 ± 0,21	
MGR	0,48 ± 0,03		0,52 ± 0,13		0,52 ± 0,08		0,53 ± 0,06	
CVG	48,41 ± 2,56		52,40 ± 13,23		52,29 ± 8,15		52,68 ± 5,53	
U	1,28 ± 0,44		1,44 ± 0,40		1,58 ± 0,19		1,54 ± 0,22	
Z	0,50 ± 0,18		0,36 ± 0,09		0,31 ± 0,06		0,33 ± 0,06	

3.3.2 ROS Profiles are influenced by the applied treatments

Once we have shown that the implemented experimental system can be used to boost or damage seed quality (in terms of germination performance), the next set of analyses was dedicated the evaluate different protocols to measure ROS levels. The two assays hereby employed, namely DCFH-DA and FOX-1, have different targets and specificities. Quantification based on the use of the DCFH-DA molecule measures the general oxidative status (Eruslanov and Kusmartsev, 2010). In particular, in the absence of metal or enzymatic catalysts, the $DCFH_2$ molecule (produced in the cells through the activity of esterases) is not able to react with some ROS (e.g., $O_2^{\cdot -}$, LOO^-, H_2O_2) whereas it can react with oxygen and nitrogen radicals, including ·OH and peroxynitrites (Eruslanov and Kusmartsev, 2010). In contrast, the FOX-1 assay directly detects peroxidic radicals ($ROO^{\cdot}$) and in particular H_2O_2 released in the medium whereas it has a low reactivity towards other molecules (Wolff, 1994; Ijaz et al., 2019). Both assays were used to assess these different aspects of ROS accumulation or release by using whole seeds. The levels of ROS detected in *G. max* seeds with the two assays are illustrated in **Fig. 3.5**.

3. ROS and seed quality

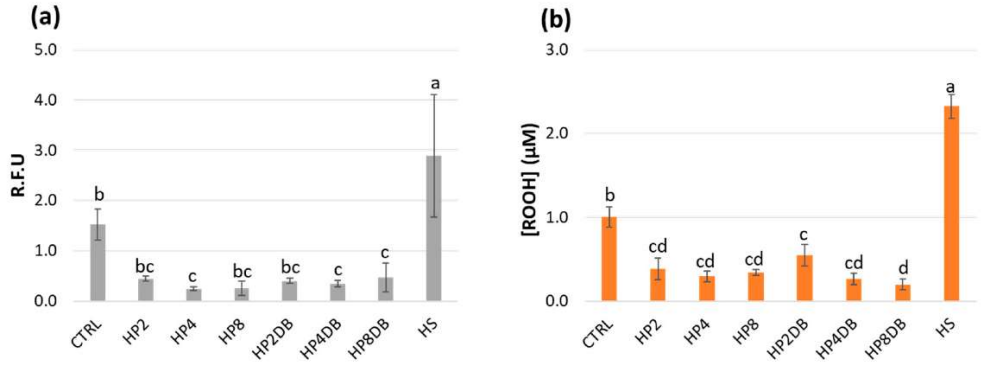

Figure 3.5. ROS detection in *G. max* seeds subjected to hydropriming and HS treatments. (**a**) Data collected by using the DCFH-DA fluorimetry assay and represented as relative fluorescence units (RFU). (**b**) Data collected from the FOX-1 assay through spectrophotometric measurements and represented as [ROOH] concentration values. Statistically significant differences ($P \leq 0.05$) are indicated by the occurrence of different letters. CTRL, non-treated control; HP2, hydropriming imbibition for 2 h; HP4, hydropriming imbibition for 4 h; HP8, hydropriming imbibition for 8 h; HP-DB, dry-back treatment following hydropriming imbibition; HS, heat-shock.

The gathered data show that the highest amount of oxidative stress (**Fig. 3.5a**) and peroxide radicals (**Fig. 3.5b**) are registered in seeds treated with HS. Moreover, the seeds subjected to HP treatments appeared to have the lowest levels of measured ROS, using both the DCFH-DA and FOX-1 assays. To validate these results, the two assays were applied to the tomato and wheat seeds following the same experimental approaches. The results of these analyses are shown in **Fig. 3.6**. As shown in the figure, although the FOX-1 results maintained a similar pattern of ROS being released from the seeds, the DCFH-DA assay presented much more elevated levels of variability.

3. ROS and seed quality

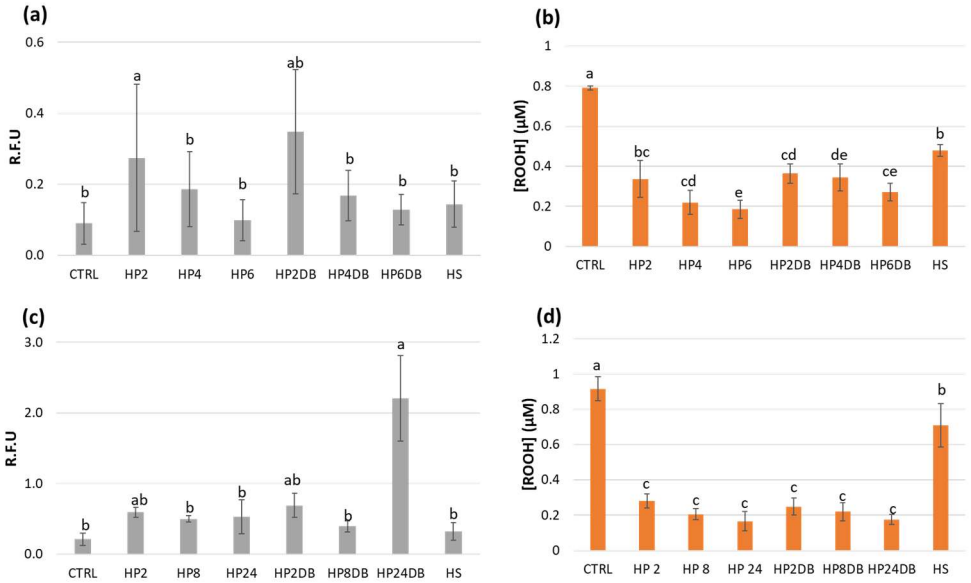

Figure 3.6. ROS detection in *Solanum lycopersicum* and *Triticum aestivum* seeds subjected to hydropriming and heat shock treatments. **(a)** Levels of relative fluorescence units (RFU) measured with the DCFH-DA assay in *T. aestivum*. **(b)** ROS levels as revealed by FOX-1 assay in *T. aestivum*. Data are reported as concentrations of hydrogen peroxide and peroxyl radicals [ROOH] in µM. **(c)** Levels of relative fluorescence units (RFU) measured with the DCFH-DA assay in *S. lycopersicum*. **(d)** ROS levels as revealed by FOX-1 assay in *S. lycopersicum*. Statistically significant differences ($P \leq 0.05$) are indicated by the occurrence of different letters. CTRL, non-treated control; HP2, hydropriming imbibition for 2 h; HP4, hydropriming imbibition for 4 h; HP8, hydropriming imbibition for 8 h; HP-DB, dry-back treatment following hydropriming imbibition; HS, heat shock.

Subsequently, a PCA analysis was carried out to evidence how the different treatments (CTRL, HP, and HS) are clustered according to the obtained data. The clustering of the group of seeds subjected to the imposed treatments in *G. max*, shown in **Fig. 3.7** shows a distinct grouping of the HP treatments compared to CTRL and HS.

3. ROS and seed quality

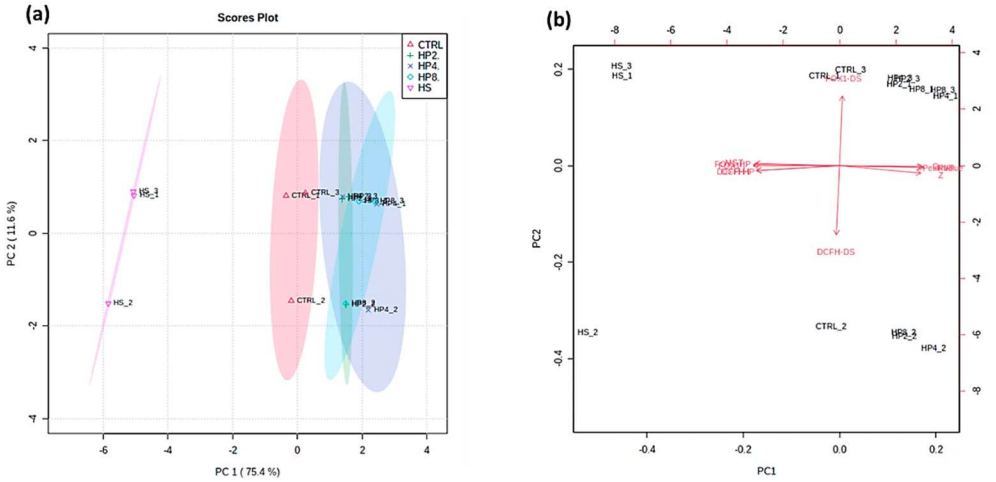

Figure 3.7. PCA using data gathered for the imposed treatments (CTRL, HP2, HP4, HP8, HS) for *G. max*. (**a**) Score plot grouping of samples subjected to different treatments. (**b**) Biplot obtained with data from germination tests (G, PV, MGT, Z, Rad) and ROS measurements (FOX-1, DCHF-DA) on the clustering of the groups subjected to the different treatments. Because the data provided consisted in triplicate values, the designation _1, _2, _3 in the plots refers to the replicate number.

According to the biplot generated by the PCA analysis (**Fig. 3.7b**), the main contributors to this this clustering are the germination parameters. The CTRL samples clustered separately from the groups subjected to HP and HS treatments, mainly due to the data obtained from the FOX-1 and DCHF-DA analyzes. Finally, the separation of the HS group is, according to the PCA analysis, mainly due to the values obtained for MGT as well as FOX1 and DCHF-DA (**Fig. 3.7b**). Similar patterns of clusters were also obtained for tomato and wheat, shown in **Fig. 3.8**.

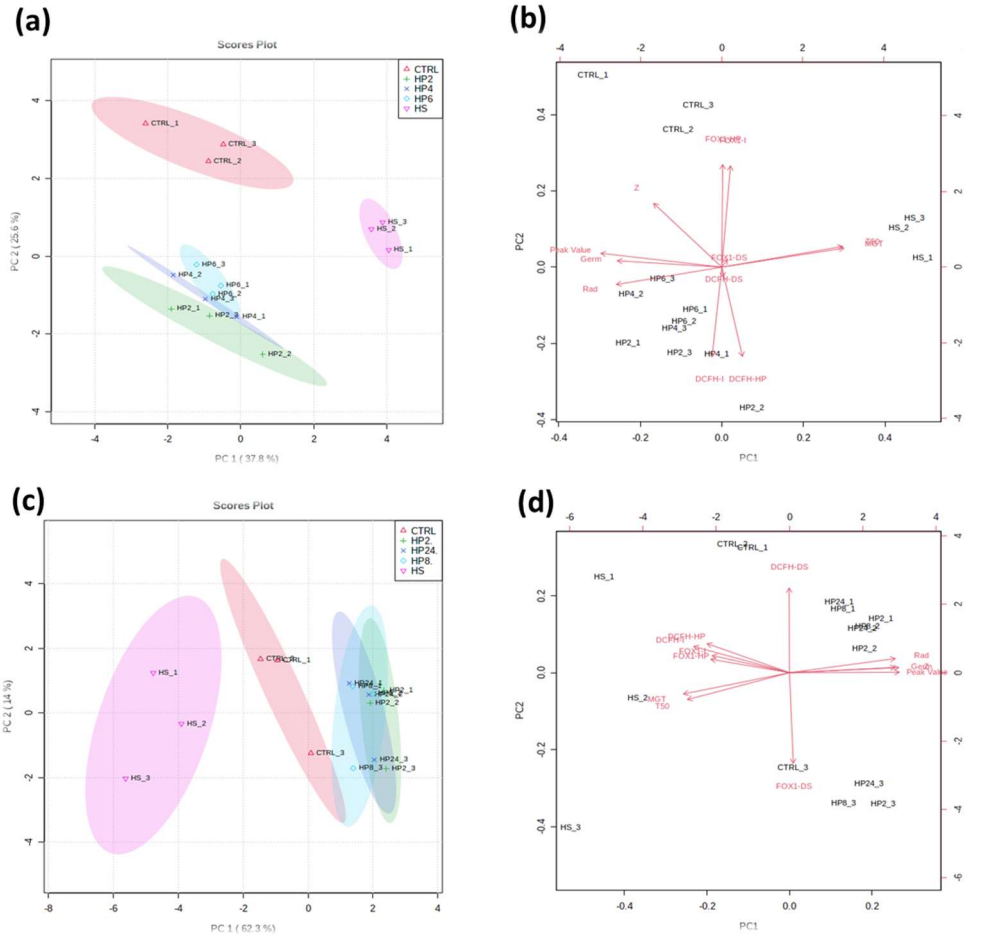

Figure 3.8. Principal Component Analysis using data gathered for the imposed treatments (CTRL, HP2, HP4, HP8, HS) for *Triticum aestivum* and *Solanum lycopersicum*. (a) Scores plot grouping of samples subjected to different treatments for *T. aestivum*. (b) Bi-plot incidence of data obtained from germination tests (G, PV, MGT, Z, Rad) and ROS measurements (FOX-1, DCHF-DA) on the clustering of the groups subjected to the different treatments *T. aestivum*. (c) Scores plot grouping of samples subjected to different treatments for *S. lycopersicum*. (d) Bi-plot incidence of data obtained from germination tests (G, PV, MGT, Z, Rad) and ROS measurements (FOX-1, DCHF-DA) on the clustering of the groups subjected to the different treatments *S. lycopersicum*.

3.3.3. ROS-related gene expression is induced by hydropriming treatments

To better investigate ROS homeostasis in the proposed working system, qRT-PCR analyses were carried out to quantify the relative expression of genes encoding enzymes involved in ROS scavenging and production. To select which genes would provide the most relevant information, a preliminary *in silico* data mining approach was conducted simultaneously for *A. thaliana* and *G. max* models. Data relative to multiple isoforms of *CAT, SOD, APX*, and *Rboh* genes were comparatively examined during seed maturation in soybean as well as during the early phases of seed germination in Arabidopsis (**Fig. 3.9**).

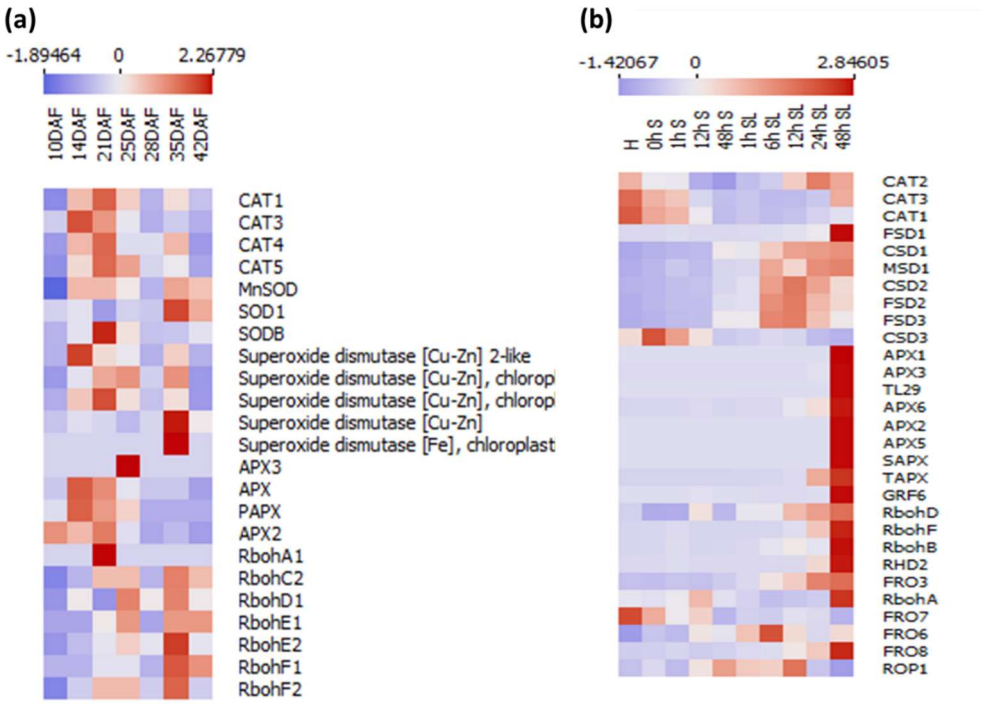

Figure 3.9. Heatmaps evidencing relative expression patters of multiple homologue genes involved in ROS scavenging (SOD, CAT, APX) and production (Rboh) in seeds of *G. max* **(a)** and *A. thaliana* **(b)**. Expression values were collected from the BAR ePLANT database (http://bar.utoronto.ca/eplant) and used after Z normalization to generate heatmaps using the Orange software (https://orangedatamining.com/). Blue color indicates gene downregulation whereas red color indicates gene upregulation.

This analysis showed that different isoforms of the studied genes are differently expressed during soybean seed maturation with the highest expression being most prevalent for 14DAF (days after flowering), 21DAF, and 35DAF, whereas for Arabidopsis the majority of genes are highly expressed at 48 h of seed imbibition/germination. Based on this investigation, the following genes were

selected to perform the qRT-PCR analyses during soybean HP treatment: *MnSOD, SOD1, CAT1, CAT5, APX2* as genes encoding enzymes involved in ROS scavenging, and *RbohE2, RbohC2* as genes encoding enzymes involved in ROS production. Their expression levels were evaluated in soybean dry seeds (CTRL), in seeds subjected to 4 h imbibition (HP4) as the most promising HP timepoint to boost germination, as well as after dry-back (HP4DB) as the last phase of the HP treatment. The results are shown in **Fig. 3.10**.

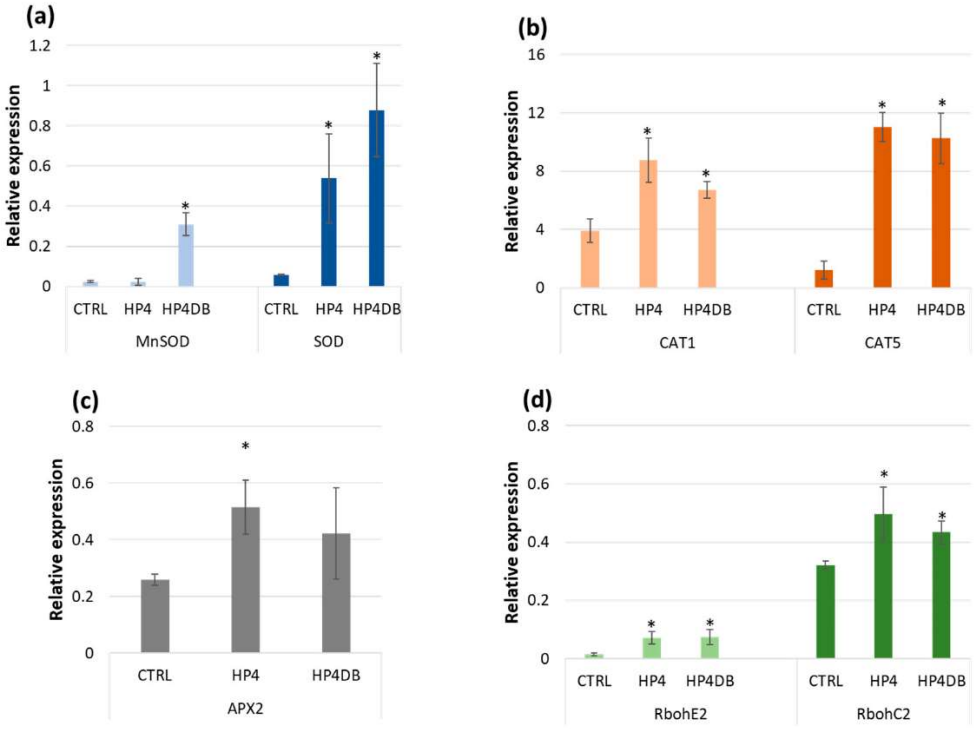

Figure 3.10. Relative expression of genes encoding enzymes involved in ROS scavenging and production mechanisms in G. max seeds subjected to hydropriming treatments. (**a**) Superoxide dismutases, *MnSOD* and *SOD1*. (**b**) Catalases, *CAT1* and *CAT5*. (**c**) Ascorbate peroxidase *APX2*. (**d**) Respiratory burst oxidase homologs, *RbohE2* and *RbohC2*. Statistically significant differences obtained by using the Student t-test ($P \leq 0.05$) are indicated with an asterisk (*). CTRL, untreated seeds; HP4, seeds soaked for four hours in water; HP4DB, seeds soaked for four hours and subjected to the desiccation required by hydropriming protocols.

The gathered data revealed that all genes were significantly upregulated both after seed imbibition (except for *MnSOD*) as well as after the dry-back treatments (except for *APX2*), as compared with the CTRL samples. Interestingly, this trend was common for genes encoding enzymes involved in ROS scavenging as well as ROS production mechanisms. Nonetheless, the highest gene expression levels were registered for the two CAT genes (ROS scavenging) whereas the lowest expression was observed for the *Rboh* genes (ROS production), namely *RbohE2* gene.

3. ROS and seed quality

Subsequently, correlation analyses were performed between data obtained from the ROS detection methods (DCFH-DA and FOX-1) and gene expression profiles (**Fig. 3.11**).

G.max	**FOX-1**	**DCFH-DA**	***CAT1***	***APX2***	***RbohE2***	***CAT5***	***RbohC2***	***MnSOD***	***SOD***
FOX-1	1	0,959 *	-0,927 *	-0,856 *	-0,908 *	-0,956 *	-0,958 *	-0,523	-0,805 *
DCFH-DA	0,959 *	1	-0,956 *	-0,916 *	-0,884 *	-0,98 *	-0,972 *	-0,429	-0,762 *
CAT1	-0,927 *	-0,956 *	1	0,943 *	0,843 *	0,973 *	0,95 *	0,254	0,624 *
APX2	-0,856 *	-0,916 *	0,943 *	1	0,776 *	0,933 *	0,888 *	0,107	0,558
RbohE2	-0,908 *	-0,884 *	0,843 *	0,776 *	1	0,884 *	0,923 *	0,624 *	0,901 *
CAT5	-0,956 *	-0,98 *	0,973 *	0,933 *	0,884 *	1	0,981 *	0,375 *	0,732 *
RbohC2	-0,958 *	-0,972 *	0,95 *	0,888 *	0,923 *	0,981 *	1	0,484	0,815 *
MnSOD	-0,523	-0,429	0,254	0,107	0,624 *	0,375	0,484	1	0,864 *
SOD	-0,805 *	-0,762 *	0,624 *	0,558	0,901 *	0,732 *	0,815 *	0,864 *	1

Figure 3.11. Pearson correlation indices calculated for G. max hydroprimed seeds taking into consideration the biochemical assays for ROS quantification (FOX-1 and DCFH-DA) and the ROS homeostasis gene (*CAT1*, *APX2*, *CAT5*, *MnSOD*, *SOD1*, *RbohE2*, *RbohC2*) expression levels. The blue color indicates negative correlations whereas red indicates positive correlations. Statistically significant correlations ($P \leq 0.05$) are indicated by an asterisk (*).

In general, a negative correlation is observed between the gene expression and ROS levels. For example, this is observed between the data obtained in the FOX-1 analysis and the *CAT*1. *RbohE*2, *APX*2, and *SOD*1 expression levels. The same trend is observed for the data obtained with the DCFH-DA analysis and the *CAT*1, *CAT*5, *RbohE*2, *APX*2, and *SOD*1 relative expression. In contrast, positive correlations are generally observed between the gene expression data, namely for *CAT*1, *CAT*5, and *APX*2 compared to *SOD*1. Furthermore, it is interesting to note that the *RbohE*2 (gene responsible for the production of ROS in seed) expression levels also showed a positive correlation with the expression levels of all the genes responsible for ROS removal (*MnSOD*, *SOD*1, *CAT*1, *CAT*5, *APX*2). A similar trend is observed also for *RbohC*2. Finally, significantly positive correlations are observed between the ROS levels measured through the FOX-1 assay (in terms of peroxide species concentration) and the DCFH-DA (in terms of oxidative stress levels) assay.

3.4 Discussion

Currently, standard germination tests approved by ISTA represent the main methods that allow the observation of seed behavior in the postsowing phase (Milivojević et al., 2018; Petrović et al., 2022). The most common methods for seed quality establishment are invasive and do not allow the continued evaluation of seeds over time. Among the invasive techniques, aside from germination tests, the evaluation of moister content (Kim, 2018; Balbaaki et al., 2012), tetrazolium test (Soares et al., 2016; França-Neto and Krzyzanowski, 2019), and accelerated aging systems (Demir et al., 2004; Dutra and Vieira, 2006) are also used often. Most of these chemical and physical techniques exhibit good accuracy and reliability but also present certain limitations, such as high cost, health hazards, lengthy duration, and high operator requirements (Huang et al., 2015). These methods also raise problems related to the direct use of seeds and the time required to obtain relevant information. The development of new techniques and procedures by which to analyze seed characteristics is driven by the need to overcome these drawbacks. Therefore, several nondestructive methodologies have been developed, many of them being based on the use of different imaging techniques supported by computer vision to rapidly collect and interpret high-resolution images (Patel et al., 2012; Rahman and Cho, 2016; Lin et al., 2019; Galletti et al., 2020). These include thermal imaging (Men et al., 2017; ElMasry et al., 2020), X-rays (Gagliardi and Marcos-Filho, 2011; Giannella et al., 2020; Musaev et al., 2021), and spectroscopic techniques such as near-infrared spectroscopy (NIRS) technologies (Font et al., 2006; Al-Amery et al., 2018; Pagano et al., 2019; Hacisalihoglu et al., 2020), Raman spectroscopy (Edwards et al., 2005; Ambrose et al., 2016; Rahman and Cho, 2016), or hyperspectral imaging (Ambrose et al., 2016; Feng et al., 2019). Although these noninvasive methods represent a faster, deeper, and more precise way to retrieve important information for the evaluation of seed quality, the associated costs, and the required expertise are still prohibitive for large-scale screening of seed lots. Therefore, there is still the need to expand the palette of methods by which to reduce their costs or to promote the development of other cost-effective and sustainable methods.

Given these premises, the current study proposes two biochemical assays that can be employed to detect the levels of ROS as a proxy of seed quality. Why focus on ROS? Because, as already indicated, these are essential molecules with well-proven roles in seed dormancy and germination (Mittler et al., 2011; Wrzaczek et al., 2013; Bailly, 2019; Pagano et al., 2019; Rehmani et al., 2022), relevant processes in the context of seed vigor and seed quality assessment. To prove that the proposed assays can be adopted as methods to test seed quality, we have first developed appropriate materials by applying treatments meant to boost (hydropriming) or inhibit (heat-shock) seed germination. We have adopted soybean as a reference species in this study because of its high agroeconomic relevance as well as possible model legume and availability of database resources (Schmutz et al., 2010; Karges et al., 2022). However, to show that these approaches can be universally applied, we have extended the study to other relevant crops like tomato and wheat, hence covering seed morphological diversity. Indeed, our results show that hydropriming improved germination performance but

this is conditioned by the soaking time. On the other hand, the HS treatments imposed in this study suppressed seed germination.

Having defined the experimental systems, the following step consisted of evaluating ROS levels and comparing the two proposed approaches. Interestingly, even if the DCFH-DA and FOX-1 assays relatively measure different components, namely oxidative status and H_2O_2 released radicals respectively, in the case of soybean the results obtained follow the same pattern: higher levels of ROS in HS and CTRL and low levels during the HP treatments. For the FOX-1 assay, this trend is also maintained in the other investigated species, whereas the DCFH-DA results were much more variable. This may be due to the different types of measurement techniques; on the one hand, the use of a fluorimeter with extracting the baseline fluorescence levels, and, on the other hand, the use of spectrophotometric readings plotted to a standard curve. Moreover, the DCFH-DA assay is generally used to quantify intracellular ROS levels (Lepage et al., 2013; Ortega-Villasante et al., 2016; Wang et al., 2016), whereas FOX-1 is used for measuring the release of specific ROS in the surrounding environment (Bellincampi et al., 2000; Balestrazzi et al., 2011; Bridi et al., 2015). The DCFH is usually oxidized to the fluorescent product DCF by multiple reactive species, and thus it is not specific for a particular ROS (Zielonka et al., 2012; Forman et al., 2015). In addition, other limitations include the fact that DCFH is not oxidized directly by H_2O_2, but only after its conversion to more reactive species, and this oxidation is also sensitive to O_2 levels, light, and pH. Consequently, several studies have indicated that the observed fluorescence may not be proportional with the accumulation of ROS (Kalyanaraman et al., 2012; Kowaltowski, 2019). By contrast, FOX-1 is generally used in an acidic environment, and it relies on the oxidation of Fe^{2+} to Fe^{3+} (Aryal et al., 2019). In this case, hydroperoxides oxidize the ferrous ion to ferric ion, subsequently treated with the XO reagent to generate a ferric-XO complex, resulting in a blue–purple color readable at 550–560 nm (Moon and Shibamoto, 2009). This approach has received much attention not only because of its low cost but also because it is not affected by environmental conditions (e.g., O_2, light) (Christodoulou et al., 2022).

To show that the applied methods are noninvasive, we have monitored the germination percentage of seeds imbibed in the DCFH-DA and FOX-1 reagents for 15 and 30 min, respectively. The results, shown in **Fig. 3.12**, indicate no significative differences were observed between CTRL and imbibed seeds.

3. ROS and seed quality

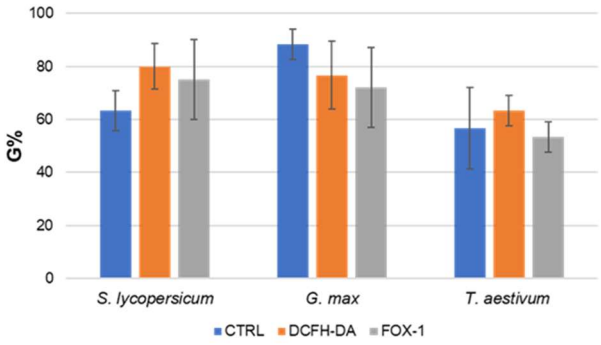

Figure 3.12. Germination percentage (G%) evaluated for *S. lycopersicum*, *G. max*, and *T. aestivum* seeds imbibed in the presence of DCFH-DA and FOX-1 for 15 min and 30 min, respectively. The number of germinated seed was monitored for three days and the data collected at the 3rd day was used to generate the graphic. Statistical differences among treatments and control are represented with asterisks (*), $P \leq 0.05$.

Lastly, to prove that the ROS turnover is influenced within the proposed system, a qRT-PCR approach was adopted to monitor the expression of genes encoding enzymes involved in both ROS production (*RbohE2*, *RbohC2*) and scavenging (*MnSOD*, *SOD1*, *CAT1*, CAT5, APX2). The scientific literature is rich in studies evidencing that seed priming treatments result in differential expression of a myriad of antioxidant genes (Wojtyla et al., 2006; Lee et al., 2010; Forti et al., 2020; Forti et al., 2020; Forti et al., 2021; Zhou et al., 2021; Pagano et al., 2022). And indeed, the observed upregulation of the selected genes is in agreement with the cited data. The upregulation of both ROS production and scavenging genes indicates active ROS turnover; thus while ROS are being produced the antioxidant systems are being activated. Additionally, a correlation analysis was carried out between the measured ROS through the two assays and the levels of expression of the investigated genes. The positive correlations observed between the DCHF-DA and FOX-1 data in the case of soybean seeds indicate that the different types of ROS detected by the two assays display a similar accumulation pattern. By contrast, during seed priming the expression of genes involved in ROS turnover increases while the observed levels of measured ROS decrease. This is statistically reinforced by the recurrent negative correlations observed between the ROS patterns and gene expression levels. This can be thus interpreted as an indication of the efficiency of the antioxidant response in reducing ROS accumulation.

The noninvasiveness and relative rapidity of the proposed assays can have promising outcomes in multiple experimental and applicative contexts. For instance, from an experimental point of view, these can be used to track the kinetics of ROS dynamics for individual seeds, providing a time-lapse to monitor the progression of priming protocols or the activation of the seed pre-germinative metabolism within the "oxidative window" (Bailly, 2019). For the applicative side, whenever seed materials are scarce these assays may allow the evaluation of the quality of a seed lot without losing valuable material. This can be applied to seed bank accessions and elite

breeding materials with important implications on biodiversity preservation in crops and wild species.

3.5 Conclusion

The current study proposes two noninvasive, rapid, cost-effective, and potentially universal techniques by which to measure ROS production in seeds as a proxy of seed quality evaluation. Although the DCFH-DA assay is more variable and subjected to certain limitations in terms of types of measured ROS and interaction with surrounding factors, the FOX-1 approach appears to be more reliable when applied to different types of seeds. Additional proof of the accuracy of the investigated methods is provided through the correlation analysis performed, taking into consideration the measured ROS levels and the expression of genes involved in ROS turnover. To further validate the obtained data, the methods could be subsequently applied to other species, varieties/genotypes, seed types, and experimental conditions, such as different seed lots collected from diverse environments, seed storage conditions, seed aging protocols, and damaging or beneficial treatments.

References

Adhikari, B.; Dhital, P.R.; Ranabhat, S.; Poudel, H. Effect of seed hydro-priming durations on germination and seedling growth of bitter gourd (*Momordica charantia*). *PLoS One*. 2021, 16, e0255258.

Al-Amery, M.; Geneve, R.L.; Sanches, M.F.; Armstrong, P.R.; Maghirang, E.B.; Lee, C.; Hildebrand, D.F. Near-infrared spectroscopy used to predict soybean seed germination and vigour. *Seed Sci. Res.* 2018, 28, 245–252.

Ambrose, A.; Lohumi, S.; Lee, W.H.; Cho, B.K. Comparative nondestructive measurement of corn seed viability using Fourier transform near-infrared (FT-NIR) and Raman spectroscopy. *Sens. Actuators B.* 2016, 224, 500–506.

Aryal, S.; Baniya, M.K.; Danekhu, K.; Kunwar, P.; Gurung, R.; Koirala, N. Total phenolic content, flavonoid content and antioxidant potential of wild vegetables from western *Nepal. Plants.* 2019, 8, 96.

Assaad, H.I.; Hou, Y.; Zhou, L.; Carroll, R.J.; Wu, G. Rapid publication-ready MS-Word tables for two-way ANOVA. *Springerplus* 2015, 4, 33.

Bailly, C. The signalling role of ROS in the regulation of seed germination and dormancy. *Biochem. J.* 2019, 476, 3019–3032.

Bailly, C.; Bogatek-Leszczynska, R.; Côme, D.; Corbineau, F. Changes in activities of antioxidant enzymes and lipoxygenase during growth of sunflower seedlings from seeds of different vigour. *Seed Sci. Res*. 2002, 12, 47–55.

Bailly, C.; El-Maarouf-Bouteau, H.; Corbineau, F. From Intracellular signaling networks to cell death: The dual role of Reactive Oxygen Species in seed physiology. *Comptes Rendus Biol*. 2008, 331, 806–814.

Baalbaki, R.Z.; McDonald, M.B.; Copeland, L.O.; Elias, S.G. Seed Testing: Principles and Practices; Michigan State University Press: *East Lansing*, MI, USA, 2012; Available online: https://www.jstor.org/stable/10.14321/j.ctt7zt51m (accessed on 12 December 2022).

Balestrazzi, A.; Agoni, V.; Tava, A.; Avato, P.; Biazzi, E.; Raimondi, E.; Macovei, A.; Carbonera, D. Cell death induction and nitric oxide biosynthesis in white poplar (*Populus alba*) suspension cultures exposed to alfalfa saponins. *Physiol. Plant* 2011, 141, 227–238.

Balestrazzi, A.; Confalonieri, M.; Macovei, A.; Carbonera, D. Seed imbibition in *Medicago truncatula* Gaertn.: Expression profiles of DNA repair genes in relation to PEG-mediated stress. J. *Plant Physiol*. 2011, 168, 706–713.

Bellincampi, D.; Dipierro, N.; Salvi, G.; Cervone, F.; De Lorenzo, G. Extracellular H2O2 induced by oligogalacturonides is not involved in the inhibition of the auxin-regulated rolB gene expression in tobacco leaf explants. *Plant Physiol*. 2000, 122, 1379–1385.

Bassel, G.W.; Fung, P.; Chow, T.F.; Foong, J.A.; Provart, N.J.; Cutler, S.R. Elucidating the germination transcriptional program using small molecules. *Plant Physiol*. 2008, 147, 143–155.

Bridi, R.; González, A.; Bordeu, E.; López-Alarcón, C.; Aspée, A.; Diethelm, B.; Versari, A. Monitoring peroxides generation during model wine fermentation by FOX-1 assay. *Food Chem*. 2015, 175, 25–28.

Carrillo-Reche, J.; Vallejo-Marín, M.; Quilliam, R.S. Quantifying the potential of 'on-farm' seed priming to increase crop performance in developing countries. A meta-analysis. *Agron. Sustain. Dev*. 2018, 38, 64.]

Ciacka, K.; Staszek, P.; Sobczynska, K.; Krasuska, U.; Gniazdowska, A. Nitric oxide in seed biology. *Int. J. Mol. Sci.* 2022, 23, 14951.

Christodoulou, M.C.; Orellana Palacios, J.C.; Hesami, G.; Jafarzadeh, S.; Lorenzo, J.M.; Domínguez, R.; Moreno, A.; Hadidi, M. Spectrophotometric methods for measurement of antioxidant activity in food and pharmaceuticals. *Antioxidants* 2022, 11, 2213.

Colombo, F.; Pagano, A.; Sangiorgio, S.; Macovei, A.; Balestrazzi, A.; Araniti, F.; Pilu, R. Study of seed ageing in lpa1-1 maize mutant and two possible approaches to restore seed germination. *Int. J. Mol. Sci*. 2023, 24, 732.

Damalas, C.A.; Koutroubas, S.D.; Fotiadis, S. Hydro-priming effects on seed germination and field performance of faba bean in spring sowing. *Agriculture* 2019, 9, 201.

Devika, O.S.; Singh, S.; Sarkar, D.; Barnwal, P.; Suman, J.; Rakshit, A. Seed priming: A potential supplement in integrated resource management under fragile intensive ecosystems. *Front. Sustain. Food Syst.* 2021, 5, 654001.

Demir, I.; Ozden, Y.S.; Yilmaz, K. Accelerated ageing test of aubergine, cucumber and melon seeds in relation to time and temperature variables. *Seed Sci. Technol*. 2004, 32, 851–855.

Dezfuli, P.M.; Sharif-Zadeh, F.; Janmohammadi, M. Influence of priming techniques on seed germination behavior of maize inbred lines (*Zea mays* L.). *A.R.P.N. J. Agric. Biol. Sci*. 2008, 3, 22–25.

Doria, E.; Pagano, A.; Ferreri, C.; Larocca, A.V.; Macovei, A.; Araújo, S.S.; Balestrazzi, A. How does the seed pre-germinative metabolism fight against imbibition damage? Emerging roles of fatty acid cohort and antioxidant defence. *Front. Plant Sci*. 2019, 10, 1505.

Dutra, A.S.; Vieira, R.D. Accelerated ageing test to evaluate seed vigor in pumpkin and zucchini seeds. *Seed Sci. Technol*. 2006, 34, 209–214.

Edwards, H.G.; Villar, S.E.J.; De Oliveira, L.F.C.; Le Hyaric, M. Analytical Raman spectroscopic study of cacao seeds and their chemical extracts. *Anal. Chim. Acta* 2005, 538, 175–180.

El-Maarouf-Bouteau, H. The seed and the metabolism regulation. *Biology* 2022, 11, 168.

ElMasry, G.; ElGamal, R.; Mandour, N.; Gou, P.; Al-Rejaie, S.; Belin, E.; Rousseau, D. Emerging thermal imaging techniques for seed quality evaluation: Principles and applications. *Food Res. Int.* 2020, 131, 109025.

Eruslanov, E.; Kusmartsev, S. Identification of ROS using oxidized DCFDA and flow-cytometry. *Methods Mol. Biol*. 2010, 594, 57–72.

Farooq, M.A.; Ma, W.; Shen, S.; Gu, A. Underlying biochemical and molecular mechanisms for seed germination. *Int. J. Mol. Sci*. 2022, 23, 8502.

Feng, L.; Zhu, S.; Liu, F.; He, Y.; Bao, Y.; Zhang, C. Hyperspectral imaging for seed quality and safety inspection: A review. *Plant Methods* 2019, 15, 1–25.

Font, R.; del Río-Celestino, M.; de Haro-Bailón, A. The use of near-infrared spectroscopy (NIRS) in the study of seed quality components in plant breeding programs. *Ind. Crop Prod*. 2006, 24, 307–313.

Forman, H.J.; Augusto, O.; Brigelius-Flohe, R.; Dennery, P.A.; Kalyanaraman, B.; Ischiropoulos, H.; Mann, G.E.; Radi, R.; Roberts, L.J.; Vina, J.; et al. Even free radicals should follow some rules: A guide to free radical research terminology and methodology. *Free Radic. Biol. Med*. 2015, 78, 233–235.

Forti, C.; Ottobrino, V.; Bassolino, L.; Toppino, L.; Rotino, G.L.; Pagano, A.; Macovei, A.; Balestrazzi, A. Molecular dynamics of pre-germinative metabolism in primed eggplant (*Solanum melongena* L.) seeds. *Hortic. Res*. 2020, 7, 87.

Forti, C.; Ottobrino, V.; Doria, E.; Bassolino, L.; Toppino, L.; Rotino, G.L.; Pagano, P.; Macovei, A.; Balestrazzi, A. Hydropriming applied on fast germinating *Solanum villosum* Miller seeds: Impact on pre-germinative metabolism. *Front. Plant Sci*. 2021, 12, 639336.

Forti, C.; Shankar, A.; Singh, A.; Balestrazzi, A.; Prasad, V.; Macovei, A. Hydropriming and biopriming improve *Medicago truncatula* seed germination and upregulate DNA repair and antioxidant genes. *Genes* 2020, 11, 242.

França-Neto, J.D.B.; Krzyzanowski, F.C. Tetrazolium: An important test for physiological seed quality evaluation. *J. Seed Sci*. 2019, 41, 359–366.

Gagliardi, B.; Marcos-Filho, J. Relationship between germination and bell pepper seed structure assessed by the X-ray test. *Scientia Agricola* 2011, 68, 411–416.

Galletti, P.A.; Carvalho, M.E.; Hirai, W.Y.; Brancaglioni, V.A.; Arthur, V.; Barboza da Silva, C. Integrating optical imaging tools for rapid and non-invasive characterization of seed quality: Tomato (*Solanum lycopersicum* L.) and carrot (*Daucus carota* L.) as study cases. *Front. Plant Sci*. 2020, 11, 577851.

Gianella, M.; Balestrazzi, A.; Pagano, A.; Müller, J.V.; Kyratzis, A.C.; Kikodze, D.; Canella, M.; Mondoni, A.; Rossi, G.; Guzzon, F. Heteromorphic seeds of wheat wild relatives show germination niche differentiation. *Plant Biol*. 2020, 22, 191–202.

Gianella, M.; Doria, E.; Dondi, D.; Milanese, C.; Gallotti, L.; Börner, A.; Zannino, L.; Macovei, A.; Pagano, A.; Guzzon, F.; et al. Physiological and molecular aspects of seed longevity: Exploring intra-species variation in eight *Pisum sativum* L. accessions. *Physiol. Plant*. 2022, 174, e13698.

Hacisalihoglu, G.; Freeman, J.; Armstrong, P.R.; Seabourn, B.W.; Porter, L.D.; Settles, A.M.; Gustin, J.L. Protein, weight, and oil prediction by single-seed near-infrared spectroscopy for selection of seed quality and yield traits in pea (*Pisum sativum*). *J. Sci. Food Agric*. 2020, 100, 3488–3497.

Hay, F.R.; Whitehouse, K.J. Rethinking the approach to viability monitoring in seed genebanks. *Conserv. Physiol*. 2017, 5, cox009.

Huang, M.; Wang, Q.G.; Zhu, Q.B.; Qin, J.W.; Huang, G. Review of seed quality and safety tests using optical sensing technologies. *Seed Sci. Technol*. 2015, 43, 337–366.

Ijaz, B.; Formentin, E.; Ronci, B.; Locato, V.; Barizza, E.; Hyder, M.Z.; Lo Schiavo, F.; Yasmin, T. Salt tolerance in indica rice cell cultures depends on a fine tuning of ROS signalling and homeostasis. *PLoS One* 2019, 14, e0213986.

Ishibashi, Y.; Yuasa, T.; Iwaya-Inoue, M. Mechanisms of maturation and germination in crop seeds exposed to environmental stresses with a focus on nutrients, water status, and Reactive Oxygen Species. *Adv. Exp. Med. Biol*. 2018, 1081, 233–257.

Johnson, R.; Puthur, J.T. Seed priming as a cost effective technique for developing plants with cross tolerance to salinity stress. *Plant Physiol. Biochem*. 2021, 162, 247–257.

Juan, C.A.; Pérez de la Lastra, J.M.; Plou, F.J.; Pérez-Lebeña, E. The chemistry of Reactive Oxygen Species (ROS) revisited: Outlining their role in biological macromolecules (DNA, lipids and proteins) and induced pathologies. *Int. J. Mol. Sci*. 2021, 22, 4642.

Jurdak, R.; Rodrigues, G.A.G.; Chaumont, N.; Schivre, G.; Bourbousse, C.; Barneche, F.; Bou Dagher Kharrat, M.; Bailly, C. Intracellular reactive oxygen species trafficking participates in seed dormancy alleviation in Arabidopsis seeds. *New Phytol*. 2022, 234, 850–866.

Kalyanaraman, B.; Darley-Usmar, V.; Davies, K.J.; Dennery, P.A.; Forman, H.J.; Grisham, M.B.; Mann, G.E.; Moore, K.; Roberts, L.J.; Ischiropoulos, H. Measuring reactive oxygen and nitrogen species with fluorescent probes: Challenges and limitations. *Free Radic. Biol. Med*. 2012, 52, 1–6.

Karges, K.; Bellingrath-Kimura, S.D.; Watson, C.A.; Stoddard, F.L.; Halwani, M.; Reckling, M. Agro-economic prospects for expanding soybean production beyond its current northerly limit in Europe. Eur. *J. Agron*. 2022, 133, 126415.

Kim, D.H. Extending Populus seed longevity by controlling seed moisture content and temperature. *PLoS One* 2018, 13, e0203080.

Klupczyńska, E.A.; Dietz, K.J.; Małecka, A.; Ratajczak, E. Mitochondrial peroxiredoxin-IIF (PRXIIF) activity and function during seed aging. *Antioxidants* 2022, 11, 1226.

Kowaltowski, A.J. Strategies to detect mitochondrial oxidants. *Redox Biol*. 2019, 21, 101065.

Kranner, I.; Roach, T.; Beckett, R.P.; Whitaker, C.; Minibayeva, F.V. Extracellular production of reactive oxygen species during seed germination and early seedling growth in *Pisum sativum*. *J. Plant Physiol*. 2010, 167, 805–811.

Kurek, K.; Plitta-Michalak, B.; Ratajczak, E. Reactive Oxygen Species as potential drivers of the seed aging process. *Plants* 2019, 8, 174.

Lechowska, K.; Kubala, S.; Wojtyla, Ł.; Nowaczyk, G.; Quinet, M.; Lutts, S.; Garnczarska, M. New insight on water status in germinating *Brassica napus* seeds in relation to priming-improved germination. *Int. J. Mol. Sci*. 2019, 20, 540.

Lee, Y.P.; Baek, K.-H.; Lee, H.-S.; Kwak, S.-S.; Bang, J.-W.; Kwon, S.-Y. Tobacco seeds simultaneously over-expressing Cu/Zn-superoxide dismutase and ascorbate peroxidase display enhanced seed longevity and germination rates under stress conditions. *J. Exp. Bot*. 2010, 61, 2499–2506.

Lepage, É.; Zampini, É.; Brisson, N. Plastid genome instability leads to reactive oxygen species production and plastid-to-nucleus retrograde signaling in Arabidopsis. *Plant Physiol*. 2013, 163, 867–881.

Lin, P.; Xiaoli, L.; Li, D.; Jiang, S.; Zou, Z.; Lu, Q.; Chen, Y. Rapidly and exactly determining postharvest dry soybean seed quality based on machine vision technology. *Sci. Rep*. 2019, 9, 1–11.

Macovei, A.; Garg, B.; Raikwar, S.; Balestrazzi, A.; Carbonera, D.; Buttafava, A.; Bremont, J.F.J.; Gill, S.S.; Tuteja, N. Synergistic exposure of rice seeds to different doses of gamma-ray and salinity stress resulted in increased antioxidant enzyme activities and gene-specific modulation of TC-NER pathway. Biomed. Res. Int. 2014, 2014, 676934.

Macovei, A.; Pagano, A.; Leonetti, P.; Carbonera, D.; Balestrazzi, A.; Araújo, S.S. Systems biology and genome-wide approaches to unveil the molecular players involved in the pre-germinative metabolism: Implications on seed technology traits. *Plant Cell Rep*. 2017, 36, 669–688.

Mal, D.; Verma, J.; Levan, A.; Reddy, M.R.; Avinash, A.V.; Velaga, P.K. Seed priming in vegetable crops: A review. *Int. J. Curr. Microb. Appl. Sci*. 2019, 8, 868–874.

Marta, B.; Szafrańska, K.; Posmyk, M.M. Exogenous melatonin improves antioxidant defense in cucumber seeds (*Cucumis sativus* L.) germinated under chilling stress. *Front. Plant Sci*. 2016, 7, 575.

Marthandan, V.; Geetha, R.; Kumutha, K.; Renganathan, V.G.; Karthikeyan, A.; Ramalingam, J. Seed priming: A feasible strategy to enhance drought tolerance in crop plants. *Int. J. Mol. Sci*. 2020, 21, 8258.

Men, S.; Yan, L.; Liu, J.; Qian, H.; Luo, Q. A classification method for seed viability assessment with infrared thermography. *Sensors* 2017, 17, 845.

Milivojević, M.; Ripka, Z.; Petrović, T. ISTA rules changes in seed germination testing at the beginning of the 21st century. *J. Process Energy Agric*. 2018, 22, 40–45.

Mirmazloum, I.; Kiss, A.; Erdélyi, É.; Ladányi, M.; Németh, É.Z.; Radácsi, P. The effect of osmopriming on seed germination and early seedling characteristics of *Carum carvi* L. *Agriculture* 2020, 10, 94.

Mittler, R.; Vanderauwera, S.; Suzuki, N.; Miller, G.; Tognetti, V.B.; Vandepoele, K.; Gollery, M.; Shulaev, V.; Van Breusegem, F. ROS signaling: The new wave? *Trends Plant Sci.* 2011, 16, 300–309.

Moon, J.K.; Shibamoto, T. Antioxidant assays for plant and food components. *J. Agric. Food Chem*. 2009, 57, 1655–1666.

Musaev, F.; Priyatkin, N.; Potrakhov, N.; Beletskiy, S.; Chesnokov, Y. Assessment of Brassicaceae seeds quality by X-ray analysis. *Horticulturae* 2021, 8, 29.

Ortega-Villasante, C.; Burén, S.; Barón-Sola, Á.; Martínez, F.; Hernández, L.E. In vivo ROS and redox potential fluorescent detection in plants: Present approaches and future perspectives. *Methods* 2016, 109, 92–104.

Pang, Z.; Chong, J.; Zhou, G.; de Lima Morais, D.A.; Chang, L.; Barrette, M.; Gauthier, C.; Jacques, P.É.; Li, S.; Xia, J. MetaboAnalyst 5.0: Narrowing the gap between raw spectra and functional insights. *Nucleic Acids Res*. 2021, 49, W388–W396.

Pagano, A.; Folini, G.; Pagano, P.; Sincinelli, F.; Rossetto, A.; Macovei, A.; Balestrazzi, A. ROS accumulation as a hallmark of dehydration stress in primed and overprimed *Medicago truncatula* seeds. *Agronomy* 2022, 12, 268.

Pagano, A.; Forti, C.; Gualtieri, C.; Balestrazzi, A.; Macovei, A. Oxidative stress and antioxidant defense in germinating seeds. A Q&A session. In Reactive Oxygen, Nitrogen and Sulfur Species in Plants: Production, Metabolism, Signaling and Defense Mechanisms; Hasanuzzaman, M., Fotopoulos, V., Nahar, K., Fujita, M., Eds.; *John Wiley & Sons Ltd*.: Hoboken, NJ, USA, 2019; pp. 267–289.

Pagano, A.; Macovei, A.; Balestrazzi, A. Molecular dynamics of seed priming at the crossroads between basic and applied research. *Plant Cell Rep*. 2023, 13, 1–32.

Paparella, S.; Araújo, S.S.; Rossi, G.; Wijayasinghe, M.; Carbonera, D.; Balestrazzi, A. Seed priming: State of the art and new perspectives. *Plant Cell Rep*. 2015, 34, 1281–1293.

Pasqualini, S.; Tedeschini, E.; Frenguelli, G.; Wopfner, N.; Ferreira, F.; D'Amato, G.; Ederli, L. Ozone affects pollen viability and NAD (P) H oxidase release from *Ambrosia artemisiifolia* pollen. *Environ. Pollut*. 2011, 159(10), 2823-2830.

Patel, K.K.; Kar, A.; Jha, S.N.; Khan, M.A. Machine vision system: A tool for quality inspection of food and agricultural products. *J. Food Sci. Technol*. 2012, 49, 123–141.

Petrović, T.; Milivojević, M.; Branković-Radojčić, D.V.; Jovanović, S.; Vujinović, J.; Vukadinović, R.; Stojadinović-Životić, J. Identification of early decline of seed quality by vigor tests. In Proceedings of the 25th EUCARPIA Maize and Sorghum Conference — Current Challenges and New Methods for Maize and Sorghum Breeding, Belgrade-Book of Abstracts, Belgrade, Serbia, 30 May–2 June 2022; p. 61.

Rahman, A.; Cho, B.K. Assessment of seed quality using non-destructive measurement techniques: A review. *Seed Sci. Res*. 2016, 26, 285–305.

Ranal, M.A.; Garcia de Santana, D. How and why to measure the germination process? *Braz. J. Bot*. 2006, 29, 1–11.

Reed, R.C.; Bradford, K.J.; Khanday, I. Seed germination and vigor: Ensuring crop sustainability in a changing climate. *Heredity* 2022, 128, 450–459.

Rehmani, M.S.; Aziz, U.; Xian, B.; Shu, K. Seed dormancy and longevity: A mutual dependence or a trade-off? *Plant Cell Physiol*. 2022, 63, 1029–1037.

Rhaman, M.S.; Imran, S.; Rauf, F.; Khatun, M.; Baskin, C.C.; Murata, Y.; Hasanuzzaman, M. Seed Priming with phytohormones: An effective approach for the mitigation of abiotic stress. *Plants* 2020, 10, 37.

Richards, S.L.; Wilkins, K.A.; Swarbreck, S.M.; Anderson, A.A.; Habib, N.; Smith, A.G.; McAinsh, M.; Davies, J.M. The hydroxyl radical in plants: From seed to seed. *J. Exp. Bot*. 2015, 66, 37–46.

Schmutz, J.; Cannon, S.B.; Schlueter, J.; Ma, J.; Mitros, T.; Nelson, W.; Hyten, D.L.; Song, Q.; Thelen, J.J.; Cheng, J.; et al. Genome sequence of the palaeopolyploid soybean. *Nature* 2010, 463, 178–183.

Schopfer, P.; Plachy, C.; Frahry, G. Release of reactive oxygen intermediates (superoxide radicals, hydrogen peroxide, and hydroxyl radicals) and peroxidase in germinating radish seeds controlled by light, gibberellin, and abscisic acid. *Plant Physiol*. 2001, 125, 1591–1602.

Severin, A.J.; Woody, J.L.; Bolon, Y.T.; Joseph, B.; Diers, B.W.; Farmer, A.D.; Muehlbauer, G.J.; Nelson, R.T.; Grant, D.; Specht, J.E.; et al. RNA-Seq Atlas of *Glycine max*: A guide to the soybean transcriptome. *BMC Plant Biol*. 2010, 10, 1–16.

Soares, V.N.; Elias, S.G.; Gadotti, G.I.; Garay, A.E.; Villela, F.A. Can the tetrazolium test be used as an alternative to the germination test in determining seed viability of grass species? *Crop Sci*. 2016, 56, 707–715.

Thomsen, R.; Sølvsten, C.A.; Linnet, T.E.; Blechingberg, J.; Nielsen, A.L. Analysis of qPCR data by converting exponentially related Ct values into linearly related X0 values. *J. Bioinform. Comput. Biol.* 2010, 8, 885–900.

Wan, Q.; Chen, S.; Shan, Z.; Yang, Z.; Chen, L.; Zhang, C.; Yuan, S.; Hao, Q.; Zhang, X.; Qiu, D.; et al. Stability evaluation of reference genes for gene expression analysis by RT-qPCR in soybean under different conditions. *PLoS One* 2017, 12, e0189405.

Wang, W.-H.; He, E.-M.; Guo, Y.; Tong, Q.-X.; Zheng, H.-L. Chloroplast calcium and ROS signaling networks potentially facilitate the primed state for stomatal closure under multiple stresses. *Environ. Exp. Bot*. 2016, 122, 85–93.

Wojtyla, Ł.; Garnczarska, M.; Zalewski, T.; Bednarski, W.; Ratajczak, L.; Jurga, S. A comparative study of water distribution, free radical production and activation of antioxidative metabolism in germinating pea seeds. *J. Plant Physiol*. 2006, 163, 1207–1220.

Wolff, S.P. Ferrous ion oxidation in presence of ferric ion indicator xylenol orange for measurement of hydroperoxides. *Methods Enzymol*. 1994, 233, 182–189.

Wrzaczek, M.; Brosché, M.; Kangasjärvi, J. ROS signaling loops—Production, perception, regulation. *Curr. Opin. Plant Biol*. 2013, 16, 575–582.

Yang, Z.; Zhi, P.; Chang, C. Priming seeds for the future: Plant immune memory and application in crop protection. *Front. Plant Sci*. 2022, 13, 961840.

Zhou, M.; Hassan, M.J.; Peng, Y.; Liu, L.; Liu, W.; Zhang, Y.; Li, Z. γ-Aminobutyric Acid (GABA) priming improves seed germination and seedling stress tolerance associated with enhanced antioxidant metabolism, DREB expression, and dehydrin accumulation in white clover under water stress. *Front. Plant Sci*. 2021, 12, 776939.

Zielonka, J.; Zielonka, M.; Sikora, A.; Adamus, J.; Joseph, J.; Hardy, M.; Ouari, O.; Dranka, B.P.; Kalyanaraman, B. Global profiling of reactive oxygen and nitrogen species in biological systems: High-throughput real-time analyses. *J. Biol. Chem*. 2012, 287, 2984–2

4. Non-invasive methods to assess seed quality based on ultra-weak photon emission and delayed luminescence

The work in this chapter was published in *Scientific Reports* (Impact Factor 3.8) on November 5, 2024 with the title "Non-invasive methods to assess seed quality based on ultra-weak photon emission and delayed luminescence" (https://www.nature.com/articles/s41598-024-74207-9#citeas). My contribution to this article is described below. I performed the UPE and DL measurements using the LIANA® light analyzer. I carried out the germination tests, calculated all the associated parameters, and integrated all data to obtain the complete datasets for machine-learning operations. I developed different predictive models, calculated the classification parameters, and carried out the statistical analysis. I was actively involved in data analysis and all the manuscript preparation steps. This work was supported by the Bayer Foundation Fellowship Program 2022 "Jeff Schell Fellowships for Agricultural Sciences" which grated me funding for the 6 months spent at IPK (https://www.bayer-foundation.com/news-stories/science/meet-our-2022-scientific-fellowship-awardees).

Abstract

Seed quality is the set of physical, genetic, and physiological characteristics, reflecting the overall germination potential. Maintaining an optimal seed quality is essential for agriculture and seed banks to preserve genetic diversity. Compared to conventional methods (e.g., germination tests), non-invasive approaches allow a more sustainable and rapid evaluation of seed quality but this is limited by high costs. The measurement of ultra-weak photon emission (UPE) and delayed fluorescence (DL), defined as biological phenomena potentially related to the physiological status of living systems, may represent a suitable approach to estimate seed quality. To test this hypothesis, seeds of five agriculturally relevant legume species (*Phaseolus vulgaris* L., *Lathyrus sativus* L., *Cicer arietinum* L., *Pisum sativum* L., and *Vicia faba* L.), stored at different conditions (room temperature or -18 °C) for several years, were analyzed using a LIANA© prototype to collect data regarding DL and UPE occurring after UV excitation. The obtained data were integrated with germination parameters which underline species-specific behaviors in response to storage conditions. The prediction models show variable efficiency in classifying seeds based on germination which underline species-dependent links between photon emission and seed quality. Therefore, these measurements represent novel, non-invasive, universal, and rapid approaches to evaluate seed quality.

4.1 Introduction

Seed quality is the set of genetic, physiological, and physical features of seeds (https://www.seedtest.org/). Since seed quality reflects the overall germination potential and influences crop production, its evaluation is crucial for seed companies and consumers to both optimize economic profits and increase the final crop yield (Huang et al., 2015). Crop production must be increased to meet the ZERO HUNGER target relative to the Sustainable Developmental Goal SDG#2 of the 2030 UN Agenda for Sustainable Development (https://www.un.org/sustainabledevelopment/). In a scenario where crop production must be sustainably enhanced, novel methods to assess seed quality can substantially increase the availability of high-quality seeds, with a positive effect on agriculture costs and food production.

Monitoring seed quality is very important for many stakeholders, including germplasm banks, breeders, agronomists, seed companies and consumers (Huang et al., 2015). The use of high-quality seeds is a proxy of the seed market, which translates into a continuous increase in the commercial seed market trends (https://www.thebusinessresearchcompany.com/report/seeds-global-market-report). Several methods are available for seed quality testing. Conventional germination, electrical conductivity, seedling growth, triphenyltetrazolium chloride (TTC) test, and accelerated ageing are approved by the International Seed Testing Association (ISTA) and constitute the most used approaches so far (McDonald, 1989; McDonald, 1998; Elizalde et al., 2016). However, these methods have some considerable limitations, including invasiveness, extensive amount of test work required, long test periods, low accuracy, and operator biases (Huang et al., 2015). To efficiently measure seed quality and avoid the waste of resources, novel methods to assess it and subsequent quality attributes are necessary and highly sought. To this purpose, non-invasive optical techniques, including machine vision (Ureña et al., 2001; Lin et al., 2019), NIR (Near-InfraRed), Raman spectroscopies (Zhu et al., 2015; Li et al., 2022), thermal, X-ray, and hyperspectral imaging (Feng et al., 2019; ElMasry et al., 2020; Musaev et al., 2022), have been developed and applied to test seed quality. Despite their advantages in gaining high-throughput information in a rapid, non-invasive, and accurate manner, the high cost and the complexity of these technologies limit their large-scale use (Rahman and Cho, 2016). So far, no universal approach has been developed to assess seed quality in a rapid, accurate, economic, and non-destructive manner. Therefore, the search for such methods is still highly required and requested.

Ultra-weak photon emission (UPE) is defined as the luminescence generated from the production of electronically excited species produced from the oxidative processes (Du et al., 2023). Since oxidative reactions are solely responsible for the spontaneous generation of photons, this phenomenon potentially occurs in living cells of all organisms, from bacteria to animals (Cifra and Pospíšil, 2014). Although the origin and the nature of the electronically excited species are partially unknown and very complex, Cilento and Adam (Cilento and Adam, 1995) described the concept of electronic excitation and the electronic configuration of molecules on the ground state T0, the singlet state S1, and the triplet state T1, which stand at the basis of this process. The transition of electrons that occurs in common oxidation and reduction

reactions results in the transition of the molecule into different energy states (T0, S1, T1) due to the different energy of the electrons exchanged. Photon release marks the transition of a molecule from an excited state (S1 or T1) to the starting state T0 (Cilento and Adam, 1995; Cifra and Pospíšil, 2014). Most of the pathways that generate electronically excited species involve radical species as well as oxygen molecules for the electronic transition (Cilento and Adam, 1995), confirming the importance of ROS (reactive oxygen species) in this process. UPE can be spontaneous, where the release of photons during the oxidative processes happens without any external stressors or stimuli, or it can be induced by stress and oxidative factors that promote oxidative reaction rates (Wang et al., 2011; Cifra and Pospíšil, 2014). Another phenomenon related to UPE is Delayed Luminescence (DL), defined as the long-term afterglow of biological systems after illumination (Popp and Yan, 2002). The DL general trend is characterized by an initial peak of intensity (in terms of the number of photons released per time) followed by a rapid decay. DL can occur for seconds or milliseconds, depending on the time of the inductor and the system used (Goltsev et al., 2009).

In recent years, the possible link between UPE, DL, and the physiological state of biological systems has gained more interest from the scientific community. Because UPE and DL are generated from oxidative processes occurring during metabolic reactions, it is connected with ROS production (Kobayashi, 2014; Pospíšil et al., 2014; Sun et al., 2022; Zhang et al., 2022), molecules involved in many biological processes (Murphy et al., 2011), including seed quality and germination (Griffo et al., 2023). UPE and DL have been successfully applied to evaluate food quality (Stolz et al., 2019). Similarly, these phenomena have been linked to germination, pointing to a connection between the physiological state and photon release (Grasso et al., 2018; Adeboye and Börner, 2020). In the context of seed evaluation, DL has been applied to detect additional features like water content (Yan et al., 2003) and viability (Costanzo et al., 2008). Although these initial reports provide insights into the UPE and DL application in seed biology, the complex features of the phenomena and their implications, require further investigation. Therefore, the aim of this study was to assess the use of UPE and DL as universal tools to predict seed quality taking into consideration multiple species and accessions. Germination performance was evaluated in five legume species (*Phaseolus vulgaris* L., *Lathyrus sativus* L., *Cicer arietinum* L., *Pisum sativum* L., and *Vicia faba* L.), using seeds stored at different conditions (room temperature or -18 °C) for more than ten years. UPE and DL occurring after UV excitation were collected using a LIANA© prototype and the generated data were integrated with the germination parameters using machine learning algorithms to generate prediction models to estimate seed quality in a non-invasive manner.

4.2 Materials and Methods

4.2.1. Seed materials and storage

Seeds of five legume species, namely bean (*Phaseolus vulgaris* L.), Faba bean (*Vicia faba* L.), pea (*Pisum sativum* L.), grass pea (*Lathyrus sativus* L.), and chickpea (*Cicer arietinum* L.), were originated from the genebank collection of the Leibniz-Institute of Plant Genetics and Crop Plant Research (IPK, Gatersleben, Germany) where the material was regenerated under field conditions. Harvest of the seeds was made by hand. After threshing and cleaning the seeds were placed in a drying chamber at a temperature of 22 ± 2°C and a relative humidity of 11 ± 3% for four weeks. Afterward, the material was divided and transferred either to the cold chamber of the genebank (Cold, sealed glass chars, silica gel on top of the seeds, -18°C ± 2°C) or to an ambient storage room (Amb, paper bags, 20°C ± 2°C, 50% ± 3% RH). For each species, 200 seeds per accession were used in the present work. These were divided into distinct seed samples (biological replicates) based on seed size; for *L. sativus* accessions, four replicates of 50 seeds each; for *C. arietinum* and *P. sativum* accessions, five replicates of 40 seeds each; for *P. vulgaris* and *V. faba* accessions, eight replicates of 25 seeds each. Different numbers of accessions per species were used as follows: 22 accessions for *P. vulgaris*, *P. sativum*, and *C. arietinum*, 12 accessions for *L. sativus*, and 11 accessions for *V. faba*. The time of storage was selected based on previous seed bank analyses carried out to identify the most suitable conditions where contrastive germination performance could be observed (Nagel and Börner, 2010). The accessions used here were collected at different harvest years: 2010 for *L. sativus* and *P. sativum*, 2012 for *P. vulgaris*, and 2013 for *V. faba* and *C. arietinum*.

4.2.2. Germination parameters

Germination tests were performed following the guidelines provided by ISTA (International Rules for Seed Testing (https://www.seedtest.org/) with some modifications. The conditions for each species/accession were as follows: for *P. vulgaris,* and *C. arietinum* seed were germinated at 25°C for 8 days; for *P. sativum* seed were germinated at 20°C for 8 days; for *V. faba* and *L. sativus* seed were germinated at 20°C for 10 days. For *V. faba*, seeds were maintained at 4°C for 7 days before starting the germination test. Seeds stored at Amb and Cold conditions were monitored in parallel. Different groups of seeds (*L. sativus*, 4 replicates of 50 seeds/replicate; *P. sativum* and *C. arietinum*, 5 replicates of 40 seeds/replicate; *V. faba* and *P. vulgaris*, 8 replicates of 25 seeds/replicate) were placed in germination trays containing filter paper moistened with distilled water. All containers were kept in a growth chamber at the indicated temperatures under 16 h dark/8 h light. At the end of germination, the following germination indices were calculated: germination percentage (G), mean germination time (MGT), and synchronicity index (Z) (Ranal and de Santana, 2006). The formulas used for the calculation of these parameters are the following.

4. UPE/DL and seed quality

$$(1)\ G\% = \left(\frac{number\ of\ germinated\ seeds)}{total\ number\ of\ seeds}\right) \times 100$$

$$(2)\ MGT = \frac{\sum_{i=1}^{k} ni\ x\ ti}{\sum_{i=1}^{k} ni}$$

$$(3)\ Z = \frac{\sum Cni,2}{\sum ni\ x\ \sum(ni-\frac{1}{2})}$$

In MGT (2) and Z (3) formulas, *ni* is the number of seeds germinated in the time *i* (not the accumulated number, but the number correspondent to the *ith* observation), *ti* corresponds to the time from the start of the experiment to the *ith* observation (day), *k* is the last time of germination, and *Cni,2* = *ni* (*ni*-1)/2. Germination data were analysed with Student *t*-test using the Microsoft Excel package using as threshold the *p*-value ≤ 0.05 ('*').

Seedling growth was monitored on the final day of the germination test by using ImageJ (https://imagej.nih.gov/ij/) software. For each accession and replicate, 20% of the seedlings were photographed and used to determine the seedling length in terms of roots and/or aerial parts.

4.2.3. Statistical analyses

Germination and physical traits data were analysed with Student *t*-test using the Microsoft Excel package using as threshold the $P \leq 0.05$ ('*'). For correlation analyses, Pearson's correlation coefficient and the relative p-values were determined by using MetaboAnalyst 6.0 (https://www.metaboanalyst.ca/) (Pang et al., 2024). The same software was also used for principal component analysis (PCA) performed by using all the germination parameters. The obtained "score plot" graphics show how the different sample groups are clustered according to the results obtained in the performed analyses.

4.2.4. UPE and DL detection

A light analyzer (LIANA©, SuperLab, Käthe-Kruse-Str. 11, 26160 Bad Zwischenahn, Germany, https://www.super-lab.de//liana.html) has been used to collect UPE and DL data of seed samples. This prototype is covered by the SuperLab IP copyright patent number EP 2613139 A1. As shown in **Fig. 4.1**, the LIANA© prototype contains seven photomultiplier tubes along with filters to form seven sensors that detect light emission at different wavelengths. The characteristics of the photomultiplier tubes (PMTs, Hamamatsu Photonics), including model type, spectrum and filter bandpass wavelength are presented in **Table 4.1**.

For the DL excitation, 6 LED with the spectral range 380-420 nm were used. The measurements were conducted with the following parameters: time, 10 (10 seconds measurement time); frequency, 100 (measure every 0.1 second); size, 100; distance,

10; surface, 10; illumination time, 1 (1-second illumination); darkcount time, 5 (5 seconds darkcount data before and after each measurement); dark-count frequency, 100 (measure every 0.1 second). For each sample, measures were taken five times (technical replicates), from which eventual outliers have been eliminated. At least three technical replicates have been retained for each seed sample. For a more realistic photon count estimation, a darkcount measurement is automatically performed before and after each measurement, averaged and subtracted from the values of the PMTs (the photon counted during the measurement time). Then a "real amount of photons" is calculated by multiplying this new value by correction factors, based on the position of the PMTs, the filter used, and the overlapping of wavelengths with other PMTs. In addition to the corrected photon counts, a large number of features reflecting the UPE and DL phenomena are acquired and included in the datasets.

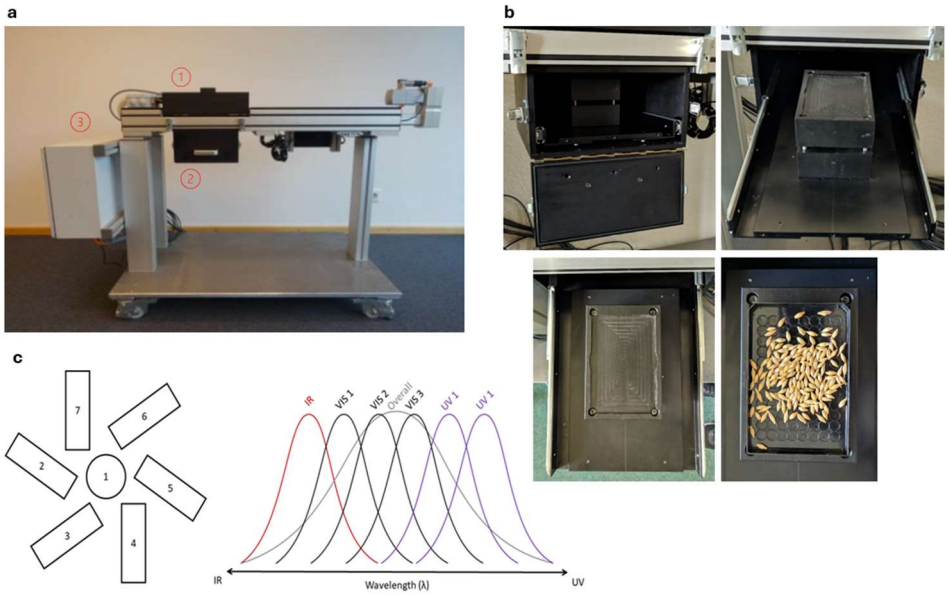

Figure 4.1. Representative images showing the structure of the LIANA© device and its use for light analysis on seeds. (**a**) The main structure of the LIANA© device illustrating (1) the excitation source, which includes the PMTs (photomultiplier tubes), (2) the sample chamber, and (3) the electrical block. (**b**) The seed chamber. It can be opened by releasing the clips on either side (top left). The front door can be drawn down to access the internal drawer with the sample holding block (top right). The drawer must be pulled out completely while inserting the seeds into the tray for the analysis (bottom). (**c**) The excitation source (UV) and the PMTs. These include seven photomultiplier tubes along with filters to form seven sensors which can detect the emission at different wavelengths.

Table 4.1. Features of the photomultiplier tubes (PMTs) of the LIANA© device, including model type, spectrum and filter bandpass wavelength.

No.	1	2	3	4	5	6	7
PMT Model	R1924P	R3788	R3788	R7154	R3788	R3896	R3896
PMT spectrum nm	300-650	185-750	185-750	160-320	185-750	185-900	185-900
Filter bandpass Wavelength nm	No Filter	280-310	315-400	No Filter	430-510	530-610	610-690

4.2.5. Generation of prediction models

Prediction models for the classification of seed samples were assigned and improved using the RapidMiner software (Kotu and Deshpande, 2014; Hofmann and Klinkenberg, 2016). Seeds were classified based on G% values into optimal (100-80%) and non-optimal (below 80%) quality. The prediction process is described in **Fig. 4.2**.

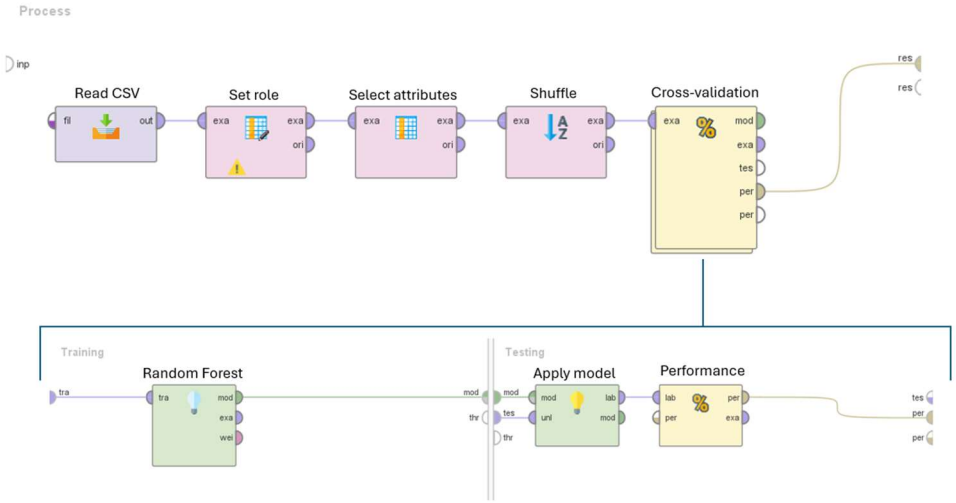

Figure 4.2. Illustration of the RapidMiner prediction model. The operators displayed in the model are connected and execute distinct actions. The Read CSV operator allows the uploading of the file. To facilitate the manual integration of germination percentages into the CSV file, the records were sorted. The Set role operator was used for data labelling. Attributes highly correlated to the label were excluded from the learning model with the operator Select attributes. The operator Shuffle was employed to randomize the records within the datasets.

The several operators used in the learning process are connected in a specific order and perform different operations. A stratified 10-fold cross-validation operation approach was used to validate the model. The classifier Random Forest was selected for outcome prediction to maximize accuracy. Accuracy %, area under the curve (AUC), sensitivity %, specificity %, positive predicted value (PPV) %, and negative predicted value (NPV) % values were obtained at the end of the validation.

4.3 Results

4.3.1. Development of an experimental system for UPE and DL data collection

The experimental system proposed in this study is based on using seeds stored at different conditions: a seed bank optimal storage conditions at -18 ºC (hereby defined as Cold) and an ambient room temperature (22-24 ºC) storage (hereby defined as Ambient). The give legume species (*P. vulgaris, L. sativus, C. arietinum, P. sativum, V. faba*) and accessions were stored for more than ten years under Ambient and Cold conditions prior to use. **Fig. 4.3** depicts the experimental model along with the analyses carried out to obtain the final dataset for the predictive models developed through machine learning approach.

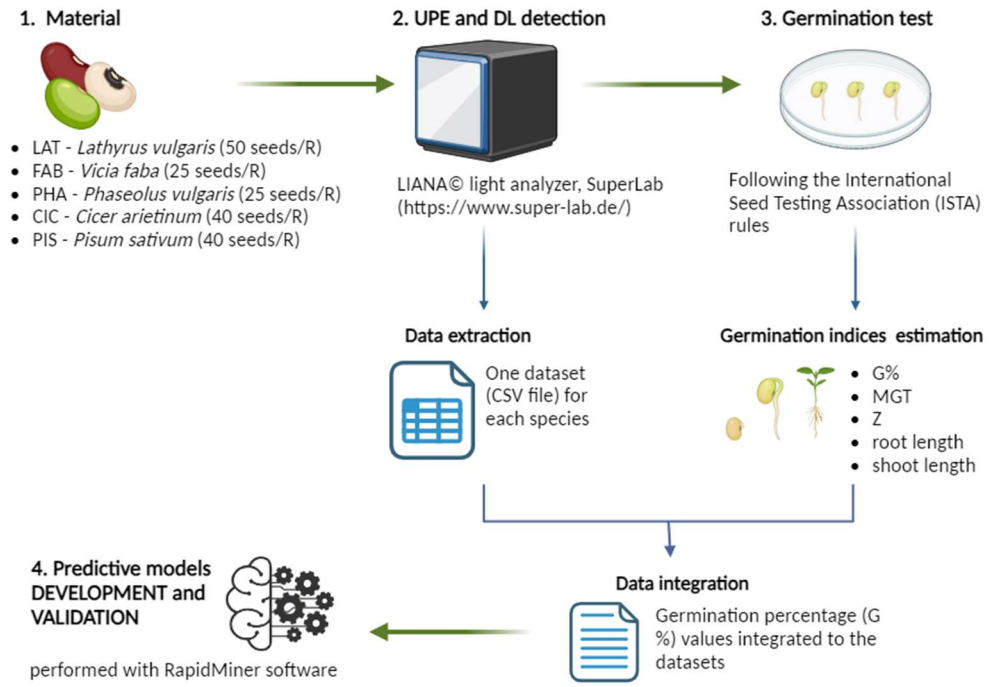

Figure 4.3. Schematic representation of the experimental system. Multiple accessions of seeds of five legume species stored at room temperature (Ambient) or -18 °C (Cold) for more than ten years were ordered in different biological replicates (R) based on their size. The

replicates were analyzed with the LIANA© light analyzer and subsequently used for germination test, following the ISTA rules for each species. At the end of the germination test, several indices were calculated (G%, Z, MGT, root and shoot length) and the germination percentage data was integrated into the extracted CSV file containing for the same replicates the UPE and DL data. The complete datasets were independently used for the development of machine learning models for germination percentage prediction from seed samples using RapidMiner® software.

Seed samples were used to detect UPE and DL and subsequently germinated to assess a set of indices indicative of seed quality. To develop the predictive models, seed samples were classified into two groups (optimal, non-optimal) based on the germination percentage, where optimal germination ranges between 80-100% while below 80% is considered as non-optimal.

4.3.2. Germination performance under different storage conditions

Germination tests were performed to estimate the effect of storage conditions on germination performances on each of the investigates species and selected accession. Given the high amount of data, the values (mean ± st.dev.) of germination percentage (G%), mean germination time (MGT), synchronicity index (Z), root and shoot length are provided for each species/accession in the Supplementary dataset. For the overall representation of these data, a principal component analysis (PCA) was performed (**Fig. 4.4**).

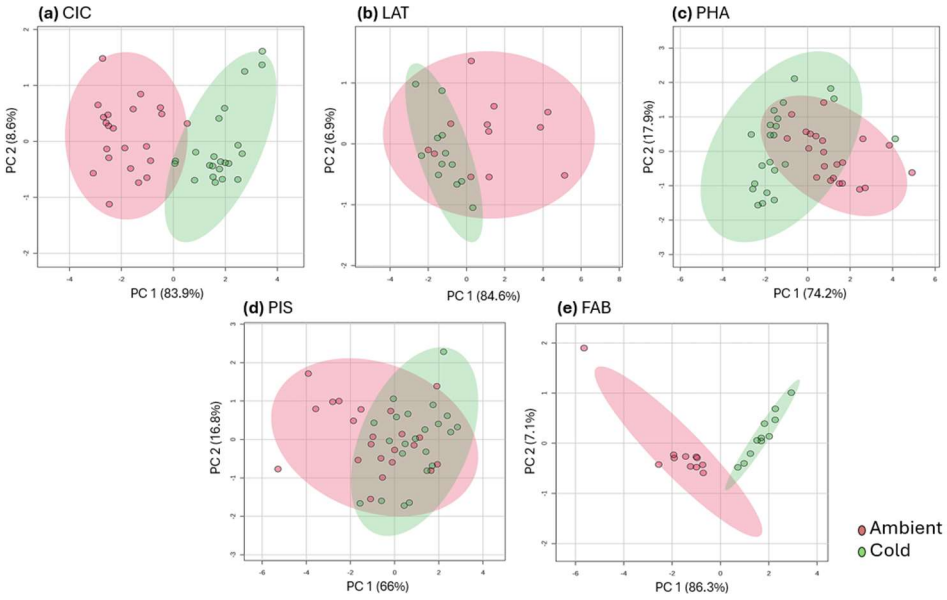

Figure 4.4. PCA score plots generated using the germination data, physical, and LIANA© parameters gathered from seeds stored at Ambient (red) and Cold (greed) storage conditions. **(a)** *Cicer arietinum* (CIC). **(b)** *Lathyrus sativus* (LAT). **(c)** *Phaseolus vulgaris* (PHA). **(d)** *Pisum sativum* (PIS). **(e)** *Vicia faba* (FAB).

The data depicts two scenarios; first, represented by *C. arietinum* (CIC) and *V. faba* (FAB), where there is a distinct clustering between the Ambient and Cold groups, and second, represented by *P. vulgaris* (PHA), *L. sativus* (LAT), and *P. sativum* (PIS) where the two clusters are overlapping. These two different trends reflect different behavior, in terms of germination performances between Amb and Cold groups, between species. Starting from *C. arietinum*, **Table 4.2** shows the germination data, in terms of G%, MGT, Z, average root length (Root), and shoot length (Shoot)

Table 4.2. Germination parameters calculated for *C. arietinum* accessions stored at room temperatures (Amb) and at -18 °C (Cold). Asterisks (*) indicate a significant difference ($P \leq 0.05$) between the Amb and Cold groups for each accession.

C. arietinum	G%		MGT		Z		Root		Shoot	
	Media	St. dev	Media	St. dev	Media	St. dev	Media	St. dev	Media	St. dev
CIC5_Amb_2013	54.5	± 11.911	2.89	± 0.179	0.38	± 0.075	5.47	± 1.758	2.17	± 0.378
CIC5_Cold_2013	95	± 1.768*	1.55	± 0.304*	0.48	± 0.159	12.82	± 0.802*	3.05	± 0.362*
CIC18_Amb_2013	50.5	± 20.872	2.50	± 0.058	0.46	± 0.056	6.11	± 2.126	2.06	± 0.693
CIC18_Cold_2013	92.5	± 8.101*	1.47	± 0.195*	0.53	± 0.109	10.50	± 2.322*	2.48	± 0.311
CIC28_Amb_2013	19.5	± 10.216	2.77	± 0.353	0.31	± 0.128	7.48	± 2.789	1.80	± 0.318
CIC28_Cold_2013	88.5	± 6.519*	1.55	± 0.104*	0.47	± 0.029*	12.00	± 0.903*	3.27	± 0.66*
CIC31_Amb_2013	25.5	± 9.421	2.92	± 0.36	0.33	± 0.083	4.70	± 1.795	1.93	± 0.549
CIC31_Cold_2013	96	± 2.85*	1.22	± 0.059*	0.66	± 0.065*	9.94	± 1.836*	3.27	± 0.329*
CIC49_Amb_2013	46	± 18.08	2.62	± 0.175	0.44	± 0.037	3.47	± 2.815	1.64	± 0.556
CIC49_Cold_2013	89	± 3.354*	1.43	± 0.306*	0.56	± 0.06*	11.21	± 1.383*	2.54	± 0.242*
CIC50_Amb_2013	41	± 5.184	2.45	± 0.166	0.51	± 0.114	8.54	± 0.888	3.52	± 0.322
CIC50_Cold_2013	90	± 3.953*	1.40	± 0.126*	0.52	± 0.042	11.09	± 3.227	3.92	± 0.597
CIC53_Amb_2013	36	± 12.324	2.90	± 0.397	0.38	± 0.144	7.34	± 2.680	2.63	± 0.751
CIC53_Cold_2013	95.5	± 2.092*	1.74	± 0.379*	0.49	± 0.018	12.83	± 1.036*	4.03	± 0.477*
CIC58_Amb_2013	31.5	± 15.969	3.63	± 0.878	0.38	± 0.111	2.43	± 1.308	0.72	± 0.585
CIC58_Cold_2013	84.5	± 11.236*	2.70	± 0.868	0.41	± 0.101	9.27	± 0.766*	2.02	± 0.513*
CIC90_Amb_2013	56.5	± 12.196	3.01	± 0.493	0.33	± 0.098	7.05	± 2.476	2.22	± 0.700
CIC90_Cold_2013	89.5	± 4.472*	1.62	± 0.269*	0.46	± 0.036*	11.14	± 0.851*	3.24	± 0.087*
CIC92_Amb_2013	25.5	± 8.732	2.86	± 0.252	0.32	± 0.091	3.32	± 1.590	0.92	± 0.376
CIC92_Cold_2013	86	± 8.404*	1.76	± 0.47*	0.43	± 0.091*	9.43	± 2.519*	3.35	± 0.32*
CIC94_Amb_2013	11	± 5.184	3.03	± 0.916	0.44	± 0.318	1.70	± 1.155	0.63	± 0.612
CIC94_Cold_2013	78.5	± 6.755*	2.38	± 0.39	0.39	± 0.076	9.17	± 0.248*	1.94	± 0.204*
CIC180_Amb_2013	24.5	± 11.911	3.09	± 0.595	0.35	± 0.215	2.61	± 1.245	1.18	± 0.529
CIC180_Cold_2013	93	± 4.809*	1.82	± 0.577*	0.45	± 0.133	12.30	± 1.276*	3.34	± 0.281*
CIC204_Amb_2013	28	± 7.786	2.88	± 0.161	0.42	± 0.143	4.84	± 2.373	1.74	± 0.493
CIC204_Cold_2013	89	± 8.023*	1.44	± 0.183*	0.52	± 0.135	11.95	± 1.697*	4.12	± 0.819*
CIC205_Amb_2013	38	± 6.471	3.36	± 0.16	0.29	± 0.044	3.61	± 1.151	1.40	± 0.280
CIC205_Cold_2013	89	± 2.85*	2.03	± 0.754*	0.48	± 0.087*	10.97	± 0.716*	3.17	± 0.632*
CIC209_Amb_2013	29.5	± 10.368	3.2	± 0.577	0.34	± 0.168	3.02	± 1.805	0.75	± 0.542
CIC209_Cold_2013	92.5	± 4.677*	2.03	± 0.445*	0.48	± 0.128	12.21	± 0.999*	3.23	± 0.411*
CIC210_Amb_2013	27	± 5.701	3.33	± 0.45	0.31	± 0.11	4.13	± 0.815	1.28	± 0.244
CIC210_Cold_2013	83	± 6.937*	2.41	± 0.741*	0.42	± 0.079	11.01	± 1.652*	2.79	± 0.31*
CIC221_Amb_2013	36	± 5.184	3.26	± 0.505	0.35	± 0.072	4.30	± 0.541	1.01	± 0.311
CIC221_Cold_2013	94.5	± 1.118*	2.13	± 0.836*	0.45	± 0.055*	11.48	± 0.816*	3.18	± 0.314*
CIC648_Amb_2013	53	± 18.235	2.56	± 0.104	0.45	± 0.057	4.51	± 1.954	2.71	± 0.697
CIC648_Cold_2013	98	± 2.092*	1.2	± 0.217*	0.75	± 0.18*	12.16	± 1.723*	3.35	± 0.424
CIC694_Amb_2013	16	± 12.068	3.25	± 0.863	0.22	± 0.204	6.14	± 2.267	1.90	± 0.738
CIC694_Cold_2013	86.5	± 9.454*	1.72	± 0.13*	0.42	± 0.049*	12.18	± 0.548*	3.07	± 0.399*
CIC701_Amb_2013	16	± 10.84	3.01	± 0.515	0.33	± 0.199	3.18	± 1.583	1.18	± 0.818
CIC701_Cold_2013	90	± 3.953*	1.18	± 0.095*	0.73	± 0.119*	12.91	± 1.333*	3.53	± 0.435*
CIC702_Amb_2013	7	± 1.118	2.83	± 0.441	0.2	± 0.183	3.92	± 1.757	0.98	± 0.431
CIC702_Cold_2013	74.5	± 9.083*	1.65	± 0.31*	0.42	± 0.055*	10.05	± 1.529*	2.32	± 0.387*
CIC737_Amb_2013	50.5	± 9.585	3.24	± 0.879	0.32	± 0.116	7.91	± 1.070	1.88	± 0.519
CIC737_Cold_2013	92.5	± 1.768*	2.12	± 0.774*	0.48	± 0.051*	13.32	± 1.975*	2.49	± 0.264*

Table 4.3. Germination parameters calculated for *V. faba* accessions stored at room temperatures (Amb) and -18 °C (Cold). Asterisks (*) indicate a significant difference ($P \leq 0.05$) between the Amb and Cold groups for each accession.

V. faba	G%		MGT		Z		Root		Shoot	
	Media	St. dev	Media	St. dev	Media	St. dev	Media	St. dev	Media	St. dev
FAB82_Amb_2013	63.5	± 8.668	3.45	± 0.311	0.28	± 0.111	3.59	± 1.104	1.58	± 0.597
FAB82_Cold_2013	98	± 2.138*	1.83	± 0.396*	0.42	± 0.104*	14.71	± 1.868*	3.92	± 0.655*
FAB129_Amb_2013	76	± 11.514	2.78	± 0.42	0.24	± 0.077	8.58	± 1.820	2.65	± 0.443
FAB129_Cold_2013	96.5	± 3.964*	1.14	± 0.127*	0.88	± 0.117*	17.42	± 2.704*	5.53	± 1.311*
FAB571_Amb_2013	71.5	± 10.351	3.41	± 0.452	0.18	± 0.038	7.59	± 1.450	3.14	± 0.681
FAB571_Cold_2013	97.5	± 2.976*	1.59	± 0.244*	0.49	± 0.104*	16.04	± 2.342*	5.37	± 0.751*
FAB6146_Amb_2013	69.5	± 12.083	2.61	± 0.455	0.24	± 0.042	6.35	± 1.202	2.80	± 0.435
FAB6146_Cold_2013	97.5	± 2.976*	1.48	± 0.157*	0.47	± 0.063*	11.14	± 2.453*	3.71	± 1.002*
FAB6956_Amb_2013	55.5	± 8.928	3.48	± 0.367	0.20	± 0.086	4.70	± 1.695	2.08	± 0.552
FAB6956_Cold_2013	98	± 3.024*	1.97	± 0.442*	0.36	± 0.116*	12.08	± 2.364*	3.52	± 1.03*
FAB6975_Amb_2013	0	± 0	NULL	±	NULL	±		±		±
FAB6975_Cold_2013	94.5	± 6.74*	1.33	± 0.172*	0.73	± 0.117*	12.26	± 1.96*	4.70	± 0.904*
FAB6997_Amb_2013	77.5	± 10.24	3.36	± 0.337	0.23	± 0.043	5.36	± 1.887	2.43	± 0.642
FAB6997_Cold_2013	97	± 2.828*	1.62	± 0.284*	0.51	± 0.135*	13.72	± 2.298*	5.02	± 0.814*
FAB6999_Amb_2013	70	± 15.269	3.62	± 0.473	0.22	± 0.068	5.99	± 1.692	2.33	± 0.890
FAB6999_Cold_2013	97	± 4.14*	1.43	± 0.364*	0.60	± 0.235*	12.80	± 2.286*	4.72	± 0.539*
FAB7200_Amb_2013	80.5	± 8.928	2.72	± 0.328	0.23	± 0.05	6.45	± 0.931	3.08	± 0.611
FAB7200_Cold_2013	100	± 0*	1.04	± 0.048*	0.95	± 0.058*	11.73	± 1.975*	4.58	± 0.636*
FAB7458_Amb_2013	43.5	± 8.124	3.20	± 0.668	0.15	± 0.037	2.39	± 0.783	1.67	± 0.945
FAB7458_Cold_2013	97.5	± 3.665*	1.17	± 0.116*	0.74	± 0.089*	14.62	± 2.650*	5.00	± 0.706*
FAB7479_Amb_2013	65	± 9.008	2.79	± 0.39	0.23	± 0.037	7.34	± 2.452	3.03	± 1.429
FAB7479_Cold_2013	99.5	± 1.414*	1.25	± 0.166*	0.69	± 0.167*	12.73	± 1.656*	3.49	± 0.614*

For CIC (**Table 4.2**) and FAB (**Table 4.3**), the majority of accessions stored under cold conditions present an optimal G% (80-100%) while storage at room temperature resulted in reduced G% below 80% (e.g., 53 – 7% in CIC648 and CIC702; 76 – 0% in FAB129 and FAB6975). For the second scenario, reflecting the trend of PIS (**Table 4.4**), PHA (**Table 4.5**), and LAT (**Table 4.6**) datasets, multiple seed samples stored under Ambient conditions (Amb group) show optimal values of germination percentage, therefore the distinction between Amb and Cold groups is less pronounced. Among the PIS accession (**Table 4.4**), 38 samples present germination above 80% while 6 samples are classified in the group below 80%.

Table 4.4. Germination parameters calculated for *P. sativum* accessions stored at room temperatures (Amb) and -18 °C (Cold). Asterisks (*) indicate a significant difference ($P \leq 0.05$) between the Amb and Cold groups for each accession.

P. sativum	G%		MGT		Z		Root		Shoot	
	Media	St. dev	Media	St. dev	Media	St. dev	Media	St. dev	Media	St. dev
PIS14_Amb_2010	74	± 5.755	3.60	± 0.165	0.34	± 0.064	8.36	± 0.800	2.39	± 0.239
PIS14_Cold_2010	99.5	± 1.118*	3.09	± 0.049*	0.69	± 0.08*	11.63	± 0.430*	3.02	± 0.324*
PIS17_Amb_2010	96.5	± 2.85	3.63	± 0.335	0.45	± 0.063	9.22	± 1.132	2.34	± 0.339
PIS17_Cold_2010	99	± 1.369	3.14	± 0.212*	0.55	± 0.112	11.65	± 0.560*	3.25	± 0.336*
PIS40_Amb_2010	64.5	± 3.26	3.47	± 0.242	0.44	± 0.119	5.93	± 0.654	1.53	± 0.338
PIS40_Cold_2010	100	± 0*	3.31	± 0.272	0.46	± 0.174	9.19	± 0.533*	2.94	± 0.347*
PIS41_Amb_2010	98	± 2.092	3.50	± 0.149	0.42	± 0.013	9.78	± 2.613	2.96	± 0.631
PIS41_Cold_2010	99.5	± 1.118	3.59	± 0.126	0.38	± 0.059	10.72	± 1.574	2.96	± 0.501
PIS108_Amb_2010	99	± 1.369	2.60	± 0.254	0.40	± 0.061	10.41	± 0.822	4.28	± 0.288
PIS108_Cold_2010	100	± 0	2.52	± 0.311	0.50	± 0.076*	10.94	± 0.969	4.27	± 0.513
PIS213_Amb_2010	81	± 8.404	4.69	± 0.297	0.36	± 0.046	5.62	± 0.852	1.01	± 0.152
PIS213_Cold_2010	98.5	± 2.236*	4.15	± 0.271*	0.40	± 0.032	9.83	± 0.732*	1.76	± 0.555*
PIS493_Amb_2010	87.5	± 10.155	4.09	± 0.331	0.35	± 0.087	10.42	± 0.891	3.34	± 0.502
PIS493_Cold_2010	79.5	± 9.253	3.74	± 0.174*	0.31	± 0.028	11.20	± 0.912	3.28	± 0.468
PIS942_Amb_2010	94.5	± 3.26	3.46	± 0.178	0.48	± 0.113	12.73	± 0.756	3.07	± 0.330
PIS942_Cold_2010	98	± 2.092*	3.73	± 0.243*	0.29	± 0.093*	12.55	± 0.711	3.38	± 0.447
PIS1135_Amb_2010	96	± 3.354	2.89	± 0.212	0.40	± 0.031	11.69	± 1.409	3.96	± 0.570
PIS1135_Cold_2010	96	± 2.85	3.27	± 0.339*	0.29	± 0.034*	11.16	± 0.964	3.75	± 0.115
PIS5049_Amb_2010	79.5	± 11.236	4.17	± 0.375	0.40	± 0.054	6.04	± 0.742	1.25	± 0.183
PIS5049_Cold_2010	100	± 0*	3.47	± 0.207*	0.46	± 0.09	9.14	± 0.529*	2.00	± 0.336*
PIS7226_Amb_2010	96	± 3.791	4.01	± 0.164	0.39	± 0.055	7.60	± 0.588	1.57	± 0.185
PIS7226_Cold_2010	98.5	± 2.236	3.37	± 0.465*	0.40	± 0.048	11.28	± 0.807*	2.54	± 0.676*
PIS7238_Amb_2010	88	± 4.809	3.98	± 0.347	0.26	± 0.052	10.34	± 0.835	2.80	± 0.552
PIS7238_Cold_2010	79.5	± 6.471*	4.06	± 0.312	0.26	± 0.056	10.21	± 0.756	2.74	± 0.308
PIS7243_Amb_2010	93	± 5.701	3.85	± 0.137	0.35	± 0.078	10.75	± 1.408	2.28	± 0.421
PIS7243_Cold_2010	100	± 0*	3.47	± 0.091*	0.41	± 0.071	14.35	± 1.095*	3.16	± 0.499*
PIS7246_Amb_2010	88	± 7.374	3.69	± 0.189	0.36	± 0.04	8.87	± 0.557	2.23	± 0.331
PIS7246_Cold_2010	99.5	± 1.118*	3.08	± 0.4*	0.52	± 0.046*	12.55	± 1.268*	3.42	± 0.436*
PIS7253_Amb_2010	53	± 8.178	4.74	± 0.273	0.24	± 0.07	5.53	± 0.613	0.95	± 0.147
PIS7253_Cold_2010	100	± 0*	3.81	± 0.284*	0.38	± 0.051*	10.72	± 0.889*	2.18	± 0.223*
PIS7261_Amb_2010	88.5	± 4.873	3.56	± 0.255	0.37	± 0.028	7.99	± 0.610	2.39	± 0.391
PIS7261_Cold_2010	100	± 0*	2.75	± 0.199*	0.54	± 0.069*	11.60	± 0.429*	3.82	± 0.210*
PIS7264_Amb_2010	97	± 2.092	3.68	± 0.15	0.38	± 0.07	10.28	± 0.436	2.80	± 0.230
PIS7264_Cold_2010	99.5	± 1.118*	3.58	± 0.188	0.45	± 0.049	11.50	± 1.134*	3.22	± 0.759
PIS7271_Amb_2010	89	± 3.791	3.98	± 0.28	0.37	± 0.058	7.15	± 0.437	1.74	± 0.113
PIS7271_Cold_2010	99.49	± 1.147*	3.05	± 0.215*	0.42	± 0.157	11.07	± 0.472*	3.62	± 0.509*
PIS7365_Amb_2010	97.5	± 1.768	3.42	± 0.161	0.43	± 0.075	10.94	± 0.873	3.36	± 0.178
PIS7365_Cold_2010	91.5	± 2.236*	3.17	± 0.296	0.45	± 0.115	11.92	± 0.817	4.41	± 0.455*
PIS7560_Amb_2010	90.5	± 6.471	5.16	± 0.157	0.4	± 0.06	3.12	± 0.944	1.11	± 0.117
PIS7560_Cold_2010	100	± 0*	3.79	± 0.27*	0.45	± 0.117	9.80	± 0.964*	2.60	± 0.253*
PIS7569_Amb_2010	99.5	± 1.118	3.74	± 0.153	0.34	± 0.042	10.49	± 0.919	2.72	± 0.413
PIS7569_Cold_2010	98	± 2.092	3.34	± 0.31*	0.49	± 0.109*	12.01	± 1.143*	3.26	± 0.476*
PIS7760_Amb_2010	99	± 1.369	2.82	± 0.175	0.58	± 0.122	10.33	± 0.524	3.34	± 0.700
PIS7760_Cold_2010	100	± 0	2.48	± 0.276*	0.53	± 0.13	12.30	± 0.754*	4.03	± 0.312*

For the PHA accessions (**Table 4.5**), 33 have optimal germination while the remaining 11 present non-optimal germination below 80%. Lastly, LAT (**Table 4.6**) is divided into 13 accessions with optimal germination above 80% and 11 accessions with non-optimal performance. The remaining germination indices follow a similar pattern as G% in the different species, accessions, and storage conditions, thus supporting the divergent PCA clustering.

Table 4.5. Germination parameters calculated for *P. vulgaris* accessions stored at room temperatures (Amb) and -18 °C (Cold). Asterisks (*) indicate a significant difference ($P \leq 0.05$) between the Amb and Cold groups for each accession.

P. vulgaris	G%		MGT		Z		Root		Shoot	
	Media	St. dev	Media	St. dev	Media	St. dev	Media	St. dev	Media	St. dev
PHA99_Amb_2012	88.48	± 5.392	3.66	± 0.32	0.19	± 0.039	15.13	± 2.774	6.40	± 1.692
PHA99_Cold_2012	97.5	± 3.665*	3.17	± 0.275*	0.17	± 0.049*	19.82	± 1.884*	8.92	± 1.850*
PHA100_Amb_2012	85.5	± 8.536	3.38	± 0.464	0.34	± 0.103	9.47	± 1.887	3.39	± 1.083
PHA100_Cold_2012	100	± 0*	1.78	± 0.181*	0.63	± 0.182*	19.26	± 2.537*	6.38	± 1.705*
PHA161_Amb_2012	87.5	± 6.908	2.98	± 0.249	0.36	± 0.091	11.46	± 1.278	3.78	± 0.496
PHA161_Cold_2012	99	± 2.828*	1.76	± 0.202*	0.66	± 0.171*	18.44	± 2.375*	7.92	± 1.986*
PHA167_Amb_2012	74.5	± 12.817	3.54	± 0.509	0.34	± 0.111	9.26	± 1.598	4.60	± 2.050
PHA167_Cold_2012	99.5	± 1.414*	1.93	± 0.361*	0.47	± 0.11	16.69	± 2.405*	8.86	± 2.544*
PHA182_Amb_2012	79.5	± 13.427	3.23	± 0.413	0.31	± 0.062	13.07	± 2.287	6.53	± 1.481
PHA182_Cold_2012	100	± 0*	2.31	± 0.245*	0.31	± 0.053	18.14	± 2.618*	9.30	± 0.940*
PHA254_Amb_2012	71	± 10.637	4.29	± 0.723	0.24	± 0.062	7.94	± 2.382	4.25	± 1.995
PHA254_Cold_2012	93.5	± 6.392*	4.06	± 0.249	0.14	± 0.02*	13.48	± 2.693*	6.47	± 1.947*
PHA309_Amb_2012	98	± 3.024	2.59	± 0.411	0.37	± 0.069	16.20	± 0.606	8.16	± 1.446
PHA309_Cold_2012	99.5	± 1.414	2.66	± 0.227	0.26	± 0.045*	18.20	± 2.046*	9.66	± 1.273*
PHA386_Amb_2012	83.83	± 10.486	2.72	± 0.395	0.42	± 0.089	10.28	± 2.311	5.70	± 1.720
PHA386_Cold_2012	98.5	± 2.07*	1.89	± 0.147*	0.48	± 0.058	14.21	± 1.928*	8.89	± 1.649*
PHA390_Amb_2012	69.5	± 18.26	2.69	± 0.458	0.36	± 0.094	8.89	± 2.078	3.64	± 1.140
PHA390_Cold_2012	98	± 3.024*	1.51	± 0.255*	0.48	± 0.219	17.63	± 1.943*	9.31	± 1.050*
PHA416_Amb_2012	91.5	± 5.831	2.57	± 0.322	0.27	± 0.062	17.16	± 3.692	9.02	± 2.719
PHA416_Cold_2012	99	± 1.852*	2.05	± 0.329*	0.46	± 0.142*	21.14	± 2.217*	12.21	± 2.228*
PHA419_Amb_2012	89	± 9.971	2.81	± 0.266	0.27	± 0.054	13.06	± 1.253	5.75	± 1.306
PHA419_Cold_2012	100	± 0*	1.74	± 0.209*	0.59	± 0.151*	20.56	± 2.303*	8.35	± 2.599*
PHA507_Amb_2012	91.5	± 7.231	2.79	± 0.36	0.34	± 0.047	13.55	± 2.176	5.91	± 1.421
PHA507_Cold_2012	99	± 1.852*	2.43	± 0.225*	0.31	± 0.075	18.42	± 2.478*	10.80	± 1.553*
PHA673_Amb_2012	43	± 15.82	4.83	± 1.193	0.24	± 0.074	2.35	± 1.942	0.79	± 0.938
PHA673_Cold_2012	50	± 13.352	4.76	± 1.129	0.17	± 0.04*	6.86	± 1.834*	2.36	± 1.103*
PHA869_Amb_2012	87.46	± 6.177	2.93	± 0.325	0.3	± 0.054	14.05	± 2.328	7.06	± 1.989
PHA869_Cold_2012	100	± 0*	2.33	± 0.285*	0.37	± 0.092*	17.65	± 2.634*	10.91	± 0.813*
PHA1448_Amb_2012	91.5	± 10.351	3.03	± 0.347	0.32	± 0.068	11.99	± 1.317	8.79	± 2.242
PHA1448_Cold_2012	100	± 0*	2.13	± 0.105*	0.38	± 0.087	13.68	± 1.499*	11.48	± 1.782*
PHA1450_Amb_2012	91.5	± 4.986	3.76	± 0.391	0.38	± 0.074	10.98	± 1.295	5.79	± 1.249
PHA1450_Cold_2012	100	± 0*	2.68	± 0.305*	0.38	± 0.087	17.54	± 2.220*	10.30	± 1.391*
PHA6017_Amb_2012	70	± 21.594	3.71	± 0.407	0.36	± 0.134	4.05	± 1.106	2.38	± 0.689
PHA6017_Cold_2012	99	± 1.852*	1.63	± 0.178*	0.57	± 0.128*	14.61	± 2.398*	8.56	± 2.582*
PHA6018_Amb_2012	65	± 11.263	2.83	± 0.45	0.37	± 0.113	7.14	± 3.206	5.07	± 2.463
PHA6018_Cold_2012	97	± 2.828*	1.8	± 0.286*	0.37	± 0.111	14.16	± 2.221*	11.90	± 1.761*
PHA6019_Amb_2012	79	± 12.048	3.55	± 0.492	0.43	± 0.147	10.03	± 1.555	4.58	± 0.636
PHA6019_Cold_2012	100	± 0*	1.63	± 0.273*	0.61	± 0.204*	19.55	± 2.548*	8.85	± 2.338*
PHA6020_Amb_2012	53.77	± 17.743	4.36	± 0.866	0.18	± 0.041	5.46	± 1.565	2.68	± 1.308
PHA6020_Cold_2012	91	± 8.485*	3.86	± 0.441	0.15	± 0.025*	11.74	± 2.835*	6.23	± 2.136*
PHA6021_Amb_2012	85.5	± 7.69	3.62	± 0.334	0.45	± 0.135	9.08	± 2.434	4.60	± 1.247
PHA6021_Cold_2012	98.5	± 2.976*	2.46	± 0.243*	0.46	± 0.117	15.35	± 0.972*	7.33	± 0.758*
PHA6022_Amb_2012	68.5	± 14.412	3.48	± 0.396	0.37	± 0.114	4.97	± 1.040	2.81	± 0.740
PHA6022_Cold_2012	99.5	± 1.414*	1.79	± 0.136*	0.58	± 0.145*	12.80	± 2.826*	7.81	± 1.571*

Table 4.6. Germination parameters calculated for *L. sativus* accessions stored at room temperatures (Amb) and -18 °C (Cold). Asterisks (*) indicate a significant difference ($P \leq 0.05$) between the Amb and Cold groups for each accession.

L. sativus	G%		MGT		Z		Root		Shoot	
	Media	St. dev	Media	St. dev	Media	St. dev	Media	St. dev	Media	St. dev
LAT227_Amb_2010	94	± 2.828	2.45	± 0.258	0.53	± 0.127	9.46	± 1.019	6.09	± 0.930
LAT227_Cold_2010	100	± 0*	2.12	± 0.054*	0.79	± 0.089*	10.81	± 1.251	5.95	± 0.415
LAT237_Amb_2010	96	± 2.828	2.46	± 0.371	0.57	± 0.161	10.46	± 0.922	6.28	± 0.771
LAT237_Cold_2010	94	± 2.828	2.33	± 0.223	0.57	± 0.173	12.03	± 2.117	6.63	± 0.523
LAT412_Amb_2010	75.5	± 8.062	3.15	± 0.707	0.55	± 0.192	10.69	± 0.774	4.05	± 0.121
LAT412_Cold_2010	98	± 1.633*	3.43	± 0.264	0.48	± 0.089	10.90	± 2.036	3.70	± 0.291*
LAT416_Amb_2010	39.5	± 6.608	3.79	± 0.322	0.36	± 0.078	6.84	± 0.642	3.14	± 0.441
LAT416_Cold_2010	97.5	± 0.993*	3.04	± 0.075*	0.70	± 0.051*	9.23	± 1.570*	4.01	± 0.230*
LAT434_Amb_2010	60	± 10.198	3.81	± 0.342	0.34	± 0.085	9.62	± 1.416	4.25	± 0.118
LAT434_Cold_2010	98	± 2.828*	2.69	± 0.269*	0.58	± 0.127*	9.91	± 0.631	5.07	± 0.257*
LAT438_Amb_2010	39	± 4.163	3.76	± 0.6	0.38	± 0.201	5.48	± 1.395	3.82	± 0.736
LAT438_Cold_2010	93	± 2*	2.62	± 0.234*	0.49	± 0.089	10.16	± 0.830*	4.39	± 0.282
LAT443_Amb_2010	47	± 3.83	4.30	± 0.158	0.26	± 0.026	6.92	± 1.897	4.05	± 1.263
LAT443_Cold_2010	90.5	± 8.699*	3.31	± 0.185*	0.58	± 0.045*	11.01	± 0.539*	4.67	± 0.481
LAT455_Amb_2010	3.5	± 1	7.75	± 1.555	0.00	± 0	0.92	± 0.712	1.19	± 0.217
LAT455_Cold_2010	98	± 2.828*	3.84	± 0.113*	0.41	± 0.087*	8.94	± 0.755*	4.00	± 0.542*
LAT456_Amb_2010	13.5	± 6.608	6.13	± 1.139	0.22	± 0.077	1.71	± 0.683	1.38	± 0.473
LAT456_Cold_2010	96	± 1.633*	3.49	± 0.526*	0.40	± 0.032*	11.32	± 1.554*	3.44	± 0.585*
LAT457_Amb_2010	21	± 1.155	3.43	± 0.277	0.37	± 0.047	6.09	± 1.087	2.89	± 0.284
LAT457_Cold_2010	92	± 1.633*	2.61	± 0.101*	0.48	± 0.021*	11.07	± 1.466*	4.74	± 0.606*
LAT458_Amb_2010	27.5	± 5.26	3.40	± 0.385	0.59	± 0.286	8.65	± 0.674	3.47	± 0.511
LAT458_Cold_2010	95.5	± 1.915*	2.29	± 0.571*	0.46	± 0.041	11.71	± 0.730*	4.75	± 0.332*
LAT468_Amb_2010	1.5	± 1.915	7.00	± 3.464	0.25	± 0.5	1.36	± 1.003	1.45	± 0.872
LAT468_Cold_2010	76	± 5.416*	4.01	± 0.645	0.27	± 0.055	8.09	± 0.975	4.71	± 0.343

To evaluate the degree of correlation between the different germination indices, the Pearson coefficient *r* was calculated and graphically represented in **Fig. 4.5**.

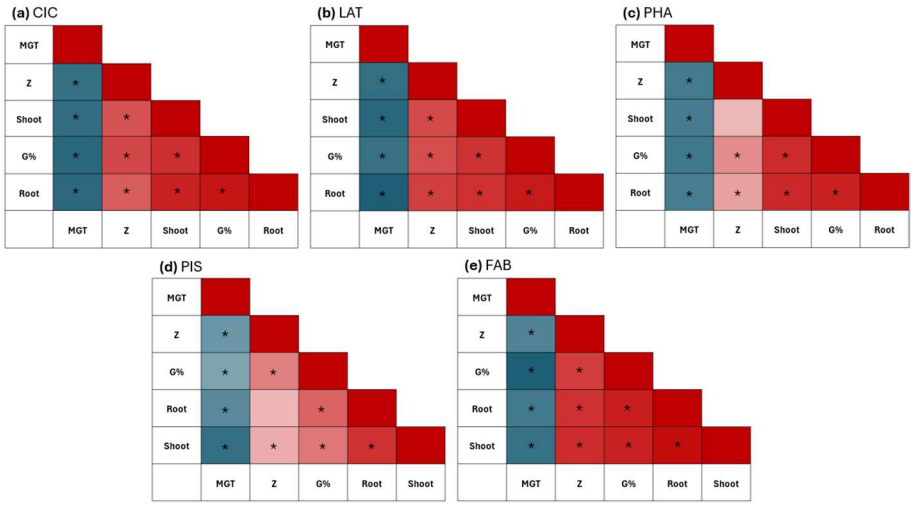

Figure 4.5. Pearson correlation analysis based on using (G%), mean germination time (MGT), synchronicity index (Z), root and shoot length. **(a)** *Cicer arietinum* (CIC). **(b)** *Lathyrus sativus* (LAT). **(c)** *Phaseolus vulgaris* (PHA). **(d)** *Pisum sativum* (PIS). **(e)** *Vicia faba* (FAB). Statistically significant correlations are indicated with an asterisk (*, $P \leq 0.05$).

4. UPE/DL and seed quality

Similar trends of correlations are observed among all the investigated species. MGT is negatively correlated with all the other parameters which are positively correlated to each other. This suggests that seed groups with optimal germination percentages are also characterized by high speed and synchrony, in addition to enhanced seedling growth.

This first step of the study allowed to characterize a system with different germinative performances that can be used to test novel methods dedicated to predicting seed viability in a non-invasive manner.

4.3.3. Application of predictive models for seed classification

Following the collection of data characterizing the investigated seeds and their germination performance, a predictive model was formulated. For each species, a dataset containing UPE, DL, and final germination percentage, was obtained from the analyses performed in this study. To train the models, the samples (records) were classified into two quality classes ranging from optimal (80-100%) and non-optimal (< 80%) germination. The 80% threshold was selected based on previous studies on genebank accessions dedicated to understanding how long seeds can retain their viability over extended periods of uncontrolled temperature or non-optimal conditions (Nagel and Börner, 2010). **Fig. 4.6** shows the accuracies of the prediction models.

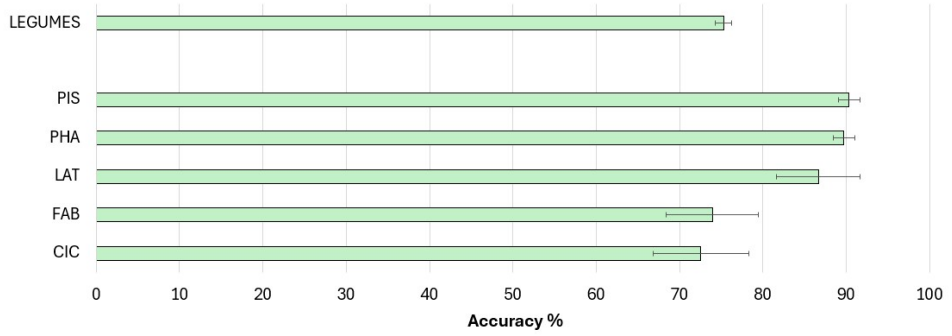

Figure 4.6. Percentage (%) of accuracy for the prediction models developed using the RapidMiner software based on germination data. Validation was performed using the "cross-validation" operator (number of folds = 10). CIC, *C. arietinum*; LAT, *L. sativus*; PHA, *P. vulgaris*; FAB, *V. faba*; PIS, *P. sativum*.

The models developed for the single species datasets (CIC, LAT, PHA, PIS, FAB) indicate different accuracy values. Models developed using *V. faba* and *C. arietinum* datasets presented a moderate accuracy (73.96% and 72.5%, respectively), while the accuracy of the other species reached higher values (above 85%). Subsequently, to uniformize these data, the dataset "Legumes" was obtained by unifying the

collections of data from the single species with the operator "append" of RapidMiner software. This operator merges two or more datasets with the same attributes building a new combined set. The accuracy of the prediction model developed with the "Legumes" dataset is around 75.29% (**Fig. 4.6**), indicating a good prediction efficiency. **Table 4.7** presents other classification metrics that describe the overall efficiency of predictive models.

Table 4.7. Predictive performance of learning models obtained after cross-validation. TP true positive, TN true negative, FN false negative, FP false positive, TPR true positive rate, FPR false positive rate. Area under the curve (AUC) = $\int_{x=0}^{1} \mathrm{TPR}(\mathrm{FPR}^{-1}(x))dx$, Sensitivity = TP/(TP + FN). Specificity = TN/(TN + FP), Positive predictive value (PPV) = TP/(TP + FP). Negative predictive value (NPV) = TN/(FN + TN).

	AUC	Sensitivity (%)	Specificity (%)	Positive predictive value (PPV) (%)	Negative predictive value (NPV) (%)
CIC	0.814 ± 0.062	55.94% ±11.56%	85.94% ± 5.89%	76.34% ± 7.88%	71.10% ± 5.22%
FAB	0.826 ± 0.048	83.04% ± 5.72%	58.32% ± 9.62%	77.51% ± 4.33%	67.00% ± 9.61%
LAT	0.963 ± 0.022	92.67% ± 6.05%	78.74% ± 11.85%	85.80% ± 6.52%	89.87% ± 7.33%
PHA	0.876 ± 0.054	98.34% ± 1.17%	58.79% ± 6.02%	89.58% ± 1.30%	91.17% ± 5.80%
PIS	0.922 ± 0.035	100.00% ± 0.00%	15.83% ± 11.42%	90.18% ± 1.21%	100.00% ± 0%
LEGUMES	0.824 ± 0.028	98.57% ± 0.76%	22.87% ± 3.23%	74.22% ± 0.77%	87.93% ± 5.81%

While positive predictive value (PPT) and negative predictive values (NPT) follow the trend exhibited by the accuracy parameter, sensitivity and specificity percentages reflect a critical issue in classifying seed samples in the appropriate group in most models. In particular, the model developed from the PIS dataset registers the lowest value of specificity (approximately 15.83%). One potential solution is represented by the "MetaCost" operator of RapidMiner, which makes the prediction cost-sensitive by utilizing a specified cost matrix (configured by the operator) (Kim et al., 2012, Wang et al., 2021).

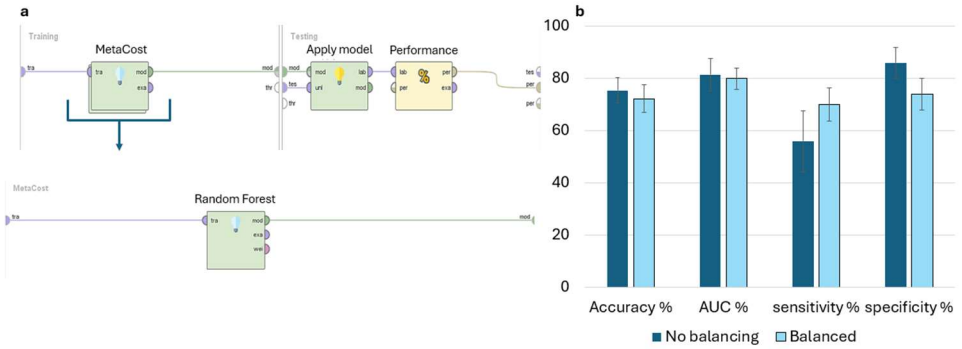

Figure 4.7. MetaCost operator utilization on CIC learning model. **(a)** Structure of the cross-validation operator, including the MetaCost operator into the Training subprocess and the

Random Forest classifier, included into the MetaCost operator. **(b)** Histograms showing the classification parameter percentages (Accuracy, AUC, sensitivity, and specificity) calculated on the CIC predictive model with (Balanced, light blue) and without (No Balancing, dark blue) MetaCost operator.

In the learning model depicted in **Fig. 4.7a**, the "MetaCost" operator was used as trial to improve the sensitivity value of the predictive model developed from the CIC dataset (55.91%, **Table 4.7**), configuring a cost matrix that assigns a cost of 5 and 4 to false negatives and false positives, respectively. The results are presented in **Fig. 4.7b**, which shows the main classification parameters of the model with (Balanced) and without (No Balancing) MetaCost operator. The histogram illustrates a notable improvement of the sensitivity, which was the objective of "MetaCost" operator utilization. However, this improvement is balanced by a reduction in specificity, while the accuracy and the AUC values exhibited a slight impact from the optimization process.

4.4 Discussion and Conclusion

The need for the development of novel, non-invasive, easy-to-use, economic, and universal methods for seed quality assessment was the driving force of this work, which proposes the use of UPE and DL as novel tools to evaluate seed quality. To maximize the number of samples with a wider range of germination percentages, this method was tested in a system composed of seeds stored for more than ten years at different conditions (Ambient and Cold) and characterized from the point of view of germination behaviour and photon emission. Following classification in quality classes (optimal, non-optimal), the generated data were used to build prediction models to test the relation between photon emission and seed quality. To our knowledge, currently, there is no study that evaluated the UPE and DL phenomena taking into consideration different species and different accessions of the same species. The LIANA© prototype used in this study is easy-to-use, fully automated, allowing rapid measurements for diverse purposes covering different surface measurements, while it was not specifically design for seeds. Although the prototype can be further optimized for more accurate analyses on seeds, the costs of its use relate mainly to covering electricity and licensing of the software.

Several studies performed on legumes (Koskosidis et al., 2022), as well as other species (Agacka et al., 2013), have evidenced differences in germination percentage between different storage conditions. In a second scenario, reflected from the data obtained from pea, beans, and lathyrus, the distinction between ambient and cold is less pronounced. The data collected from *P. sativum* can be given as an example from this group. In this case, it appears that seeds stored at both ambient and cold conditions are able to maintain seed germinability in several accessions. A recent study reported similar results in ten varieties of soybeans stored at cold and room temperatures (Koskosidis et al., 2022). Other studies showed that pea seeds stored under ambient conditions retained their viability for more than twenty years (Nagel

and Börner, 2010). In addition, Giannella et al. reported different germination performance when analysing eight accessions from which one proved to be maintained prolonged seed longevity also at room temperature (Giannella et al., 2022). This accession was characterized by low levels of ROS and increased antioxidant activity and genome stability. Different germination performances between varieties may be explained by several aspects. Genetic variability influences plant hormone signalling and other crucial processes related to seed germination (Miransari and Smith, 2014).

The results of the learning models exhibit variable results, which can be grouped in two scenarios. The models developed from the datasets CIC and FAB exhibit a moderate efficiency in classifying seed samples appropriately, while the processes obtained from the remaining datasets show high performances. Several factors can affect the quality of prediction and explain the differences in accuracy between the different types of models. For instance, the size of dataset is a crucial issue for machine learning: an optimal training process require an appropriate number of examples representing a wide variety of conditions (Barbedo, 2018). The choice of the classifier substantially affects the efficiency of the model. In this study, the predictive models are based on a Random Forest classifier, an ensemble approach widely used for classification tasks that allows the optimization of accuracy and prevents overfitting of the models (Rodriguez-Galiano et al., 2012). However, an efficient data-cleaning phase is crucial for optimizing the efficiency of the predictive models since the presence of outliers can interfere with the classification (Fernández et al., 2022). A cost-sensitive classification with the MetaCost operator of RapidMiner has been demonstrated to enhance sensitivity, improving the efficiency of prediction. Thus, this approach may be employed with other models to enhance the balancing of error rates between optimal and non-optimal classes. Apart from the technical aspects related to machine learning, the trend observed may confirms the hypothesis of a correlation between seed quality and UPE and DL phenomena. This is in agreement with other publications indicating that DL and UPE measurements can be used to assess seed viability (Grasso et al., 2018; Li et al., 2022). In addition, the results obtained from the single datasets may suggest the hypothesis of a species-dependent photon emission.

To conclude, seed quality evaluation is a complex aspect since different features (genetic, physiological, and physical factors) are involved in its determination (Rahman and Cho, 2016). UPE and DL have been previously correlated to oxidative stress (Pospíšil et al., 2014), water content (Yan et al., 2003), and seeds vigour (Grasso et al., 2018), therefore this can be envisioned an accurate method to assess seed quality. The data collected in this report suggest a complex scenario, in which intrinsic seed characteristics of different species may play an important role in the link between seed quality and photon emission. Despite its potential, UPE and DL phenomena require further in-depth characterization to understand their biological relevance in the seed context. The use of machine learning allows to bypass some of the drawbacks related to the lack of information about UPE and DL, enabling more accurate prediction of a specific outcome, while contributing to a better understanding of these phenomena.

References

Adeboye, K. & Börner, A. (2020). Delayed luminescence of seeds: are shining seeds viable? *SST*, 48(2), 167–177.

Agacka, M., Depta, A., Börner, M., Doroszewska, T., Hay, F. R., & Börner, A. (2013). Viability of Nicotiana spp. seeds stored under ambient temperature. *Seed Science and Technology*, 41(3), 474-478.

Barbedo, J. G. A. (2018). Impact of dataset size and variety on the effectiveness of deep learning and transfer learning for plant disease classification. *Comput. Electron. Agr*., 153, 46-53.

Cifra, M., & Pospíšil, P. (2014). Ultra-weak photon emission from biological samples: Definition, mechanisms, properties, detection and applications. *J. Photochem. Photobiol. B.*, 139, 2–10.

Cilento, G. & Adam, W. (1995). From free radicals to electronically excited species. *Free Radic. Biol. Med.*, 19(1), 103–114.

Costanzo, E., Gulino, M., Lanzanò, L., Musumeci, F., Scordino, A., Tudisco, S., & Sui, L. (2008). Single seed viability checked by delayed luminescence. *European Biophysics Journal*, *37*, 235-238.

Du, J., Deng, T., Cao, B., Wang, Z., Yang, M., & Han, J. (2023). The application and trend of ultra-weak photon emission in biology and medicine. *Frontiers in Chemistry*, 11, 1140128.

Elizalde, V., García, J. R., Peña-Valdivia, C. B., Ybarra, M. C., Leiva, O. R., & Trejo, C. (2016). Viability and germination of *Hechtia perotensis* (*Bromeliaceae*) seed.

ElMasry, G., ElGamal, R., Mandour, N., Gou, P., Al-Rejaie, S., Belin, E., & Rousseau, D. (2020). Emerging thermal imaging techniques for seed quality evaluation: Principles and applications. *Food Research International*, 131, 109025.

Feng, L., Zhu, S., Liu, F., He, Y., Bao, Y., & Zhang, C. (2019). Hyperspectral imaging for seed quality and safety inspection: A review. *Plant Methods*, 15, 1-25.

Fernández, Á., Bella, J. & Dorronsoro, J. R. (2022). Supervised outlier detection for classification and regression. *Neurocomputing*, 486, 77-92.

Gianella, M., Doria, E., Dondi, D., Milanese, C., Gallotti, L., Börner, A., Lorena Zannino, L., Macovei, A., Pagano, A., Guzzon, F., Biggiogera, M., & Balestrazzi, A. (2022). Physiological and molecular aspects of seed longevity: exploring intra-species variation in eight *Pisum sativum* L. accessions. *Physiologia Plantarum*, 174(3), e13698.

Goltsev, V., Zaharieva, I., Chernev, P. & Strasser, R. J. (2009). Delayed fluorescence in photosynthesis. *Photosynth. Res.*, 101, 217-232.

Grasso, R., Gulino, M., Giuffrida, F., Agnello, M., Musumeci, F., & Scordino, A. (2018). Non-destructive evaluation of watermelon seeds germination by using Delayed Luminescence. *Journal of Photochemistry and Photobiology B: Biology*, 187, 126-130.

Griffo, A., Bosco, N., Pagano, A., Balestrazzi, A. & Macovei, A. (2023). Noninvasive methods to detect reactive oxygen species as a proxy of seed quality. *Antioxidants,* 12(3), 626.

Hofmann, M. & Klinkenberg, R. (2016). RapidMiner: Data mining use cases and business analytics applications. *CRC Press.*

Huang, M., Wang, Q. G., Zhu, Q. B., Qin, J. W. & Huang, G. (2015). Review of seed quality and safety tests using optical sensing technologies. *SST*, 43(3), 337–366.

Kim, J., Choi, K., Kim, G., & Suh, Y. (2012). Classification cost: An empirical comparison among traditional classifier, Cost-Sensitive Classifier, and MetaCost. *Expert Syst. Appl.*, 39(4), 4013-4019.

Kobayashi, M. (2014). Highly sensitive imaging for ultra-weak photon emission from living organisms. *J. Photochem. Photobiol. B.*, 139, 34–38.

Kotu, V. & Deshpande, B. (2014). Predictive Analytics and Data Mining. *Elsevier Science & Technology*.

Koskosidis, A., Khah, E. M., Pavli, O. I & Vlachostergios, D. N. (2022). Effect of storage conditions on seed quality of soybean (*Glycine max* L.) germplasm. *AIMS Agric. Food*, 7(2), 387–402.

Li, W., Tan, F., Cui, J. & Ma, B. (2022). Fast identification of soybean varieties using Raman spectroscopy. *Vib. Spectrosc.*, 123, 103447.

Lin, P., Xiaoli, L., Li, D., Jiang, S., Zou, Z., Lu, Q., & Chen, Y. (2019). Rapidly and exactly determining postharvest dry soybean seed quality based on machine vision technology. *Scientific Reports*, 9(1), 17143.

McDonald, M. B. Assessment of Seed Quality1. (1980). *HortScience*, 15(6), pp.784–788.

McDonald, M. B. Seed quality assessment. (1998). *Seed Sci. Res.*, 8(2), 265–276.

Miransari, M. & Smith, D. L. (2014). Plant hormones and seed germination. *EEB*, 99, 110–121.

Murphy, M. P., Holmgren, A., Larsson, N. G., Halliwell, B., Chang, C. J., Kalyanaraman, B., Rhee, S. G., Thornalley, P. J., Partridge, L., Gems, D., · Nyström, T., Belousov, V., Schumacker, P. T., Winterbourn, C. C., & Winterbourn, C. C. (2011). Unraveling the biological roles of reactive oxygen species. *Cell Metabolism*, 13(4), 361-366.

Musaev, F., Priyatkin, N., Potrakhov, N., Beletskiy, S. & Chesnokov, Y. (2022). Assessment of *Brassicaceae* Seeds Quality by X-ray Analysis. *Hortic.*, 8(1), 29.

Nagel, M. & Börner, A. (2010). The longevity of crop seeds stored under ambient conditions. *Seed Sci. Res.*, 20(1), 1-12.

Pang, Z., Lu, Y., Zhou, G., Hui, F., Xu, L., Viau, C., Spigelman, A. F., MacDonald, P. E., Wishart, D. S., Li, S., & Xia, J. (2024). MetaboAnalyst 6.0: towards a unified platform for metabolomics data processing, analysis and interpretation. *Nucleic Acids Research*, gkae253.

Popp, F. A. & Yan, Y. (2002). Delayed luminescence of biological systems in terms of coherent states. *Phys. Lett.*, 293(1-2), 93–97.

Pospíšil, P., Prasad, A. & Rác, M. (2014). Role of reactive oxygen species in ultra-weak photon emission in biological systems. *J. Photochem. Photobiol. B*., 139, 11–23.

Rahman, A. & Cho, B. K. (2016) Assessment of seed quality using non-destructive measurement techniques: a review. *Seed Sci. Res.*, 26(4), 285–305.

Ranal, M. A. & de Santana, D. G. (2006). How and why to measure the germination process? *Rev. Bras. Bot*, 29(1), 1–11.

Rodriguez-Galiano, V. F., Ghimire, B., Rogan, J., Chica-Olmo, M., & Rigol-Sanchez, J. P. (2012). An assessment of the effectiveness of a random forest classifier for land-cover classification. *P&RS*, 67, 93-104.

Stolz, P., Wohlers, J. & Mende G. (2019). Measuring delayed luminescence by FES to evaluate special quality aspects of food samples – an overview. *Open Agric.,* 4(1), 410–417.

Sun, C., Liu, J., Liu, H. & Guo, J. (2022). Reactive oxygen species mediate the relationship between mitochondrial function and delayed luminescence during senescence of strawberry (*Fragaria ananassa*) fruits. *Acta Physiol. Plant*., 44(2).

Ureña, R., Rodríguez, F. & Berenguel, M. (2001). A machine vision system for seeds quality evaluation using fuzzy logic. *Comput. Electron. Agr.*, 32(1), 1–20.

Wang, C., Bókkon, I., Dai, J. & Antal I. (2011). Spontaneous and visible light-induced ultraweak photon emission from rat eyes. *Brain Res.*, 1369, 1–9

Wang, Y. C. & Cheng, C. H. (2021). A multiple combined method for rebalancing medical data with class imbalances. *Computers in Biology and Medicine*, 134, p.104527.

www.thebusinessresearchcompany.com. (n.d.). (2024). *Seeds Market Size, Share, Growth, Trend Analysis, Forecast 2033*. Available at: https://www.thebusinessresearchcompany.com/report/seeds-global-market-report.

Yan, Y., Popp, F. A. & Rothe, G. M. (2003). Correlation between germination capacity and biophoton emission of barley seeds (*Hordeum vulgare* L.). *SST*, 31(2), 249–258.

Zhang, J., Fang, B., Sun, L., Zhang, X., Liu, J., Yang, Y., Zhang, W., Wang, X., & Ding, Y. (2022). Roles of NOD1/Rip2 signal pathway in carotid artery remodelling in spontaneous hypertensive rats. *General Physiology & Biophysics*, 41(1).

Zhu, L. W., Ma, W. G., Hu, J., Zheng, Y. Y., Tian, Y. X. Y. J., & Hu, W. M. (2015). Advances of NIR spectroscopy technology applied in seed quality detection. *Spectroscopy and Spectral Analysis*, 35(2), 346-349.

5. Volatilome profiling as a tool to assess legume seed quality in a non-invasive manner

This manuscript is currently in preparation for submission in the *Physiologia Plantarum* (Impact Factor 5.4) journal, with the title "Volatilome profiling as a tool to assess legume seed quality in a non-invasive manner". My contribution to this article is hereby described. I performed germination tests to assess the efficacy of hydropriming and artificial aging treatments to improve and reduce seed quality, respectively. I contributed to the VOCs analyses through PTR-Qi-TOF-MS, carried out at the INFRA-VOL phenotyping platform, and performed statistical analyses. This work was supported by the SeedGrant 2023 program awarded by SIBV (Società Italiana di Biologia Vegetale) (https://www.sibv.eu/premi-e-borse-di-studio/seed-grants/seed-grants-2023).

Abstract

Seed quality is a complex trait related to seed biology, defined as a set of physical, genetic, and physiological characteristics. Since seed quality reflects the overall germination potential, its accurate, sustainable, and cost-effective evaluation is important for the agrifood sector. Non-invasive techniques to estimate seed quality are highly requested in view of sustainability principles. In this context, the emission of volatile organic compounds (VOCs) from seeds can constitute a non-invasive and accurate approach since the emission of these molecules reflects the metabolic activity of seeds and the occurrence of processes involved in the acceleration of seed deterioration. In the present work, the volatilome profiles of *Glycine max* (accessions EM PURA and OL996), *Pisum sativum var. arvense* (accessions Forrimax and Guifredo), *Lathyrus sativus* (accessions Maleme-107 and Sofades), and *Trigonella foenum-graecum* (accessions Tborsek and Rayhane) seeds, treated with hydropriming and artificial aging, were investigated. Proton transfer reaction – time of flight – mass spectrometry (PTR-Qi-TOF-MS) was used for real-time monitoring of VOCs at very low concentrations and without prior sample concentration and destruction. The results show significant differences in the quantity and quality of VOCs emitted by different species and in response to the imposed treatments. All the 440 m/z values detected through PTR-Qi-TOF-MS exhibited statistically significant differences among treatments. From correlation analysis and machine-learn model utilization a list of relevant m/z to germination were identified. Apart from ethanol, whose emission is a known indicator of low seed quality, 2(3H)-furanone and cresol isomers were also found to be associated with aging or stress, while methanetriol release was identified to be positively related with an high quality of seeds.

5.1 Introduction

The role of agriculture encompasses every aspect of modern society. It is not only fundamental for food production, but it also has a significant impact on global and local economies, particularly in low-income countries where agricultural practices account for a substantial proportion of income and employment (Dethier & Effenberger, 2012). Although crop production has continuously increased since the year 2000 thanks to the enhancement of technologies and the intensification of farming activities (FAO 2022), the current output is not sufficient to meet the future global demand, strongly affected by the steadily growing world population (Lee, 2011) and the negative impact of climate changes of crop yield (Zwiers et al., 2013; Shi and Chen, 2018). In recent years the application of novel technologies of plant breeding (Raman, 2017) and genetically modified (GM) crops (Singh et al., 2022) resulting from modern scientific research, reported a positive impact on agricultural production (Tester and Langridge, 2010; Kavhiza et al., 2022). However, their large-scale utilization is strongly limited by the potential negative effect on biodiversity (Schmeller and Henle, 2008; Carpenter, 2011) and the uncertainties of public opinion regarding GM safety (Kvakkestad and Vatn, 2011). An effective approach to promote the sustainable improvement of crop production is represented by the utilization of high-quality seeds for agricultural practices, which are characterized by optimal germination performances. Seed quality is a complex trait related to seed biology, defined as the set of genetic, physiological, and physical features of seeds (https://www.seedtest.org/). As seed quality is indicative of the overall germination potential, the use of high-quality seeds can also be related to improved crop yield (Huang et al., 2015).

A number of techniques are currently available for the assessment of seed quality. The International Seed Testing Association (ISTA) has approved and standardized several methods for seed quality assessment, including conventional germination tests, which represent the standard method for seed quality estimation (McDonald, 1998). However, these methods present notable limitations, including invasiveness, prolonged test periods, low accuracy, and operator bias (Huang et al., 2015). To ensure the efficient measurement of seed quality and to prevent the waste of resources, novel methods for assessing seed quality and subsequent quality attributes are required. Non-invasive optical techniques have been developed and applied to assess seed quality, including machine vision (Lin et al., 2019), NIR (near-infrared) spectroscopy (Zhu et al., 2015), Raman spectroscopies (Li et al., 2022), thermal imaging, X-ray imaging, and hyperspectral imaging (Feng et al., 2019, ElMasry et al., 2020, Musaev et al., 2021). Despite the advantages these technologies offer, their high cost and complexity present significant limitations for large-scale use (Rahman and Cho, 2016).

Since one of the main products of chemical reactions occurring in dry seeds is represented by volatile organic compounds (VOCs), defined as small molecular weight carbonyl compounds that escape into the airspace as volatile molecules (Mira et al., 2016), the analysis of the seed volatilome profile can be used for the non-invasive collection of information regarding seed metabolism and the rate of seed

deterioration. The analysis of VOCs released from seeds was investigated in different works to estimate seed quality, and mainly seed deterioration (Umarani et al., 2020; Zhang et al., 2022). These studies revealed different patterns of VOCs release, including several aldehydes, alcohols, ketones, alkanes, alkenes, terpenes, and furans (Lee et al., 2000; Mira et al., 2010), reflecting specific processes occurring, such as lipid peroxidation, alcoholic fermentation, glycation, and respiration (Colville et al., 2012).

Given these premises, the following study aims to investigate the seed volatilome profiles in multiple legume species and accession. The seed collection includes two commercial accessions of *Glycine max* (OL996 and EM PURA), one of the most cultivated corps worldwide, along with different orphan legume species, namely *Lathyrus sativus* (Maleme-107 and Sofades), *Pisum sativum var. arvense* (Forrimax and Guifredo), and *Trigonella foenum-graecum* (Tborsek and Rayhane). Recently, orphan legumes are being considered as 'climate-smart' crops having important agronomic and nutritional features (Balestrazzi et al., 2024). To obtain seeds with different qualitative traits, hydropriming and artificial aging treatments were applied. Priming is a well-known approach for enhancing seed germination performance and resistance to stress, by triggering the seed pre-germinative metabolism (Paparella et al., 2015; Pagano et al., 2023). Differently, artificial aging is an approach based on the storage of seeds at high temperatures and relative humidity (Tian et al., 2019; Wang et al., 2022), thus causing seed deterioration without modifying the molecular pathway that acts during natural aging (TeKrony, 2005).

5.2 Materials and Methods

5.2.1. Seed material

Seeds of *Glycine max* (accessions EM PURA and OL996, provided by Sipcam Italia S.P.A, Italy), *Pisum sativum var. arvense* (accessions Forrimax and Guifredo, provided by Batlle Desde 1802, Spain), *Lathyrus sativus* (accessions Maleme-107, provided by Hellenic Agricultural Organization ELGO-DIMITRA and Sofades, provided by Agroland S. A, Greece), and *Trigonella foenum-graecum* (accessions Tborsek and Rayhane, provided by Université de Sfax, Tunisia), were used in this study.

5.2.2. Seed treatments

Seeds from each accession were subjected to two distinct treatments: hydropriming (HP8) and artificial aging (AA). For the HP8 treatment, seeds were imbibed in distilled water for eight hours and subsequently dried for 24 hours at room temperature (22-24°C). The AA treatment involved heating the seeds in sealed glass containers with 150 ml of distilled water at 55°C (for *T. foenum-graecum* Tborsek and Rayhane, *G. max* OL996 and EM PURA, and *P. sativum* Guifredo) or 60°C (for *L. sativus* Maleme-107 and Sofades, and *P. sativum* Forrimax) for eight hours.

Treated and untreated seeds were subsequently used for further analyses. The experimental design used in this work is illustrated in **Fig. 5.1**.

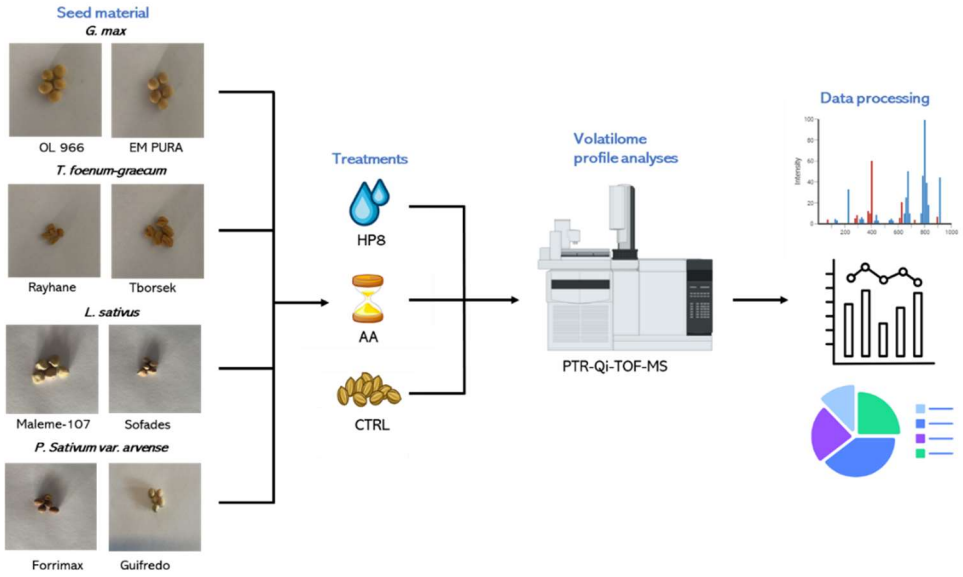

Figure 5.1. Schematic representation of the experimental system. HP8, hydropriming; AA, artificial aging; CTRL, non-treated seeds (control group); PTR-Qi-TOF-MS, proton transfer reaction-quadrupole ion guide-time of flight-mass spectrometry.

5.2.3. Germination test

Germination tests were performed following the guidelines provided by ISTA (International Rules for Seed Testing (https://www.seedtest.org/) with some modifications. For all species, seeds were placed in germination trays containing filter paper moistened with distilled water and kept in a growth chamber (25°C ± 1°C) under 16 h dark/8 h light for 7 days. Three replicates of 30 seeds each were used. At the end of germination, the following germination indices were calculated: germination percentage (G%), mean germination time (MGT), synchronicity index (Z) (Ranal and de Santana, 2006). The formulas used for the calculation of these parameters are the following:

$$(1)\ G\% = \left(\frac{number\ of\ germinated\ seeds)}{total\ number\ of\ seeds}\right) \times 100$$

$$(2)\ MGT = \frac{\sum_{i=1}^{k} ni\ x\ ti}{\sum_{i=1}^{k} ni}$$

$$(3)\ Z = \frac{\sum Cni,2}{\sum ni\ x\ \sum(ni-\frac{1}{2})}$$

In MGT (2) and Z (3) formulas, *ni* is the number of seeds germinated in the time *i* (not the accumulated number, but the number correspondent to the *ith* observation),

ti corresponds to the time from the start of the experiment to the *ith* observation (day), *k* is the last time of germination, and *Cni,2* = *ni* (*ni*-1)/2.

5.2.4. VOC analysis of legume seeds by PTR-Qi-ToF-MS

Seed volatile fingerprints were analyzed with a commercial PTR-MS equipped with Time of flight and quadrupole ion guide (PTR-Qi-TOF-MS, Ionicon Analytik GmbH, Innsbruck, Austria) by using H_3O^+ as reagent ion for the proton transfer reaction. For each sample, 50 grams (weight recorded before each treatment) were weighed and transferred in a 100-mL glass bottle, equipped with a GL45 3-valve screw cap. Four replicates per sample were used. Before each measurement, samples were incubated at 60°C for 10 minutes. Headspace VOCs profiles were measured by direct injection of the volatile mixture into the PTR-Qi-TOF-MS drift tube via a heated (80°C) peek inlet tube connected to a valve of the GL45 3-valve screw cap with a flow rate of 35 sccm (standard cubic centimeters per minute) for 6 min. To avoid low pressure inside the vial, clean air was continuously flushed through the glass bottle at 1 liter per minute (LPM). The drift tube conditions were 80°C temperature, 3.80 mbar drift pressure, and 900 V drift voltage corresponding to an E/N ratio of about 128 Townsend (1 Td = 10-17 V cm^2) (with E corresponding to the electric field strength and N to the gas number density). The acquisition rate of TOF mass spectrometer was one spectrum per second with a mass spectrum ranging from m/z 15 and 373. The raw PTR-Qi-TOF-MS data were acquired by the TofDaq software (Tofwerk AG, Switzerland) and processed using the R package ptairMS (Roquencourt et al., 2022). To achieve a good mass accuracy an internal calibration was performed on three calibration points: m/z=21.022 ($H3O^+$), m/z=203.943 (1,3-diiodobenzene fragment of internal gas standard) and m/z=330.848 (1,3-diiodobenzene internal gas standard). Seeds' volatile concentrations were expressed as normalized count per second (ncps) by normalization to the primary ion signal. The m/z signals were blank corrected by subtracting the signal obtained from the empty glass bottle and the peaks associated with the PTR-MS ion source, including those ascribed to water chemistry or other interfering ions; m/z=32 (O_2^+), m/z=31.022 (NO^+), m/z=37, and m/z= 39.033 (corresponding to $H_3{}^{18}O^+$ and water cluster ions H_2O-$H_3{}^{18}O^+$, respectively), were manually removed from the data set. Most of the mass peaks were tentatively identified based on the available literature or by comparisons with genuine standards.

5.2.5. Statistical analysis

Germination data were analyzed with Student *t*-test using the Microsoft Excel package using as threshold the $P \leq 0.05$ ('*'). Principal component analysis (PCA), analysis of variance (ANOVA, $P \leq 0.05$), Pearson's correlation analyses, and the relative p-values were determined by using MetaboAnalyst 6.0 (https://www.metaboanalyst.ca/, Pang et al., 2024). R internal statistical functions were also used for volatilome data elaboration. Two-way ANOVA test was performed using GraphPad 8.0 software (https://www.graphpad.com/scientific-software/prism/www.graphpad.com/scientific-software/prism/) to assess significative differences between groups in terms of volatile emission.

5.2.6. Machine-learning modeling

The Altair® RapidMiner® software (https://altair.com/altair-rapidminer) was used to develop learning model for the classification of seed samples. Model validation was performed with a stratified 3-fold cross-validation system, using the "Cross-Validation" operator. "Performance" operator was set to perform the calculation of classification parameters, based on the number of TP (true positive), TN (true negative), FP (false positive), FN (false negative), and the estimation of the TPR (true positive rate) and FPR (false positive rate) obtained through the confusion matrix: accuracy = (TP + TN)/(TP + TN + FP + FN), area under the curve (AUC) = $\int_{x=0}^{1} \mathrm{TPR}(\mathrm{FPR}^{-1}(x))dx$, sensitivity = TP/(TP + FN). specificity = TN/(TN + FP), positive predictive value (PPV) = TP/(TP + FP). negative predictive value (NPV) = TN/(FN + TN).

5.3 Results and Discussions

5.3.1. Germination performance of primed and aged seeds

Germination performance of treated/untreated seeds were evaluated to establish seed quality through ISTA indicated methods. A pronounced decline in germinability resulting from the aging treatment was observed in all the accessions tested in the following experiments (**Fig. 5.2**). However, the extent of deterioration varies among accessions. In the *L. sativus* accessions (**Fig. 5.2a,b**) and *G. max* EM PURA (**Fig. 5.2h**), the AA-treated seeds exhibit a significantly lower percentage of germination (17,78% ± 5,1 in Maleme-107, 22,22% ± 12,6 in Sofades, and 18,89 ± 1,9 in EM PURA) compared to the other species/accessions, where the G% values were approximately 40%. With regard to *T. foenum-graecum* seeds (**Figs 5.2e,f**), G% reached values ranges between 33.33% and 57.78%. For *L. sativus* Maleme-107 (**Fig. 5.2a**) and Sofades (**Fig. 5.2b**), as well as *P. sativum* Forrimax (**Fig. 5.2d**), the temperature utilized for the AA treatment was 60°C, while for the other species was 55 °C. This modification of the AA protocol was due to the fact that these accessions were more resistant to the high temperature and humidity treatments.

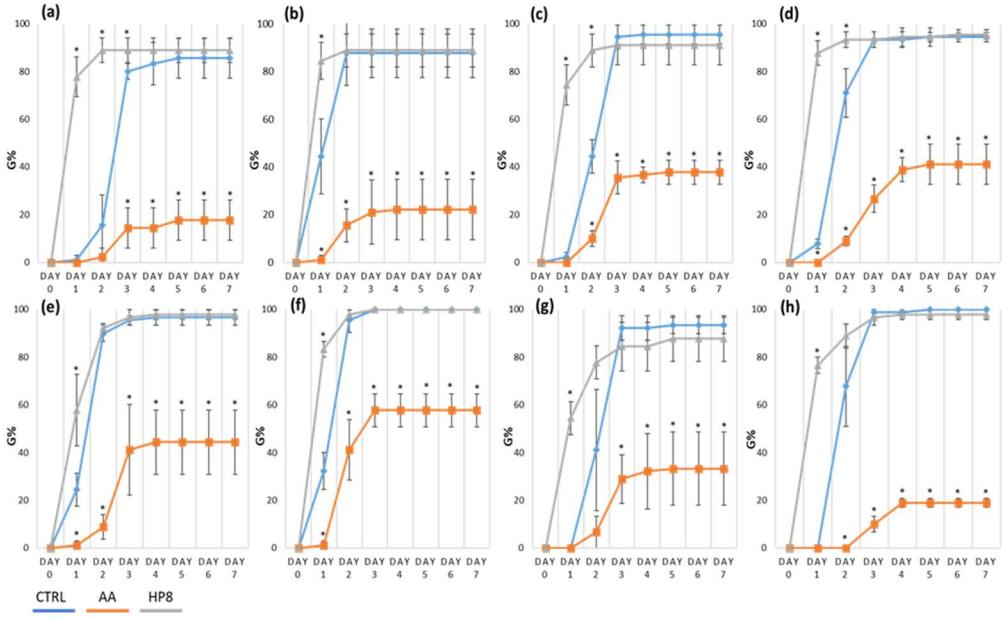

Figure 5.2. Time course of germination percentage (G%) in *L. sativus* **(a)** Maleme-107 and **(b)** Sofades, *P. sativum var. arvense* **(c)** Guifredo and **(d)** Forrimax, *T. foenum-graecum* **(e)** Rayhane and **(f)** Tborsek, *G. max* **(g)** OL996 and **(h)** EM PURA. Significant differences are indicated by asterisks (*, $P \leq 0.05$). CTRL, control (non-treated seeds); HP8, hydro-primed seeds; AA, artificially aged seeds.

Concerning the HP treatments (**Fig. 5.2**), the results obtained in all the accessions tested exhibit significantly higher G% values compared to CTRL mainly during the initial days of germination, while no significant differences are observed towards the end of the experimental period. These findings suggested that HP promotes an improvement in the speed of germination without significantly influencing the germination percentage. To confirm this, additional features reflecting germination speed (MGT) and synchrony (Z), were calculated (**Fig. 5.3**). The data show that HP8 treatments result in lower MGT value compared to CTRL, thus supporting the trend observed for the time course of germination. AA decreases the speed of germination in most of the accessions, except for *L. sativus* Maleme-107. Regarding the Z values (rhombus), no statistically significant differences are observed among species/accesses in the absence of treatments. is not observed in all the accessions tested. However, significantly higher Z values are observed on the HP8 seeds of *L. sativus* Sofades (**Fig. 5.3b**), *P. sativum* Guifredo (**Fig. 5.3c**) and Forrimax (**Fig. 5.3d**), and *T. foenum-graecum* Tborsek (**Fig. 5.3f**), while a negative influence of AA treatments is observed only in *P. sativum* Forrimax (**Fig. 5.3d**).

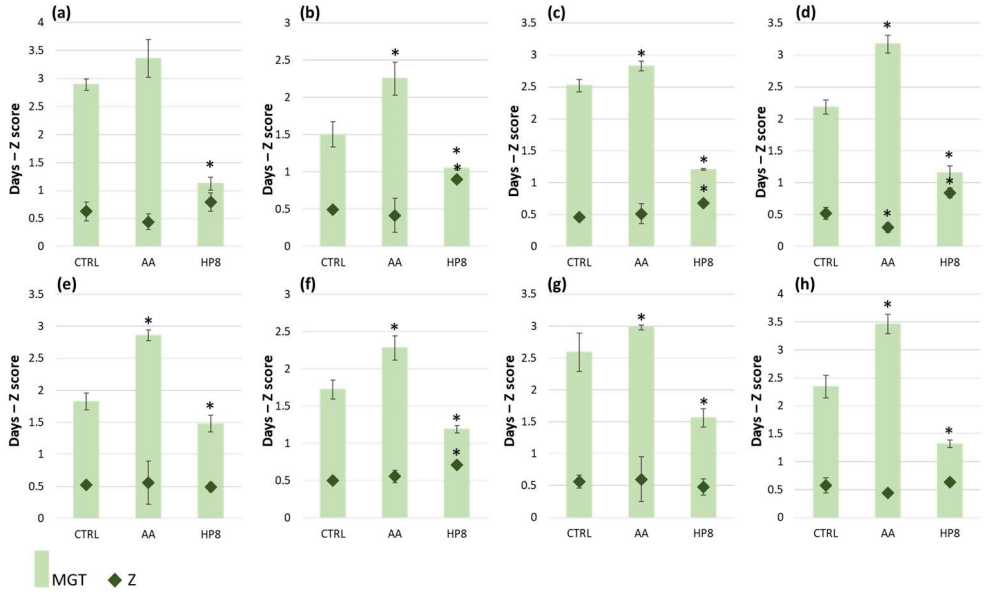

Figure 5.3. Graphical representation of the mean germination time (MGT) and synchronicity index (Z) in *L. sativus* **(a)** Maleme-107 and **(b)** Sofades, *P. sativum* **(c)** Guifredo and **(d)** Forrimax, *T. foenum-graecum* **(e)** Rayhane and **(f)** Tborsek, and *G. max* **(g)** OL996 and **(h)** EM PURA. MGT values are shown as histograms and Z score in rhomboids. A significant difference from the MGT and Z values of control is indicated by asterisks (*, $P \leq 0.05$). CTRL, control (non-treated seeds); HP8, hydro-primed seeds; AA, artificially aged seeds.

Overall, the information collected from the germination tests indicate a variation in seed quality induced by the treatments; namely, AA inhibits seed germination and therefore lowers the quality of the seeds, while HP improves germination and enhances seed quality. In agreement with the hereby obtained results, several other studies evidenced a negative effect of AA on the germination performance in legumes (Kapoor et al., 2010; Mohammadzadeh et al., 2019). At the same time, the positive effect of HP on legume seed germination is reported (Singh et al., 2017; Damalas et al., 2019; Pagano et al., 2022). So far, no data are available concerning the study of germination in orphan legumes; therefore, the current study provides novel and relevant information about this system, showing that these seeds are more resistant to high-temperature treatments and that their quality can be still improved by the use of priming.

5.3.2. General overview of volatilome profiles

After defining the experimental system with high- and low-quality seeds, encompassing a range of genetic variability in terms of different legume species and

accessions, these were subjected to PTR-Qi-TOF MS analyses to identify and measure VOC profiles. From the analyses, a total of 440 mass-to-charge values (m/z) were found. From the whole m/z groups, only 123 present a specific VOC or a group of VOCs identified. As an initial characterization, the whole volatilome was used to conduct a principal component analysis (PCA) distinguishing between the treatments and species/accessions (**Fig. 5.4**).

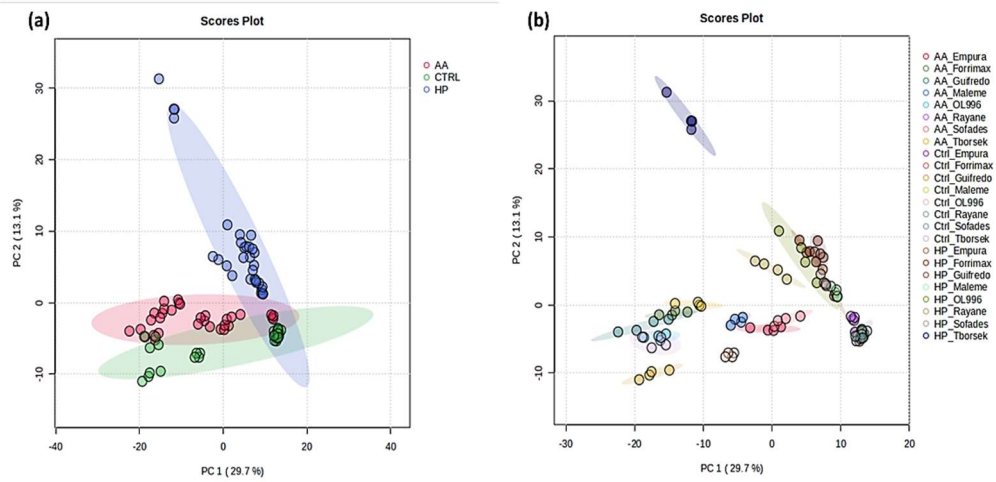

Figure 5.4. Principal component analysis (PCA) of volatilome profiles obtained through PTR-Qi-TOF-MS for characterization of **(a)** treatments and **(b)** groups (defined by the treatment and the accession). The variance explained by each component is reported in brackets.

Overall, the principal components obtained with the analysis present low values, reflecting a complexity in differentiating the groups based on the whole dataset. However, as shown in **Fig. 5.4a**, the treatments are clearly separated from each other, while for the accessions (**Fig. 5.4b**), most of the groups tested are separated, except for the CTRL groups of Rayhane, EM PURA, Sofades, Maleme-107, and Forrimax, suggesting a similar behavior in terms of volatile detected in the absence of treatments. The group with the highest level of separation is represented by HP Tborsek (dark blue), while the other treatments of the same accession (AA_Tborsek, yellow; CTRL_Tborsek, pink) occupy a near position in the scores plot.

A deeper exploration of volatilome profiles among treatments/groups is provided by the heatmaps (**Fig. 5.5**), where defined clusters among treatments and groups can be observed. Namely, the CTRL and AA groups of the Tborsek accession are clustered together in the lower part of the heat map (1 and 2, respectively), while the HP_Tborsek group present a distinct cluster of volatiles on the top of the heat map (3) (**Fig. 5.5a**). In the heatmap showing the difference among treatments (Fig. 41b), distinct groupings can be observed for each treatment, supporting the diversification obtained in the PCA.

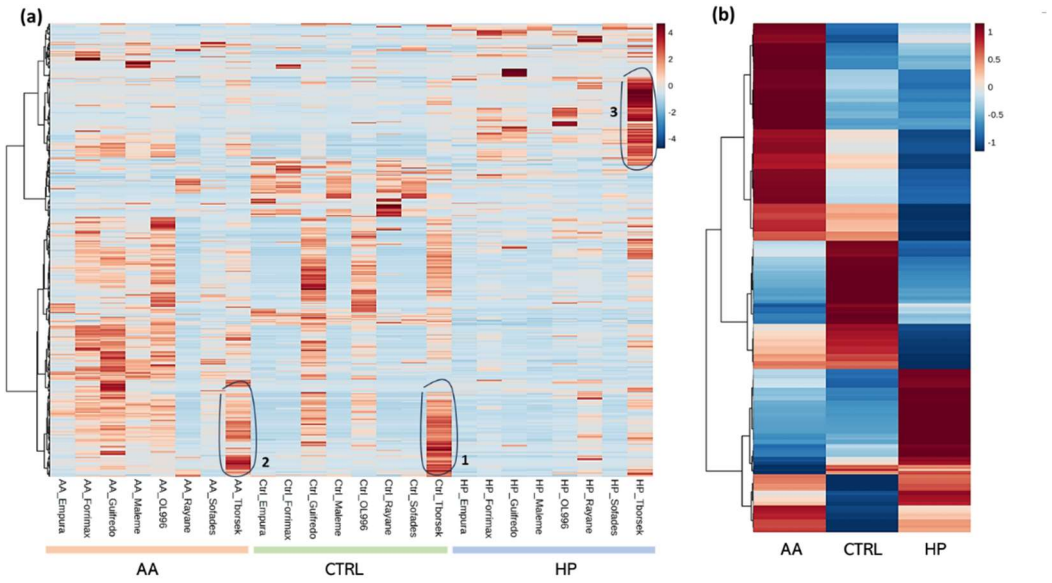

Figure 5.5. Heat maps of VOCs emitted from different **(a)** groups and **(b)** treatments. Seed groups are in columns (24) and the volatiles m/z values are in rows (440). Each colored cell on the map corresponds to a concentration value following a blue/red chromatic scale. All the m/z detected in the following study are significant (ANOVA $P \leq 0.01$).

Additionally, the hierarchical clustering (**Fig. 5.6**) provides an overview of the behavior of the seed groups/treatments based on the volatilome emitted. The resulting dendrogram confirms the peculiar behavior of the HP_Tborsek group, which cluster separately from the other HP group. Moreover, AA and CTRL groups of Tborsek accession are located nearby, which reflects a similar behavior, in terms of VOCs emitted. This data also shows a partial overlapping of the treatments CTRL and AA, as observed in the PCA.

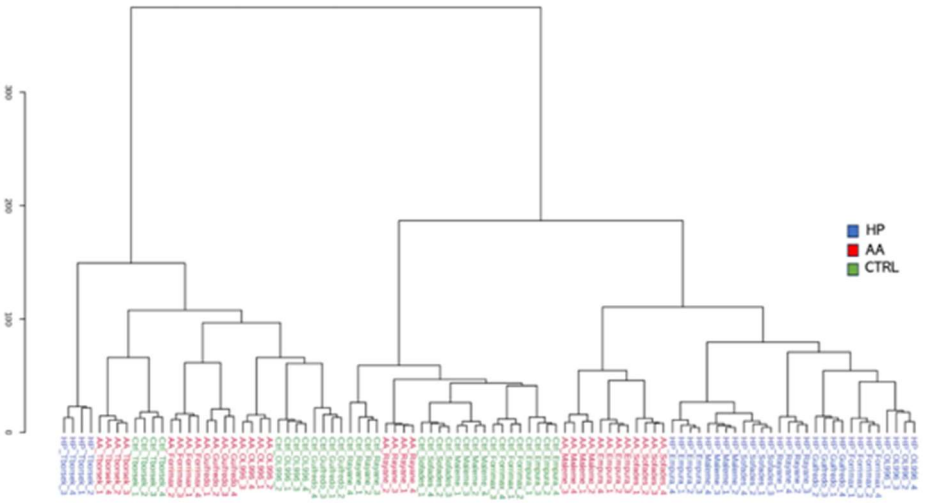

Figure 5.6. Cluster Dendrogram of seed samples produced by Hierarchical Clustering. Colors indicate the treatments of seed samples: blue, hydropriming (HP); red, artificial aging (AA); green, non-treated seeds (CTRL). Euclidean distance measure and Ward clustering algorithm were used.

Overall, the data collected and shown through PCA, heatmaps, and hierarchical clustering, report differences in the volatilome among treatments and accessions. Several studies evidenced quantitative and qualitative differences in terms of VOCs emissions between non-treated and artificially (Han et al., 2021; Liu et al., 2024) or naturally aged seeds (Zhang et al., 2022). So far, no study has looked into the VOCs profiles during HP treatments, therefore, the hereby results are useful to fill in the gaps regarding this topic. Importantly, the substantially different emission of VOCs observed in the HP seeds appear to be be consistent with the effect that priming has on the seed metabolism (Ali et al., 2019; Pagano et al., 2023). Concerning the differences in VOC profiles observed between the different investigated species/accessions, this is in agreement with other studies conducted on different species (Colville et al., 2012; Mira et al., 2016; Michalak et al., 2021). Considering that seed metabolism, and potentially the volatilome emission, is strongly affected by the chemical composition and genetic variability (Wilson, 2004; Toubiana et al., 2012), the different volatilome profiles obtained are coherent with the chemical and genetic differences characterizing the species/accessions tested in this study.

5.3.3. Selection of the most relevant compounds based on seed quality and germination behavior

To identify the m/z values that are crucial to the diversification among treatments, two different approaches were utilized: one based on PCA and correlation analyses and another based on machine learning prediction models.

5. VOCs and seed quality

First, the most relevant parameters (m/z values) included in the PCA analysis were observed, in order to highlight the most differently emitted VOCs among CTRL, HP, and AA (**Table 5.1**). The degree of relevance is indicated by the weight score. These data indicate that many VOCs, such as acetaldehyde (m/z 45.0328), 1-2 ethanediol (63.0427), ethanol (m/z 47.0482), methanetriol (49.0098), and sesquiterpenes (m/z 205.193), are actively involved in the obtained grouping regarding the different treatments.

Table 5.1. List of the most relevant m/z for the PCA grouping (weight score higher than 0.7). For each m/z value detected through PTR-TOF-MS, the weight score (from 1 to 0), the putative identification, and the reference articles of the putative identification are reported. High weight scores indicate a relevant impact on the classification of seed groups in the different treatments (CTRL, AA, HP8). M/z values without a putative identification were not included in the list.

m/z	Weight score	Putative identification	References
45.0328	0.983	Acetaldehyde	Vita et al., 2015
63.0427	0.977	1,2-Ethanediol	Cappellin et al., 2012
59.0479	0.926	Oxetane, Propanal, Acetone , 2-Propen-1-ol, 2-Propen-1-ol, Methyl vinyl ether	Cappellin et al., 2012; Taiti et al., 2018; Brilli et al., 2011; Graus et al., 2010
47.0482	0.913	Ethanol	Jordan et al., 2009
77.059	0.901	1,3-Propanediol, Propylene glycol (Propane-1,2-diol)	Cappellin et al., 2012
51.0428	0.851	Methanol water cluster	Fasbender et al., 2018
205.193	0.835	Sesquiterpenes	Cappellin et al., 2012; Taiti et al., 2018
49.0098	0.827	Methanetriol	Vita et al., 2015; Pedrotti et al., 2021
71.0475	0.817	2-Butenal, fragment of isoprene hydroperoxide, Methacrolein, Methyl Vinyl Ketone	Cappellin et al., 2012; Liu et al., 2013
89.0583	0.782	1,3-Dioxane, Ethyl acetate, 1,4-Dioxane	Cappellin et al., 2012; Vita et al., 2015; Feilberg et al., 2015, Pedrotti et al., 2021
87.0777	0.706	2-Pentanone, 3-Pentanone, 2-Methylbutanal, Pentanal, 2-Methyl-3-buten-2-ol, 3-Methyl-2-buten-1-ol	Cappellin et al., 2012; Vita et al., 2015; Yáñez-Serrano et al., 2019, Pedrotti et al., 2021

The current study also examined the potential link between volatile compounds emitted and germination performance. A Pearson correlation analysis was conducted to investigate the correlation between the m/z values detected through PTR-Qi-TOF-MS and the germination performances, defined by the percentage of germination (G%), the mean germination time (MGT), and the synchronicity of germination (Z), using all the seed groups tested in this study. **Table 5.2** illustrates the list of the most 20 m/z values with the highest or lowest coefficient of correlations. M/z with no identification of VOCs were excluded from the representation, as well as the neutral correlation, defined by the Pearson coefficient near 0. From the lists provided, most of the m/z values are associated with negative germination performances. For instance, there are no m/z values exhibiting a positive correlation coefficient in the case of G%, while for Z there is only one m/z value with a positive Pearson coefficient. For MGT, three m/z values are negatively correlated with MGT. Comparing the different lists, the VOCs that are correlated with all the germination parameters, include 2(3H)-furanone (m/z 85.0266) and cresol (m/z 109.0626).

Table 5.2. Lists of the top 20 m/z with the highest or lowest Person correlation coefficient. For each germination parameter (G%, MGT, Z), a list of the 20 most positively or negatively correlated m/z is represented with their putative identification. All the correlations shown are statistically significant ($P \leq 0.05$). G%, percentage of germination; MGT, mean germination time; Z, synchronicity index. Pc, Pearson correlation coefficient.

G%			MGT			Z		
m/z	Pc	Putative identification	m/z	Pc	Putative identification	m/z	Pc	Putative identification
Z	0.44993		85.0266	0.7302	2(3H)-Furanone	49.0098	0.5823	Methanetriol
195.1743	-0.41013	Geranyl acetone (6,10-Dimethyl-5,9-undecadien-2-one /)	73.0268	0.62948	2-Propenoic acid, Methyl glyoxal	G%	0.44993	
111.0435	-0.42631	2-Acetylfuran (1-(2-Furanyl)-ethanone)	79.0517	0.60898	Benzene	141.1275	-0.40987	3-Nonen-2-one, 2-Nonenal
69.0313	-0.4495	Furan	93.0351	0.60397	2-Methylmercaptoethanol	73.0268	-0.4247	2-Propenoic acid, Methyl glyoxal
109.0626	-0.49083	m-Cresol, o-Cresol, p-Cresol	97.0998	0.5778	Alkyl fragment	79.0211	-0.42546	Dimethyl sulfoxide
79.0517	-0.49096	Benzene	123.1156	0.57241	Santene, 2-Norbornene	67.0527	-0.42684	Monoterpene fragments (myrcene, camphene)
125.1313	-0.51928	3,3,5-Trimethylcyclohexene	43.0172	0.56032	Ketene, Hexyl acetate fragment	93.0351	-0.42705	2-Methylmercaptoethanol
57.0321	-0.52224	1-Butanol fragment, Hexanal fragment, 1-Octanol fragment	61.0273	0.55955	Ethyl acetate fragment, Acetic acid, Hydroxyacetaldehyde, Methyl formate	123.1156	-0.43185	Santene, 2-Norbornene
69.0684	-0.53669	Isoprene, 1,4-Pentadiene, 2-Methyl-3-buten-2-ol fragment, Cyclopentene, 2-Pentyne	83.0839	0.55266	Cyclohexene, 1-Hexyne, 2-Hexyne	46.0646	-0.43493	Dimethylamine, Ethylamine
171.1747	-0.54381	2-Undecanone	97.0245	0.54358	2-Furancarboxaldehyde (Furfural)	81.0322	-0.4521	2,4-Cyclopentadiene-1-one
93.0351	-0.59134	2-Methylmercaptoethanol	141.1275	0.53098	3-Nonen-2-one, 2-Nonenal	83.0839	-0.45622	Cyclohexene, 1-Hexyne, 2-Hexyne
143.1424	-0.60318	Nonanal, 2-Nonanone	109.0626	0.52796	m-Cresol, o-Cresol, p-Cresol	107.0485	-0.45785	Benzaldehyde
73.0268	-0.60906	2-Propenoic acid, Methyl glyoxal	125.1313	0.5216	3,3,5-Trimethylcyclohexene	97.0998	-0.47198	Alkyl fragment
157.1588	-0.64421	Decanal, Decanone, Menthol	57.0321	0.50692	1-Butanol fragment, Hexanal fragment, 1-Octanol fragment	91.0509	-0.4909	Thujone fragment, Linalool fragment
83.0839	-0.65174	Cyclohexene, 1-Hexyne, 2-Hexyne	47.0118	0.50265	Formic acid	109.0626	-0.49334	m-Cresol, o-Cresol, p-Cresol
97.0998	-0.65989	Alkyl fragment	47.0482	-0.45741	Ethanol	79.0517	-0.50297	Benzene
123.1156	-0.67328	Santene, 2-Norbornene	49.0098	-0.47893	Methanetriol	105.0684	-0.50713	Styrene
MGT	-0.73239		45.0328	-0.54101	Acetaldehyde	97.0245	-0.50804	2-Furancarboxaldehyde (Furfural)
141.1275	-0.75098	3-Nonen-2-one, 2-Nonenal	Z	-0.63382		85.0266	-0.51772	2(3H)-Furanone
85.0266	-0.86595	2(3H)-Furanone	G%	-0.73239		MGT	-0.63382	

Secondly, a prediction model based on a classification in three classes corresponding to the treatments (CTRL, AA, HP8A), was developed using the same dataset used for PCA analysis. To optimize the classification process through the machine-learning model, a Random Forest algorithm was utilized, which generates 10 different random trees based on different sub-sets of parameters (m/z) in the dataset. Together with the accuracy, the model was developed to provide a list of the most relevant parameters for the classification process. The weight score obtained (from 0 to 1) reflects the importance of a specific parameter to classification. The structure of the program developed using the Altair® RapidMiner® software (https://altair.com/altair-rapidminer) is illustrated in **Fig 5.7**. The model developed with the volatilome data demonstrated 100% accuracy in the classification process. Furthermore, the most influential m/z values indicated a specific set of VOCs that are pivotal in characterizing the individual treatments. The most relevant VOCs are shown in **Table 5.3**. The degree of relevance is indicated by the weight score. The results suggest the potential involvement of multiple VOCs, including 2,3-dimethyl-2-cyclopentenone (m/z 111.079), 2(3H)-furanone (m/z 85.0266), 2-butyl furan (125.095), and dimethyl

sulfide (63.0266). Despite the indication of different m/z values by the learning models as responsible for the differentiation of the treatments, many of the most relevant VOCs emitted remain unidentified.

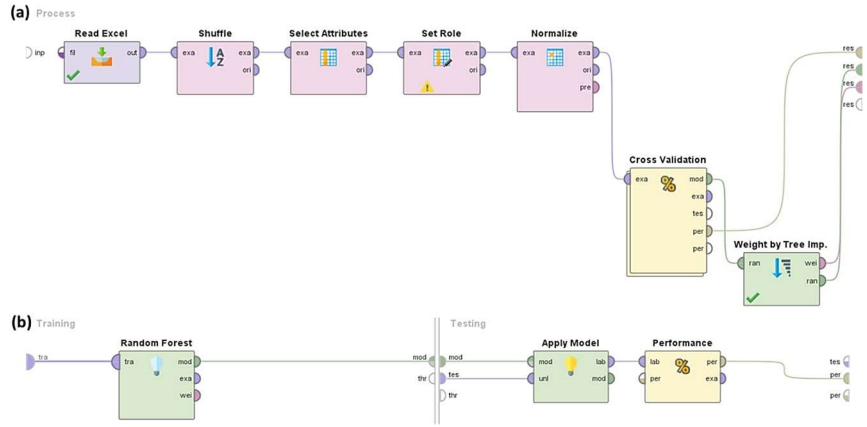

Figure 5.7. Illustration of the prediction model developed using the Altair® RapidMiner® software.

Table 5.3. List of the most relevant m/z for the classification of seed groups performed with the predictive model (weight score higher than 0.3). For each m/z value detected through PTR-TOF-MS, the weight score (from 1 to 0), the putative identification, and the reference articles of the putative identification are reported. A higher weight score indicates a relevant impact on the classification of seed groups in the different treatments (CTRL, AA, HP8). ND, no VOCs identified.

m/z	Weight score	Putative identification	References
373.093	1	ND	
91.9422	0.842	ND	
111.078	0.575	2,3-dimethyl-2-cyclopentenone	Taiti et al., 2018
30.0128	0.501	ND	
55.0855	0.497	ND	
27.0033	0.480	ND	
19.0116	0.468	ND	
29.0058	0.442	ND	
85.0266	0.408	2(3H)-furanone	Vita et al., 2015
99.0052	0.398	ND	
125.095	0.373	2-butylfuran	Taiti et al., 2018
121.027	0.368	ND	
88.0747	0.366	ND	
136.12	0.355	ND	
74.0226	0.347	ND	
68.993	0.344	ND	
102.084	0.343	ND	
114.06	0.323	ND	
63.0266	0.310	dimethyl sulfide	Cappellin et al., 2012
32.0646	0.310	ND	
27.9939	0.310	ND	
357.069	0.304	ND	

5. VOCs and seed quality

The same machine-learning approach was also used to detect the most relevant VOCs for the prediction of seed germination. In the following model, two classes were defined based on G% values: optimal (including all the seed groups with G% ≥ 80%) and non-optimal (G% < 80%). The classification in two classes (binomial classification) allowed the calculation of further parameters that reflect the efficiency of prediction. The efficiency of the model, shown in **Table 5.4**, indicates that all parameters reach very high values. In particular, the accuracy reaches 98%, reflecting an overall efficiency in class prediction, while the high percentages obtained for the sensitivity (98.41%) and specificity (96.67%) indicate that the model is able to classify the seed samples in the appropriate groups. The list of the most relevant m/z also shows a group of VOCs possibly implicated in class prediction. Interestingly, 2(3H)-furanone (m/z 85.0266) and Cresol (m/z 109.0626), which exhibited a negative correlation with germination performances, presents a significant weight score in this model. Despite the putative identification available for m/z 71.084 and 69.0684, the association of multiple VOCs to these values limits the identification of a unique component highly involved in class prediction.

Table 5.4. Classification parameters and list of the most relevant m/z to the prediction of germination classes (optimal and non-optimal). **(a)** Predictive performance of learning models obtained after cross-validation (Validation). TP true positive, TN true negative, FN false negative, FP false positive, TPR true positive rate, FPR false positive rate. Area under the curve (AUC) = $\int_{x=0}^{1} TPR(FPR^{-1}(x))dx$, Sensitivity = TP/(TP + FN). Specificity = TN/(TN + FP), Positive predictive value (PPV) = TP/(TP + FP). Negative predictive value (NPV) = TN/(FN + TN). **(b)** List of the top 20 relevant m/z for the classification of seed samples in optimal (G%≥80%) and non-optimal (G%<80%) classes. ND, no VOCs identified.

(a)

Parameters	Value
Accuracy	97.92% ± 1.80%
AUC	0.999 ± 0.001
Sensitivity	98.41% ± 2.75%
Specificity	96,67% ± 5.77%
Positive predicted value (PPV)	98.55% ± 2.51%
Negative predicted value (NPV)	97.22% ± 4.81%

(b)

	weight score	putative identification	References
25.96	1	ND	
7.949	0.998	ND	
1.102	0.992	ND	
1.084	0.984	Butyric acid fragment, Isobutyric acid fragment, Pentanal fragment, Alcohol fragment, Ethyl acetate fragment, (E)-2-pentene, 2-Methyl-1-butene, 2-Methyl-2-butene, 1-Pentene, Butanoic acid fragment,(Z)-2-pentene, 3-Methyl-1-butene, Cyclopentane	Cappellin et al., 2012; Vita et al., 2015; Feilberg et al., 2015
.1022	0.892	ND	
2.982	0.842	ND	
.0266	0.840	2(3H)-Furanone	Vita et al., 2015
.0026	0.751	ND	
.1157	0.751	ND	
.0353	0.751	ND	
.0684	0.684	Isoprene, 1,4-Pentadiene, 2-Methyl-3-buten-2-ol fragment, Cyclopentene, 2-Pentyne	Cappellin et al., 2012; Brilli et al., 2011; Kaser et al., 2013; Yáñez-Serrano et al., 2019
7.301	0.680	ND	
7.089	0.672	Ethyl butanoate (Ethylbutyrate)	Taiti et al., 2018
4.145	0.639	ND	
.0582	0.601	ND	
3.093	0.599	ND	
9.978	0.554	ND	
.0583	0.491	1,3-Dioxane, Ethyl acetate, 1,4-Dioxane	Cappellin et al., 2012; Vita et al., 2015; Feilberg et al., 2015, Pedrotti et al., 2021
9.063	0.467	m-Cresol, o-Cresol, p-Cresol	Cappellin et al., 2012

Overall, most of the VOCs detected are correlated with more than one germination parameter. Interestingly, ethanol and acetaldehyde, VOCs commonly released during seed aging (Zhang et al., 1994), show a significant correlation with MGT, reflecting a link with germination speed. Generally, VOC emissions reflect the activation of specific metabolic processes, which negatively affect germination performances (Colville et al., 2012). Although most of them are correlated with a negative germination capacity (hereby the AA groups), in this study we also identified VOCs showing a correlation with positive germination performance as in the case of HP seeds. These VOCs may reflect the activation of specific reactions that are essential for promoting optimal germination. Additionally, by using machine learning predicting models, we were able to identify VOCs correlated with different germination parameters, further confirming that these compounds may be differentially emitted in seeds with a different quality. Concerning the non-invasive seed quality estimation, the classification models provide an additional result given that the models for germination class prediction exhibited a high accuracy value; this reflects an elevated efficiency in predicting the germination performances of seed groups based on volatilome data. Although many of the m/z used by the model are not associated to any VOCs, the efficiency in predicting the correct germination class confirms the possibility of using the detection of VOCs as an approach to accurately estimate seed quality. However, the restricted number of examples contained characterizing the dataset for model development limits the affordability of the classification parameters results. As reported by a recent study, small datasets may be characterized by unbalanced data (unbalanced numbers of examples belonging to the different groups of the parameter to predict), and high dimensionality (high ratio between the number of parameters and the number of examples) (Kokol et al., 2022). Moreover, the validation of models developed from small datasets may not explore properly the possibility of overfitting and provide non-realistic accuracy values (Vabalas et al., 2019).

5.3.4. Comparative analyses of VOCs with differential profiles among treatments

Given the results of the correlation analysis and the identification of the most relevant VOCs in prediction of class of germinability, the next step involved analysing the emission levels of selected VOCs among the performed treatments and species/accessions.

The first group of investigated VOCs is represented by ethanol (EtOH), methanol (MetOH), and acetaldehyde (MeCHO). Apart from being the most common volatile compounds released during aging, ethanol, and acetaldehyde exhibited a negative correlation with MGT, suggesting an emission of these volatiles on seeds with a positive germination speed. As illustrated in **Fig. 5.8**, the AA group shows the highest level of methanol (MetOH) emission in both pea and soybean accessions. In *L. sativus*, the Maleme-107 accession presents a similar trend, whereas Sofades has the lowest level of methanol emission in the AA group. In *T. foenum-graecum* seeds, the

AA group exhibits higher level of methanol emission compared to the HP8 group. No significant differences in emission levels were observed between the CTRL and AA groups. Regarding acetaldehyde (MeCHO), the levels of emission of the HP8 groups are significantly higher than in the CTRL and AA groups in the majority of accessions. Ethanol (EtOH) is the volatile compound that is least emitted among those shown in **Fig. 5.8**. Although the low levels of emission preclude an accurate illustration of the emission pattern, in most accessions, the HP8 and AA groups exhibit significantly higher emissions compared to CTRL. Overall, the results support the findings that methanol is mainly emitted from aged seeds, as well as the fact that acetaldehyde and ethanol emission patterns may be influenced by specific reactions occurring in primed seeds.

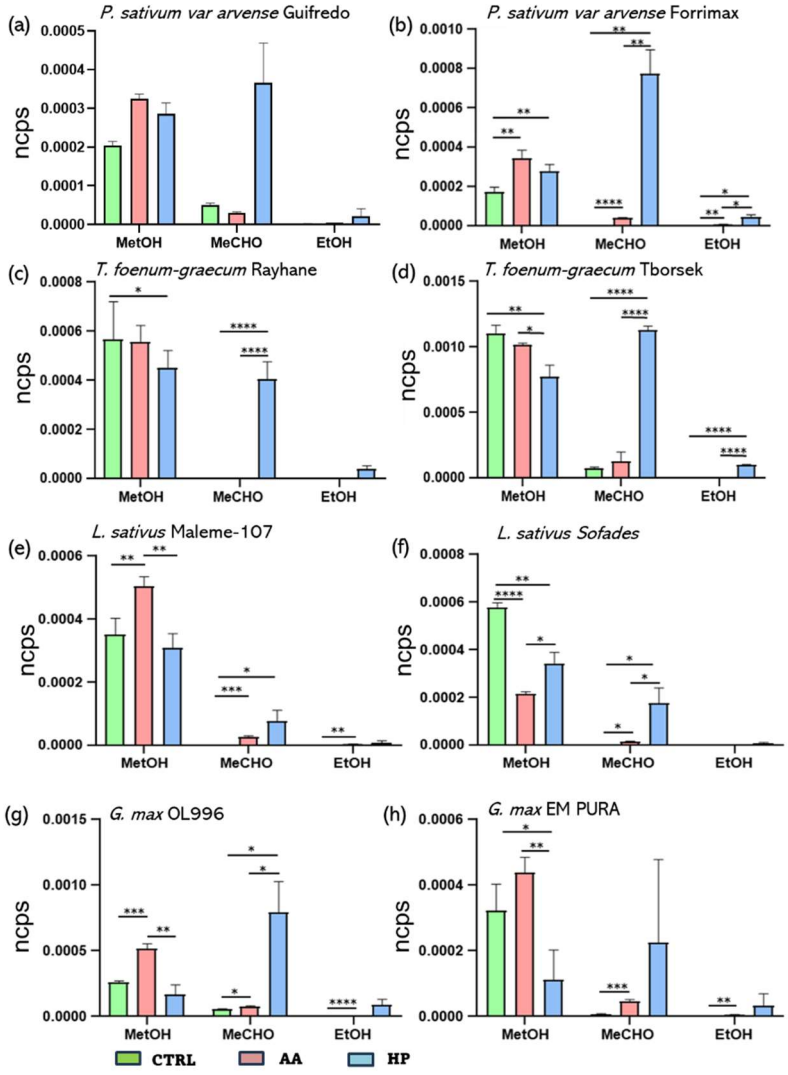

Figure 5.8. Comparison between the levels of methanol (MetOH), acetaldehyde (MeCHO), and ethanol (EtOH) of applied treatments in **(a)** *P. sativum var. arvense* Guifredo, **(b)** *P.*

sativum var. arvense Forrimax, **(c)** *T. foenum-graecum* Rayhane, **(d)** *T. foenum-graecum* Tborsek, **(e)** *L. sativus* Maleme-107, **(f)** *L. sativus* Sofades, **(g)** *G. max* OL996, and **(h)** *G. max* EM PURA. Volatile levels emitted are expressed as normalized count per second (ncps). Statistically significant differences are highlighted by asterisks (*'* $P < 0.0332$, '** $P < 0.0021$, '*** $P < 0.0002$, '**** $P < 0.0001$*). CTRL, control non-treated seeds; AA, artificially aged seeds; HP, hydroprimed seeds.

The next group of VOCs is represented by 2(3H)-furanone (m/z 85.0266), cresol isomers (m/z 109.0626), and methanetriol (m/z 49.0098). Furanone and cresol isomers were found to be correlated with G%, MGT, and Z. In particular, furanone presents a strong negative correlation with G%, Z, and a strong positive correlation with MGT, indicating that this volatile is emitted mainly in low-quality seeds. Although the correlation coefficient is less marked compared to furanone, cresol isomers (m-cresol, o-cresol, p-cresol) follow a similar trend. Moreover, both furanone and cresol are relevant VOCs obtained from the classification of seed samples with the machine-learning model, indicating a specific emission of these volatile linked to germination performance. As shown in **Fig. 5.9**, the levels of emission of 2(3H)-furanone exhibit a conserved trend among species and accession, where AA seeds present significantly higher values compared to CTRL and HP8. No significant differences are observed between CTRL and HP8 groups, except for the accession Guifredo for *P. sativum* (**Fig. 5.9a**) and the accession Tborsek for *T. foenum-graecum* (**Fig. 5.9d**). The observed pattern supports the evidence provided by the correlation analyses, which identifies 2(3H)-furanone as a marker of negative germination performance.

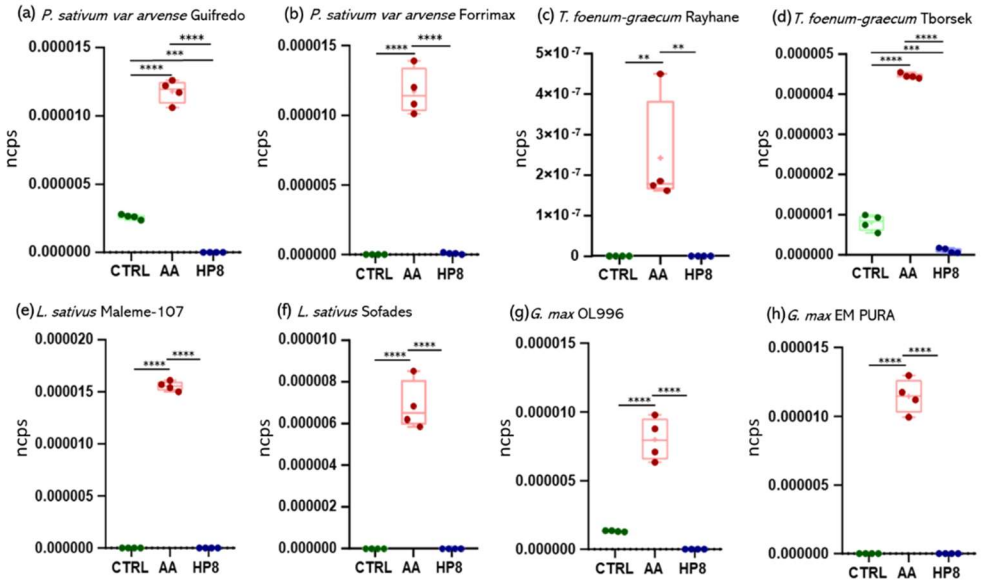

Figure 5.9. Box plots showing the levels of 2(3H)-furanone (m/z 85.0266) among different treatments in **(a)** *P. sativum var. arvense* Guifredo, **(b)** *P. sativum var. arvense* Forrimax, **(c)** *T. foenum-graecum* Rayhane, **(d)** *T. foenum-graecum* Tborsek, **(e)** *L. sativus* Maleme-107, **(f)** *L. sativus* Sofades, **(g)** *G. max* OL996, and **(h)** *G. max* EM PURA. Volatile levels emitted are

expressed as normalized count per second (ncps). Dots indicate the emission levels of single seed groups of each treatment. Statistically significant differences are highlighted by asterisks (*'*P < 0.0332, '**'P < 0.0021, '***'P < 0.0002, '****'P < 0.0001*).

The levels of cresol isomers (m-cresol, o-cresol, and p-cresol) are illustrated in **Fig. 5.10**. Cresol isomer emission levels are markedly elevated in the AA group, similar to 2(3H)-furanone. Exceptions include the *T. foenum-graecum* Rayhane (Fig. **5.10c**), where the HP8 group shows higher levels of emissions, and *G. max* EM PURA (**Fig. 5.10h**), where cresol isomers were not detected. Differently, the emission pattern of methanetriol (**Fig. 5.11**) indicate significantly higher levels in HP seeds. Only in *G. max* OL 996 (**Fig. 5.11g**) the methanetriol levels are not significant difference between AA and HP8 groups. Interestingly, in the Tborsek (**Fig. 5.11d**), Maleme-107 (**Fig. 5.11e**), and OL 996 (**Fig. 5.11g**) accessions, the levels of emission recorded in AA groups are significantly higher compared to the CTRL groups.

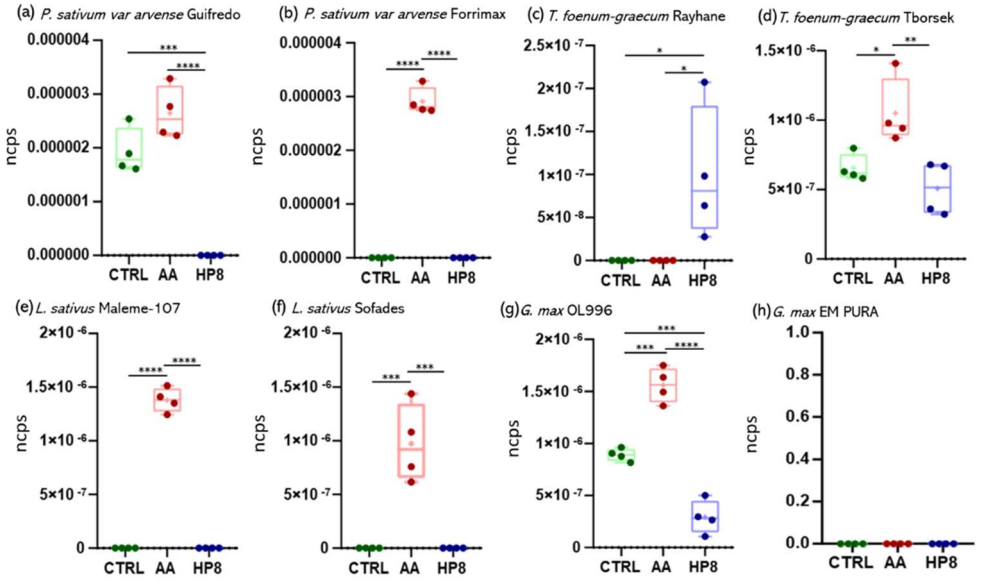

Figure 5.10. Box plots showing the levels of m-Cresol, o-Cresol, and p-Cresol (m/z 109.0626) among different treatments in **(a)** *P. sativum var. arvense* Guifredo, **(b)** *P. sativum var. arvense* Forrimax, **(c)** *T. foenum-graecum* Rayhane, **(d)** *T. foenum-graecum* Tborsek, **(e)** *L. sativus* Maleme-107, **(f)** *L. sativus* Sofades, **(g)** *G. max* OL996, and **(h)** *G. max* EM PURA. Volatile levels emitted are expressed as normalized count per second (ncps). Dots indicate the emission levels of single seed groups of each treatment. Statistically significant differences are highlighted by asterisks (*'*P < 0.0332, '**'P < 0.0021, '***'P < 0.0002, '****'P < 0.0001*).

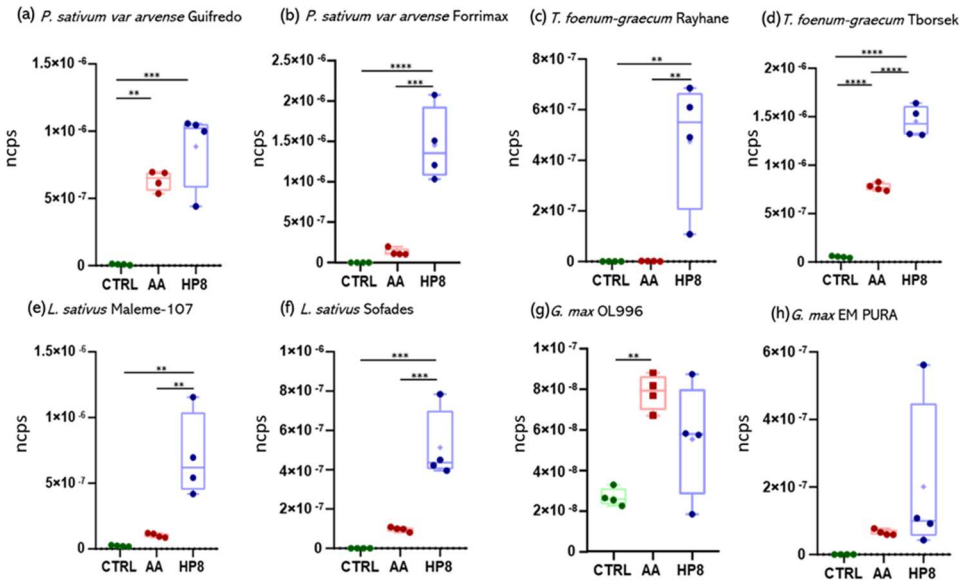

Figure 5.11. Box plots showing the levels of methanetriol (m/z 49.0098) among different treatments in **(a)** *P. sativum var. arvense* Guifredo, **(b)** *P. sativum var. arvense* Forrimax, **(c)** *T. foenum-graecum* Rayhane, **(d)** *T. foenum-graecum* Tborsek, **(e)** *L. sativus* Maleme-107, **(f)** *L. sativus* Sofades, **(g)** *G. max* OL996, and **(h)** *G. max* EM PURA. Volatile levels emitted are expressed as normalized count per second (ncps). Dots indicate the emission levels of single seed groups of each treatment. Statistically significant differences are highlighted by asterisks (*'*' $P < 0.0332$, '**' $P < 0.0021$, '***' $P < 0.0002$, '****' $P < 0.0001$).

Overall, the emission levels of selected VOCs reflect the information provided by the correlation analyses and the machine-learning models. The emission of ethanol, commonly used as seed vigour test in many species, such as *Brassica napus* (Buckley and Huang, 2011) and *Brassica oleracea* (Kodde et al., 2012), exhibited higher emission levels in AA groups, supporting the evidence from literature (Zhang et al., 1994). In addition, further VOCs showed a treatment-related emission. In particular, cresol isomers and 2(3H)-furanone, showing elevated weight scores and correlated with negative germination performances, are present in high amounts in the AA groups. Differently, methanetriol, negatively correlated with MGT, was more present in the HP groups. Therefore, the current study brings new and relevant information related to the emission of 2(3H)-furanone, cresol, and methanetriol in low- and high-quality seeds. A recent study reported the emission of furanone from quinoa (*Chenopodium quinoa*) after micro-wave treatments, partially supporting the hypothesis of furanone emission from seeds with a reduced quality (Cao et al., 2024).

5.4 Conclusions

The present work explored the utilization of volatilome profiles as “fingerprint” of seed quality. Profiles emerged the presence of VOCs differently emitted among low and high-quality seeds, already emerged from the general overview of volatilome profiling. The levels of emissions of acetaldehyde, ethanol, and methanol, most common volatile compounds released from seeds during deterioration, were evaluated. The results indicated a more complex trend, in which methanol is mostly emitted by HP, while acetaldehyde and ethanol are emitted by CTRL and AA groups in most accession tested. A more indicative information regarding the link between VOCs emission and seed quality was provided by the correlation and predictive model analyses, highlighting specific compounds potentially connected with seed quality. These results led to the identification of VOCs correlated with a low (furanone and cresol isomers) and high (methanetriol) seed quality, supporting the possibility of using VOCs emission level to estimate seed quality in a non-invasive manner. Despite these promising data, many m/z values detected through PTR-Qi-TOF-MS could not be associated with specific VOCs, while other m/z values are associated with multiple volatile compounds, thus complicating the correct identification of the VOCs potentially limiting seed quality discrimination. In this context, the utilization of machine-learning model can help the estimation of seed quality overcoming the lack of knowledge related to unidentified VOCs of relevant m/z values.

References

Ali, Q., Ashraf, S., Kamran, M., Rehman, A., & Ahmad, S. (2019). Alterations in plant secondary metabolism by seed priming. *Priming and Pretreatment of Seeds and Seedlings: Implication in Plant Stress Tolerance and Enhancing Productivity in Crop Plants*, 147-161.

Balestrazzi, A., Calvio, C., Macovei, A., Pagano, A., Laux, P., Moutahir, H., Rajjou, L., Tani E., Chachalis, D., Katsis, C., Ghaouti, L., Gmouh, S., Majid, S., Elleuch, A., Hanin, M., Khemakhem, B., El Abed, H., Nunes, J., Araújo, S., Benhamrouche, A. & Bersi, M. (2024). Seed quality as a proxy of climate-ready orphan legumes: the need for a multidisciplinary and multi-actor vision. *Frontiers in Plant Science*, 15, 1388866.

Brilli, F., Ruuskanen, T. M., Schnitzhofer, R., Müller, M., Breitenlechner, M., Bittner, V., Wohlfahrt, G., Loreto, F., & Hansel, A. (2011). Detection of plant volatiles after leaf wounding and darkening by proton transfer reaction “time-of-flight” mass spectrometry (PTR-TOF). *PLoS One*, 6(5), e20419.

Buckley, W. T., & Huang, J. (2011). An ethanol-based seed vigour assay for canola. *Seed Science and Technology*, *39*(2), 510-526.

Cao, H., Han, J., Sun, R., Li, Z., Zhang, Y., Song, H., Huang, K., Zhang, Y., & Guan, X. (2024). Analysis of key enzyme activity and aroma volatile compounds in microwave-irradiated quinoa during storage. *Journal of Cereal Science*, 116, 103857.

Cappellin, L., Karl, T., Probst, M., Ismailova, O., Winkler, P. M., Soukoulis, C., Aprea, E., Märk, T. D., Gasperi, F., & Biasioli, F. (2012). On quantitative determination of volatile organic compound concentrations using proton transfer reaction time-of-flight mass spectrometry. *Environmental Science & Technology*, 46(4), 2283-2290.

Carpenter, J. E. (2011). Impact of GM crops on biodiversity. *GM Crops*, 2(1), 7-23.

Colville, L., Bradley, E. L., Lloyd, A. S., Pritchard, H. W., Castle, L. & Kranner, I. (2012). Volatile fingerprints of seeds of four species indicate the involvement of alcoholic fermentation, lipid peroxidation, and Maillard reactions in seed deterioration during aging and desiccation stress. *Journal of Experimental Botany*, 63(18), 6519-6530.

Damalas, C. A., Koutroubas, S. D., & Fotiadis, S. (2019). Hydro-priming effects on seed germination and field performance of faba bean in spring sowing. *Agriculture*, 9(9), 201.

Dethier, J. J., & Effenberger, A. (2012). Agriculture and development: A brief review of the literature. *Economic Systems*, 36(2), 175-205.

ElMasry, G., ElGamal, R., Mandour, N., Gou, P., Al-Rejaie, S., Belin, E., & Rousseau, D. (2020). Emerging thermal imaging techniques for seed quality evaluation: Principles and applications. *Food Research International*, 131, 109025.

Fasbender, L., Yáñez-Serrano, A. M., Kreuzwieser, J., Dubbert, D., & Werner, C. (2018). Real-time carbon allocation into biogenic volatile organic compounds (BVOCs) and respiratory carbon dioxide (CO2) traced by PTR-TOF-MS, 13CO2 laser spectroscopy and 13C-pyruvate labelling. *PLoS One*, *13*(9), e0204398.

Feilberg, A., Bildsoe, P., & Nyord, T. (2015). Application of PTR-MS for measuring odorant emissions from soil application of manure slurry. *Sensors*, 15(1), 1148-1167.

Feng, L., Zhu, S., Liu, F., He, Y., Bao, Y., & Zhang, C. (2019). Hyperspectral imaging for seed quality and safety inspection: A review. *Plant Methods*, 15, 1-25.

Ghasemi-Golezani, K., Japparpour-Bonyadi, Z., Shafagh-Kolvanagh, J., & Nikpour-Rashidabad, N. (2013). Effects of water stress and hydro-priming duration on field performance of lentil. *International Journal of Farming and Allied Sciences*, 2(21), 922-925.

Graus, M., Müller, M., & Hansel, A. (2011). High resolution PTR-TOF: quantification and formula confirmation of VOC in real time. *Journal of the American Society for Mass Spectrometry*, 21(6), 1037-1044.

Huang, M., Wang, Q. G., Zhu, Q. B., Qin, J. W. & Huang, G. Review of seed quality and safety tests using optical sensing technologies. *SST*, 43(3), 337–366 (2015).

Kapoor, N., Arya, A., Siddiqui, M. A., Amir, A., & Kumar, H. (2010). Seed deterioration in chickpea (*Cicer arietinum* L.) under accelerated ageing. *Asian Journal of Plant Sciences*, 9(3), 158-162.

Kaser, L., Karl, T., Schnitzhofer, R., Graus, M., Herdlinger-Blatt, I. S., DiGangi, J. P., Sive, B., Turnipseed, A., Hornbrook, R.S., Zheng, W., Flocke, F. M., Guenther, A., Keutsch, F. N., Apel, E., & Hansel, A. (2013). Comparison of different real time VOC measurement techniques in a ponderosa pine forest. *Atmospheric Chemistry and Physics*, 13(5), 2893-2906.

Kavhiza, N. J., Zargar, M., Prikhodko, S. I., Pakina, E. N., Murtazova, K. M. S., & Nakhaev, M. R. (2022). Improving crop productivity and ensuring food security through the adoption of genetically modified crops in sub-Saharan Africa. *Agronomy*, 12(2), 439.

Kodde, J., Buckley, W. T., de Groot, C. C., Retiere, M., Zamora, A. M. V., & Groot, S. P. (2012). A fast ethanol assay to detect seed deterioration. *Seed Science Research*, *22*(1), 55-62.

Kokol, P., Kokol, M., & Zagoranski, S. (2022). Machine learning on small size samples: A synthetic knowledge synthesis. *Science Progress*, 105(1), 00368504211029777.

Kvakkestad, V., & Vatn, A. (2011). Governing uncertain and unknown effects of genetically modified crops. *Ecological Economics*, 70(3), 524-532.

Lee, R. (2011). The outlook for population growth. *Science*, 333(6042), 569-573.

Lee, P. C., Taylor, A. G., Zhang, M., & Esashi, Y. (2000). Volatile compounds and accumulation of acetaldehyde-protein adducts in relation to seed quality and storage conditions. *Journal of New Seeds*, 2(1), 59-76.

Li, W., Tan, F., Cui, J., & Ma, B. (2022). Fast identification of soybean varieties using Raman spectroscopy. *Vibrational Spectroscopy*, 123, 103447.

Lin, P., Xiaoli, L., Li, D., Jiang, S., Zou, Z., Lu, Q., & Chen, Y. (2019). Rapidly and exactly determining postharvest dry soybean seed quality based on machine vision technology. *Scientific Reports*, 9(1), 17143.

Liu, Y., Ren, S., Sun, Q., Guo, B., Zhang, Y., Li, M., & Zhang, R. (2024). GC-IMS determination of volatile organic compounds as potential indicators of wheat germination rate. *Food Bioscience*, 57, 103535.

Liu, Y. J., Herdlinger-Blatt, I., McKinney, K. A., & Martin, S. T. (2013). Production of methyl vinyl ketone and methacrolein via the hydroperoxyl pathway of isoprene oxidation. *Atmospheric Chemistry and Physics*, 13(11), 5715-5730.

McDonald, M. B. (1998). Seed quality assessment. *Seed Science Research*, 8(2), 265-276.

Michalak, M., Plitta-Michalak, B. P., Nadarajan, J., & Colville, L. (2021). Volatile signature indicates viability of dormant orthodox seeds. *Physiologia Plantarum*, 173(3), 788-804.

Mira, S., González-Benito, M. E., Hill, L. M., & Walters, C. (2010). Characterization of volatile production during storage of lettuce (*Lactuca sativa*) seed. *Journal of Experimental Botany*, 61(14), 3915-3924.

Mira, S., Hill, L. M., González-Benito, M. E., Ibáñez, M. A., & Walters, C. (2016). Volatile emission in dry seeds as a way to probe chemical reactions during initial asymptomatic deterioration. *Journal of Experimental Botany*, 67(6), 1783-1793.

Mohammadzadeh, A., Majnon Hoseini, N., Asadi, S., Moghadam, H., & Jamali, M. (2019). Effects of artificial seed ageing on germination indices, seedling establishment and yield of two red kidney bean (*Phaseolus vulgaris* L.) cultivars. *Iranian Journal of Seed Science and Technology*, *7*(2), 75-94.

Musaev, F., Priyatkin, N., Potrakhov, N., Beletskiy, S., & Chesnokov, Y. (2021). Assessment of Brassicaceae seeds quality by X-ray analysis. *Horticulturae*, 8(1), 29.

Pagano, A., Macovei, A., & Balestrazzi, A. (2023). Molecular dynamics of seed priming at the crossroads between basic and applied research. *Plant Cell Reports*, 42(4), 657–688.

Pang, Z., Lu, Y., Zhou, G., Hui, F., Xu, L., Viau, C., Spigelman, A. F, MacDonald, P. E., Wishart, D. S., Li, S. & Xia, J. (2024). MetaboAnalyst 6.0: towards a unified platform for metabolomics data processing, analysis and interpretation. *Nucleic Acids Research*, gkae253.

Paparella, S., Araújo, S. S., Rossi, G., Wijayasinghe, M., Carbonera, D., & Balestrazzi, A. (2015). Seed priming: state of the art and new perspectives. *Plant Cell Reports*, 34, 1281-1293.

Pedrotti, M., Khomenko, I., Genova, G., Castello, G., Spigolon, N., Fogliano, V., & Biasioli, F. (2021). Quality control of raw hazelnuts by rapid and non-invasive fingerprinting of volatile compound release. *LWT*, 143, 111089.

Rahman, A., & Cho, B. K. (2016). Assessment of seed quality using non-destructive measurement techniques: a review. *Seed Science Research*, 26(4), 285-305.

Ranal, M. A. & de Santana, D. G. (2006). How and why to measure the germination process? *Revista Brasileira de Botanica*, 29(1), 1–11.

Roquencourt, C., Grassin-Delyle, S., & Thévenot, E. A. (2022). ptairMS: real-time processing and analysis of PTR-TOF-MS data for biomarker discovery in exhaled breath. *Bioinformatics*, 38(7), 1930-1937.

Schmeller, D. S., & Henle, K. (2008). Cultivation of genetically modified organisms: resource needs for monitoring adverse effects on biodiversity. *Biodiversity and Conservation*, 17, 3551-3558

Shi, H., & Chen, J. (2018). Characteristics of climate change and its relationship with land use/cover change in Yunnan Province, China. *International Journal of Climatology*.

Singh, R. B., Mishra, S., Saxena, P., Saxena, M., Smail, M. M., & Velluri, S. R. (2022). Genetically modified organisms and foods: perspectives and challenges. *Functional Foods and Nutraceuticals in Metabolic and Non-Communicable Diseases*, 493-505.

Singh, S., Lal, G. M., Bara, B. M., & Mishra, S. N. (2017). Effect of hydropriming and osmopriming on seed vigour and germination of Pea (Pisum sativum L.) seeds. *Journal of Pharmacognosy and Phytochemistry*, 6(3), 820-824.

Taiti, C., Costa, C., Figorilli, S., Billi, M., Caparrotta, S., Comparini, D., & Mancuso, S. (2018). Volatome analysis approach for the taxonomic classification of tree exudate collection using Proton Transfer Reaction Time of Flight Mass Spectrometry. *Flavour and Fragrance Journal*, 33(3), 245-262.

TeKrony, D. M. (2005). Accelerated aging test: principles and procedures. *Seed Technology*, 135-146.

Tester, M., & Langridge, P. (2010). Breeding technologies to increase crop production in a changing world. *Science*, 327(5967), 818-822.

Tian, P. P., Lv, Y. Y., Yuan, W. J., Zhang, S. B., & Hu, Y. S. (2019). Effect of artificial aging on wheat quality deterioration during storage. *Journal of Stored Products Research*, 80, 50-56.

Toubiana, D., Semel, Y., Tohge, T., Beleggia, R., Cattivelli, L., Rosental, L., Nikoloski, Z., Zamir, D., Fernie, A. R., & Fait, A. (2012). Metabolic profiling of a mapping population exposes new insights in the regulation of seed metabolism and seed, fruit, and plant relations. *PLoS Genetics*, 8(3), e1002612.

Vabalas, A., Gowen, E., Poliakoff, E., & Casson, A. J. (2019). Machine learning algorithm validation with a limited sample size. *PloS One*, 14(11), e0224365.

Vita, F., Taiti, C., Pompeiano, A., Bazihizina, N., Lucarotti, V., Mancuso, S., & Alpi, A. (2015). Volatile organic compounds in truffle (*Tuber magnatum Pico*): comparison of samples from different regions of Italy and from different seasons. *Scientific Reports*, 5(1), 1-15.

Wang, B., Yang, R., Ji, Z., Zhang, H., Zheng, W., Zhang, H., & Feng, F. (2022). Evaluation of biochemical and physiological changes in sweet corn seeds under natural aging and artificial accelerated aging. *Agronomy*, 12(5), 1028.

Wilson, R. F. (2004). Seed composition. *Soybeans: Improvement, Production, and Uses*, 16, 621-677.

Umarani, R., Bhaskaran, M., Vanitha, C., & Tilak, M. (2020). Fingerprinting of volatile organic compounds for quick assessment of vigour status of seeds. *Seed Science Research*, 30(2), 112-121.

Yáñez-Serrano, A. M., Mahlau, L., Fasbender, L., Byron, J., Williams, J., Kreuzwieser, J., & Werner, C. (2019). Heat stress increases the use of cytosolic pyruvate for isoprene biosynthesis. *Journal of Experimental Botany*, 70(20), 5827-5838.

Zhang, M., Maeda, Y., Furihata, Y., Nakamaru, Y., & Esashi, Y. (1994). A mechanism of seed deterioration in relation to the volatile compounds evolved by dry seeds themselves. *Seed Science Research*, 4(1), 49-56.

Zhang, T., Ayed, C., Fisk, I. D., Pan, T., Wang, J., Yang, N., & Sun, Q. (2022). Evaluation of volatile metabolites as potential markers to predict naturally-aged seed vigour by coupling rapid analytical profiling techniques with chemometrics. *Food Chemistry*, 367, 130760.

Zhu, L. W., Ma, W. G., Hu, J., Zheng, Y. Y., Tian, Y. X. Y. J., & Hu, W. M. (2015). Advances of NIR spectroscopy technology applied in seed quality detection. *Spectroscopy and Spectral Analysis*, 35(2), 346-349.

Zwiers, F. W., Alexander, L. V., Hegerl, G. C., Knutson, T. R., Kossin, J. P., Naveau, P., Nicholls N., Schär C., Seneviratne S.I. & Zhang, X. (2013). Climate Extremes: Challenges in Estimating and Understanding Recent Changes in the Frequency and Intensity of Extreme Climate and Weather Events. In: Asrar, G., Hurrell, J. (eds) Climate Science for Serving Society. *Springer*, Dordrecht.

6. Final conclusions

In the present project, three approaches, based on the detection of specific markers of seed quality, have been developed and tested on multiple species. Although an exhaustive exploration of the potentiality of these methods requires further analyses, the promising results obtained for each approach confirm the possibility of using these methodologies for non-invasive, rapid, and accurate estimation of seed quality.

The non-invasive detection of ROS performed in non-treated (CTRL), imbibed (HP), hydroprimed (HBDB), and damaged seeds (HS), obtained mainly with the FOX-1 assay [ROOH], provided a general trend in ROS release levels that reflect the quality of the different seed groups. According to the data collected, CTRL and HS groups present higher [ROOH] values released compared to HP and HPDB groups. Although in tomato and wheat, the CTRL group exhibits higher levels of [ROOH] compared to HS, in soybean this trend was not confirmed. However, these results show significant differences, in terms of [ROOH], between high-quality (HPDB) and low-quality (HS) seeds. For soybean, the measured ROS was correlated data obtained from gene expression analyses. The data relative to the investigated genes (*MnSOD*, *SOD1*, *CAT1*, *CAT5*, *RbohE2*, *RbohC2*, related with ROS production or scavenging, is in line with other studies reporting increased antioxidant gene expression during seed imbibition (Zhao et al., 2020; Dey and Bhattacharjee, 2023). Overall, the following results indicate that controlled ROS levels are required to ensure optimal germination; when this equilibrium is broken, uncontrolled ROS accumulation is indicative of damaged seeds.

The method based on UPE and DL measurements provided positive results, confirming the possibility of using the photon emission as an index of the physiological seed status. The predictive model developed from the used datasets (CIC, *C. arietinum*; LAT, *L. sativus*; FAB, *V. faba*; PHA; *P. vulgaris*; PIS, *P. sativum*) provided different efficiency values. The models derived from the datasets CIC and FAB exhibit moderate efficiency in classifying seed samples, while the processes obtained from the remaining datasets show high performances. This discrepancy in efficiency can be attributed to different factors: (1) the datasets differ in the number of examples, which can affect the efficiency of class prediction (Barbedo, 2018); (2) the presence of outliers can interfere with the classification (Fernández et al., 2022); (3) balancing the different predictive models, represents a critical issue in most of the models developed. In this context, the application of the “MetaCost” operator of RapidMiner® software induced an improvement in sensitivity, indicating that a similar approach can be used also for other models. Overall, the results obtained confirmed the correlation between seed quality and UPE and DL phenomena, in agreement with other studies (Grasso et al., 2018; Li et al., 2022). These results support the possibility of integrating the application of artificial intelligence (AI) models to improve the elaboration and interpretation of complex data (Jordan and Mitchell, 2015; Milo and Somech, 2020).

VOCs detection provided relevant information related to the volatilome profiles of different quality seeds. The obtained results indicate a different clusterization of non-

treated (CTRL), hydro-primed (HP), and artificially aged (AA) seeds, reflecting different patterns of VOCs emission among treatments. In recent years, other studies have also evidenced a quantitative and qualitative difference, in terms of VOC emissions, between non-treated and artificially aged (Han et al., 2021; Liu et al., 2024) or naturally aged seeds (Zhang et al., 2022). However, prior to this study, no data regarding the emission of VCOs from HP seeds was available. The obtained data allowed the identification of VOCs mainly related to negative germination performances, where different metabolic activity is linked with the accelerated seed aging process (Colville et al., 2012; Umarani et al., 2020). By applying machine learning approaches, the efficiency of the predictive model for the classification of seed groups, based on germination percentage (G%), revealed a high efficiency. Although the size of the dataset needs to be adjusted to further evaluate the obtained accuracy values (Vabalas et al., 2019), the results confirm the possibility of using the real-time VOCs emission to non-invasively estimate seed quality.

To conclude, the present PhD thesis exploited multiple approaches for the non-invasive evaluation of seed quality. Among the methodologies developed in this work, ROS detection can be considered as the most rapid, easy-to-use and cost-effective, being based mainly of the availability of an array of chemical substances and spectrophotometric reader. However, the accuracy and large-scale use of this methodology still requires further developments. On the other hand, the detection of UPE/DL and VOCs, provide a much higher quantity and accuracy of data, but require advanced equipment and skills to be performed and analyzed. In these cases, the use of machine learning algorithms was necessary to provide models able to distinguish between seeds with different characteristics. Overall, the data hereby provided represent a good starting point for the optimization and development of accurate, rapid, and easy-to-use non-invasive technologies to support the seed industry sector. In the future, additional analyses conducted on a wider panel of species will offer a stronger validation and more precise estimation of the cost related to large-scale use.

7. References

Agati, G., Azzarello, E., Pollastri, S., & Tattini, M. (2012). Flavonoids as antioxidants in plants: location and functional significance. *Plant Science*, 196, 67-76.

Ali, F., Qanmber, G., Li, F., & Wang, Z. (2021). Updated role of ABA in seed maturation, dormancy, and germination. *Journal of Advanced Research*, 35, 199–214.

Ali, M. R., Rahman, M. M., & Ahammad, K. U. (2014). Effect of relative humidity, initial seed moisture content and storage container on soybean (Glycine max L. Meril.) seed quality. *Bangladesh Journal of Agricultural Research*, 39(3), 461-469.

Alscher, R. G., Erturk, N., & Heath, L. S. (2002). Role of superoxide dismutases (SODs) in controlling oxidative stress in plants. *Journal of Experimental Botany*, 53(372), 1331-1341.

Ambrose, A., Kandpal, L. M., Kim, M. S., Lee, W. H., & Cho, B. K. (2016). High speed measurement of corn seed viability using hyperspectral imaging. *Infrared Physics & Technology*, 75, 173-179.

Ambrose, A., Lohumi, S., Lee, W. H., & Cho, B. K. (2016). Comparative nondestructive measurement of corn seed viability using Fourier transform near-infrared (FT-NIR) and Raman spectroscopy. *Sensors and Actuators B: Chemical*, 224, 500-506.

Ansari, N., Ratri, S. S., Jahan, A., Ashik-E-Rabbani, M., & Rahman, A. (2021). Inspection of paddy seed varietal purity using machine vision and multivariate analysis. *Journal of Agriculture and Food Research*, 3, 100109.

Anupama, K., Pranathi, K., & Meenakshi Sundaram, R. (2020). Assessment of genetic purity of bulked-seed of rice CMS lines using capillary electrophoresis. *Electrophoresis*, 41(20), 1749-1751.

Arora, N. K. (2019). Impact of climate change on agriculture production and its sustainable solutions. *Environmental Sustainability*, 2(2), 95-96.

Bailly, C., El-Maarouf-Bouteau, H., & Corbineau, F. (2008). From intracellular signaling networks to cell death: the dual role of reactive oxygen species in seed physiology. *Comptes Rendus. Biologies*, 331(10), 806-814.

Bailly, C., & Gomez Roldan, M. V. (2023). Impact of climate perturbations on seeds and seed quality for global agriculture. *The Biochemical Journal*, 480(3), 177–196.

Bakhtavar, M. A., & Afzal, I. (2020). Seed storage and longevity: mechanism, types and management. *Advances in Seed Production and Management*, 451-468.

Balestrazzi, A., Calvio, C., Macovei, A., Pagano, A., Laux, P., Moutahir, H., Rajjou, L., Tani, E., Chachalis, D., Katsis, C., Ghaouti, L., Gmouh, S., Majid, S., Elleuch, A., Hanin, M., Khemakhem, B., El Abed, H., Nunes, J., Araújo, S., Benhamrouche, A. & Bersi, M. (2024). Seed quality as a proxy of climate-ready orphan legumes: the need for a multidisciplinary and multi-actor vision. *Frontiers in Plant Science*, *15*, 1388866.

Bailly, C. (2019). The signalling role of ROS in the regulation of seed germination and dormancy. *Biochemical Journal*, 476(20), 3019-3032.

7. References

Balestrazzi, A., Confalonieri, M., Macovei, A., Donà, M., & Carbonera, D. (2011). Genotoxic stress and DNA repair in plants: emerging functions and tools for improving crop productivity. *Plant Cell Reports*, 30, 287-295.

Barbedo, J. G. A. (2018). Impact of dataset size and variety on the effectiveness of deep learning and transfer learning for plant disease classification. *Computers and Electronics in Agriculture*, 153, 46-53.

Barbedo, C. J., Centeno, D. D. C., & Ribeiro, R. D. C. L. F. (2013). Do recalcitrant seeds really exist?. *Hoehnea*, 40, 583-593.

Barnard, A., & Calitz, F. J. (2011). The effect of poor quality seed and various levels of grading factors on the germination, emergence and yield of wheat. *South African Journal of Plant and Soil*, 28(1), 23–33.

Bennett, M. A., Grassbaugh, E. M., Evans, A. F., & Kleinhenz, M. D. (2004). Saturated salt accelerated aging (SSAA) and other vigor tests for vegetable seeds. *Seed Technology*, 67-74.

Berhe, M., Subramanyam, B., Demissie, G., Chichaybelu, M., Abera, F. A., Mahroof, R., & Harvey, J. (2023). Effect of storage duration and storage technologies on pest infestations and post-harvest quality loss of stored sesame seeds in Ethiopia. *Journal of Stored Products Research*, 103, 102161.

Berhe, M., Subramanyam, B., Demissie, G., Chichaybelu, M., Abera, F. A., Mahroof, R., & Harvey, J. (2023). Investigation of insect population density, species composition and associated losses in chickpea seeds stored on farms in Ethiopia. *Heliyon*, 9(7).

Bose, J., Rodrigo-Moreno, A., & Shabala, S. (2014). ROS homeostasis in halophytes in the context of salinity stress tolerance. *Journal of Experimental Botany*, 65(5), 1241-1257.

Bray, C. M. (2017). Biochemical processes during the osmopriming of seeds. In *Seed Development and Germination* (pp. 767-789). Routledge.

Buijs G. (2020). A Perspective on Secondary Seed Dormancy in *Arabidopsis thaliana*. *Plants (Basel, Switzerland)*, 9(6), 749.

Carrillo-Barral, N., Rodríguez-Gacio, M. D. C., & Matilla, A. J. (2020). Delay of Germination-1 (DOG1): A Key to Understanding Seed Dormancy. *Plants (Basel, Switzerland)*, 9(4), 480.

Cazzonelli, C. I. (2011). Carotenoids in nature: insights from plants and beyond. *Functional Plant Biology*, 38(11), 833-847.

Ceccarelli, S. (2009). Evolution, plant breeding and biodiversity. *Journal of Agriculture and Environment for International Development (JAEID)*, 103(1/2), 131-145.

Chakraborti, S., Bera, K., Sadhukhan, S., & Dutta, P. (2022). Bio-priming of seeds: Plant stress management and its underlying cellular, biochemical and molecular mechanisms. *Plant Stress*, 3, 100052.

7. References

Chauffour, F., Bailly, M., Perreau, F., Cueff, G., Suzuki, H., Collet, B., Frey, A., Clément, G., Soubigou-Taconnat, L., Balliau, T., Krieger-Liszkay, A., Rajjou, L., & Marion-Poll, A. (2019). Multi-omics Analysis Reveals Sequential Roles for ABA during Seed Maturation. *Plant Physiology*, 180(2), 1198–1218.

Chen, C. (2003). Evaluation of air oven moisture content determination methods for rough rice. *Biosystems Engineering*, 86(4), 447-457.

Chinnasamy, G. P., Sundareswaran, S., Subramaniyan, K. S., Raja, K., Renganayaki, P. R., & Marimuthu, S. (2022). Volatile organic compound analysis as advanced technology to detect seed quality in groundnut. *Journal of Applied and Natural Science*, 14(3), 885-894.

Chongtham, S. K., Devi, E. L., Samantara, K., Yasin, J. K., Wani, S. H., Mukherjee, S., Razzaq, A., Bhupenchandra, I., Jat, A. L., Singh, L. K., & Kumar, A. (2022). Orphan legumes: harnessing their potential for food, nutritional and health security through genetic approaches. *Planta*, 256(2), 24.

Cialla-May, D., Schmitt, M., & Popp, J. (2019). Theoretical principles of Raman spectroscopy. *Physical Sciences Reviews*, 4(6).

Colville, L., Bradley, E. L., Lloyd, A. S., Pritchard, H. W., Castle, L. & Kranner, I. (2012). Volatile fingerprints of seeds of four species indicate the involvement of alcoholic fermentation, lipid peroxidation, and Maillard reactions in seed deterioration during ageing and desiccation stress. *Journal of Experimental Botany*, 63(18), 6519-6530.

Csanádi, G. Y., Vollmann, J., Stift, G., & Lelley, T. (2001). Seed quality QTLs identified in a molecular map of early maturing soybean. *Theoretical and Applied Genetics*, 103, 912-919.

Cullis, C., Chimwamurombe, P., Barker, N., Kunert, K., & Vorster, J. (2018). Orphan Legumes Growing in Dry Environments: Marama Bean as a Case Study. *Frontiers in Plant Science*, 9, 1199.

Cullis, C., & Kunert, K. J. (2017). Unlocking the potential of orphan legumes. *Journal of Experimental Botany*, 68(8), 1895–1903.

Czarna, M., Kolodziejczak, M., & Janska, H. (2016). Mitochondrial Proteome Studies in Seeds during Germination. *Proteomes*, 4(2), 19.

Damalas, C. A., Koutroubas, S. D., & Fotiadis, S. (2019). Hydro-priming effects on seed germination and field performance of faba bean in spring sowing. *Agriculture*, 9(9), 201.

Dat, J., Vandenabeele, S., Vranova, E. V. M. M., Van Montagu, M., Inzé*, D., & Van Breusegem, F. (2000). Dual action of the active oxygen species during plant stress responses. *Cellular and Molecular Life Sciences CMLS*, 57, 779-795.

Davière, J. M., & Achard, P. (2013). Gibberellin signaling in plants. *Development*, 140(6), 1147-1151.

7. References

Delgado, A., Quemada, M., & Villalobos, F. J. (2016). Fertilizers. *Principles of Agronomy for Sustainable Agriculture*, 321-339.

Del Río, L. A., & López-Huertas, E. (2016). ROS generation in peroxisomes and its role in cell signaling. *Plant and Cell Physiology*, 57(7), 1364-1376.

Delseny, M., Bies-Etheve, N., Carles, C., Hull, G., Vicient, C., Raynal, M., Grellet, F., & Aspart, L. (2001). Late Embryogenesis Abundant (LEA) protein gene regulation during Arabidopsis seed maturation. *Journal of Plant Physiology*, 158(4), 419-427.

Dey, A., & Bhattacharjee, S. (2023). Imbibitional redox and hormonal priming revealed regulation of oxidative window as a key factor for progression of germination of indica rice cultivars. *Physiology and Molecular Biology of Plants : an International Journal of Functional Plant Biology*, 29(4), 471–493.

Domergue, J., Abadie, C., Limami, A., Way, D. & Tcherkez, G. (2019). Seed quality and carbon primary metabolism. Plant, *Cell & Environment*, 42(10), pp.2776–2788.

Dvořák, P., Krasylenko, Y., Zeiner, A., Šamaj, J., & Takáč, T. (2021). Signaling toward reactive oxygen species-scavenging enzymes in plants. *Frontiers in Plant Science*, 11, 618835.

Ebone, L. A., Caverzan, A., & Chavarria, G. (2019). Physiologic alterations in orthodox seeds due to deterioration processes. *Plant Physiology and Biochemistry: PPB*, 145, 34–42.

ElMasry, G., ElGamal, R., Mandour, N., Gou, P., Al-Rejaie, S., Belin, E., & Rousseau, D. (2020). Emerging thermal imaging techniques for seed quality evaluation: Principles and applications. *Food Research International*, 131, 109025.

Elemike, E. E., Uzoh, I. M., Onwudiwe, D. C., & Babalola, O. O. (2019). The role of nanotechnology in the fortification of plant nutrients and improvement of crop production. *Applied Sciences*, 9(3), 499.

El-Sanatawy, A. M., Ash-Shormillesy, S. M., Qabil, N., Awad, M. F., & Mansour, E. (2021). Seed halo-priming improves seedling vigor, grain yield, and water use efficiency of maize under varying irrigation regimes. *Water*, 13(15), 2115.

Enfissi, E. M. A., Drapal, M., Perez-Fons, L., Nogueira, M., Berry, H. M., Almeida, J., & Fraser, P. D. (2021). New plant breeding techniques and their regulatory implications: An opportunity to advance metabolomics approaches. *Journal of Plant Physiology*, 258-259, 153378.

Ermiş, S., Kara, F., Özden, E., & Demir, İ. (2016). Solid matrix priming of cabbage seed lots: repair of ageing and increasing seed quality. *Journal of Agricultural Sciences*, 22(4), 588-595.

Ezeh, A. C., Bongaarts, J., & Mberu, B. (2012). Global population trends and policy options. *The Lancet*, 380(9837), 142-148.

7. References

FAO. (2022). Agricultural production statistics 2000–2020. *FAOSTAT Analytical Brief Series no.* 41.

Fantazzini, T. B., Rosa, D. V. F. D., Pereira, C. C., Pereira, D. D. S., Cirillo, M. Â., & Ossani, P. C. (2018). Association between the artificial aging test and the natural storage of coffee seeds. *Journal of Seed Science*, 40(2), 164-172.

Farooq, M. S. M. A., Basra, S. M. A., & Ahmad, N. (2007). Improving the performance of transplanted rice by seed priming. *Plant Growth Regulation*, 51, 129-137.

Fawzy, S., Osman, A. I., Doran, J., & Rooney, D. W. (2020). Strategies for mitigation of climate change: a review. *Environmental Chemistry Letters*, 18, 2069-2094.

Fazel-Niari, Z., Afkari-Sayyah, A. H., Abbaspour-Gilandeh, Y., Herrera-Miranda, I., Hernández-Hernández, J. L., & Hernández-Hernández, M. (2022). Quality assessment of components of wheat seed using different classifications models. *Applied Sciences*, 12(9), 4133.

Feng, L., Zhu, S., Liu, F., He, Y., Bao, Y., & Zhang, C. (2019). Hyperspectral imaging for seed quality and safety inspection: A review. *Plant Methods*, 15, 1-25.

Fernández, Á., Bella, J. & Dorronsoro, J. R. (2022). Supervised outlier detection for classification and regression. *Neurocomputing*, 486, 77-92.

Fessel, S. A., Vieira, R. D., Cruz, M. C. P. D., Paula, R. C. D., & Panobianco, M. (2006). Electrical conductivity testing of corn seeds as influenced by temperature and period of storage. *Pesquisa Agropecuária Brasileira*, 41, 1551-1559.

Finch-Savage, W. E., & Leubner-Metzger, G. (2006). Seed dormancy and the control of germination. *The New Phytologist*, 171(3), 501–523.

Forti, C., Ottobrino, V., Bassolino, L., Toppino, L., Rotino, G. L., Pagano, A., Macovei, A., & Balestrazzi, A. (2020). Molecular dynamics of pre-germinative metabolism in primed eggplant (*Solanum melongena* L.) seeds. *Horticulture Research*, 7(1), 87.

França-Neto, J. D. B., & Krzyzanowski, F. C. (2019). Tetrazolium: an important test for physiological seed quality evaluation. *Journal of Seed Science*, 41(3), 359-366.

França-Neto, J. D. B., & Krzyzanowski, F. C. (2022). Use of the tetrazolium test for estimating the physiological quality of seeds. *Seed Science and Technology*, 50(2), 31-44.

França-Silva, F., Gomes-Junior, F. G., Rego, C. H. Q., Marassi, A. G., & Tannús, A. (2023). Advances in imaging technologies for soybean seed analysis. *Journal of Seed Science*, 45, e202345022.

Freitas, R. A., Dias, D. C. F. S., Oliveira, G. A., Dias, L. A. S., & Jose, I. C. (2006). Physiological and biochemical changes in naturally and artificially aged cotton seeds. *Seed Science and Technology*, 34(2), 253-264.

7. References

Gagliardi, B., & Marcos-Filho, J. (2011). Relationship between germination and bell pepper seed structure assessed by the X-ray test. *Scientia Agricola*, 68, 411-416.

Garg, N., & Manchanda, G. J. P. B. (2009). ROS generation in plants: boon or bane?. *Plant Biosystems*, 143(1), 81-96.

Gebeyehu, B. (2020). Review on: Effect of seed storage period and storage environment on seed quality. *International Journal of Applied Agricultural Sciences*, 6(6), 185-190.

Genkawa, T., Uchino, T., Inoue, A., Tanaka, F., & Hamanaka, D. (2008). Development of a low-moisture-content storage system for brown rice: storability at decreased moisture contents. *Biosystems Engineering*, 99(4), 515-522.

Glasauer, A., & Chandel, N. S. (2013). Ros. *Current Biology*, 23(3), R100-R102.

Goettel, W., Zhang, H., Li, Y., Qiao, Z., Jiang, H., Hou, D., Song, Q., Pantalone, V. R., Song, B. H., Yu, D., & An, Y. C. (2022). *POWR1* is a domestication gene pleiotropically regulating seed quality and yield in soybean. *Nature Communications*, 13(1), 3051.

Görlach, A., Bertram, K., Hudecova, S., & Krizanova, O. (2015). Calcium and ROS: A mutual interplay. *Redox Biology*, 6, 260-271.

Grasso, R., Gulino, M., Giuffrida, F., Agnello, M., Musumeci, F., & Scordino, A. (2018). Non-destructive evaluation of watermelon seeds germination by using Delayed Luminescence. *Journal of Photochemistry and Photobiology B: Biology*, 187, 126-130.

Griffo, A., Bosco, N., Pagano, A., Balestrazzi, A., & Macovei, A. (2023). Noninvasive methods to detect reactive oxygen species as a proxy of seed quality. *Antioxidants*, 12(3), 626.

Groot, S. P., Surki, A. A., de Vos, R. C., & Kodde, J. (2012). Seed storage at elevated partial pressure of oxygen, a fast method for analysing seed ageing under dry conditions. *Annals of Botany*, 110(6), 1149–1159

Gu, D., Andreev, K., & Dupre, M. E. (2021). Major Trends in Population Growth Around the World. *China CDC Weekly*, 3(28), 604–613.

Gutierrez, L., Van Wuytswinkel, O., Castelain, M., & Bellini, C. (2007). Combined networks regulating seed maturation. *Trends in Plant Science*, 12(7), 294–300.

Haj Sghaier, A., Tarnawa, Á., Khaeim, H., Kovács, G. P., Gyuricza, C., & Kende, Z. (2022). The Effects of Temperature and Water on the Seed Germination and Seedling Development of Rapeseed (*Brassica napus* L.). *Plants (Basel, Switzerland)*, 11(21), 2819.

Hamdy, S., Charrier, A., Corre, L. L., Rasti, P., & Rousseau, D. (2024). Toward robust and high-throughput detection of seed defects in X-ray images via deep learning. *Plant Methods*, 20(1), 63.

Han, B., Fernandez, V., Pritchard, H. W., & Colville, L. (2021). Gaseous environment modulates volatile emission and viability loss during seed artificial ageing. *Planta*, 253, 1-16.

7. References

Harris, D., Rashid, A., Miraj, G., Arif, M., & Yunas, M. (2008). 'On-farm'seed priming with zinc in chickpea and wheat in Pakistan. *Plant and Soil*, 306, 3-10.

Hay, F. R., Rezaei, S., Wolkis, D., & McGill, C. (2023). Determination and control of seed moisture. *Seed Science and Technology*, 51(2), 267-285.

Hay, F. R., Valdez, R., Lee, J. S., & Sta. Cruz, P. C. (2019). Seed longevity phenotyping: recommendations on research methodology. *Journal of Experimental Botany*, 70(2), 425-434.

Hirsch, S., & Oldroyd, G. E. (2009). GRAS-domain transcription factors that regulate plant development. *Plant signaling & Behavior*, 4(8), 698-700.

Hou, J. J., Cao, C. M., Xu, Y. W., Yao, S., Cai, L. Y., Long, H. L., Bi, Q. R., Zhen, Y. Y., Wu, W. Y. & Guo, D. A. (2018). Exploring lipid markers of the quality of coix seeds with different geographical origins using supercritical fluid chromatography mass spectrometry and chemometrics. *Phytomedicine*, 45, 1-7.

Hourston, J. E., Steinbrecher, T., Chandler, J. O., Pérez, M., Dietrich, K., Turečková, V., Tarkowská, D., Strnad, M., Weltmeier, F., Meinhard, J., Fischer, U., Fiedler-Wiechers, K., Ignatz, M., & Leubner-Metzger, G. (2022). Cold-induced secondary dormancy and its regulatory mechanisms in *Beta vulgaris*. *Plant, Cell & Environment*, 45(4), 1315–1332.

Ishibashi, Y., Koda, Y., Zheng, S. H., Yuasa, T., & Iwaya-Inoue, M. (2013). Regulation of soybean seed germination through ethylene production in response to reactive oxygen species. *Annals of Botany*, 111(1), 95-102.

Jakoby, M., Weisshaar, B., Dröge-Laser, W., Vicente-Carbajosa, J., Tiedemann, J., Kroj, T., Parcy, F., & bZIP Research Group (2002). bZIP transcription factors in Arabidopsis. *Trends in Plant Science*, 7(3), 106–111.

Jhanji, S., Goyal, E., Chumber, M., & Kaur, G. (2024). Exploring fine tuning between phytohormones and ROS signaling cascade in regulation of seed dormancy, germination and seedling development. *Plant Physiology and Biochemistry*, 108352.

Jisha, K. C., Vijayakumari, K., & Puthur, J. T. (2013). Seed priming for abiotic stress tolerance: an overview. *Acta Physiologiae Plantarum*, 35, 1381-1396.

Jordan, M. I., & Mitchell, T. M. (2015). Machine learning: Trends, perspectives, and prospects. *Science*, 349(6245), 255-260.

Kaburu, T. W., Mushimiyimana, D., & Muchiri, J. (2024). Enhancing Maize Growth and Yield through Hydropriming in Buuri East Sub-County, Kenya. *International Journal of Professional Practice*, 12(2), 15-26.

Khan, A., Khan, V., Pandey, K., Sopory, S. K., & Sanan-Mishra, N. (2022). Thermo-priming mediated cellular networks for abiotic stress management in plants. *Frontiers in Plant Science*, 13, 866409.

7. References

Kibinza, S., Vinel, D., Côme, D., Bailly, C., & Corbineau, F. (2006). Sunflower seed deterioration as related to moisture content during ageing, energy metabolism and active oxygen species scavenging. *Physiologia Plantarum*, 128(3), 496-506.

Kozaki, A., & Aoyanagi, T. (2022). Molecular Aspects of Seed Development Controlled by Gibberellins and Abscisic Acids. *International Journal of Molecular Sciences*, 23(3), 1876.

Krishnamurthy, A., & Rathinasabapathi, B. (2013). Oxidative stress tolerance in plants: novel interplay between auxin and reactive oxygen species signaling. *Plant Signaling & Behavior*, 8(10), e25761.

Kulik, M. M. (2020). Seed quality and microorganisms. In: Gough, R.E (eds) Seed Quality (pp. 153-171). *CRC Press*.

Kumar, B. (2012). Prediction of Germination Potential in Seeds of Indian Basil (*Ocimum basilicum* L.). *Journal of Crop Improvement*, 26(4), 532–539.

Kumar, M., Pant, B., Mondal, S., & Bose, B. (2016). Hydro and halo priming: influenced germination responses in wheat Var-HUW-468 under heavy metal stress. *Acta Physiologiae Plantarum*, 38, 1-7.

Lamichhane, S., & Thapa, S. (2022). Advances from conventional to modern plant breeding methodologies. *Plant breeding and Biotechnology*, 10(1), 1-14.

Lee, R. (2011). The outlook for population growth. *Science*, 333(6042), 569-573.

Lee, P. C., Taylor, A. G., Zhang, M., & Esashi, Y. (2000). Volatile compounds and accumulation of acetaldehyde-protein adducts in relation to seed quality and storage conditions. *Journal of New Seeds*, 2(1), 59-76.

Lei, C., Bagavathiannan, M., Wang, H., Sharpe, S. M., Meng, W., & Yu, J. (2021). Osmopriming with polyethylene glycol (PEG) for abiotic stress tolerance in germinating crop seeds: A review. *Agronomy*, 11(11), 2194.

Lewandowska, S., Łoziński, M., Marczewski, K., Kozak, M., & Schmidtke, K. (2020). Influence of priming on germination, development, and yield of soybean varieties. *Open Agriculture*, 5(1), 930-935.

Li, J., Liu, Y., Zhang, J., Cao, L., Xie, Q., Chen, G., Chen, X., & Hu, Z. (2023). Suppression of a hexokinase gene *SlHXK1* in tomato affects fruit setting and seed quality. *Plant Physiology and Biochemistry: PPB*, 205, 108160.

Li, M., & Kim, C. (2022). Chloroplast ROS and stress signaling. *Plant Communications*, *3*(1).

Li, W., Tan, F., Cui, J. & Ma, B. (2022). Fast identification of soybean varieties using Raman spectroscopy. *Vibrational Spectroscopy.*, 123, 103447.

Li, Z., Lu, W., Yang, L., Kong, X., & Deng, X. (2015). Seed weight and germination behavior of the submerged plant *Potamogeton pectinatus* in the arid zone of northwest China. *Ecology and Evolution*, 5(7), 1504–1512.

7. References

Liu, D., Wu, Y., Gao, Z., & Yun, Y. H. (2019). Comparative non-destructive classification of partial waxy wheats using near-infrared and Raman spectroscopy. *Crop and Pasture Science*, 70(5), 437-441.

Liu, X., Zhang, H., Zhao, Y., Feng, Z., Li, Q., Yang, H. Q., Luan, S., Li, J., & He, Z. H. (2013). Auxin controls seed dormancy through stimulation of abscisic acid signaling by inducing ARF-mediated ABI3 activation in Arabidopsis. *Proceedings of the National Academy of Sciences*, 110(38), 15485-15490.

Liu, X., & Hou, X. (2018). Antagonistic regulation of ABA and GA in metabolism and signaling pathways. *Frontiers in Plant Science*, 9, 251.

Liu, Y., Ren, S., Sun, Q., Guo, B., Zhang, Y., Li, M., & Zhang, R. (2024). GC-IMS determination of volatile organic compounds as potential indicators of wheat germination rate. *Food Bioscience*, 57, 103535.

Locascio, A., Blázquez, M. A., & Alabadí, D. (2013). Genomic analysis of DELLA protein activity. *Plant and Cell Physiology*, 54(8), 1229-1237.

Logan, D. C., Millar, A. H., Sweetlove, L. J., Hill, S. A., & Leaver, C. J. (2001). Mitochondrial biogenesis during germination in maize embryos. *Plant Physiology*, 125(2), 662-672.

López-Fernández, M. P., Moyano, L., Correa, M. D., Vasile, F., Burrieza, H. P., & Maldonado, S. (2018). Deterioration of willow seeds during storage. *Scientific Reports*, 8(1), 17207.

Macovei, A., Balestrazzi, A., Confalonieri, M., & Carbonera, D. (2010). The tyrosyl-DNA phosphodiesterase gene family in Medicago truncatula Gaertn.: bioinformatic investigation and expression profiles in response to copper-and PEG-mediated stress. *Planta*, *232*(2), 393-407.

Macovei, A., Pagano, A., Leonetti, P., Carbonera, D., Balestrazzi, A., & Araújo, S. S. (2017). Systems biology and genome-wide approaches to unveil the molecular players involved in the pre-germinative metabolism: implications on seed technology traits. *Plant Cell Reports*, 36, 669-688.

Mahajan, S., Mittal, S. K., & Das, A. (2018). Machine vision based alternative testing approach for physical purity, viability and vigour testing of soybean seeds (Glycine max). *Journal of Food Science and Technology*, 55(10), 3949-3959.

Malaker, P. K., Mian, I. H., Bhuiyan, K. A., Akanda, A. M., & Reza, M. M. A. (2008). Effect of storage containers and time on seed quality of wheat. *Bangladesh Journal of Agricultural Research*, 33(3), 469-477.

Malhi, G. S., Kaur, M., & Kaushik, P. (2021). Impact of climate change on agriculture and its mitigation strategies: A review. *Sustainability*, 13(3), 1318.

Marcos Filho, J. (2015). Seed vigor testing: an overview of the past, present and future perspective. *Scientia Agricola*, 72, 363-374.

7. References

Marinoni, L., Zabala, J. M., Quiroga, R. E., Richard, G. A., & Pensiero, J. F. (2022). Seed Weight and Trade-Offs: An Experiment in False Rhodes Grasses under Different Aridity Conditions. *Plants (Basel, Switzerland)*, 11(21), 2887

Marler, T. E. (2019). Temperature and imbibition influence Serianthes seed germination behavior. *Plants*, *8*(4), 107.

Martin, R. E., Postiglione, A. E., & Muday, G. K. (2022). Reactive oxygen species function as signaling molecules in controlling plant development and hormonal responses. *Current Opinion in Plant Biology*, 69, 102293.

Matilla A. J. (2020). Seed Dormancy: Molecular Control of Its Induction and Alleviation. *Plants (Basel, Switzerland)*, 9(10), 1402.

Matthews, S., Noli, E., Demir, I., Khajeh-Hosseini, M., & Wagner, M. H. (2012). Evaluation of seed quality: from physiology to international standardization. *Seed Science Research*, 22(S1), S69–S73.

Matthews, S., & Powell, A. (2006). Electrical conductivity vigour test: physiological basis and use. *Seed Testing International*, *131*(32.35).

Maurya, D. K., Hasanain, M., Verma, S. K., Singh, P. K., Kumar, V., Singh, S., & Mishra, R. (2020). Seed priming and its effect on enhancing pulse productivity. *Food and Scientific Reports*, 1, 20-22.

McGuire, S., & Sperling, L. (2016). Seed systems smallholder farmers use. *Food Security*, 8, 179-195.

Men, S., Yan, L., Liu, J., Qian, H., & Luo, Q. (2017). A classification method for seed viability assessment with infrared thermography. *Sensors*, 17(4), 845.

Mesa, T., & Munné-Bosch, S. (2023). α-Tocopherol in chloroplasts: nothing more than an antioxidant?. *Current Opinion in Plant Biology*, 74, 102400.

Milo, T., & Somech, A. (2020). Automating exploratory data analysis via machine learning: An overview. In *Proceedings of the 2020 ACM SIGMOD International Conference on Management of Data* (pp. 2617-2622).

Milošević, M., Vujaković, M., & Karagić, D. (2010). Vigour tests as indicators of seed viability. *Genetika*, *42*(1), 103-118.

Mira, S., González-Benito, M. E., Hill, L. M., & Walters, C. (2010). Characterization of volatile production during storage of lettuce (*Lactuca sativa*) seed. *Journal of Experimental Botany*, 61(14), 3915-3924.

Mira, S., Hill, L. M., González-Benito, M. E., Ibáñez, M. A., & Walters, C. (2016). Volatile emission in dry seeds as a way to probe chemical reactions during initial asymptomatic deterioration. *Journal of Experimental Botany*, 67(6), 1783-1793.

7. References

Mizutani, M., & Todoroki, Y. (2006). ABA 8′-hydroxylase and its chemical inhibitors. *Phytochemistry Reviews*, 5, 385-404.

Moon, J., Li, M., Ramirez-Cuesta, A. J., & Wu, Z. (2023). Raman spectroscopy. In *Springer Handbook of Advanced Catalyst Characterization* (pp. 75-110). Cham: *Springer International Publishing*.

Motsa, M. M., Slabbert, M. M., Bester, C., Mokwena, L., & Taylor, M. (2017). Volatile organic compounds from germinating seeds of Cyclopia species as affected by temperature. *Seed Science and Technology*, 45(1), 43-55.

Murphey, M., Kovach, K., Elnacash, T., He, H., Bentsink, L., & Donohue, K. (2015). DOG1-imposed dormancy mediates germination responses to temperature cues. *Environmental and Experimental Botany*, 112, 33-43.

Nawaz, J., Hussain, M., Jabbar, A., Nadeem, G. A., Sajid, M., Subtain, M. U., & Shabbir, I. (2013). Seed priming a technique. *International Journal of Agriculture and Crop Sciences*, 6(20), 1373.

Nie, P., Zhang, J., Feng, X., Yu, C., & He, Y. (2019). Classification of hybrid seeds using near-infrared hyperspectral imaging technology combined with deep learning. *Sensors and Actuators B: Chemical*, 296, 126630.

Obi, O. F., Ezeoha, S. L., & Egwu, C. O. (2016). Evaluation of air oven moisture content determination procedures for pearl millet (Pennisetum glaucum L.). *International Journal of Food Properties*, 19(2), 454-466.

OECD (2018). Concentration in Seed Markets: Potential Effects and Policy Responses, *OECD Publishing*, Paris

Ozyigit, I. I., Filiz, E., Vatansever, R., Kurtoglu, K. Y., Koc, I., Öztürk, M. X., & Anjum, N. A. (2016). Identification and comparative analysis of H2O2-scavenging enzymes (ascorbate peroxidase and glutathione peroxidase) in selected plants employing bioinformatics approaches. *Frontiers in Plant Science*, 7, 301.

Pagano, A., de Sousa Araújo, S., Macovei, A., Dondi, D., Lazzaroni, S., & Balestrazzi, A. (2019). Metabolic and gene expression hallmarks of seed germination uncovered by sodium butyrate in *Medicago truncatula*. *Plant, Cell & Environment*, 42(1), 259-269.

Pagano, A., Macovei, A., & Balestrazzi, A. (2023). Molecular dynamics of seed priming at the crossroads between basic and applied research. *Plant cell Reports*, 42(4), 657–688.

Pan, J., Wang, H., You, Q., Cao, R., Sun, G., & Yu, D. (2023). Jasmonate-regulated seed germination and crosstalk with other phytohormones. *Journal of Experimental Botany*, 74(4), 1162–1175.

Paparella, S., Araújo, S. S., Rossi, G., Wijayasinghe, M., Carbonera, D., & Balestrazzi, A. (2015). Seed priming: state of the art and new perspectives. *Plant Cell Reports*, 34, 1281-1293.

7. References

Penfield S. (2017). Seed dormancy and germination. *Current Biology: CB*, 27(17), R874–R878.

Pérez, H. E., Shiels, A. B., Zaleski, H. M., & Drake, D. R. (2008). Germination after simulated rat damage in seeds of two endemic Hawaiian palm species. *Journal of Tropical Ecology*, 24(5), 555–558.

Pessoa, H. P., Copati, M. G. F., Azevedo, A. M., Dariva, F. D., Almeida, G. Q. D., & Gomes, C. N. (2023). Combining deep learning and X-ray imaging technology to assess tomato seed quality. *Scientia Agricola*, 80, e20220121.

Pimbert, M. (2022). Introduction: Thinking About Seeds. In: Nishikawa, Y., Pimbert, M. (eds) Seeds for Diversity and Inclusion. *Palgrave Macmillan*, Cham.

Pirredda, M., Fañanás-Pueyo, I., Oñate-Sánchez, L., & Mira, S. (2023). Seed Longevity and Ageing: A Review on Physiological and Genetic Factors with an Emphasis on Hormonal Regulation. *Plants*, 13(1), 41.

Popoola, J. O., Aworunse, O. S., Ojuederie, O. B., Adewale, B. D., Ajani, O. C., Oyatomi, O. A., Eruemulor, D. I., Adegboyega, T. T., & Obembe, O. O. (2022). The Exploitation of Orphan Legumes for Food, Income, and Nutrition Security in Sub-Saharan Africa. *Frontiers in Plant Science*, 13, 782140.

Pradhan, N., Fan, X., Martini, F., Chen, H., Liu, H., Gao, J., & Goodale, U. M. (2022). Seed viability testing for research and conservation of epiphytic and terrestrial orchids. *Botanical Studies*, 63(1), 3.

Prieto, N., Pawluczyk, O., Dugan, M. E. R., & Aalhus, J. L. (2017). A review of the principles and applications of near-infrared spectroscopy to characterize meat, fat, and meat products. *Applied Spectroscopy*, 71(7), 1403-1426.

Puga-Guzmán, P. S., Magallán-Hernández, F., Queijeiro-Bolaños, M., Valencia-Hernández, J. A., & Vergara-Pineda, S. (2023). Seed morphology and germination of <*Turnera diffusa*> Willd. ex Schult. emulating environmental conditions within ant nest. *PloS One*, 18(10), e0292626.

Racca, S., Gras, D. E., Canal, M. V., Ferrero, L. V., Rojas, B. E., Figueroa, C. M., Ariel, F. D., Welchen, E., & Gonzalez, D. H. (2022). Cytochrome c and the transcription factor ABI4 establish a molecular link between mitochondria and ABA-dependent seed germination. *The New Phytologist*, 235(5), 1780–1795.

Rahman, A. & Cho, B. K. (2016). Assessment of seed quality using non-destructive measurement techniques: a review. Seed Science Research, 26(4), 285–305.

Raina, A., Sahu, P. K., Laskar, R. A., Rajora, N., Sao, R., Khan, S., & Ganai, R. A. (2021). Mechanisms of genome maintenance in plants: playing it safe with breaks and bumps. *Frontiers in Genetics*, 12, 675686.

7. References

Raman R. (2017). The impact of Genetically Modified (GM) crops in modern agriculture: A review. *GM Crops & Food*, 8(4), 195–208.

Ranal, M. A., & Santana, D. G. D. (2006). How and why to measure the germination process?. *Brazilian Journal of Botany*, 29, 1-11.

Rastin, S., Madani, H., & Shoaei, S. (2013). Effect of seed priming on red bean (*Phaseolus calcaratus*) growth and yield. *Annals of Biological Research*, 4(2), 292-296.

Reddy, P., Guthridge, K. M., Panozzo, J., Ludlow, E. J., Spangenberg, G. C., & Rochfort, S. J. (2022). Near-infrared hyperspectral imaging pipelines for pasture seed quality evaluation: An overview. *Sensors*, 22(5), 1981.

Reddy, P. P., & Reddy, P. P. (2013). Bio-priming of seeds. *Recent Advances in Crop Protection*, 83-90.

Rehmani, M. S., Aziz, U., Xian, B., & Shu, K. (2022). Seed Dormancy and Longevity: A Mutual Dependence or a Trade-Off?. *Plant & Cell Physiology*, 63(8), 1029–1037.

Reich, G. (2005). Near-infrared spectroscopy and imaging: basic principles and pharmaceutical applications. *Advanced Drug Delivery Reviews*, 57(8), 1109-1143.

Rhaman, M.S., Rauf, F., Tania, S.S., & Khatun, M. (2020). Seed Priming Methods: Application in Field Crops and Future Perspectives. *Asian Journal of Research in Crop Science*.

Rodo, A. B., & Marcos Filho, J. (2003). Accelerated aging and controlled deterioration for the determination of the physiological potential of onion seeds. *Scientia Agricola*, 60, 465-469.

Sajeev, N., Bai, B., & Bentsink, L. (2019). Seeds: a unique system to study translational regulation. *Trends in Plant Science*, 24(6), 487-495.

Salvi, P., Varshney, V., & Majee, M. (2022). Raffinose family oligosaccharides (RFOs): role in seed vigor and longevity. *Bioscience Reports*, 42(10), BSR20220198.

Sano, N., & Marion-Poll, A. (2021). ABA Metabolism and Homeostasis in Seed Dormancy and Germination. *International Journal of Molecular Sciences*, 22(10), 5069.

Sano, N., Rajjou, L., North, H. M., Debeaujon, I., Marion-Poll, A., & Seo, M. (2016). Staying alive: molecular aspects of seed longevity. *Plant and Cell Physiology*, 57(4), 660-674.

Santos, F. D., Medina, P. F., Lourenção, A. L., Parisi, J. J. D., & Godoy, I. J. D. (2016). Damage caused by fungi and insects to stored peanut seeds before processing. *Bragantia*, 75(2), 184-192.

Schmeller, D. S., & Henle, K. (2008). Cultivation of genetically modified organisms: resource needs for monitoring adverse effects on biodiversity. *Biodiversity and Conservation*, 17, 3551-3558.

7. References

Scott, S. J., Jones, R. A., & Williams, W. (1984). Review of data analysis methods for seed germination 1. *Crop Science*, 24(6), 1192-1199.

Schmidt, L. (2007). Seed Testing. In: Tropical Forest Seed, 281-322. Tropical Forestry. *Springer*, Berlin, Heidelberg.

Sedah, P., Djedatin, L. G., Loko, L. Y. E., Ewedje, E. B. K., Orobiyi, A., Gbemavo, C. D. S. J., Toffa, J., Tchakpa, C., Cubry, P., & Sabot, F. (2023). Impact of Seed Origin and Genetic Drift of Improved Rice Variety IR841 in Benin. *Rice (New York, N.Y.)*, 16(1), 48.

Selvarani, K., & Umarani, R. (2011). Evaluation of seed priming methods to improve seed vigour of onion (*Allium cepa* cv. aggregatum) and carrot (*Daucus carota*). *Journal of Agricultural Technology*, 7(3), 857-867.

Sen, S. K., & Mandal, P. (2016). Solid matrix priming with chitosan enhances seed germination and seedling invigoration in mung bean under salinity stress. *Journal of Central European Agriculture*.

Seo, Y. W., Ahn, C. K., Lee, H., Park, E., Mo, C., & Cho, B. K. (2016). Non-destructive sorting techniques for viable pepper (Capsicum annuum L.) seeds using Fourier transform near-infrared and raman spectroscopy. *Journal of Biosystems Engineering*, *41*(1), 51-59.

Sharma, I., & Ahmad, P. (2014). Catalase: a versatile antioxidant in plants. In: Oxidative Damage to Plants (pp. 131-148). *Academic Press*.

Shi, H., & Chen, J. (2018). Characteristics of climate change and its relationship with land use/cover change in Yunnan Province, China. *International Journal of Climatology*.

Shi, H., Guan, W., Shi, Y., Wang, S., Fan, H., Yang, J., Chen, W., Zhang, W., Sun, D., & Jing, R. (2020). QTL mapping and candidate gene analysis of seed vigor-related traits during artificial aging in wheat (Triticum aestivum). *Scientific Reports*, 10(1), 22060.

Shimada, T. L., Ueda, T., & Hara-Nishimura, I. (2021). Excess sterol accumulation affects seed morphology and physiology in *Arabidopsis thaliana*. *Plant signaling & behavior*, 16(4), 1872217.

Shrestha, S., Knapič, M., Žibrat, U., Deleuran, L. C., & Gislum, R. (2016). Single seed near-infrared hyperspectral imaging in determining tomato (*Solanum lycopersicum* L.) seed quality in association with multivariate data analysis. *Sensors and Actuators B: Chemical*, 237, 1027-1034.

Shu, K., Liu, X. D., Xie, Q., & He, Z. H. (2016). Two Faces of One Seed: Hormonal Regulation of Dormancy and Germination. *Molecular Plant*, 9(1), 34–45.

Siesler, H. W. (2007). Basic principles of near-infrared spectroscopy. In Handbook of Near-Infrared Analysis (pp. 25-38). *CRC press*.

7. References

Singh, R. B., Mishra, S., Saxena, P., Saxena, M., Smail, M. M., & Velluri, S. R. (2022). Genetically modified organisms and foods: perspectives and challenges. *Functional Foods and Nutraceuticals in Metabolic and Non-Communicable Diseases*, 493-505.

Smolikova, G., Strygina, K., Krylova, E., Leonova, T., Frolov, A., Khlestkina, E., & Medvedev, S. (2021). Transition from Seeds to Seedlings: Hormonal and Epigenetic Aspects. *Plants (Basel, Switzerland)*, 10(9), 1884.

Soares, V. N., Elias, S. G., Gadotti, G. I., Garay, A. E., & Villela, F. A. (2016). Can the tetrazolium test be used as an alternative to the germination test in determining seed viability of grass species?. *Crop Science*, 56(2), 707-715.

Son, Y., Cheong, Y. K., Kim, N. H., Chung, H. T., Kang, D. G., & Pae, H. O. (2011). Mitogen-activated protein kinases and reactive oxygen species: how can ROS activate MAPK pathways?. *Journal of Signal Transduction*, 2011(1), 792639.

Souri, M. K. (2016). Aminochelate fertilizers: the new approach to the old problem; a review. *Open Agriculture*, 1(1), 118-123.

Stamm, P., Ravindran, P., Mohanty, B., Tan, E. L., Yu, H., & Kumar, P. P. (2012). Insights into the molecular mechanism of RGL2-mediated inhibition of seed germination in Arabidopsis thaliana. *BMC Plant Biology*, 12, 179.

Storr, S. J., Woolston, C. M., Zhang, Y., & Martin, S. G. (2013). Redox environment, free radical, and oxidative DNA damage. *Antioxidants & Redox Signaling*, 18(18), 2399-2408.

Sun, H., Xu, H., Li, B., Shang, Y., Wei, M., Zhang, S., Zhao, C., Qin, R., Cui, F., & Wu, Y. (2021). The brassinosteroid biosynthesis gene, *ZmD11*, increases seed size and quality in rice and maize. *Plant Physiology and Biochemistry: PPB*, 160, 281–293.

Sundareswaran, S., Ray Choudhury, P., Vanitha, C., Yadava, D.K. (2023). Seed Quality: Variety Development to Planting—An Overview. In: Dadlani, M., Yadava, D.K. (eds) *Seed Science and Technology*. *Springer*, Singapore.

Tang, S., TeKrony, D. M., Egli, D. B., & Cornelius, P. L. (2000). An alternative model to predict corn seed deterioration during storage. *Crop Science*, 40(2), 463-470.

Taylor, A. G., Lee, P. C., & Zhang, M. (1999). Volatile compounds as indicators of seed quality and their influence on seed aging. *Seed Technology*, 21(1), 57-65.

TeKrony, D. M. (2005). Accelerated aging test: principles and procedures. *Seed Technology*, 135-146.

Tester, M., & Langridge, P. (2010). Breeding technologies to increase crop production in a changing world. *Science*, 327(5967), 818-822.

Tripathi, P. C., & Lawande, K. E. (2014). Effect of seed moisture and packing material on viability and vigour of onion seed. *Journal of Engineering Computers & Applied Sciences*, 3(7), 1-5.

7. References

Tu, K. L., Li, L. J., Yang, L. M., Wang, J. H., & Qun, S. U. N. (2018). Selection for high quality pepper seeds by machine vision and classifiers. *Journal of Integrative Agriculture*, 17(9), 1999-2006.

Tuan, P. A., Sun, M., Nguyen, T. N., Park, S., & Ayele, B. T. (2019). Molecular mechanisms of seed germination. In Sprouted Grains (pp. 1-24). *AACC International Press*.

Umarani, R., Bhaskaran, M., Vanitha, C., & Tilak, M. (2020). Fingerprinting of volatile organic compounds for quick assessment of vigour status of seeds. *Seed Science Research*, 30(2), 112-121.

Vabalas, A., Gowen, E., Poliakoff, E., & Casson, A. J. (2019). Machine learning algorithm validation with a limited sample size. *PloS One*, 14(11), e0224365.

Vallejo-Marín, M., Domínguez, C. A., & Dirzo, R. (2006). Simulated seed predation reveals a variety of germination responses of neotropical rain forest species. *American Journal of Botany*, *93*(3), 369-376.

Van Dijk, M., Morley, T., Rau, M. L., & Saghai, Y. (2021). A meta-analysis of projected global food demand and population at risk of hunger for the period 2010–2050. *Nature Food*, *2*(7), 494-501.

van Treuren, R., Bas, N., Kodde, J., Groot, S. P. C., & Kik, C. (2018). Rapid loss of seed viability in *ex situ* conserved wheat and barley at 4°C as compared to -20°C storage. *Conservation Physiology*, 6(1), coy033.

Vaneeckhaute, C., Meers, E., Michels, E., Buysse, J., & Tack, F. M. G. (2013). Ecological and economic benefits of the application of bio-based mineral fertilizers in modern agriculture. *Biomass and Bioenergy*, 49, 239-248.

Ventura, L., Donà, M., Macovei, A., Carbonera, D., Buttafava, A., Mondoni, A., Rossi, G., & Balestrazzi, A. (2012). Understanding the molecular pathways associated with seed vigor. *Plant Physiology and Biochemistry*: PPB, 60, 196–206.

VijayaVenkataRaman, S., Iniyan, S., & Goic, R. (2012). A review of climate change, mitigation and adaptation. *Renewable and Sustainable Energy Reviews*, *16*(1), 878-897.

Vithu, P., & Moses, J. A. (2016). Machine vision system for food grain quality evaluation: A review. *Trends in Food Science & Technology*, 56, 13-20.

Walters, C., Ballesteros, D., & Vertucci, V. A. (2010). Structural mechanics of seed deterioration: standing the test of time. *Plant Science*, 179(6), 565-573.

Walters, C., Hill, L. M., & Wheeler, L. J. (2005). Dying while dry: kinetics and mechanisms of deterioration in desiccated organisms. *Integrative and Comparative Biology*, 45(5), 751-758.

Wang, P., Xue, L., Batelli, G., Lee, S., Hou, Y. J., Van Oosten, M. J., Zhang, H., Tao, W. A., & Zhu, J. K. (2013). Quantitative phosphoproteomics identifies SnRK2 protein kinase

substrates and reveals the effectors of abscisic acid action. *Proceedings of the National Academy of Sciences*, 110(27), 11205-11210.

Wang, S., Liu, S., Wang, J., Yokosho, K., Zhou, B., Yu, Y. C., Liu, Z., Frommer, W. B., Ma, J. F., Chen, L. Q., Guan, Y., Shou, H., & Tian, Z. (2020). Simultaneous changes in seed size, oil content and protein content driven by selection of *SWEET* homologues during soybean domestication. *National Science Review*, *7*(11), 1776–1786.

Wang, X., Cai, J., Liu, F., Dai, T., Cao, W., Wollenweber, B., & Jiang, D. (2014). Multiple heat priming enhances thermo-tolerance to a later high temperature stress via improving subcellular antioxidant activities in wheat seedlings. *Plant Physiology and Biochemistry*, 74, 185-192.

Wang, Z., Tang, L., Hu, H., Guo, Y., Peng, T., Yan, F., & Chen, F. (2012). Metabolic profiling assisted quality control of phorbolesters in *Jatropha curcas* seed by high-performance liquid chromatography using a fused-core column. *Journal of Agricultural and Food Chemistry*, 60(38), 9567-9572.

Waterworth, W., Balobaid, A., & West, C. (2024). Seed longevity and genome damage. *Bioscience Reports*, 44(2), BSR20230809.

Waterworth, W. M., Bray, C. M., & West, C. E. (2019). Seeds and the art of genome maintenance. *Frontiers in Plant Science*, 10, 706.

Waterworth, W. M., Latham, R., Wang, D., Alsharif, M., & West, C. E. (2022). Seed DNA damage responses promote germination and growth in Arabidopsis thaliana. *Proceedings of the National Academy of Sciences*, 119(30), e2202172119.

Wojtyla, Ł., Lechowska, K., Kubala, S., & Garnczarska, M. (2016). Different modes of hydrogen peroxide action during seed germination. *Frontiers in Plant Science*, 7, 66.

Wonggasem, K., Wongchaisuwat, P., Chakranon, P., & Onwimol, D. (2024). Utilization of Machine Learning and Hyperspectral Imaging Technologies for Classifying Coated Maize Seed Vigor: A Case Study on the Assessment of Seed DNA Repair Capability. *Agronomy*, 14(9), 1991.

Wu, B., & Wang, B. (2019). Comparative analysis of ascorbate peroxidases (APXs) from selected plants with a special focus on *Oryza sativa* employing public databases. *Plos One*, 14(12), e0226543.

Wu, L., Huo, W., Yao, D., & Li, M. (2019). Effects of solid matrix priming (SMP) and salt stress on broccoli and cauliflower seed germination and early seedling growth. *Scientia Horticulturae*, *255*, 161-168.

Wu, W., Cao, S. F., Shi, L. Y., Chen, W., Yin, X. R., & Yang, Z. F. (2023). Abscisic acid biosynthesis, metabolism and signaling in ripening fruit. *Frontiers in Plant Science*, 14, 1279031.

7. References

Xue, L. W., Du, J. B., Yang, H., Xu, F., Yuan, S., & Lin, H. H. (2009). Brassinosteroids counteract abscisic acid in germination and growth of Arabidopsis. *Zeitschrift fur Naturforschung. C, Journal of Biosciences*, 64(3-4), 225–230.

Yamaguchi S. (2008). Gibberellin metabolism and its regulation. *Annual Review of Plant Biology*, 59, 225–251.

Yang, C., Li, X., Chen, S., Liu, C., Yang, L., Li, K., Liao, J., Zheng, X., Li, H., Li, Y., Zeng, S., Zhuang, X., Rodriguez, P. L., Luo, M., Wang, Y., & Gao, C. (2023). ABI5-FLZ13 module transcriptionally represses growth-related genes to delay seed germination in response to ABA. *Plant Communications*, 4(6), 100636.

Zabala, J. M., Widenhorn, P., & Pensiero, J. F. (2011). Germination patterns of species of the genus Trichloris in arid and semiarid environments. *Seed Science and Technology*, *39*(2), 338-353.

Zhang, K., Zhang, Y., Sun, J., Meng, J., & Tao, J. (2021). Deterioration of orthodox seeds during ageing: Influencing factors, physiological alterations and the role of reactive oxygen species. *Plant Physiology and Biochemistry*, 158, 475-485.

Zhang, M., Liu, S., Wang, Z., Yuan, Y., Zhang, Z., Liang, Q., Yang, X., Duan, Z., Liu, Y., Kong, F., Liu, B., Ren, B., & Tian, Z. (2022). Progress in soybean functional genomics over the past decade. *Plant Biotechnology Journal*, 20(2), 256–282.

Zhang, M., Maeda, Y., Furihata, Y., Nakamaru, Y., & Esashi, Y. (1994). A mechanism of seed deterioration in relation to the volatile compounds evolved by dry seeds themselves. *Seed Science Research*, 4(1), 49-56.

Zhang, T., Ayed, C., Fisk, I. D., Pan, T., Wang, J., Yang, N., & Sun, Q. (2022). Evaluation of volatile metabolites as potential markers to predict naturally-aged seed vigour by coupling rapid analytical profiling techniques with chemometrics. *Food Chemistry*, 367, 130760.

Zhang, W., Zhao, J., Xue, L., Dai, H., & Lei, J. (2023) Seed Morphology and Germination of Native *Tulipa* Species. *Agriculture*, 13(2):466.

Zhang, X. L., Jiang, L., Xin, Q., Liu, Y., Tan, J. X., & Chen, Z. Z. (2015). Structural basis and functions of abscisic acid receptors PYLs. *Frontiers in Plant Science*, *6*, 88.

Zhao, H., Nie, K., Zhou, H., Yan, X., Zhan, Q., Zheng, Y., & Song, C. P. (2020). ABI5 modulates seed germination via feedback regulation of the expression of the *PYR/PYL/RCAR ABA* receptor genes. *The New Phytologist*, 228(2), 596–608.

Zhao, J., He, Y., Li, X., Weng, X., Feng, D., Ying, J., & Wang, Z. (2020). An integrated RNA-Seq and physiological study reveals gene responses involving in the initial imbibition of seed germination in rice. *Plant Growth Regulation*, 90, 249-263.

Zhao, L., Haque, S. M., & Wang, R. (2022). Automated seed identification with computer vision: challenges and opportunities. *Seed Science and Technology*, 50(2), 75-102.

7. References

Zhao, S., Zou, H., Jia, Y., Pan, X., & Huang, D. (2022). Carrot (*Daucus carota* L.) Seed Germination Was Promoted by Hydro-Electro Hybrid Priming Through Regulating the Accumulation of Proteins Involved in Carbohydrate and Protein Metabolism. *Frontiers in Plant Science*, 13, 824439.

Zheng, J., Chen, F., Wang, Z., Cao, H., Li, X., Deng, X., Soppe, W. J. J., Li, Y., & Liu, Y. (2012). A novel role for histone methyltransferase KYP/SUVH4 in the control of Arabidopsis primary seed dormancy. *New Phytologist*, 193(3), 605-616.

Zheng, J., Wen, D., Zhao, H., & Zhang, C. (2017). Acetic acid urea-polyacrylamide gel electrophoresis: a rapid method for testing the genetic purity of sunflower seeds. *Quality Assurance and Safety of Crops & Foods*, 9(1), 41-46.

Zhou, G., Zhang, F., & Wu, S. (2016). Improvement on The Ellis and Roberts Viability Model. *Turkish Journal of Agriculture-Food Science and Technology*, 4(5), 321-329.

Zhu, Q., Feng, Z., Huang, M., & Zhu, X. (2012). Maize seed classification based on image entropy using hyperspectral imaging technology. *Transactions of the Chinese Society of Agricultural Engineering*, 28(23), 271-276.

Zhu, Y., Fan, S., Zuo, M., Zhang, B., Zhu, Q., & Kong, J. (2024). Discrimination of New and Aged Seeds Based on On-Line Near-Infrared Spectroscopy Technology Combined with Machine Learning. *Foods*, 13(10), 1570.

Zinsmeister, J., Lalanne, D., Terrasson, E., Chatelain, E., Vandecasteele, C., Vu, B. L., Dubois-Laurent, C., Geoffriau, E., Signor, C. L., Dalmais, M., Gutbrod, K., Dörmann, P., Gallardo, K., Bendahmane, A., Buitink, J., & Leprince, O. (2016). ABI5 Is a Regulator of Seed Maturation and Longevity in Legumes. *The Plant Cell*, 28(11), 2735–2754.

Zinsmeister, J., Leprince, O., & Buitink, J. (2020). Molecular and environmental factors regulating seed longevity. *Biochemical Journal*, 477(2), 305-323.

Zuo, Y., & Xu, Y. (2020). Research progress on the mechanism of GA and ABA during seed germination. *Molecular Plant Breeding*, 11.

Zwiers, F. W., Alexander, L. V., Hegerl, G. C., Knutson, T. R., Kossin, J. P., Naveau, P., Nicholls N., Schär C., Seneviratne S.I. & Zhang, X. (2013). Climate Extremes: Challenges in Estimating and Understanding Recent Changes in the Frequency and Intensity of Extreme Climate and Weather Events. In: Asrar, G., Hurrell, J. (eds) Climate Science for Serving Society. *Springer*, Dordrecht.

Publications

antioxidants

MDPI

Article

Noninvasive Methods to Detect Reactive Oxygen Species as a Proxy of Seed Quality

Adriano Griffo [1,†], Nicola Bosco [1,†], Andrea Pagano [1], Alma Balestrazzi [1,2] and Anca Macovei [1,2,*]

[1] Department of Biology and Biotechnology 'L. Spallanzani', University of Pavia, Via Ferrata 9, 27100 Pavia, Italy
[2] National Biodiversity Future Center (NBFC), 90133 Palermo, Italy
* Correspondence: anca.macovei@unipv.it
† These authors contributed equally to this work.

Abstract: ROS homeostasis is crucial to maintain radical levels in a dynamic equilibrium within physiological ranges. Therefore, ROS quantification in seeds with different germination performance may represent a useful tool to predict the efficiency of common methods to enhance seed vigor, such as priming treatments, which are still largely empirical. In the present study, ROS levels were investigated in an experimental system composed of hydroprimed and heat-shocked seeds, thus comparing materials with improved or damaged germination potential. A preliminary phenotypic analysis of germination parameters and seedling growth allowed the selection of the best-per-forming priming protocols for species like soybean, tomato, and wheat, having relevant agroeconomic value. ROS levels were quantified by using two noninvasive assays, namely dichloro-dihydro-fluorescein diacetate (DCFH-DA) and ferrous oxidation-xylenol orange (FOX-1). qRT-PCR was used to assess the expression of genes encoding enzymes involved in ROS production (respiratory burst oxidase homolog family, RBOH) and scavenging (catalase, superoxide dismutase, and peroxidases). The correlation analyses between ROS levels and gene expression data suggest a possible use of these indicators as noninvasive approaches to evaluate seed quality. These findings are relevant given the centrality of seed quality for crop production and the potential of seed priming in sustainable agricultural practices.

Keywords: DCFH-DA; FOX-1; gene expression; *Glycine max*; heat-shock; ROS; seed priming; seed quality

Citation: Griffo, A.; Bosco, N.; Pagano, A.; Balestrazzi, A.; Macovei, A. Noninvasive Methods to Detect Reactive Oxygen Species as a Proxy of Seed Quality. *Antioxidants* **2023**, *12*, 626. https://doi.org/10.3390/antiox12030626

Academic Editors: Francisco J. Corpas and José M. Palma

Received: 9 February 2023
Revised: 25 February 2023
Accepted: 28 February 2023
Published: 3 March 2023

1. Introduction

Seed quality can be defined based on the set of physical, genetic, and physiological characteristics, as per the guidelines given by the International Seed Testing Association (ISTA) [1]. Because seed quality affects germination, its evaluation has become increasingly important for consumers and seed companies, as it constitutes a valuable tool to optimize crop production, with practical and economic benefits [2]. This can be achieved through the development of approaches aimed at determining seed quality in an efficient, noninvasive manner [3]. The current standard approach to monitoring seed viability is mostly based on germination tests which are time-consuming and destructive [4]. Research efforts dedicated to improving seed viability testing are constantly performed, but so far no universal approach has been developed.

Starting from the primordial state of development on the mother plant, seeds undergo endogenous and exogenous stresses that may undermine cellular structures and functions. As a consequence, reactive oxygen species (ROS) are produced during all phases of seed development, from seed dehydration to storing and germination, posing different outcomes on seed longevity and quality [5–7]. In addition to ROS, more recently reactive nitrogen species (RNS) and especially nitric oxide (NO) have also been shown to carry

essential functions in seed biology, from their intervention in the regulation of seed dormancy, germination, and aging, to their possible use as seed pretreatments to increase seed quality [8].

ROS production is a side effect of many metabolic pathways (e.g., mitochondrial and plastid electron transport chains, peroxisomal reactions, lipid autooxidation) occurring both under physiological and stress conditions [9–12]. Uncontrolled ROS accumulation causes oxidative damage and compromises seed viability [13,14]. Aside from detrimental effects, positive physiological functions of ROS were highlighted during the pre-germinative metabolism, related to signaling, dormancy release, reservoir mobilization, and radicle elongation [15–18]. Thus, ROS play a key role in the activation of pre-germinative metabolism [16,17]. Accumulation of ROS in seeds has been well documented in multiple species and at different developmental stages [19–21]. At the cellular level, several components (e.g., mitochondria, peroxisomes, cell membrane, and apoplast) act as preferred production sites. The reactivation of metabolism during seed imbibition causes an enhanced accumulation of ROS, generally resulting from electron leakage within the mitochondrial electron transport chain [22]. Due to their dual nature, ROS must be kept under stringent control by antioxidant defenses. If the balance between ROS production and scavenging is lost, the seeds undergo oxidative stress which can induce seed death. In this view, the presence and diffusion of ROS throughout the cell compartments are spatially and temporally regulated to avoid damage [23,24]. Given the double nature of ROS functions in seeds, the concept of an "oxidative window" of germination is used to evidence this critical range in which ROS can play a positive role in seed metabolism without being detrimental [6].

Fast and uniform seed germination and successful seedling establishment are high priorities for enhancing crop yields. Technologies designed to improve germination performance (generally known as seed priming) can contribute to building up dynamic and sustainable agriculture practices [25–27]. Seed priming is the process of regulating seed germination by managing a series of parameters during the initial stages of germination [28–30]. For instance, the so-called "on-farm" seed priming, a low-cost technique consisting of soaking seeds in water before sowing, has led to 22% faster seed emergence translated into a 21% yield increase, whereas under stress conditions the plants proved to be more tolerant, gaining up to 22–28% in yield improvements [31]. The main effect of priming is the activation of the metabolic processes triggered during the early phase of germination, or the pre-germinative metabolism [16,27,28]. Although the success of seed priming is strongly correlated to plant species, genotype, seed lot, and vigor, it has also been proven to be effective in improving germination performances during environmental constraints [28,29,32–34]. Among the different priming treatments, hydropriming (water soaking with or without aeration) is especially useful in those agricultural areas where crop cultivation is impaired by adverse climate conditions, and it does not require the use of chemical substances [31,35–38]. Despite its simplicity, hydropriming has been reported to improve germination performances (in terms of germination time, speed, and percentage) in many species [35–41]. In the case of some practices (e.g., osmopriming, chemopriming), several studies have indicated that these act by delaying water entrance into the seed and thus may limit ROS oxidative injury [42–44], whereas in most cases priming acts at the level of seed transition from dormancy toward full germination, touching processes like the activation of DNA repair and antioxidant mechanisms, essential to obtain seeds with improved quality (see comprehensive reviews [16,27,28]). When considering the antioxidant response, enhanced enzymatic activity or increased expression of genes encoding antioxidant enzymes (e.g., SOD, APX, CAT, GR), were evidenced during seed germination and priming treatments [45–48].

As seed priming is still an empirical procedure, hallmarks useful to monitor the seed response to priming and to discriminate between high- and low-quality lots are necessary to enable the development of efficient protocols [5,35–37]. Because ROS play a vital role in seed dormancy and germination, measuring their levels can provide relevant information

about seed viability under different conditions. ROS levels have been evaluated as a possible indicator of overpriming seed performance in *Medicago truncatula*, showing that their accumulation during dehydration positively correlates with the loss of desiccation tolerance [49]. ROS levels were also used as a tool to monitor seed quality in *Solanum melongena*, pinpointing that low-quality seed lots defined by low germination rates were characterized by enhanced accumulation of ROS [35]. Additionally, in *Pisum sativum*, accessions with low ROS levels were associated with long-lived seeds, which maintained good germination profiles, whereas short-lived seeds were characterized by higher ROS accumulation [50].

Despite recent advances, the thresholds at which ROS induces toxicity are unknown and conditioned by many factors. Moreover, the necessity to avail of a palette of universal, cost-effective, and noninvasive tools or techniques to monitor seed quality, is highly requested by seed technologists working in industry and seed banks. To this purpose, the current study employed two different biochemical assays, namely dichloro-dihydrofluorescein diacetate (DCFH-DA) and ferrous oxidation-xylenol orange (FOX-1), to quantify ROS levels in seeds subjected to contrastive treatments leading to enhanced (hydropriming) or impaired (heat-shock) seed quality, in different plant species. These data were also integrated with the expression profiles of genes encoding enzymes involved in ROS production and scavenging.

2. Materials and Methods

2.1. Seed Materials and Treatments

Seeds of *Glycine max* (commercial variety, provided by Sipcam Oxon SpA, Milan, Italy), *Solanum lycopersicum* (commercial variety, provided by ISI Sementi S.p.A., Fidenza, Italy), and *Triticum aestivum* (commercial variety, provided by ITQB NOVA, Oeiras, Portugal) were used. The seeds were collected from the respective providers and stored at 4 °C until use.

Hydroprimng (HP) treatments were conducted in a species-specific manner, especially regarding the time spent during the seed imbibition phase. For instance, in soybean seeds, HP treatments were carried out for 2, 4, and 8 h of imbibition (Figure 1). Considering the *S. lycopersicum* and *T. aestivum* systems, the HP treatments based on seed imbibition in water were carried out at different intervals of time, namely 2 h, 8 h, 24 h for tomato, and 2 h, 4 h, 6 h for wheat seeds. Subsequently, the seeds were air-dried overnight at room temperature to perform the dry-back (DB) phase of the priming treatment. The heat-shock (HS) treatment was carried out in an oven at 90 °C for 30 min for *G. max* and *T. aestivum*, while *S. lycopersicum* seeds were kept in the oven for 3 h. Nontreated controls (CTRL) consisting of dry seeds were also used in the experimental system. A schematic representation of the experimental design representative for *G. max* treatments is given in Figure 1.

2.2. Germination Parameters

For germination tests, treated/untreated seeds were monitored in parallel compatibly with the guidelines provided by ISTA [1]. For this purpose, all germination tests were performed in triplicate, where 20 seeds/replicate were placed in Petri dishes containing a filter of blotting paper moistened with 2.5 mL water. All containers were kept in a growth chamber at 25 °C under light conditions with a photon flux density of 150 µmol m^{-2} s^{-1}, a photoperiod of 16/8 h, and 70–80% relative humidity. Germination was assessed daily for a period of three days for soybean, five days for wheat, and six days for tomato seeds.

At the end of the indicated periods, the following germination indices were calculated: germinability (G), peak value (PV), mean germination time (MGT), mean germination rate (MGR), coefficient of velocity (CVG), uncertainty index (U), and synchronicity index (Z) [51]. G is defined as the percentage (%) of germinated seeds at the end of the germination test. PV is the highest ratio between the number of germinated seeds at a given time point and the corresponding time, providing an indication of germination rates both in terms

of percentage and speed. MGT calculates the average germination time, in which lower MGT values indicate a faster germination. MGR is calculated as the reciprocal of MGT, and it provides an estimation of germination frequency, in which higher MGT values correspond to higher germination frequency. CVG is calculated as the MGR expressed in percentage (%); hence it provides an estimation of germination frequency, in which higher CVG values correspond to higher germination frequency. U is associated with the distribution of germination during the germination test timespan, and higher U values indicate lower synchronization and more dispersion. Z is relative to the synchrony of germination during the experimental monitoring, in which higher Z values indicate high degree of synchronization and lower dispersion in time [51]. The formulas used for the calculation of these parameters is given in the Supplementary Table S1.

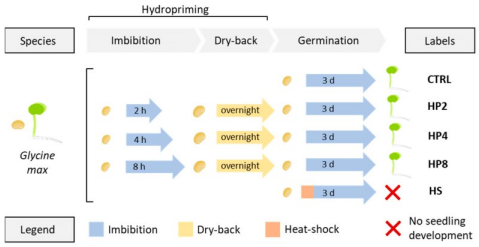

Figure 1. Example of the experimental system applied to *Glycine max* seeds. Imbibition steps are indicated in blue, dry-back is indicated in yellow, and heat-shock is indicated in orange. CTRL, non-treated control; HP2, hydropriming for 2 h; HP4, hydropriming for 4 h; HP8, hydro-priming for 8 h; HS, heat-shock.

Aside from the aforementioned germination parameters, seedling growth was biometrically assessed. The seedling growth was monitored at the end of the experiment by using ImageJ (https://imagej.nih.gov/ij/) software. To this purpose, at least five seedlings/replicate were photographed and used to determine the seedling length (in terms of roots and/or aerial parts).

2.3. DCFH-DA Assay

ROS levels were quantified in CTRL and HP, HS, and DB seeds. The assay was carried out by using the fluorogenic dye 2,7-dichlorofluorescin diacetate (DCFH-DA; Sigma-Aldrich, Milan, Italy). The dye is converted to a nonfluorescent molecule following deacetylation mediated by esterases, and it is subsequently oxidized by ROS into the fluorescent compound 2,7-dichlorofluorescein (DCF), which can be detected by fluorescence spectroscopy with maximum excitation and emission spectra of 495 nm and 529 nm, respectively. The assay was carried out as described by Pagano et al. [49], with the following modifications. Seed samples were incubated for 30 min with 500 µL of 10 µM DCFH-DA (for *G. max* and *T. aestivum*) and 70 µL of 50 µM DCFH-DA (for *S. lycopersicum*) or for 15 min. Subsequently, the fluorescence sensor (at 517 nm) of the Rotor-Gene 6000 PCR apparatus (Corbett Robotics, Brisbane, Australia) was used, setting the program for one cycle of 30 s at 25 °C. A sample containing only DCFH-DA was used as a negative technical control to subtract the baseline fluorescence. Data were expressed as relative fluorescence units (RFU).

2.4. FOX-1 Assay

Peroxyl radicals and hydrogen peroxide (H_2O_2) concentrations were quantified in control and treated seeds at the indicated time points as presented in Section 2.1. The assay

was carried out by using the reagent xylenol orange (Carlo Erba, Milan, Italy), which reacts with Fe^{3+} (derived from the oxidation of Fe^{2+} induced by peroxyl radicals and H_2O_2) to give a blue-violet complex with an absorption maximum at 560 nm. The working solution (FOX-1 solution) was prepared as described by Bridi et al. [52]. A solution containing ammonium ferrous (II) sulphate $(NH_4)2Fe(SO_4)2{\cdot}6H_2O$ 25 mM (Merk's Reagents, Darmstadt, Germany) in H_2SO_4 0.25 M (Honeywell, Charlotte, NC, USA) was added to a Milli-Q water solution containing Xylenol Orange 125 µM (Carlo Erba, Milan, Italy) and D-sorbitol 100 mM (Duchefa Biochemie, Haarlem, The Netherlands) in a ratio of 1:100. The solutions were mixed gently until the color became uniform. Seed samples were incubated in a sufficient volume (1.5 mL for *S. lycopersicum* and 3 mL for *T. aestivum* and *G. max*) of FOX-1 working solution to allow seeds complete immersion for 45 min. Five replicates of one seed each were used per sample. Subsequently, 1 mL of medium was recovered from each sample and the absorbance was determined at 560 nm by using a Biochrom WPA Biowave (Biochrom Ltd., Cambridge, United Kingdom) spectrophotometer. A calibration curve (Figure S1) was performed by using FOX-1 solution with different concentrations (0, 1.25, 2.50, 5 µM) of H_2O_2, and data were represented as [ROOH] concentration values.

2.5. Quantitative Real-Time-Polymerase Chain Reaction (qRT-PCR)

Total RNA was isolated from *G. max* treated/untreated seeds by using TRIzol™ (Thermo Fisher Scientific, Monza, Italia), as indicated by the provider. Subsequently, a DNase (Thermo Fisher Scientific) treatment was performed. RNA was quantified by using NanoDrop (Biowave DNA, WPA, Thermo Fisher Scientific). Subsequently, cDNAs were obtained by using the RevertAid First Strand cDNA Synthesis Kit (Thermo Fisher Scientific) according to the manufacturer's suggestions.

The qRT-PCR reactions were performed with the Maxima SYBR Green qPCR Master Mix (Thermo Fisher Scientific) according to the supplier's indications, by using a CFX Duet, Real-Time PCR System (BIO-RAD, Milano, Italy). Amplification conditions were as follows: denaturation at 95 °C for 10 min, and 45 cycles of 95 °C for 15 s and 60 °C for 60 s. Oligonucleotide sequences (Table S2) were designed by using Primer3Plus1 (https://primer3plus.com/) and verified with Oligo Analyzer.2 (https://eu.idtdna.com/pages/tools/oligoanalyzer). Relative quantification was carried out by using the *CYP* (peptidyl-prolyl cis-trans isomerase) and RP40S (ribosomal protein 40S) as reference genes [53]. Raw fluorescence data provided by Software 1.7 (BIO-RAD) were used to determine the threshold cycle number (Ct) values for each transcript quantification. Relative quantification of transcript accumulation was performed as described by Thomsen et al. [54] by using the X_0 method in which a conversion of the exponentially related Ct values is introduced to arrive to linearly related values, representing the amount of starting material in a qPCR reaction. All reactions were performed in triplicate.

The choice of investigated genes was based on in silico gene expression data mining obtained from *Arabidopsis thaliana* and *G. max* orthologues, recovered from BAR ePLANT (http://bar.utoronto.ca/eplant_soybean/) [55] and Arabidopsis eFP browser (http://bar.utoronto.ca/efp/cgi-bin/efpWeb.cgi) [56], respectively. The selected genes encoding enzymes involved in ROS production and scavenging include superoxide dismutase (*SOD*1, Phytozome accession No. Glyma.19G240400) manganese superoxide dismutase (*MnSOD*, Phytozome accession No. Glyma.04G221300), catalase 1 (*CAT*1, Phytozome accession No. Glyma.06G017900), catalase 5 (*CAT*5, Phytozome accession No. Glyma.17G261700), ascorbate peroxidase 2 (*APX*2, Phytozome accession No. Glyma.12G073100), respiratory burst oxidase homolog E2 (*RbohE*2, Phytozome accession No. Glyma.08G005900), and respiratory burst oxidase homolog C2 (*RbohC*2, Phytozome accession No. Glyma.06G162300).

2.6. Statistical Analyses

Germination data were analyzed with the Student *t*-test by using the Microsoft Excel package using as threshold the p-value < 0.05 ('*'). Estimation of oxidative stress and ROS data were analyzed by two-way ANOVA and Tuckey–Kramer test, where $p < 0.05$ is

considered as significantly different, by using the software developed by Assaad et al. [57]. Letters were used to indicate significant differences among all samples. For correlation analyses, Pearson's correlation coefficient and the relative *p*-values were determined by using MetaboAnalyst 5.0 (https://www.metaboanalyst.ca/) [58]. The same software was also used for principal component analysis (PCA) performed by using the germination parameters and ROS detection data. The obtained "biplot" and "score plot" graphics show how the different sample groups are clustered according to the results obtained in the performed analyses.

3. Results

3.1. Hydropriming Improves Germination Performance in Multiple Species

Because hydropriming has been already proven to be effective in improving seed germination potential [31,35–38], this initial part of the work was dedicated to select the most appropriate time points of seed imbibition as this is generally dependent not only on plant variety/genotype but also on the respective seed lots [28,36]. To test the efficiency of hydropriming treatment in improving seed germination, we first focused on soybean, as it is one of the most cultivated species that dominate global agriculture [59]. It has a sequenced and well-annotated genome [60], with data present in several bioinformatics platforms (e.g., Phytozome, BAR ePLANT). Due to the time-specific sensitivity of hydropriming treatments, several imbibition time points were tested. Additionally, to develop a competent experimental design, HS treatments were implemented to decrease seed quality and germination were included along with the control (CTRL). The subsequent analyses indicated that hydropriming resulted in a significantly enhanced germination percentage (G%) compared to CTRL (Figure 2a) for all the tested treatments during the first two days of monitoring. This improved G% was also translated into significantly enhanced root growth when measured at the end of the experiment (after three days) (Figure 2b,c). Data collected for other germination parameters (Table 1) confirm that HP improves germination performance. Specifically for soybean, all the imposed HP treatments showed significant differences compared to CTRL, in terms of PV, MGT, MGR, and CVG, whereas the U and Z parameters were improved only with the HP4 treatment. This indicates that the best time point at which to stop the priming treatment for this soybean commercial variety is after 4 h of imbibition in water, a treatment that brings positive outcomes in terms of germination percentage, speed, and uniformity. The HS treatment was highly damaging and no seed germinated, showing that this can be used as a system to decrease seed quality.

Table 1. Germination parameters calculated for *Glycine max*. Statistical differences among treatments and control are represented with asterisks (*), $p < 0.05$. Formulas and measure units for each parameter are provided in the supplementary materials. PV, peak value; MGT, mean germination time; MGR, mean germination rate; CVG coefficient of velocity; U, uncertainty index; Z, synchronicity index; CTRL, nontreated control; HP2, hydropriming for 2 h; HP4, hydropriming for 4 h; HP8, hydropriming for 8 h; HS, heat-shock.

	CTRL	HP2	HP4	HP8	HS
PV	6.67 ± 0.76	11.67 ± 0.58 *	14 ± 2.65 *	14 ± 2 *	0 ± 0 *
MGT	2.18 ± 0.09	1.41 ± 0.06 *	1.22 ± 0.12 *	1.33 ± 0.17 *	n.d.
MGR	0.46 ± 0.02	0.71 ± 0.03 *	0.82 ± 0.08 *	0.76 ± 0.10 *	n.d.
CVG	45.89 ± 1.87	70.98 ± 2.76 *	82.24 ± 7.84 *	75.7 ± 9.95 *	n.d.
U	1.28 ± 0.08	1.1 ± 0.13	0.72 ± 0.21 *	1 ± 0.34	0 ± 0 *
Z	0.43 ± 0.02	0.48 ± 0.03	0.65 ± 0.13 *	0.56 ± 0.15	0 ± 0 *

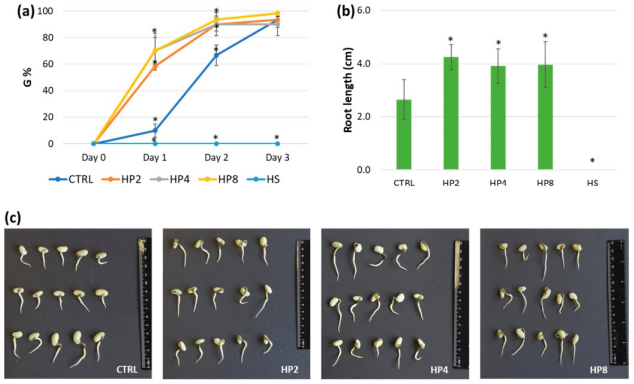

Figure 2. Evaluation of hydropriming efficiency in *Glycine max* seeds. (**a**) Germination percentage (%). (**b**) Root length (cm). (**c**) Representative images of germinated soybean seedlings after three days of treatments. Statistical differences among treatments and control are represented with asterisks (*). $p < 0.05$. CTRL, non-treated control; HP2, hydropriming for 2 h; HP4, hydropriming for 4 h; HP8, hydropriming for 8 h; HS, heat-shock.

To confirm that these treatments can be universally implemented for different plant species and seed types, additional experiments were carried out by using *S. lycopersicum* and *T. aestivum* seeds (Figures S2 and S3, Table S3). The gathered results show that HP2 and HP8 treatments were efficient in improving germination and seedling growth in tomatoes, whereas for wheat the only significant data regarded G% after one day of monitoring. The results indicate that hydropriming treatments are efficient in boosting germination, but the imbibition time points need to be tailored for each species/genotype/seed lots, as evidenced in other cases [35–38].

3.2. ROS Profiles Are Influenced by the Applied Treatments

Once we have shown that the implemented experimental system can be used to boost or damage seed quality (in terms of germination performance), the next set of analyses was dedicated the evaluate different protocols to measure ROS levels. The two assays hereby employed, namely DCFH-DA and FOX-1, have different targets and specificities. Quantification based on the use of the DCFH-DA molecule measures the general oxidative status [61]. In particular, in the absence of metal or enzymatic catalysts, the $DCFH_2$ molecule (produced in the cells through the activity of esterases) is not able to react with some ROS (e.g., $O_2^{\cdot -}$, LOO^-, H_2O_2) whereas it can react with oxygen and nitrogen radicals, including $\cdot OH$ and peroxynitrites [61]. In contrast, the FOX-1 assay directly detects peroxidic radicals ($ROO^{\cdot}$) and in particular H_2O_2 released in the medium whereas it has a low reactivity towards other molecules [62,63].

Both assays were used to assess these different aspects of ROS accumulation or release by using whole seeds. The gathered data show that the highest amount of oxidative stress (Figure 3a) and peroxide radicals (Figure 3b) are registered in seeds treated with HS. Moreover, the seeds subjected to HP treatments appeared to have the lowest levels of measured ROS, using both the DCFH-DA and FOX-1 assays (Figure 3a,b).

To validate these results, the two assays were applied to the tomato and wheat seeds following the same experimental approaches (Figure S4). Although the FOX-1 results

maintained a similar pattern of ROS being released from the seeds (Figure S4b,d), the DCFH-DA assay presented much more elevated levels of variability (Figure S4a,c).

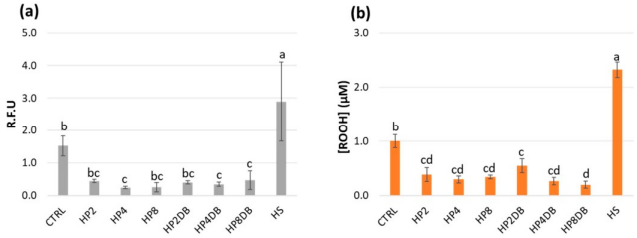

Figure 3. ROS detection in *G. max* seeds subjected to hydropriming and HS treatments. (**a**) Data collected by using the DCFH-DA fluorimetry assay and represented as relative fluorescence units (RFU). (**b**) Data collected from the FOX-1 assay through spectrophotometric measurements and represented as [ROOH] concentration values. Statistically significant differences ($p < 0.05$) are indicated by the occurrence of different letters. CTRL, non-treated control; HP2, hydropriming imbibition for 2 h; HP4, hydropriming imbibition for 4 h; HP8, hydropriming imbibition for 8 h; HP-DB, dry-back treatment following hydropriming imbibition; HS, heat-shock.

Subsequently, a PCA analysis was carried out to evidence how the different treatments (CTRL, HP, and HS) are clustered according to the obtained data. The clustering of the group of seeds subjected to the imposed treatments in *G. max* (Figure 4a) shows a distinct grouping of the HP treatments compared to CTRL and HS.

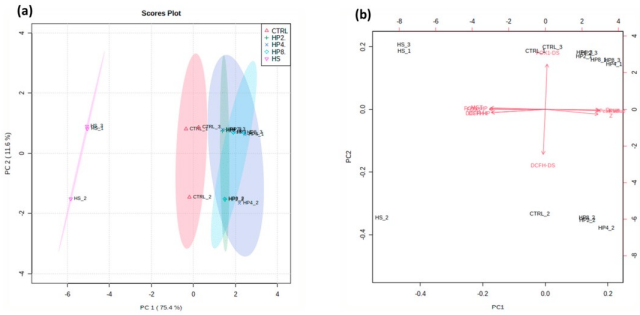

Figure 4. PCA using data gathered for the imposed treatments (CTRL, HP2, HP4, HP8, HS) for *G. max*. (**a**) Score plot grouping of samples subjected to different treatments. (**b**) Biplot obtained with data from germination tests (G, PV, MGT, Z, Rad) and ROS measurements (FOX-1, DCHF-DA) on the clustering of the groups subjected to the different treatments. Because the data provided consisted in triplicate values, the designation _1, _2, _3 in the plots refers to the replicate number.

According to the biplot generated by the PCA analysis (Figure 4b), the main contributors to this this clustering are the germination parameters. The CTRL samples clustered separately from the groups subjected to HP and HS treatments, mainly due to the data obtained from the FOX-1 and DCHF-DA analyzes. Finally, the separation of the HS group is, according to the PCA analysis, mainly due to the values obtained for MGT as well as

FOX1 and DCHF-DA (Figure 4b). Similar patterns of clusters were also obtained for tomato and wheat (Figure S5).

3.3. ROS-Related Gene Expression Is Induced by Hydropriming Treatments

To better investigate ROS homeostasis in the proposed working system, qRT-PCR analyses were carried out to quantify the relative expression of genes encoding enzymes involved in ROS scavenging and production. To select which genes would provide the most relevant information, a preliminary *in silico* data mining approach was conducted simultaneously for *A. thaliana* and *G. max* models. Data relative to multiple isoforms of *CAT, SOD, APX*, and *Rboh* genes were comparatively examined during seed maturation in soybean as well as during the early phases of seed germination in Arabidopsis (Figure S6). This analysis showed that different isoforms of the studied genes are differently expressed during soybean seed maturation with the highest expression being most prevalent for 14DAF (days after flowering), 21DAF, and 35DAF, whereas for Arabidopsis the majority of genes are highly expressed at 48 h of seed imbibition/germination. Based on this investigation, the following genes were selected to perform the qRT-PCR analyses during soybean HP treatment: *MnSOD, SOD1, CAT1, CAT5, APX2* as genes encoding enzymes involved in ROS scavenging, and *RbohE2, RbohC2* as genes encoding enzymes involved in ROS production. Their expression levels were evaluated in soybean dry seeds (CTRL), in seeds subjected to 4 h imbibition (HP4) as the most promising HP timepoint to boost germination, as well as after dry-back (HP4DB) as the last phase of the HP treatment (Figure 5). The gathered data revealed that all genes were significantly upregulated both after seed imbibition (except for *MnSOD*) as well as after the dry-back treatments (except for *APX2*), as compared with the CTRL samples. Interestingly, this trend was common for genes encoding enzymes involved in ROS scavenging as well as ROS production mechanisms. Nonetheless, the highest gene expression levels were registered for the two CAT genes (ROS scavenging) whereas the lowest expression was observed for the *Rboh* genes (ROS production), namely *RbohE2* gene.

Subsequently, correlation analyses were performed between data obtained from the ROS detection methods (DCFH-DA and FOX-1) and gene expression profiles (Figure 6). In general, a negative correlation is observed between the gene expression and ROS levels. For example, this is observed between the data obtained in the FOX-1 analysis and the *CAT*1. *RbohE*2, *APX*2, and *SOD*1 expression levels. The same trend is observed for the data obtained with the DCFH-DA analysis and the *CAT*1, *CAT*5, *RbohE*2, *APX*2, and *SOD*1 relative expression. In contrast, positive correlations are generally observed between the gene expression data, namely for *CAT*1, *CAT*5, and *APX*2 compared to *SOD*1. Furthermore, it is interesting to note that the *RbohE*2 (gene responsible for the production of ROS in seed) expression levels also showed a positive correlation with the expression levels of all the genes responsible for ROS removal (*MnSOD*, *SOD*1, *CAT*1, *CAT*5, *APX*2). A similar trend is observed also for *RbohC*2. Finally, significantly positive correlations are observed between the ROS levels measured through the FOX-1 assay (in terms of peroxide species concentration) and the DCFH-DA (in terms of oxidative stress levels) assay.

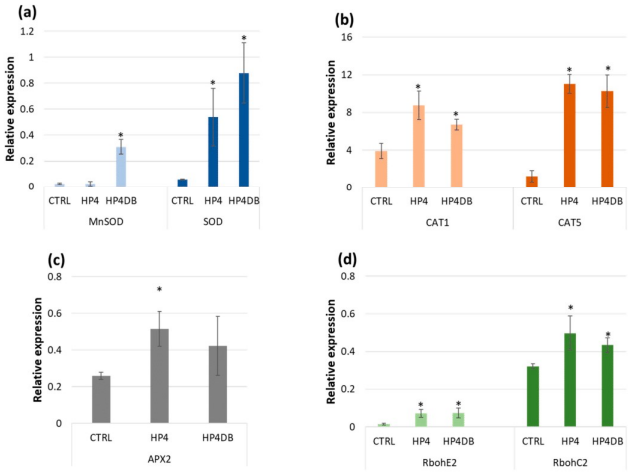

Figure 5. Relative expression of genes encoding enzymes involved in ROS scavenging and production mechanisms in *G. max* seeds subjected to hydropriming treatments. (**a**) Superoxide dismutases, *MnSOD* and *SOD*1. (**b**) Catalases, *CAT*1 and *CAT*5. (**c**) Ascorbate peroxidase *APX*2. (**d**) Respiratory burst oxidase homologs, *RbohE*2 and *Rboh*C2. Statistically significant differences obtained by using the Student *t*-test ($p < 0.05$) are indicated with an asterisk (*). CTRL, untreated seeds; HP4, seeds soaked for four hours in water; HP4DB, seeds soaked for four hours and subjected to the desiccation required by hydropriming protocols.

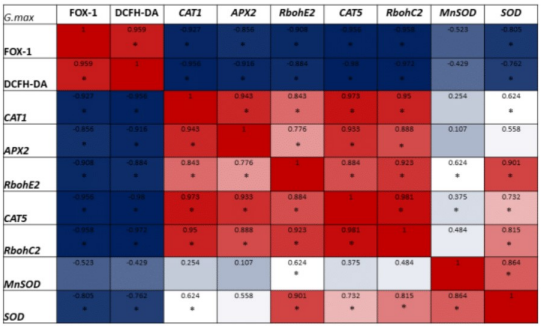

Figure 6. Pearson correlation indices calculated for *G. max* hydroprimed seeds taking into consideration the biochemical assays for ROS quantification (FOX-1 and DCFH-DA) and the ROS homeostasis gene (*CAT*1, *APX*2, *CAT*5, *MnSOD*, *SOD*1, *RbohE*2, *Rboh*C2) expression levels. The blue color indicates negative correlations whereas red indicates positive correlations. Statistically significant correlations ($p < 0.05$) are indicated by an asterisk (*).

4. Discussion

Currently, standard germination tests approved by ISTA represent the main methods that allow the observation of seed behavior in the postsowing phase [1,64]. The most common methods for seed quality establishment are invasive and do not allow the continued evaluation of seeds over time. Among the invasive techniques, aside from germination tests, the evaluation of moister content [65,66], tetrazolium test [67,68], and accelerated aging systems [69,70] are also used often. Most of these chemical and physical techniques exhibit a good accuracy and reliability but also present certain limitations, such as high cost, health hazards, lengthy duration, and high operator requirements [2]. These methods also raise problems related to the direct use of seeds and the time required to obtain relevant information. The development of new techniques and procedures by which to analyze seed characteristics is driven by the need to overcome these drawbacks. Therefore, several nondestructive methodologies have been developed, many of them being based on the use of different imaging techniques supported by computer vision to rapidly collect and interpret high-resolution images [3,71–73]. These include thermal imaging [74,75], X-rays [76–78], and spectroscopic techniques such as near-infrared spectroscopy (NIRS) technologies [5,79–81], Raman spectroscopy [3,82,83], or hyperspectral imaging [83,84]. Although these noninvasive methods represent a faster, deeper, and more precise way to retrieve important information for the evaluation of seed quality, the associated costs, and the required expertise are still prohibitive for large-scale screening of seed lots. Therefore, there is still the need to expand the palette of methods by which to reduce their costs or to promote the development of other cost-effective and sustainable methods.

Given these premises, the current study proposes two biochemical assays that can be employed to detect the levels of ROS as a proxy of seed quality. Why focus on ROS? Because, as already indicated, these are essential molecules with well-proven roles in seed dormancy and germination [5–7,23,24], relevant processes in the context of seed vigor and seed quality assessment. To prove that the proposed assays can be adopted as methods to test seed quality, we have first developed appropriate materials by applying treatments meant to boost (hydropriming) or inhibit (heat-shock) seed germination. We have adopted soybean as a reference species in this study because of its high agroeconomic relevance as well as possible model legume and availability of database resources [59,60]. However, to show that these approaches can be universally applied, we have extended the study to other relevant crops like tomato and wheat, hence covering seed morphological diversity. Indeed, our results show that hydropriming improved germination performance but this is conditioned by the soaking time. On the other hand, the HS treatments imposed in this study suppressed seed germination.

Having defined the experimental systems, the following step consisted of evaluating ROS levels and comparing the two proposed approaches. Interestingly, even if the DCFH-DA and FOX-1 assays relatively measure different components, namely oxidative status and H_2O_2 released radicals respectively, in the case of soybean the results obtained follow the same pattern: higher levels of ROS in HS and CTRL and low levels during the HP treatments. For the FOX-1 assay, this trend is also maintained in the other investigated species, whereas the DCFH-DA results were much more variable. This may be due to the different types of measurement techniques; on the one hand, the use of a fluorimeter with extracting the baseline fluorescence levels, and, on the other hand, the use of spectrophotometric readings plotted to a standard curve. Moreover, the DCFH-DA assay is generally used to quantify intracellular ROS levels [85–87], whereas FOX-1 is used for measuring the release of specific ROS in the surrounding environment [52,88,89]. The DCFH is usually oxidized to the fluorescent product DCF by multiple reactive species, and thus it is not specific for a particular ROS [90,91]. In addition, other limitations include the fact that DCFH is not oxidized directly by H_2O_2, but only after its conversion to more reactive species, and this oxidation is also sensitive to O_2 levels, light, and pH. Consequently, several studies have indicated that the observed fluorescence may not be proportional with the accumulation of ROS [92,93]. By contrast, FOX-1 is generally used in an acidic environment,

and it relies on the oxidation of Fe^{2+} to Fe^{3+} [94]. In this case, hydroperoxides oxidize the ferrous ion to ferric ion, subsequently treated with the XO reagent to generate a ferric-XO complex, resulting in a blue–purple color readable at 550–560 nm [95]. This approach has received much attention not only because of its low cost but also because it is not affected by environmental conditions (e.g., O_2, light) [96].

To show that the applied methods are noninvasive, we have monitored the germination percentage of seeds imbibed in the DCFH-DA and FOX-1 reagents for 15 and 30 min, respectively, and no significative differences were observed between CTRL and imbibed seeds (Figure S7).

Lastly, to prove that the ROS turnover is influenced within the proposed system, a qRT-PCR approach was adopted to monitor the expression of genes encoding enzymes involved in both ROS production (*RbohE*2, *Rboh*C2) and scavenging (*MnSOD*, *SOD*1, *CAT*1, *CAT*5, *APX*2). The scientific literature is rich in studies evidencing that seed priming treatments result in differential expression of a myriad of antioxidant genes [35–37,45,46,97,98]. And indeed, the observed upregulation of the selected genes is in agreement with the cited data. The upregulation of both ROS production and scavenging genes indicates active ROS turnover; thus while ROS are being produced the antioxidant systems are being activated. Additionally, a correlation analysis was carried out between the measured ROS through the two assays and the levels of expression of the investigated genes. The positive correlations observed between the DCHF-DA and FOX-1 data in the case of soybean seeds indicate that the different types of ROS detected by the two assays display a similar accumulation pattern. By contrast, during seed priming the expression of genes involved in ROS turnover increases while the observed levels of measured ROS decrease. This is statistically reinforced by the recurrent negative correlations observed between the ROS patterns and gene expression levels. This can be thus interpreted as an indication of the efficiency of the antioxidant response in reducing ROS accumulation.

The noninvasiveness and relative rapidity of the proposed assays can have promising outcomes in multiple experimental and applicative contexts. For instance, from an experimental point of view, these can be used to track the kinetics of ROS dynamics for individual seeds, providing a time-lapse to monitor the progression of priming protocols or the activation of the seed pre-germinative metabolism within the "oxidative window" [6]. For the applicative side, whenever seed materials are scarce these assays may allow the evaluation of the quality of a seed lot without losing valuable material. This can be applied to seed bank accessions and elite breeding materials with important implications on biodiversity preservation in crops and wild species.

5. Conclusions

The current study proposes two noninvasive, rapid, cost-effective, and potentially universal techniques by which to measure ROS production in seeds as a proxy of seed quality evaluation. Although the DCFH-DA assay is more variable and subjected to certain limitations in terms of types of measured ROS and interaction with surrounding factors, the FOX-1 approach appears to be more reliable when applied to different types of seeds. Additional proof of the accuracy of the investigated methods is provided through the correlation analysis performed, taking into consideration the measured ROS levels and the expression of genes involved in ROS turnover. To further validate the obtained data, the methods could be subsequently applied to other species, varieties/genotypes, seed types, and experimental conditions, such as different seed lots collected from diverse environments, seed storage conditions, seed aging protocols, and damaging or beneficial treatments.

Supplementary Materials: The following supporting information can be downloaded at: https://www.mdpi.com/article/10.3390/antiox12030626/s1. Table S1: Germination parameters formulas; Table S2: List of oligonucleotides sequences used for the qRT-PCR analysis; Table S3: Germination parameters calculated for *S. lycopersicum*, and *T. aestivum*; Figure S1: FOX-1 calibration curve; Figure S2: Representative images of *S. lycopersicum* and *T. aestivum* HP germinated seedlings. Figure S3: Evalua-

tion of HP efficiency in tomato and wheat seeds; Figure S4: ROS detection in *S. lycopersicum* and *T. aestivum* seeds subjected to HP and HS treatments; Figure S5: PCA analysis for wheat and tomato; Figure S6: Gene expression heatmaps in seeds of *G. max* and *A. thaliana*; Figure S7: Germination percentage (G%) for soybean, tomato and wheat seeds imbibed in DCFH-DA and FOX-1.

Author Contributions: Conceptualization, A.M. and A.B.; methodology, formal analysis, investigation. Data curation, A.G. and N.B.; writing-original draft preparation, review and editing, A.P., A.B. and A.M. All authors have read and agreed to the published version of the manuscript.

Funding: This research received no external funding.

Institutional Review Board Statement: Not applicable.

Informed Consent Statement: Not applicable.

Data Availability Statement: The data presented in this study are available in the article and supplementary materials.

Acknowledgments: The authors wish to acknowledge the support provided by the National Recovery and Resilience Plan (NRRP) NextGenerationEU: "Node 4-Ecosystems functions, services and solutions", Activity 5 (Conceptual framework and methodological tools of Nature Based Solution and Restoration Ecology) and Mission 4 Education and research "NODES-Nord Ovest Digitale E Sostenibile", Spoke 6-Primary Agroindustry. The authors would also like to thank all the institutions (ITQB NOVA) and companies (Sipcam Oxon SpA, ISI Sementi S.p.A.) who kindly provided the seed materials used in this study.

Conflicts of Interest: The authors declare no conflict of interest.

References

1. Milivojević, M.; Ripka, Z.; Petrović, T. ISTA rules changes in seed germination testing at the beginning of the 21st century. *J. Process Energy Agric.* **2018**, *22*, 40–45. [CrossRef]
2. Huang, M.; Wang, Q.G.; Zhu, Q.B.; Qin, J.W.; Huang, G. Review of seed quality and safety tests using optical sensing technologies. *Seed Sci. Technol.* **2015**, *43*, 337–366. [CrossRef]
3. Rahman, A.; Cho, B.K. Assessment of seed quality using non-destructive measurement techniques: A review. *Seed Sci. Res.* **2016**, *26*, 285–305. [CrossRef]
4. Hay, F.R.; Whitehouse, K.J. Rethinking the approach to viability monitoring in seed genebanks. *Conserv. Physiol.* **2017**, *5*, cox009. [CrossRef] [PubMed]
5. Pagano, A.; Forti, C.; Gualtieri, C.; Balestrazzi, A.; Macovei, A. Oxidative stress and antioxidant defense in germinating seeds. A Q&A session. In *Reactive Oxygen, Nitrogen and Sulfur Species in Plants: Production, Metabolism, Signaling and Defense Mechanisms*; Hasanuzzaman, M., Fotopoulos, V., Nahar, K., Fujita, M., Eds.; John Wiley & Sons Ltd.: Hoboken, NJ, USA, 2019; pp. 267–289.
6. Bailly, C. The signalling role of ROS in the regulation of seed germination and dormancy. *Biochem. J.* **2019**, *476*, 3019–3032. [CrossRef] [PubMed]
7. Rehmani, M.S.; Aziz, U.; Xian, B.; Shu, K. Seed dormancy and longevity: A mutual dependence or a trade-off? *Plant Cell Physiol.* **2022**, *63*, 1029–1037. [CrossRef]
8. Ciacka, K.; Staszek, P.; Sobczynska, K.; Krasuska, U.; Gniazdowska, A. Nitric oxide in seed biology. *Int. J. Mol. Sci.* **2022**, *23*, 14951. [CrossRef]
9. Richards, S.L.; Wilkins, K.A.; Swarbreck, S.M.; Anderson, A.A.; Habib, N.; Smith, A.G.; McAinsh, M.; Davies, J.M. The hydroxyl radical in plants: From seed to seed. *J. Exp. Bot.* **2015**, *66*, 37–46. [CrossRef]
10. Ishibashi, Y.; Yuasa, T.; Iwaya-Inoue, M. Mechanisms of maturation and germination in crop seeds exposed to environmental stresses with a focus on nutrients, water status, and Reactive Oxygen Species. *Adv. Exp. Med. Biol.* **2018**, *1081*, 233–257.
11. Farooq, M.A.; Ma, W.; Shen, S.; Gu, A. Underlying biochemical and molecular mechanisms for seed germination. *Int. J. Mol. Sci.* **2022**, *23*, 8502. [CrossRef]
12. Klupczyńska, E.A.; Dietz, K.J.; Małecka, A.; Ratajczak, E. Mitochondrial peroxiredoxin-IIF (PRXIIF) activity and function during seed aging. *Antioxidants* **2022**, *11*, 1226. [CrossRef]
13. Kurek, K.; Plitta-Michalak, B.; Ratajczak, E. Reactive Oxygen Species as potential drivers of the seed aging process. *Plants* **2019**, *8*, 174. [CrossRef] [PubMed]
14. Juan, C.A.; Pérez de la Lastra, J.M.; Plou, F.J.; Pérez-Lebeña, E. The chemistry of Reactive Oxygen Species (ROS) revisited: Outlining their role in biological macromolecules (DNA, lipids and proteins) and induced pathologies. *Int. J. Mol. Sci.* **2021**, *22*, 4642. [CrossRef] [PubMed]
15. Bailly, C.; El-Maarouf-Bouteau, H.; Corbineau, F. From Intracellular signaling networks to cell death: The dual role of Reactive Oxygen Species in seed physiology. *Comptes Rendus Biol.* **2008**, *331*, 806–814. [CrossRef] [PubMed]

16. Macovei, A.; Pagano, A.; Leonetti, P.; Carbonera, D.; Balestrazzi, A.; Araújo, S.S. Systems biology and genome-wide approaches to unveil the molecular players involved in the pre-germinative metabolism: Implications on seed technology traits. *Plant Cell Rep.* **2017**, *36*, 669–688. [CrossRef]
17. Doria, E.; Pagano, A.; Ferreri, C.; Larocca, A.V.; Macovei, A.; Araújo, S.S.; Balestrazzi, A. How does the seed pre-germinative metabolism fight against imbibition damage? Emerging roles of fatty acid cohort and antioxidant defence. *Front. Plant Sci.* **2019**, *10*, 1505. [CrossRef]
18. El-Maarouf-Bouteau, H. The seed and the metabolism regulation. *Biology* **2022**, *11*, 168. [CrossRef]
19. Schopfer, P.; Plachy, C.; Frahry, G. Release of reactive oxygen intermediates (superoxide radicals, hydrogen peroxide, and hydroxyl radicals) and peroxidase in germinating radish seeds controlled by light, gibberellin, and abscisic acid. *Plant Physiol.* **2001**, *125*, 1591–1602. [CrossRef]
20. Bailly, C.; Bogatek-Leszczynska, R.; Côme, D.; Corbineau, F. Changes in activities of antioxidant enzymes and lipoxygenase during growth of sunflower seedlings from seeds of different vigour. *Seed Sci. Res.* **2002**, *12*, 47–55. [CrossRef]
21. Jurdak, R.; Rodrigues, G.A.G.; Chaumont, N.; Schivre, G.; Bourbousse, C.; Barneche, F.; Bou Dagher Kharrat, M.; Bailly, C. Intracellular reactive oxygen species trafficking participates in seed dormancy alleviation in Arabidopsis seeds. *New Phytol.* **2022**, *234*, 850–866. [CrossRef] [PubMed]
22. Kranner, I.; Roach, T.; Beckett, R.P.; Whitaker, C.; Minibayeva, F.V. Extracellular production of reactive oxygen species during seed germination and early seedling growth in *Pisum sativum*. *J. Plant Physiol.* **2010**, *167*, 805–811. [CrossRef]
23. Mittler, R.; Vanderauwera, S.; Suzuki, N.; Miller, G.; Tognetti, V.B.; Vandepoele, K.; Gollery, M.; Shulaev, V.; Van Breusegem, F. ROS signaling: The new wave? *Trends Plant Sci.* **2011**, *16*, 300–309. [CrossRef]
24. Wrzaczek, M.; Brosché, M.; Kangasjärvi, J. ROS signaling loops—Production, perception, regulation. *Curr. Opin. Plant Biol.* **2013**, *16*, 575–582. [CrossRef]
25. Devika, O.S.; Singh, S.; Sarkar, D.; Barnwal, P.; Suman, J.; Rakshit, A. Seed priming: A potential supplement in integrated resource management under fragile intensive ecosystems. *Front. Sustain. Food Syst.* **2021**, *5*, 654001. [CrossRef]
26. Reed, R.C.; Bradford, K.J.; Khanday, I. Seed germination and vigor: Ensuring crop sustainability in a changing climate. *Heredity* **2022**, *128*, 450–459. [CrossRef] [PubMed]
27. Pagano, A.; Macovei, A.; Balestrazzi, A. Molecular dynamics of seed priming at the crossroads between basic and applied research. *Plant Cell Rep.* **2023**, *13*, 1–32. [CrossRef] [PubMed]
28. Paparella, S.; Araújo, S.S.; Rossi, G.; Wijayasinghe, M.; Carbonera, D.; Balestrazzi, A. Seed priming: State of the art and new perspectives. *Plant Cell Rep.* **2015**, *34*, 1281–1293. [CrossRef] [PubMed]
29. Mal, D.; Verma, J.; Levan, A.; Reddy, M.R.; Avinash, A.V.; Velaga, P.K. Seed priming in vegetable crops: A review. *Int. J. Curr. Microb. Appl. Sci.* **2019**, *8*, 868–874. [CrossRef]
30. Marthandan, V.; Geetha, R.; Kumutha, K.; Renganathan, V.G.; Karthikeyan, A.; Ramalingam, J. Seed priming: A feasible strategy to enhance drought tolerance in crop plants. *Int. J. Mol. Sci.* **2020**, *21*, 8258. [CrossRef]
31. Carrillo-Reche, J.; Vallejo-Marín, M.; Quilliam, R.S. Quantifying the potential of 'on-farm' seed priming to increase crop performance in developing countries. A meta-analysis. *Agron. Sustain. Dev.* **2018**, *38*, 64. [CrossRef]
32. Rhaman, M.S.; Imran, S.; Rauf, F.; Khatun, M.; Baskin, C.C.; Murata, Y.; Hasanuzzaman, M. Seed Priming with phytohormones: An effective approach for the mitigation of abiotic stress. *Plants* **2020**, *10*, 37. [CrossRef]
33. Johnson, R.; Puthur, J.T. Seed priming as a cost effective technique for developing plants with cross tolerance to salinity stress. *Plant Physiol. Biochem.* **2021**, *162*, 247–257. [CrossRef]
34. Yang, Z.; Zhi, P.; Chang, C. Priming seeds for the future: Plant immune memory and application in crop protection. *Front. Plant Sci.* **2022**, *13*, 961840. [CrossRef]
35. Forti, C.; Shankar, A.; Singh, A.; Balestrazzi, A.; Prasad, V.; Macovei, A. Hydropriming and biopriming improve *Medicago truncatula* seed germination and upregulate DNA repair and antioxidant genes. *Genes* **2020**, *11*, 242. [CrossRef]
36. Forti, C.; Ottobrino, V.; Bassolino, L.; Toppino, L.; Rotino, G.L.; Pagano, A.; Macovei, A.; Balestrazzi, A. Molecular dynamics of pre-germinative metabolism in primed eggplant (*Solanum melongena* L.) seeds. *Hortic. Res.* **2020**, *7*, 87. [CrossRef]
37. Forti, C.; Ottobrino, V.; Doria, E.; Bassolino, L.; Toppino, L.; Rotino, G.L.; Pagano, P.; Macovei, A.; Balestrazzi, A. Hydropriming applied on fast germinating *Solanum villosum* Miller seeds: Impact on pre-germinative metabolism. *Front. Plant Sci.* **2021**, *12*, 639336. [CrossRef] [PubMed]
38. Adhikari, B.; Dhital, P.R.; Ranabhat, S.; Poudel, H. Effect of seed hydro-priming durations on germination and seedling growth of bitter gourd (*Momordica charantia*). *PLoS ONE* **2021**, *16*, e0255258. [CrossRef] [PubMed]
39. Dezfuli, P.M.; Sharif-Zadeh, F.; Janmohammadi, M. Influence of priming techniques on seed germination behavior of maize inbred lines (*Zea mays* L.). *A.R.P.N. J. Agric. Biol. Sci.* **2008**, *3*, 22–25.
40. Damalas, C.A.; Koutroubas, S.D.; Fotiadis, S. Hydro-priming effects on seed germination and field performance of faba bean in spring sowing. *Agriculture* **2019**, *9*, 201. [CrossRef]
41. Colombo, F.; Pagano, A.; Sangiorgio, S.; Macovei, A.; Balestrazzi, A.; Araniti, F.; Pilu, R. Study of seed ageing in *lpa1-1* maize mutant and two possible approaches to restore seed germination. *Int. J. Mol. Sci.* **2023**, *24*, 732. [CrossRef]
42. Marta, B.; Szafrańska, K.; Posmyk, M.M. Exogenous melatonin improves antioxidant defense in cucumber seeds (*Cucumis sativus* L.) germinated under chilling stress. *Front. Plant Sci.* **2016**, *7*, 575. [CrossRef]

43. Lechowska, K.; Kubala, S.; Wojtyla, Ł.; Nowaczyk, G.; Quinet, M.; Lutts, S.; Garnczarska, M. New insight on water status in germinating Brassica napus seeds in relation to priming-improved germination. *Int. J. Mol. Sci.* **2019**, *20*, 540. [CrossRef]
44. Mirmazloum, I.; Kiss, A.; Erdélyi, É.; Ladányi, M.; Németh, É.Z.; Radácsi, P. The effect of osmopriming on seed germination and early seedling characteristics of *Carum carvi* L. *Agriculture* **2020**, *10*, 94. [CrossRef]
45. Wojtyla, Ł.; Garnczarska, M.; Zalewski, T.; Bednarski, W.; Ratajczak, L.; Jurga, S. A comparative study of water distribution, free radical production and activation of antioxidative metabolism in germinating pea seeds. *J. Plant Physiol.* **2006**, *163*, 1207–1220. [CrossRef]
46. Lee, Y.P.; Baek, K.-H.; Lee, H.-S.; Kwak, S.-S.; Bang, J.-W.; Kwon, S.-Y. Tobacco seeds simultaneously over-expressing Cu/Zn-superoxide dismutase and ascorbate peroxidase display enhanced seed longevity and germination rates under stress conditions. *J. Exp. Bot.* **2010**, *61*, 2499–2506. [CrossRef]
47. Balestrazzi, A.; Confalonieri, M.; Macovei, A.; Carbonera, D. Seed imbibition in *Medicago truncatula* Gaertn.: Expression profiles of DNA repair genes in relation to PEG-mediated stress. *J. Plant Physiol.* **2011**, *168*, 706–713.
48. Macovei, A.; Garg, B.; Raikwar, S.; Balestrazzi, A.; Carbonera, D.; Buttafava, A.; Bremont, J.F.J.; Gill, S.S.; Tuteja, N. Synergistic exposure of rice seeds to different doses of gamma-ray and salinity stress resulted in increased antioxidant enzyme activities and gene-specific modulation of TC-NER pathway. *Biomed. Res. Int.* **2014**, *2014*, 676934. [CrossRef]
49. Pagano, A.; Folini, G.; Pagano, P.; Sincinelli, F.; Rossetto, A.; Macovei, A.; Balestrazzi, A. ROS accumulation as a hallmark of dehydration stress in primed and overprimed *Medicago truncatula* seeds. *Agronomy* **2022**, *12*, 268. [CrossRef]
50. Gianella, M.; Doria, E.; Dondi, D.; Milanese, C.; Gallotti, L.; Börner, A.; Zannino, L.; Macovei, A.; Pagano, A.; Guzzon, F.; et al. Physiological and molecular aspects of seed longevity: Exploring intra-species variation in eight *Pisum sativum* L. accessions. *Physiol. Plant.* **2022**, *174*, e13698. [CrossRef]
51. Ranal, M.A.; Garcia de Santana, D. How and why to measure the germination process? *Braz. J. Bot.* **2006**, *29*, 1–11.
52. Bridi, R.; González, A.; Bordeu, E.; López-Alarcón, C.; Aspée, A.; Diethelm, B.; Versari, A. Monitoring peroxides generation during model wine fermentation by FOX-1 assay. *Food Chem.* **2015**, *175*, 25–28. [CrossRef] [PubMed]
53. Wan, Q.; Chen, S.; Shan, Z.; Yang, Z.; Chen, L.; Zhang, C.; Yuan, S.; Hao, Q.; Zhang, X.; Qiu, D.; et al. Stability evaluation of reference genes for gene expression analysis by RT-qPCR in soybean under different conditions. *PLoS ONE* **2017**, *12*, e0189405. [CrossRef]
54. Thomsen, R.; Sølvsten, C.A.; Linnet, T.E.; Blechingberg, J.; Nielsen, A.L. Analysis of qPCR data by converting exponentially related C_t values into linearly related X_0 values. *J. Bioinform. Comput. Biol.* **2010**, *8*, 885–900. [CrossRef]
55. Severin, A.J.; Woody, J.L.; Bolon, Y.T.; Joseph, B.; Diers, B.W.; Farmer, A.D.; Muehlbauer, G.J.; Nelson, R.T.; Grant, D.; Specht, J.E.; et al. RNA-Seq Atlas of *Glycine max*: A guide to the soybean transcriptome. *BMC Plant Biol.* **2010**, *10*, 1–16. [CrossRef]
56. Bassel, G.W.; Fung, P.; Chow, T.F.; Foong, J.A.; Provart, N.J.; Cutler, S.R. Elucidating the germination transcriptional program using small molecules. *Plant Physiol.* **2008**, *147*, 143–155. [CrossRef]
57. Assaad, H.I.; Hou, Y.; Zhou, L.; Carroll, R.J.; Wu, G. Rapid publication-ready MS-Word tables for two-way ANOVA. *Springerplus* **2015**, *4*, 33. [CrossRef] [PubMed]
58. Pang, Z.; Chong, J.; Zhou, G.; de Lima Morais, D.A.; Chang, L.; Barrette, M.; Gauthier, C.; Jacques, P.É.; Li, S.; Xia, J. MetaboAnalyst 5.0: Narrowing the gap between raw spectra and functional insights. *Nucleic Acids Res.* **2021**, *49*, W388–W396. [CrossRef]
59. Karges, K.; Bellingrath-Kimura, S.D.; Watson, C.A.; Stoddard, F.L.; Halwani, M.; Reckling, M. Agro-economic prospects for expanding soybean production beyond its current northerly limit in Europe. *Eur. J. Agron.* **2022**, *133*, 126415. [CrossRef]
60. Schmutz, J.; Cannon, S.B.; Schlueter, J.; Ma, J.; Mitros, T.; Nelson, W.; Hyten, D.L.; Song, Q.; Thelen, J.J.; Cheng, J.; et al. Genome sequence of the palaeopolyploid soybean. *Nature* **2010**, *463*, 178–183. [CrossRef]
61. Eruslanov, E.; Kusmartsev, S. Identification of ROS using oxidized DCFDA and flow-cytometry. *Methods Mol. Biol.* **2010**, *594*, 57–72.
62. Wolff, S.P. Ferrous ion oxidation in presence of ferric ion indicator xylenol orange for measurement of hydroperoxides. *Methods Enzymol.* **1994**, *233*, 182–189.
63. Ijaz, B.; Formentin, E.; Ronci, B.; Locato, V.; Barizza, E.; Hyder, M.Z.; Lo Schiavo, F.; Yasmin, T. Salt tolerance in indica rice cell cultures depends on a fine tuning of ROS signalling and homeostasis. *PLoS ONE* **2019**, *14*, e0213986. [CrossRef]
64. Petrović, T.; Milivojević, M.; Branković-Radojčić, D.V.; Jovanović, S.; Vujinović, J.; Vukadinović, R.; Stojadinović-Životić, J. Identification of early decline of seed quality by vigor tests. In Proceedings of the 25th EUCARPIA Maize and Sorghum Conference —Current Challenges and New Methods for Maize and Sorghum Breeding, Belgrade-Book of Abstracts, Belgrade, Serbia, 30 May–2 June 2022; p. 61.
65. Kim, D.H. Extending Populus seed longevity by controlling seed moisture content and temperature. *PLoS ONE* **2018**, *13*, e0203080. [CrossRef]
66. Baalbaki, R.Z.; McDonald, M.B.; Copeland, L.O.; Elias, S.G. *Seed Testing: Principles and Practices*; Michigan State University Press: East Lansing, MI, USA, 2012. Available online: https://www.jstor.org/stable/10.14321/j.ctt7zt51m (accessed on 12 December 2022).
67. França-Neto, J.D.B.; Krzyzanowski, F.C. Tetrazolium: An important test for physiological seed quality evaluation. *J. Seed Sci.* **2019**, *41*, 359–366. [CrossRef]
68. Soares, V.N.; Elias, S.G.; Gadotti, G.I.; Garay, A.E.; Villela, F.A. Can the tetrazolium test be used as an alternative to the germination test in determining seed viability of grass species? *Crop Sci.* **2016**, *56*, 707–715. [CrossRef]

69. Dutra, A.S.; Vieira, R.D. Accelerated ageing test to evaluate seed vigor in pumpkin and zucchini seeds. *Seed Sci. Technol.* **2006**, *34*, 209–214. [CrossRef]
70. Demir, I.; Ozden, Y.S.; Yilmaz, K. Accelerated ageing test of aubergine, cucumber and melon seeds in relation to time and temperature variables. *Seed Sci. Technol.* **2004**, *32*, 851–855. [CrossRef]
71. Patel, K.K.; Kar, A.; Jha, S.N.; Khan, M.A. Machine vision system: A tool for quality inspection of food and agricultural products. *J. Food Sci. Technol.* **2012**, *49*, 123–141. [CrossRef]
72. Lin, P.; Xiaoli, L.; Li, D.; Jiang, S.; Zou, Z.; Lu, Q.; Chen, Y. Rapidly and exactly determining postharvest dry soybean seed quality based on machine vision technology. *Sci. Rep.* **2019**, *9*, 1–11. [CrossRef]
73. Galletti, P.A.; Carvalho, M.E.; Hirai, W.Y.; Brancaglioni, V.A.; Arthur, V.; Barboza da Silva, C. Integrating optical imaging tools for rapid and non-invasive characterization of seed quality: Tomato (*Solanum lycopersicum* L.) and carrot (*Daucus carota* L.) as study cases. *Front. Plant Sci.* **2020**, *11*, 577851. [CrossRef]
74. Men, S.; Yan, L.; Liu, J.; Qian, H.; Luo, Q. A classification method for seed viability assessment with infrared thermography. *Sensors* **2017**, *17*, 845. [CrossRef]
75. ElMasry, G.; ElGamal, R.; Mandour, N.; Gou, P.; Al-Rejaie, S.; Belin, E.; Rousseau, D. Emerging thermal imaging techniques for seed quality evaluation: Principles and applications. *Food Res. Int.* **2020**, *131*, 109025. [CrossRef]
76. Gagliardi, B.; Marcos-Filho, J. Relationship between germination and bell pepper seed structure assessed by the X-ray test. *Scientia Agricola* **2011**, *68*, 411–416. [CrossRef]
77. Gianella, M.; Balestrazzi, A.; Pagano, A.; Müller, J.V.; Kyratzis, A.C.; Kikodze, D.; Canella, M.; Mondoni, A.; Rossi, G.; Guzzon, F. Heteromorphic seeds of wheat wild relatives show germination niche differentiation. *Plant Biol.* **2020**, *22*, 191–202. [CrossRef]
78. Musaev, F.; Priyatkin, N.; Potrakhov, N.; Beletskiy, S.; Chesnokov, Y. Assessment of Brassicaceae seeds quality by X-ray analysis. *Horticulturae* **2021**, *8*, 29. [CrossRef]
79. Font, R.; del Río-Celestino, M.; de Haro-Bailón, A. The use of near-infrared spectroscopy (NIRS) in the study of seed quality components in plant breeding programs. *Ind. Crop Prod.* **2006**, *24*, 307–313. [CrossRef]
80. Al-Amery, M.; Geneve, R.L.; Sanches, M.F.; Armstrong, P.R.; Maghirang, E.B.; Lee, C.; Hildebrand, D.F. Near-infrared spectroscopy used to predict soybean seed germination and vigour. *Seed Sci. Res.* **2018**, *28*, 245–252. [CrossRef]
81. Hacisalihoglu, G.; Freeman, J.; Armstrong, P.R.; Seabourn, B.W.; Porter, L.D.; Settles, A.M.; Gustin, J.L. Protein, weight, and oil prediction by single-seed near-infrared spectroscopy for selection of seed quality and yield traits in pea (*Pisum sativum*). *J. Sci. Food Agric.* **2020**, *100*, 3488–3497. [CrossRef]
82. Edwards, H.G.; Villar, S.E.J.; De Oliveira, L.F.C.; Le Hyaric, M. Analytical Raman spectroscopic study of cacao seeds and their chemical extracts. *Anal. Chim. Acta* **2005**, *538*, 175–180. [CrossRef]
83. Ambrose, A.; Lohumi, S.; Lee, W.H.; Cho, B.K. Comparative nondestructive measurement of corn seed viability using Fourier transform near-infrared (FT-NIR) and Raman spectroscopy. *Sens. Actuators B.* **2016**, *224*, 500–506. [CrossRef]
84. Feng, L.; Zhu, S.; Liu, F.; He, Y.; Bao, Y.; Zhang, C. Hyperspectral imaging for seed quality and safety inspection: A review. *Plant Methods* **2019**, *15*, 1–25. [CrossRef]
85. Lepage, É.; Zampini, É.; Brisson, N. Plastid genome instability leads to reactive oxygen species production and plastid-to-nucleus retrograde signaling in Arabidopsis. *Plant Physiol.* **2013**, *163*, 867–881. [CrossRef]
86. Wang, W.-H.; He, E.-M.; Guo, Y.; Tong, Q.-X.; Zheng, H.-L. Chloroplast calcium and ROS signaling networks potentially facilitate the primed state for stomatal closure under multiple stresses. *Environ. Exp. Bot.* **2016**, *122*, 85–93. [CrossRef]
87. Ortega-Villasante, C.; Burén, S.; Barón-Sola, Á.; Martínez, F.; Hernández, L.E. In vivo ROS and redox potential fluorescent detection in plants: Present approaches and future perspectives. *Methods* **2016**, *109*, 92–104. [CrossRef]
88. Bellincampi, D.; Dipierro, N.; Salvi, G.; Cervone, F.; De Lorenzo, G. Extracellular H_2O_2 induced by oligogalacturonides is not involved in the inhibition of the auxin-regulated rolB gene expression in tobacco leaf explants. *Plant Physiol.* **2000**, *122*, 1379–1385. [CrossRef]
89. Balestrazzi, A.; Agoni, V.; Tava, A.; Avato, P.; Biazzi, E.; Raimondi, E.; Macovei, A.; Carbonera, D. Cell death induction and nitric oxide biosynthesis in white poplar (*Populus alba*) suspension cultures exposed to alfalfa saponins. *Physiol. Plant* **2011**, *141*, 227–238. [CrossRef]
90. Zielonka, J.; Zielonka, M.; Sikora, A.; Adamus, J.; Joseph, J.; Hardy, M.; Ouari, O.; Dranka, B.P.; Kalyanaraman, B. Global profiling of reactive oxygen and nitrogen species in biological systems: High-throughput real-time analyses. *J. Biol. Chem.* **2012**, *287*, 2984–2995. [CrossRef]
91. Forman, H.J.; Augusto, O.; Brigelius-Flohe, R.; Dennery, P.A.; Kalyanaraman, B.; Ischiropoulos, H.; Mann, G.E.; Radi, R.; Roberts, L.J.; Vina, J.; et al. Even free radicals should follow some rules: A guide to free radical research terminology and methodology. *Free Radic. Biol. Med.* **2015**, *78*, 233–235. [CrossRef]
92. Kalyanaraman, B.; Darley-Usmar, V.; Davies, K.J.; Dennery, P.A.; Forman, H.J.; Grisham, M.B.; Mann, G.E.; Moore, K.; Roberts, L.J.; Ischiropoulos, H. Measuring reactive oxygen and nitrogen species with fluorescent probes: Challenges and limitations. *Free Radic. Biol. Med.* **2012**, *52*, 1–6. [CrossRef]
93. Kowaltowski, A.J. Strategies to detect mitochondrial oxidants. *Redox Biol.* **2019**, *21*, 101065. [CrossRef]
94. Aryal, S.; Baniya, M.K.; Danekhu, K.; Kunwar, P.; Gurung, R.; Koirala, N. Total phenolic content, flavonoid content and antioxidant potential of wild vegetables from western Nepal. *Plants* **2019**, *8*, 96. [CrossRef]
95. Moon, J.K.; Shibamoto, T. Antioxidant assays for plant and food components. *J. Agric. Food Chem.* **2009**, *57*, 1655–1666. [CrossRef]

96. Christodoulou, M.C.; Orellana Palacios, J.C.; Hesami, G.; Jafarzadeh, S.; Lorenzo, J.M.; Domínguez, R.; Moreno, A.; Hadidi, M. Spectrophotometric methods for measurement of antioxidant activity in food and pharmaceuticals. *Antioxidants* **2022**, *11*, 2213. [CrossRef]
97. Zhou, M.; Hassan, M.J.; Peng, Y.; Liu, L.; Liu, W.; Zhang, Y.; Li, Z. γ-Aminobutyric Acid (GABA) priming improves seed germination and seedling stress tolerance associated with enhanced antioxidant metabolism, DREB expression, and dehydrin accumulation in white clover under water stress. *Front. Plant Sci.* **2021**, *12*, 776939. [CrossRef]
98. Pagano, A.; Zannino, L.; Pagano, P.; Doria, E.; Dondi, D.; Macovei, A.; Biggiogera, M.; Araújo, S.S.; Balestrazzi, A. Changes in genotoxic stress response, ribogenesis and PAP (3′-phosphoadenosine 5′-phosphate) levels are associated with loss of desiccation tolerance in overprimed *Medicago truncatula* seeds. *Plant Cell Environ.* **2022**, *45*, 1457–1473. [CrossRef]

www.nature.com/scientificreports

scientific reports

Check for updates

OPEN

Non-invasive methods to assess seed quality based on ultra-weak photon emission and delayed luminescence

Adriano Griffo[1,2], Stefanie Sehmisch[2], Frédéric Laager[3], Andrea Pagano[1], Alma Balestrazzi[1], Anca Macovei[1]✉ & Andreas Börner[2]✉

Seed quality is the set of physical, genetic, and physiological characteristics, reflecting the overall germination potential. Maintaining an optimal seed quality is essential for agriculture and seed banks to preserve genetic diversity. Compared to conventional methods (e.g., germination tests), non-invasive approaches allow a more sustainable and rapid evaluation of seed quality but this is limited by high costs. The measurement of ultra-weak photon emission (UPE) and delayed fluorescence (DL), defined as biological phenomena potentially related to the physiological status of living systems, may represent a suitable approach to estimate seed quality. To test this hypothesis, seeds of five agriculturally relevant legume species (*Phaseolus vulgaris* L., *Lathyrus sativus* L., *Cicer arietinum* L., *Pisum sativum* L., and *Vicia faba* L.), stored at different conditions (room temperature or -18 °C) for several years, were analysed using a LIANA© prototype to collect data regarding DL and UPE occurring after UV excitation. The obtained data were integrated with germination parameters which underline species-specific behaviours in response to storage conditions. The prediction models show variable efficiency in classifying seeds based on germination which underline species-dependent links between photon emission and seed quality. Therefore, these measurements represent novel, non-invasive, and rapid approaches to evaluate seed quality.

Keywords Delayed luminescence, Leguminosae, Machine learning, Non-invasive assessment, Seed quality, Ultra-weak photon emission

Seed quality is the set of genetic, physiological, and physical features of seeds (https://www.seedtest.org/). Since seed quality reflects the overall germination potential and influences crop production, its evaluation is crucial for seed companies and consumers to both optimize economic profits and increase the final crop yield[1]. Crop production must be increased to meet the ZERO HUNGER target relative to the Sustainable Developmental Goal SDG#2 of the 2030 UN Agenda for Sustainable Development (https://www.un.org/sustainabledevelopment/). In a scenario where crop production must be sustainably enhanced, novel methods to assess seed quality can substantially increase the availability of high-quality seeds, with a positive effect on agriculture costs and food production.

Monitoring seed quality is very important for many stakeholders, including germplasm banks, breeders, agronomists, seed companies and consumers[1]. The use of high-quality seeds is a proxy of the seed market, which translates into a continuous increase in the commercial seed market trends (Seeds Global Market Report 2024)[2]. Several methods are available for seed quality testing. Conventional germination, electrical conductivity, seedling growth, triphenyltetrazolium chloride (TTC) test, and accelerated ageing are approved by the International Seed Testing Association (ISTA) and constitute the most used approaches so far[3–5]. However, these methods have some considerable limitations, including invasiveness, extensive amount of test work required, long test periods, low accuracy and operators biases[1]. To efficiently measure seed quality and avoid the waste of resources, novel methods to assess it and subsequent quality attributes are necessary and highly sought. To this purpose, non-invasive optical techniques, including machine vision[6,7], NIR (Near InfraRed), Raman spectroscopies[8,9],

[1]Department of Biology and Biotechnology 'L. Spallanzani', University of Pavia, Via Ferrata 9, Pavia PV 27100, Italy. [2]Leibniz Institute of Plant Genetics and Crop Plant Research, Corrensstr. 3, Gatersleben, 06466 Seeland, Saxony-Anhalt, Germany. [3]SUPER Lab, 26160 Bad Zwischenahn, Germany. ✉email: anca.macovei@unipv.it; boerner@ipk-gatersleben.de

thermal, X-ray, and hyperspectral imaging[10–12], have been developed and applied to test seed quality. Despite their advantages in gaining high-throughput information in a rapid, non-invasive, and accurate manner, the high cost and the complexity of these technologies limit their large-scale use[13]. So far, no universal approach has been developed to assess seed quality in a rapid, accurate, economic, and non-destructive manner. Therefore, the search for such methods is still highly required and requested.

Ultra-weak photon emission (UPE) is defined as the luminescence generated from the production of electronically excited species produced from the oxidative processes[14]. Since oxidative reactions are solely responsible for the spontaneous generation of photons, this phenomenon potentially occurs in living cells of all organisms, from bacteria to animals[15]. Although the origin and the nature of the electronically excited species are partially unknown and very complex, Cilento and Adam[16] described the concept of electronic excitation and the electronic configuration of molecules on the ground state T_0, the singlet state S_1, and the triplet state T_1, which stand at the basis of this process. The transition of electrons that occurs in common oxidation and reduction reactions results in the transition of the molecule into different energy states (T_0, S_1, T_1) due to the different energy of the electrons exchanged. Photon release marks the transition of a molecule from an excited state (S_1 or T_1) to the starting state T_0[15,16]. Most of the pathways that generate electronically excited species involve radical species as well as oxygen molecules for the electronic transition[16], confirming the importance of ROS (reactive oxygen species) in this process. UPE can be spontaneous, where the release of photons during the oxidative processes happens without any external stressors or stimuli, or it can be induced by stress and oxidative factors that promote oxidative reactions[15,17]. Another phenomenon related to UPE is Delayed Luminescence (DL), defined as the long-term afterglow of biological systems after illumination[18]. The DL general trend is characterized by an initial peak of intensity (in terms of the number of photons released per time) followed by a rapid decay. DL can occur for seconds or milliseconds, depending on the time of the inductor and the used system[19].

In recent years, the possible link between UPE, DL, and the physiological state of biological systems has gained more interest from the scientific community. Because UPE and DL are generated from oxidative processes occurring during metabolic reactions, it is connected with ROS production[20–23], molecules involved in many biological processes[24], including seed quality and germination[25]. UPE and DL have been successfully applied to evaluate food quality[26]. Similarly, these phenomena have been linked to germination, pointing to a connection between the physiological state and photon release[27,28]. In the context of seed evaluation, DL has been applied to detect additional features like water content[29] and viability[30]. Although, these initial reports provide insights into the UPE and DL application in seed biology, the complex features of the phenomena and their implications, require further investigation. Therefore, the aim of this study was to assess the use of UPE and DL as tools to predict seed quality taking into consideration multiple legume species and accessions. Germination performance was evaluated in five legume species (*Phaseolus vulgaris* L., *Lathyrus sativus* L., *Cicer arietinum* L., *Pisum sativum* L., and *Vicia faba* L.), using seeds stored at different conditions (room temperature or -18 °C) for more than ten years. The study has focused on legumes as these are economically important crops characterized by high nutrient content and have important agronomic applications given their symbiosis with nitrogen-fixing bacteria. The species with the highest number of accessions available at the IPK genebank collection were selected to take into account intraspecific variability. UPE and DL occurring after UV excitation were collected using a LIANA© prototype and the generated data were integrated with the germination parameters using machine learning algorithms to generate prediction models to estimate seed quality in a non-invasive manner.

Results

Development of an experimental system for UPE and DL data collection

The experimental system proposed in this study is based on using seeds stored at different conditions: a seed bank optimal storage conditions at -18°C (hereby defined as Cold) and an ambient room temperature (22–24 °C) storage (hereby defined as Ambient). The investigated legume species (*P. vulgaris*, *L. sativus*, *C. arietinum*, *P. sativum*, *V. faba*) and multiple accessions were stored for more than ten years under Ambient and Cold conditions prior to use. Information describing the species and accessions, including time of harvest, years of storage, and origin, are provided in Supplementary Tables S1-S5. Figure 1 depicts the experimental model along with the analyses carried out to obtain the final dataset for the predictive models developed through machine learning approach. Seed samples were used to detect UPE and DL and subsequently germinated to assess a set of indices indicative of seed quality. To develop the predictive models, seed samples were classified into two groups (optimal, non-optimal) based on the germination percentage, where optimal germination ranges between 80 and 100% while below 80% is considered as non-optimal.

Germination performance under different storage conditions

Germination tests were performed to estimate the effect of storage conditions on germination performances on each of the investigates species and selected accession. Given the high amount of data, the values (mean ± st. dev.) of germination percentage (G%), mean germination time (MGT), synchronicity index (Z), root and shoot length are provided for each species/accession in the Supplementary dataset. For the overall representation of these data, a principal component analysis (PCA) was performed (Fig. 2). The data depicts two scenarios; first, represented by *C. arietinum* (CIC) and *V. faba* (FAB), where there is a distinct clustering between the Ambient and Cold groups, and second, represented by *P. vulgaris* (PHA), *L. sativus* (LAT), and *P. sativum* (PIS) where the two clusters are overlapping. For CIC and FAB, the majority of accessions stored under cold conditions present an optimal G% (80–100%) while storage at room temperature resulted in reduced G% below 80% (e.g., 53–7% in CIC648 and CIC702; 76–0% in FAB129 and FAB6975, see Supplementary dataset). For the second scenario, multiple seed samples stored under Ambient conditions show optimal values of G%, therefore the distinction

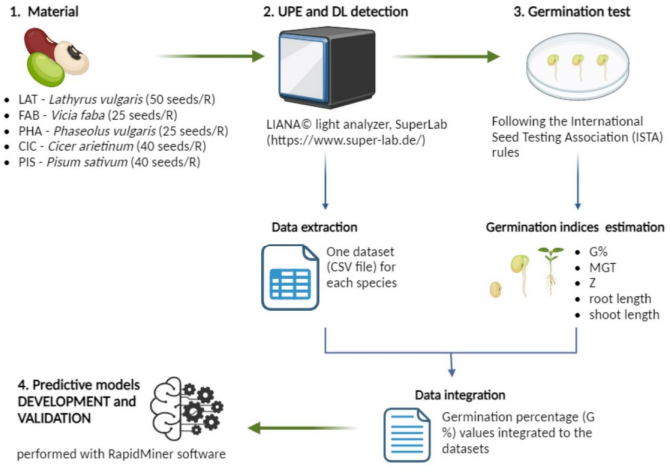

Fig. 1. Schematic representation of the experimental system. Multiple accessions of seeds of five legume species stored at room temperature (Ambient) or -18 °C (Cold) for more than ten years were ordered in different biological replicates (R) based on their size. The replicates were analyzed with the LIANA© light analyzer and subsequently used for germination test, following the ISTA rules for each species. At the end of the germination test, several indices (G%, Z, MGT, root and shoot length) were calculated and the germination percentage data was integrated into the extracted CSV file containing the UPE and DL data for the same replicates. The complete datasets were independently used for the development of machine learning models for germination prediction using RapidMiner® software.

between Ambient and Cold is less pronounced. Among the PIS accession, 38 samples present germination above 80% while 6 samples are classified in the group below 80%. For the PHA accessions, 33 have optimal germination while the remaining 11 present non-optimal germination. Lastly, LAT is divided into 13 accessions with optimal germination and 11 accessions with non-optimal performance (Supplementary dataset). The remaining germination indices follow a similar pattern as G% in the different species, accessions, and storage conditions, thus supporting the divergent PCA clustering.

To evaluate the degree of correlation between the different germination indices, the Pearson coefficient *r* was calculated and graphically represented in Fig. 3. Similar trends of correlations are observed among all the investigated species. MGT is negatively correlated with all the other parameters which are positively correlated to each other. This suggests that seeds with optimal germination percentage are also characterized by high speed and synchrony, in addition to enhanced seedling growth.

This first step of the study allowed to characterize a system with different germinative performances that can be used to test novel methods dedicated to predict seed viability in a non-invasive manner.

Analysis of photon counts in correlation with germination percentage

The LIANA© prototype, used in this study for UPE and DL detection, collects 1334 parameters reflecting the entire photon release phenomena. The prototype includes seven sensors (photomultiplier tubes, PMTs) that allow the detection of photons at different wavelengths (see Methods paragraph UPE and DL detection). An example of a time course of phonon emission curve is shown in Fig. 4a. The "RAW_DATA" parameter corresponds to the total of photon counted for each sensor while "R_A_O_P" corresponds to the corrected value of photons, obtained by subtracting the photon courted during dark count and by multiplying to correction factors. The values of "RAW_DATA" and "R_A_O_P" are provided in the Supplementary dataset for each sensor per species. To investigate if the values of photon counts (in terms of "RAW_DATA" and "R_A_O_P" for each sensor) can be related to G%, a correlation analysis was performed (Fig. 4b). Significant negative correlations can be observed for the following parameters: RAW_DATA sensors 3, 4, 5, 7, and R_A_O_P sensors 1, 2, 5, 7. Among these, data from "R_A_O_P sensor 1", showing the most relevant correlation value (dark blue in Fig. 4b), was used to plot photon counts for each accession in relation to germination (Fig. S1). To generate these plots taking account of the Amb and Cold groups, fold-change (FC, Amb/Cold) values were used for both parameters. Among species and accessions, the ratio of photon counts is heterogeneous; however, a higher number of accessions show FC

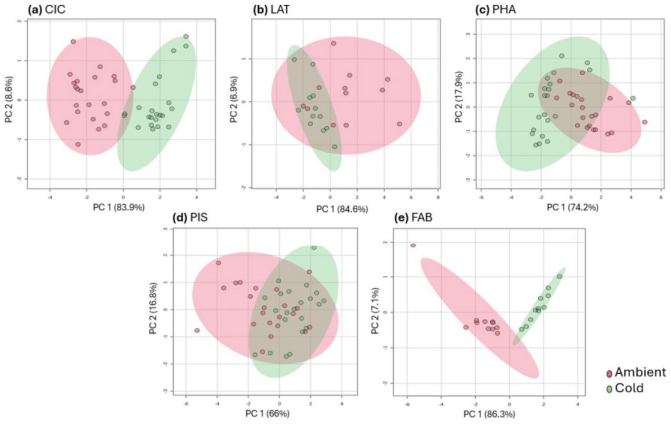

Fig. 2. PCA score plots generated using the germination data, and LIANA© parameters gathered from seeds stored at Ambient (red) and Cold (greed) storage conditions. (**a**) *Cicer arietinum* (CIC). (**b**) *Lathyrus sativus* (LAT). (**c**) *Phaseolus vulgaris* (PHA). (**d**) *Pisum sativum* (PIS). (**e**) *Vicia faba* (FAB).

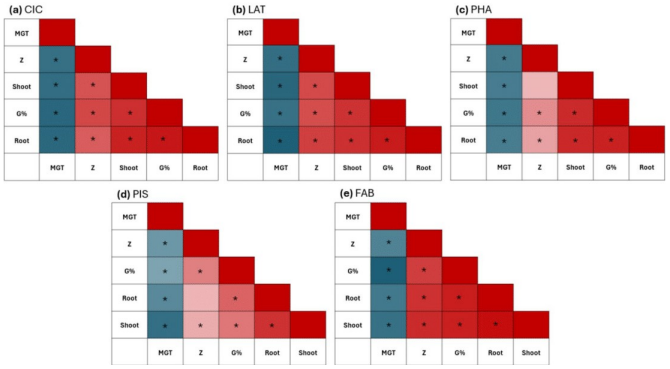

Fig. 3. Pearson correlation analysis based on using (G%), mean germination time (MGT), synchronicity index (Z), root and shoot length. (**a**) *Cicer arietinum* (CIC). (**b**) *Lathyrus sativus* (LAT). (**c**) *Phaseolus vulgaris* (PHA). (**d**) *Pisum sativum* (PIS). (**e**) *Vicia faba* (FAB). Statistically significant correlations are indicates with an asterisk ($^{*}p \leq 0.05$).

values below 1, reflecting a lower emission of photons from Amb groups. Despite this trend, the FC values regarding G% do not indicate a precise trend between these parameters. Overall, this indicates that considering only the photon counts does not explain the complete UPE and DL phenomena and their possible link with germination performance. Given the high number of parameters provided by the prototype, it is therefore highly required to use more complex data analysis systems, such as machine learning.

(a)

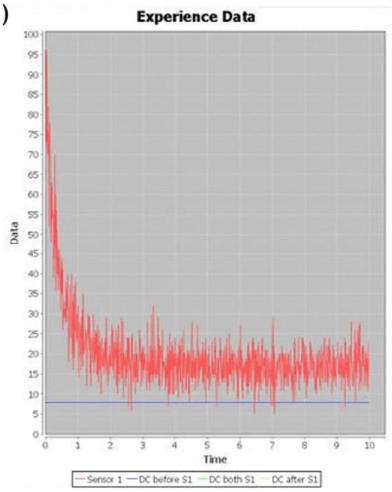

(b)

	germ %
germ %	1
R_A_O_P_SENSOR_5	-0.12186 ***
RAW_DATA_SENSOR_7	-0.11971 ***
R_A_O_P_SENSOR_1	-0.28721 ***
RAW_DATA_SENSOR_5	-0.14945 ***
R_A_O_P_SENSOR_2	-0.15264 ***
R_A_O_P_SENSOR_7	-0.17347 ***
RAW_DATA_SENSOR_2	-0.01108
RAW_DATA_SENSOR_6	-0.01449
RAW_DATA_SENSOR_1	-0.02666
RAW_DATA_SENSOR_3	-0.11066 ***
RAW_DATA_SENSOR_4	-0.0414 **
R_A_O_P_SENSOR_4	0.0143

Fig. 4. Photon count determination. (**a**) Example of a time course of phonon emission curve as provided by the integrated software of LIANA© prototype. (**b**) Pearson correlation table of LIANA© parameters indicating the photon counted (raw and corrected) through each sensor (1–7) with the percentage of germination (G%), using the data of all the tested species. Statistically significant correlations are indicated by asterisks (*$p < 0.05$; **$p < 0.01$; ***$p < 0.001$). R_A_O_P, real amount of photons, obtained by subtracting the photons counted before and after the measurement time and by multiplying by correction factors, which consider the position of the PMTs, the filter used, and the overlapping of wavelengths with other PMTs; RAW_DATA, initial photon counts not corrected.

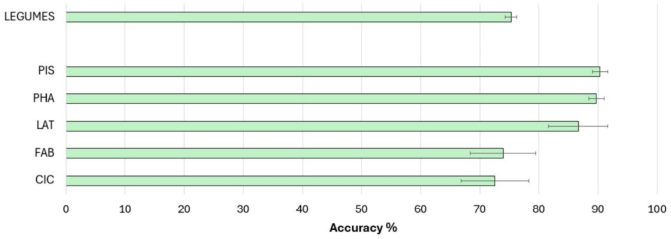

Fig. 5. Percentage (%) of accuracy for the prediction models developed using the RapidMiner software based on germination data. Validation was performed using the "cross-validation" operator (number of folds = 10). CIC, *C. arietinum*; LAT, *L. sativus*; PHA, *P. vulgaris*; FAB, *V. faba*; PIS, *P. sativum*.

Application of predictive models for seed classification

Using the UPE/DL data provided by the prototype and the germination performance classification, a predictive model was formulated. To train the models, the samples (records) were classified into two quality classes ranging from optimal (80–100%) and non-optimal (< 80%) germination. The 80% threshold was selected based on previous studies on genebank accessions dedicated to understand how long seeds can retain their viability over extended periods of uncontrolled temperature or non-optimal conditions[31]. Figure 5 shows the accuracies of

	AUC	Sensitivity (%)	Specificity (%)	Positive predictive value (PPV) (%)	Negative predictive value (NPV) (%)
CIC	0.814 ± 0.062	55.94% ±11.56%	85.94% ± 5.89%	76.34% ± 7.88%	71.10% ± 5.22%
FAB	0.826 ± 0.048	83.04% ± 5.72%	58.32% ± 9.62%	77.51% ± 4.33%	67.00% ± 9.61%
LAT	0.963 ± 0.022	92.67% ± 6.05%	78.74% ± 11.85%	85.80% ± 6.52%	89.87% ± 7.33%
PHA	0.876 ± 0.054	98.34% ± 1.17%	58.79% ± 6.02%	89.58% ± 1.30%	91.17% ± 5.80%
PIS	0.922 ± 0.035	100.00% ± 0.00%	15.83% ± 11.42%	90.18% ± 1.21%	100.00% ± 0%
LEGUMES	0.824 ± 0.028	98.57% ± 0.76%	22.87% ± 3.23%	74.22% ± 0.77%	87.93% ± 5.81%

TP true positive, *TN* true negative, *FN* false negative, *FP* false positive, *TPR* true positive rate, *FPR* false positive rate. Area under the curve (AUC) = $\int_{x=0}^{1} \mathrm{TPR}(\mathrm{FPR}^{-1}(x))dx$, Sensitivity = TP/(TP + FN). Specificity = TN/(TN + FP), Positive predictive value (PPV) = TP/(TP + FP). Negative predictive value (NPV) = TN/(FN + TN).

Table 1. Predictive performance of learning models obtained after cross-validation.

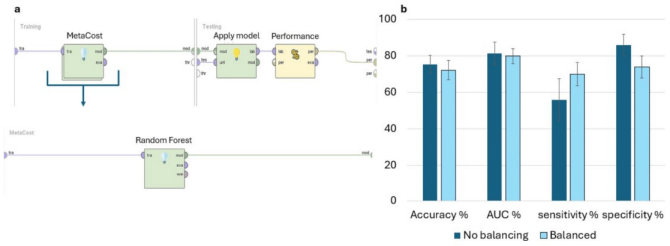

Fig. 6. MetaCost operator utilization on CIC learning model. (**a**) Structure of the cross-validation operator, including the MetaCost operator into the Training subprocess and the Random Forest classifier, included into the MetaCost operator. (**b**) Histograms showing the classification parameter percentages (Accuracy, AUC, sensitivity, and specificity) calculated on the CIC predictive model with (Balanced, light blue) and without (No Balancing, dark blue) MetaCost operator.

the prediction models. The models developed for the single species datasets (CIC, LAT, PHA, PIS, FAB) indicate different accuracy values. Models developed using *V. faba* and *C. arietinum* datasets presented a moderate accuracy (73.96% and 72.5%, respectively), while the accuracy of the other species reached higher values (above 85%). Subsequently, to uniformize these data, the dataset "Legumes" was obtained by unifying the collections of data from the single species with the operator "append" of RapidMiner software. This operator merges two or more datasets with the same attributes building a new combined set. The accuracy of the prediction model developed with the "Legumes" dataset is around 75.29% (Fig. 5), indicating a good prediction efficiency. Table 1 presents other classification metrics that describe the overall efficiency of predictive models. While positive predictive value (PPT) and negative predictive values (NPT) follow the trend exhibited by the accuracy parameter, sensitivity and specificity percentages reflect a critical issue in classifying seed samples in the appropriate group in most models. In particular, the model developed from the PIS dataset registers the lowest value of specificity (approximately 15.83%). One potential solution is represented by the MetaCost operator of RapidMiner, which makes the prediction cost-sensitive by utilizing a specified cost matrix (configured by the operator)[32,33]. In the learning model depicted in Fig. 6a, the MetaCost operator was used as trial to improve the sensitivity value of the predictive model developed from the CIC dataset (55.91%, Table 1), configuring a cost matrix that assigns a cost of 5 and 4 to false negatives and false positives, respectively. The results are presented in Fig. 6b, which shows the main classification parameters of the model with (Balanced) and without (No Balancing) MetaCost operator. The histogram illustrates a notable improvement of the sensitivity, which was the objective of MetaCost operator utilization. However, this improvement is balanced by a reduction in specificity, while the accuracy and the AUC values exhibited a slight impact from the optimization process. In general, the application of machine

learning allowed a more efficient and a complete handling of the parameters provided by the LIANA© prototype to estimate seed quality.

Discussion

The need to develop novel, non-invasive, easy-to-use, and economic methods for seed quality assessment was the driving force of this work, which proposes the use of UPE and DL as novel tools to evaluate seed quality. To maximize the number of samples with a wider range of germination percentages, this method was tested in a system composed of seeds stored for more than ten years at different conditions (Ambient and Cold) and characterized from the point of view of germination behaviour and photon emission. Following classification in quality classes (optimal, non-optimal), the generated data were used to build prediction models to test the relation between photon emission and seed quality. To our knowledge, currently there is no study that evaluated the UPE and DL phenomena taking into consideration different species and different accessions of the same species. The LIANA© prototype is easy-to-use, fully automated, allowing rapid measurements for diverse purposes covering different surface measurements, while it was not specifically design for seeds. Although the prototype can be further optimized for more accurate analyses on seeds, the costs of its use relate mainly to covering electricity and licensing of the software.

When considering seed germination, several studies performed in legumes[34], as well as other species[35], has evidenced differences in G% between storage conditions. In the scenario reflected from the data obtained from pea, beans and lathyrus, the distinction between ambient and cold is less pronounced. The data collected from *P. sativum* can be given as an example from this group. In this case, is appears that seeds stored at both ambient and cold conditions are able to maintain seed germinability in several accessions. A recent study reported similar results in ten varieties of soybeans stored at cold and room temperatures[34]. Other studies showed that pea seeds stored under ambient conditions retained their viability for more than twenty years[31]. In addition, Giannella et al.[36] reported different germination performance when analysing eight accessions from which one proved to maintain prolonged seed longevity also at room temperature. This accession was characterized by low levels of ROS and increased antioxidant activity and genome stability. Different germination performances between varieties may be explained by other aspects, such as genetic variability that influences plant hormone signalling and other processes related to seed germination[37].

When considering the results of the machine learning models, these exhibit variable results which can be grouped in two scenarios. The models developed from the datasets CIC and FAB exhibit a moderate efficiency in classifying seed samples appropriately, while the processes obtained from the remaining datasets show high performances. Several factors can affect the quality of prediction and explain the differences in accuracy between the different types of models. For instance, the size of dataset is a crucial issue for machine learning: an optimal training process require an appropriate number of examples representing a wide variety of conditions[38]. The choice of the classifier substantially affects the efficiency of the model. In this study, the predictive models are based on a Random Forest classifier, an ensemble approach widely used for classification tasks that allow the optimization of accuracy and prevent from overfitting of the models[39]. However, an efficient data cleaning phase is important for optimizing the efficiency of the predictive models since the presence of outliers can interfere with the classification[40]. A cost-sensitive classification with the MetaCost operator of RapidMiner has been demonstrated to enhance sensitivity, improving the efficiency of prediction. Thus, this approach may be employed with other models to enhance the balancing of error rates between optimal and non-optimal classes. Apart from the technical aspects related to machine learning, the obtained results support the use of UPE and DL phenomena to estimate seed quality. This is in agreement with other publications indicating that DL and UPE measurements can be used to assess seed viability[9,27]. In addition, the results obtained from the single datasets may suggest the hypothesis of a species-dependent photon emission.

To conclude, seed quality evaluation is a complex aspect since different features (genetic, physiological, and physical factors) are involved in its determination[13]. UPE and DL have been previously correlated to oxidative stress[21], water content[29], and seeds vigour[27], therefore this can be envisioned an accurate method to assess seed quality. The data collected in this work suggests a complex scenario, in which intrinsic seed characteristics of different species may play an important role in the link between seed quality and photon emission. Despite its potential, UPE and DL phenomena require further in-depth characterization to understand their biological relevance in the seed context. The use of machine learning allows to bypass some of the drawbacks related to the lack information about UPE and DL, enabling more accurate prediction of a specific outcome, while contributing to a better understanding of these phenomena.

Methods

Seed materials and storage

Seeds of five legume species, namely bean (*Phaseolus vulgaris* L.), faba bean (*Vicia faba* L.), pea (*Pisum sativum* L.), grass pea (*Lathyrus sativus* L.), and chickpea (*Cicer arietinum* L.), were originated from the genebank collection of the Leibniz-Institute of Plant Genetics and Crop Plant Research (IPK, Gatersleben, Germany) where the material was regenerated under field conditions. Harvest of the seeds was made by hand. After threshing and cleaning the seeds were placed in a drying chamber at a temperature of 22 ± 2 °C and a relative humidity of 11 ± 3% for four weeks. Afterwards the material was divided and transferred either to the cold chamber of the genebank (Cold, sealed glass chars, silica gel on top of the seeds, -18 °C $\pm$ 2 °C) or to an ambient storage room (Amb, paper bags, 20 °C $\pm$ 2 °C, 50% $\pm$ 3% RH).

For each species, 200 seeds per accession were used in the present work. These were divided into distinct seed samples (biological replicates) based on seed size; for *L. sativus* accessions, four replicates of 50 seeds each; for *C. arietinum* and *P. sativum* accessions, five replicates of 40 seeds each; for *P. vulgaris* and *V. faba* accessions, eight replicates of 25 seeds each. Different number of accessions per species were used as follows: 22 accession

for *P. vulgaris*, *P. sativum*, and *C. arietinum*, 12 accession for *L. sativus*, and 11 accessions for *V. faba*. The time of storage was selected based on previous seed bank analyses carried out to identify the most suitable conditions where contrastive germination performance could be observed[31]. The accessions used here were collected at different harvest years: 2010 for *L. sativus* and *P. sativum*, 2012 for *P. vulgaris*, and 2013 for *V. faba* and *C. arietinum*.

Germination parameters

Germination tests were performed following the guidelines provided by ISTA (International Rules for Seed Testing (https://www.seedtest.org/) with some modifications. The conditions for each species/accession were as follows: for *P. vulgaris*, and *C. arietinum* seed were germinated at 25 °C for 8 days; for *P. sativum* seed were germinated at 20 °C for 8 days; for *V. faba* and *L. sativus* seed were germinated at 20 °C for 10 days. For *V. faba*, seeds were maintained at 4 °C for 7 days before starting the germination test. Seeds stored at Amb and Cold conditions were monitored in parallel. Different groups of seeds (*L. sativus*, 4 replicates of 50 seeds/replicate; *P. sativum* and *C. arietinum*, 5 replicates of 40 seeds/replicate; *V. faba* and *P. vulgaris*, 8 replicates of 25 seeds/replicate) were placed in germination trays containing filter paper moistened with distilled water. All containers were kept in a growth chamber at the indicated temperatures under 16 h dark/8 h light. At the end of germination, the following germination indices were calculated: germination percentage (G), mean germination time (MGT), and synchronicity index (Z)[41]. The formulas used for the calculation of these parameters are the following.

$$(1)\quad G\% = \left(\frac{number\ of\ germinated\ seeds)}{total\ number\ of\ seeds}\right) \times 100$$

$$(2)\quad MGT = \frac{\sum_{i=1}^{k} ni\ x\ ti}{\sum_{i=1}^{k} ni}$$

$$(3)\quad Z = \frac{\sum Cni,2}{\sum ni\ x \sum \left(ni - \frac{1}{2}\right)}$$

In MGT (2) and Z (3) formulas, *ni* is the number of seeds germinated in the time *i* (not the accumulated number, but the number correspondent to the *ith* observation), *ti* corresponds to the time from the start of the experiment to the *ith* observation (day), *k* is the last time of germination, and *Cni*,2 = *ni* (*ni*-1)/2. Germination data were analysed with Student *t*-test using the Microsoft Excel package using as threshold the *p*-value ≤ 0.05 ('*').

Seedling growth was monitored on the final day of the germination test by using ImageJ (https://imagej.nih.gov/ij/) software. For each accession and replicate, 20% of the seedlings were photographed and used to determine the seedling length in terms of roots and/or aerial parts.

Statistical analyses

Germination and physical traits data were analysed with Student *t*-test using the Microsoft Excel package using as threshold the *p*-value ≤ 0.05 ('*'). For correlation analyses, Pearson's correlation coefficient and the relative p-values were determined by using MetaboAnalyst 6.0 (https://www.metaboanalyst.ca/)[42]. The same software was also used for principal component analysis (PCA) performed by using all the germination parameters. The obtained "score plot" graphics show how the different sample groups are clustered according to the results obtained in the performed analyses.

UPE and DL detection

A light analyzer (LIANA©, SuperLab, Käthe-Kruse-Str. 11, 26160 Bad Zwischenahn, Germany, https://www.super-lab.de//liana.html) has been used to collect UPE and DL data of seed samples. This prototype is covered by the SuperLab IP copyright patent number EP 2,613,139 A1. The LIANA© prototype (Fig. 7) contains seven photomultiplier tubes along with filters to form seven sensors that detect light emission at different wavelengths. The characteristics of the photomultiplier tubes (PMTs, Hamamatsu Photonics), including model type, spectrum and filter bandpass wavelength are presented in Supplementary Table S6. For the DL excitation, 6 LED with the spectral range 380–420 nm were used. The measurements were conducted with the following parameters: time, 10 (10 s measurement time); frequency, 100 (measure every 0.1 s); size, 100; distance, 10; surface, 10; illumination time, 1 (1-second illumination); darkcount time, 5 (5 s darkcount data before and after each measurement); dark-count frequency, 100 (measure every 0.1 s). For each sample, measures were taken five times (technical replicates), from which eventual outliers have been eliminated. At least three technical replicates have been retained for each seed sample. For a more realistic photon count estimation, a darkcount measurement is automatically performed before and after each measurement, averaged and subtracted from the values of the PMTs (the photon counted during the measurement time). Then a "real amount of photons" is calculated by multiplying this new value by correction factors, based on the position of the PMTs, the filter used, and the overlapping of wavelengths with other PMTs. In addition to the corrected photon counts, a large number of features reflecting the UPE and DL phenomena are acquired and included in the datasets.

Generation of prediction models

Prediction models for the classification of seed samples were assigned and improved using the RapidMiner software[43,44]. Seeds were classifieds based on G% values into optimal (100 − 80%) and non-optimal (below 80%) quality. The prediction process is described in Fig. 8. The several operators used in the learning process are connected in a specific order and perform different operations. A stratified 10-fold cross-validation operation approach was used to validate the model. The classifier Random Forest was selected for outcome prediction to maximize accuracy. Accuracy %, area under the curve (AUC), sensitivity %, specificity %, positive predicted value (PPV) %, and negative predicted value (NPV) % values were obtained at the end of the validation.

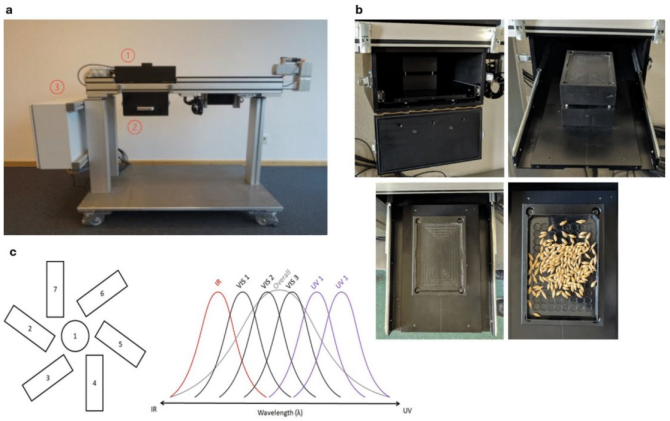

Fig. 7. Representative images showing the structure of the LIANA© device and its use for light analysis on seeds. (**a**) The main structure of the LIANA© device illustrating (1) the excitation source, which includes the PMTs (photomultiplier tubes), (2) the sample chamber, and (3) the electrical block. (**b**) The seed chamber. It can be opened by releasing the clips on either sides (top left). The front door can be drawn down to access the internal drawer with the sample holding block (top right). The drawer must be pulled out completely while inserting the seeds into the tray for the analysis (bottom). (**c**) The excitation source (UV) and the PMTs. These include seven photomultiplier tubes along with filters to form seven sensors which can detect the emission at different wavelengths.

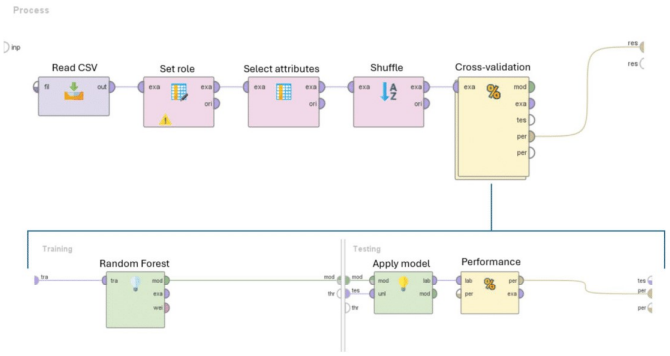

Fig. 8. Illustration of the RapidMiner prediction model. The operators displayed in the model are connected and execute distinct actions. The Read CSV operator allows the uploading of the file. To facilitate the manual integration of germination percentages into the CSV file, the records were sorted. The Set role operator was used for data labelling. Attributes highly correlated to the label were excluded from the learning model with the operator Select attributes. The operator Shuffle was employed to randomize the records within the datasets.

Data availability

The datasets used and/or analysed during the current study are available from the corresponding author on reasonable request.

Received: 17 May 2024; Accepted: 24 September 2024
Published online: 05 November 2024

References

1. Huang, M., Wang, Q. G., Zhu, Q. B., Qin, J. W. & Huang, G. Review of seed quality and safety tests using optical sensing technologies. *SST* **43** (3), 337–366 (2015).
2. www.thebusinessresearchcompany.com. (n.d.). *Seeds Market Size, Share, Growth, Trend Analysis, Forecast 2033*. https://www.thebusinessresearchcompany.com/report/seeds-global-market-report (2024).
3. McDonald, M. B. Assessment of seed Quality1. *HortScience* **15** (6), 784–788 (1980).
4. McDonald, M. B. Seed quality assessment. *Seed Sci. Res.* **8** (2), 265–276 (1998).
5. Elizalde, V. et al. Viability and germination of *Hechtia perotensis* (*Bromeliaceae*) seed. *Rev. Biol. Trop.* **65** (1), 153–165 (2017).
6. Ureña, R., Rodríguez, F. & Berenguel, M. A machine vision system for seeds quality evaluation using fuzzy logic. *Comput. Electron. Agric.* **32** (1), 1–20 (2001).
7. Lin, P. et al. Rapidly and exactly determining postharvest dry soybean seed quality based on machine vision technology. *Sci. Rep.* **9** (1), 17143 (2019).
8. Zhu, L. et al. Advances of NIR spectroscopy technology applied in seed quality detection. *Spectrosc. Spect. Anal.* **35** (2), 346–349 (2015).
9. Li, W., Tan, F., Cui, J. & Ma, B. Fast identification of soybean varieties using Raman spectroscopy. *Vib. Spectrosc.* **123**, 103447 (2022).
10. Feng, L. et al. Hyperspectral imaging for seed quality and safety inspection: a review. *Plant. Methods* **91** (1), 15 (2019).
11. ElMasry, G. et al. Emerging thermal imaging techniques for seed quality evaluation: principles and applications. *Food Res. Int.* **131**, 109025 (2020).
12. Musaev, F., Priyatkin, N., Potrakhov, N., Beletskiy, S. & Chesnokov, Y. Assessment of *Brassicaceae* seeds Quality by X-ray analysis. *Hortic* **8** (1), 29 (2022).
13. Rahman, A. & Cho, B. K. Assessment of seed quality using non-destructive measurement techniques: a review. *Seed Sci. Res.* **26** (4), 285–305 (2016).
14. Du, J. et al. The application and trend of ultra-weak photon emission in biology and medicine. *Fchem* **11**, 1140128 (2023).
15. Cifra, M. & Pospíšil, P. Ultra-weak photon emission from biological samples: definition, mechanisms, properties, detection and applications. *J. Photochem. Photobiol B* **139**, 2–10 (2014).
16. Cilento, G. & Adam, W. From free radicals to electronically excited species. *Free Radic Biol. Med.* **19** (1), 103–114 (1995).
17. Wang, C., Bókkon, I., Dai, J. & Antal, I. Spontaneous and visible light-induced ultraweak photon emission from rat eyes. *Brain Res.* **1369**, 1–9 (2011).
18. Popp, F. A. & Yan, Y. Delayed luminescence of biological systems in terms of coherent states. *Phys. Lett.* **293** (1–2), 93–97 (2002).
19. Goltsev, V., Zaharieva, I., Chernev, P. & Strasser, R. J. Delayed fluorescence in photosynthesis. *Photosynth Res.* **101**, 217–232 (2009).
20. Kobayashi, M. Highly sensitive imaging for ultra-weak photon emission from living organisms. *J. Photochem. Photobiol B* **139**, 34–38 (2014).
21. Pospíšil, P., Prasad, A. & Rác, M. Role of reactive oxygen species in ultra-weak photon emission in biological systems. *J. Photochem. Photobiol B* **139**, 11–23 (2014).
22. Sun, C., Liu, J., Liu, H. & Guo, J. Reactive oxygen species mediate the relationship between mitochondrial function and delayed luminescence during senescence of strawberry (*Fragaria ananassa*) fruits. *Acta Physiol. Plant.* **44**(2) (2022).
23. Zhang, J. et al. Roles of NOD1/*Rip2* signal pathway in carotid artery remodelling in spontaneous hypertensive rats. *Gen. Physiol. Biophys.* **41** (01), 31–42 (2022).
24. Murphy, M. P. et al. Unraveling the Biological roles of reactive oxygen species. *Cell. Metab.* **13** (4), 361–366 (2011).
25. Griffo, A., Bosco, N., Pagano, A., Balestrazzi, A. & Macovei, A. Noninvasive methods to detect reactive oxygen species as a proxy of seed quality. *Antioxidants* **12** (3), 626 (2023).
26. Stolz, P., Wohlers, J. & Mende, G. Measuring delayed luminescence by FES to evaluate special quality aspects of food samples – an overview. *Open. Agric.* **4** (1), 410–417 (2019).
27. Grasso, R. et al. Non-destructive evaluation of watermelon seeds germination by using delayed luminescence. *J. Photochem. Photobiol. B* **187**, 126–130 (2018).
28. Adeboye, K. & Börner, A. Delayed luminescence of seeds: are shining seeds viable? *SST* **48** (2), 167–177 (2020).
29. Yan, Y., Popp, F. A. & Rothe, G. M. Correlation between germination capacity and biophoton emission of barley seeds (*Hordeum vulgare* L). *SST* **31** (2), 249–258 (2003).
30. Costanzo, E. et al. Single seed viability checked by delayed luminescence. *EBJ* **37** (2), 235–238 (2007).
31. Nagel, M. & Börner, A. The longevity of crop seeds stored under ambient conditions. *Seed Sci. Res.* **20** (1), 1–12 (2010).
32. Kim, J., Choi, K., Kim, G. & Suh, Y. Classification cost: an empirical comparison among traditional classifier, cost-sensitive classifier, and MetaCost. *Expert Syst. Appl.* **39** (4), 4013–4019 (2012).
33. Wang, Y. C. & Cheng, C. H. A multiple combined method for rebalancing medical data with class imbalances. *Comput. Biol. Med.* **134**, 104527 (2021).
34. Koskosidis, A., Khah, E. M., Pavli, O. I. & Vlachostergios, D. N. Effect of storage conditions on seed quality of soybean (*Glycine max* L.) germplasm. *AIMS Agric. Food* **7** (2), 387–402 (2022).
35. Agacka, M. et al. Viability of *Nicotiana* spp. seeds stored under ambient temperature. *SST* **41** (3), 474–478 (2013).
36. Gianella, M. et al. Physiological and molecular aspects of seed longevity: exploring intra-species variation in eight *Pisum sativum* L. accessions. *Physiol. Plant.* **174**(3), e13698. (2022).
37. Miransari, M. & Smith, D. L. Plant hormones and seed germination. *EEB* **99**, 110–121 (2014).
38. Barbedo, J. G. A. Impact of dataset size and variety on the effectiveness of deep learning and transfer learning for plant disease classification. *Comput. Electron. Agr.* **153**, 46–53 (2018).
39. Rodriguez-Galiano, V. F., Ghimire, B., Rogan, J., Chica-Olmo, M. & Rigol-Sanchez, J. P. An assessment of the effectiveness of a random forest classifier for land-cover classification. *P&RS* **67**, 93–104 (2012).
40. Fernández, Á., Bella, J. & Dorronsoro, J. R. Supervised outlier detection for classification and regression. *Neurocomputing* **486**, 77–92 (2022).
41. Ranal, M. A. & de Santana, D. G. How and why to measure the germination process? *Rev. Bras. Bot.* **29** (1), 1–11 (2006).
42. Pang, Z. et al. MetaboAnalyst 6.0: towards a unified platform for metabolomics data processing, analysis and interpretation. *Nucleic Acids Res.* gkae253 (2024).
43. Kotu, V. & Deshpande, B. *Predictive Analytics and Data Mining* (Elsevier Science & Technology, 2014).
44. Hofmann, M., Klinkenberg, R. & RapidMiner *Data Mining use Cases and Business Analytics Applications* (CRC, 2016).

Publications

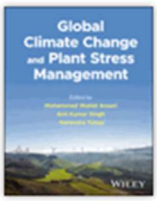

Global Climate Change and Plant Stress Management

Editor(s): Mohammad Wahid Ansari, Anil Kumar Singh, Narendra Tuteja

First published: 14 August 2023

Print ISBN: 9781119858522 | Online ISBN: 9781119858553 | DOI: 10.1002/9781119858553

Chapter 22

Seed Quality Assessment and Improvement Between Advancing Agriculture and Changing Environments

Andrea Pagano, Paola Pagano, Conrado Dueñas, Adriano Griffo, Shraddha Shridhar Gaonkar, Francesca Messina, Alma Balestrazzi, Anca Macovei

Book Editor(s):Mohammad Wahid Ansari, Anil Kumar Singh, Narendra Tuteja

First published: 07 July 2023 | https://doi.org/10.1002/9781119858553.ch22